Self Healing of Asphalt Mixtures

Towards a Better Understanding of the Mechanism

J. Qiu

Self Healing of Asphalt Mixtures
Towards a Better Understanding of the Mechanism

Proefschrift

ter verkrijging van de graad van doctor
aan de Technische Universiteit Delft,
op gezag van de Rector Magnificus prof. ir. K.C.A.M. Luyben,
voorzitter van het College voor Promoties,
in het openbaar te verdedigen op woensdag 6 juni 2012 om 15:00 uur

door

Jian QIU

Master of Science in Material Science
Wuhan University of Technology, P.R. China
geboren te Liaozhong, Liaoning, P.R. China

Dit proefschrift is goedgekeurd door de promotoren:
Prof. dr. ir. A.A.A. Molenaar
Prof. S.P. Wu, BSc, MSc, PhD

Copromotor:
Ir. M.F.C. van de Ven

Samenstelling promotiecommissie:

Rector Magnificus	Technische Universiteit Delft, voorzitter
Prof. dr. ir. A.A.A. Molenaar	Technische Universiteit Delft, promotor
Prof. S.P. Wu, BSc, MSc, PhD	Wuhan University of Technology, promotor
Ir. M.F.C. van de Ven	Technische Universiteit Delft, copromotor
Prof. D.N. Little, BSCE, MSc, PhD	Texas A&M University
Prof. I.L. Al-Qadi, BSc, MEng, PhD	University of Illinois at Urbana-Champaign
Prof. B. Birgisson, BSCE, MSc, PhD	Royal Institute of Technology
Prof. dr. ir. S. van der Zwaag	Technische Universiteit Delft
Prof. dr. ir. K. van Breugel	Technische Universiteit Delft, reservelid

To Lili and Ruizhe

Acknowledgements

Everything started with the successful cooperation between TU Delft and Wuhan University of Technology (WHUT), where I obtained my Bachelor's and Master's degree. Without all the efforts of Prof. dr. ir. André Molenaar from Delft and Prof. Shaopeng Wu from Wuhan, it would have been impossible for me to do a PhD thesis in TU Delft.

The supervision by Prof. dr. ir. André Molenaar during my PhD study is gratefully acknowledged. His encouragement and clear scientific mind were invaluable for me. His criticism and suggestions on my research are highly appreciated. I would like to thank Prof. Shaopeng Wu for being my promotor throughout my bachelor, master and PhD study, and also for showing me the way how to become a researcher in pavement materials.

I would like to thank my daily supervisor Associate Professor Martin van de Ven. He was always there for me whenever I needed him. Sharing with me his broad knowledge and valuable suggestions for both research and life are highly appreciated. I will always remember his motto on the definition of the student and will always keep it if I will become a teacher. Thank you, Martin!

I would like to thank Prof. dr. ir. Erik Schlangen for his guidance on the modeling work. I am very grateful for the valuable suggestions from my former officemate Ir. Ad Pronk. His broad knowledge on fatigue and healing, and his ideas and suggestions to research were always excellent. The valuable suggestions from Prof. dr. ir. Sybrand van der Zwaag, Prof. dr. ir. Stephen Picken, Dr. Zhao Su, Dr. Alvaro Garcia Hernandez, Dr. Liantong Mo, Dr. Milliyon Woldekidan and Dr. Xueyan Liu are greatly appreciated. Special thanks go to all the colleagues from the IOP self healing program. I was always very happy to join the meetings and to gain knowledge about innovative ideas on developing other types of self healing materials.

I would like to thank the staff of the Road and Railway Engineering group. I am very grateful for the help from Associate Professor Lambert Houben, Marco Poot, Jan Moraal, Jan-Willem Bientjes, Dirk Doedens and Jacqueline Barnhoorn. Special thanks also go to my valuable PhD colleagues Mo, Gang, Dongxing, Yue, Ning, Quantao, Jingang, Yuan, Milliyon, Diederik, Mohamad, Wim, Pungky, Sadegh, Xin, Mingliang, Pengpeng and of course my officemates Dongya and Mauricio. I would also like to thank my former colleagues for their support, Abdol, Dr. ir. Rien Huurman, Sonja, Radjan, Alem, Eyassu and Oscar.

In case I forgot to mention other colleagues and friends, sorry for that, but I am definitely very grateful for your help in one way or another.

I would like to thank my parents for their endless support during all these years I was pursuing my study, although they didn't really know what I was doing with the black-sticky stuff.

My special gratitude goes to my beloved wife, Lili Wu. I thank you for your endless love and support. I was always the guy who only knows and cares about asphalt, even in daily life. I was amazed that you spoke the term "Marshall Compactor" to me, and I realized how big our life was influenced by each other for all these years since 2003. All the love, understanding, encouragement and happiness that you gave me are greatly appreciated. And our lovely son, Ruizhe, your big smile is always a great gift to me.

Jian Qiu 邱 健

May 2012 in Delft

Summary

Traffic is increasing rapidly in terms of number of vehicles and also in axle loads. In order to maximize the availability of the pavement and to minimize hindrances to traffic because of maintenance works, long life pavements are needed. An asphalt pavement with self repairing capabilities is believed to be very useful to this respect. The self healing phenomenon of asphalt mixtures is known for many years by road engineers. Bituminous materials are expected to repair themselves during hot summers and (long) rest periods. However, the underlying mechanism is not well understood, and a proper way to measure it is not available. Research questions are: what is the self healing phenomenon, how to measure it effectively and efficiently and how to upgrade it if possible. In order to answer these questions, investigations were carried out in this thesis. This research focuses on understanding the self healing mechanism of bituminous materials and the effects of material modifications, by means of testing and modelling.

The research started with a critical literature review. Preliminary research was conducted to explore possible self healing modifiers. Novel self healing modifiers like ionomers, supermolecular rubbers and nanoparticles were chosen and investigated. Upon analyzing the change of the material properties and the self healing capability due to modifications, it was observed however, that all the novel modifications used in this research are not quite beneficial for the self healing improvement of bituminous materials. A normal soft bitumen was observed to be the best healer among all the modified bitumens tested.

Further research was conducted to assess the self healing capability of bituminous materials in further detail. Three test methods were developed to mimic the self healing phenomenon at different levels being from bitumen level to mixture level. The self healing phenomenon was directly related to a measurable crack. In each of the test methods used, cracks were produced first in a controlled way, and after that the healing process of these cracks was investigated. The test methods covered the following aspects:

- A two-piece healing (TPH) test was developed to investigate the self healing behaviour of pure bitumen using the Dynamic Shear Rheometer (DSR). During the TPH test, the healing process was mimicked by pressing two pieces of bitumen together in a parallel-plate system. The development of the complex shear modulus during the closure of the gap width and during healing rest periods was monitored and used as a healing indicator.

- A modified direct tension test was developed to assess the self healing capability of bituminous mastics. The cracks were first introduced via mechanical loading, and then healing rest periods were applied. After healing, the specimens were reloaded to determine the recovery of the

material strength; this recovery was used as a healing indicator. This test can be used to investigate the self healing capability of an open crack with two total fractured surfaces and to determine the self healing capability of meso cracks.

- A beam on elastic foundation test (BOEF) was developed to investigate the self healing phenomenon of asphalt mixtures with a notched asphalt concrete beam fully glued on a low modulus rubber foundation. After a crack is produced by imposing monotonic loading, the BOEF setup allows fully closure of the crack due to the confinement of the rubber foundation. After a healing period, the beams were reloaded and the stiffness recovery and strength recovery were used as indicators of healing.

- The results of the various tests showed that the self healing capability of bituminous materials can be ranked successfully at different healing times, temperatures and damage levels. The self healing process of damage in bituminous materials consists of two main phases, namely the crack closure and the strength gain phase. The driving force can be either thermal (temperature) or mechanical (by confinement, pressure). The self healing capability is related to the viscosity of the bitumen, which increases with increasing healing time, temperature and when the crack size is very small.

Finite element modelling was done to further investigate the self healing phenomenon in the tests. A smeared type cohesive zone model was used to model healing by defining the stiffness and strength recovery process. In this way, the self healing phenomenon was directly linked to a crack repairing process.

Based on the research results, a better understanding of the self healing phenomenon was achieved. This thesis ends by discussing some important aspects of building a durable asphalt pavement with self healing capabilities. The self healing capability of an asphalt mixture should be optimized to obtain pavements with an enhanced durability.

Samenvatting

De laatste decennia is de verkeersbelasting van onze wegen sterk toegenomen zowel in termen van het aantal voertuigen als wel de zwaarte van de aslasten. Om de beschikbaarheid van wegen voor het verkeer te maximaliseren dienen onderhoudswerkzaamheden tot een minimum te worden beperkt en is een lange levensduur van de verharding vereist. Asfaltverhardingen met zelf herstellend vermogen (healing) spelen hierbij een belangrijke rol. Het healing fenomeen van asfaltmengsels is al vele jaren bekend bij ingenieurs werkzaam in de wegenbouw. Van bitumineuze materialen is bekend dat zij zelf herstellend gedrag vertonen tijdens warme zomers en/of relatief lange rusttijden. Echter, het onderliggende mechanisme is niet goed bekend en er is geen goede manier beschikbaar om dit te bepalen. Onderzoeksvragen zijn: wat is het healing fenomeen, hoe is het effectief en efficiënt te bepalen en wat zijn de mogelijkheden om het healinggedrag te verbeteren. Dit proefschrift heeft als doel om deze vragen te beantwoorden. Het uitgevoerde onderzoek is gericht op het begrijpen van het healing mechanisme van bitumineuze materialen en de daarvoor mogelijk te gebruiken materiaal modificaties door middel van, mechanisch onderzoek en modellering.

De thesis start met een samenvatting van een uitgebreide literatuurstudie over het onderwerp. Dit heeft geresulteerd in een orienterend onderzoek vooraf om de mogelijkheden van in de literatuur als veelbelovend omschreven "self healing modifiers" voor toepassing in bitumineuze materialen af te tasten. Nieuwe self healing modifiers als ionomeren, supermoleculaire rubbers en nanodeeltjes zijn hierbij gebruikt. Bij een kritische analyse van de verandering in materiaal eigenschappen en het zelfherstellend vermogen als gevolg van deze bitumenmodificaties bleek, dat toevoeging van deze self healing modifiers meestal niet gunstig zijn voor het zelfherstellend vermogen van bitumineuze materialen. Vastgesteld werd dat ongemodificeerd "zacht" bitumen (met een relatief hoge penetratie) beter herstellend gedrag vertoont dan alle geteste gemodificeerde bitumina.

De focus van het onderzoek is vervolgens gericht op het bepalen van het healing vermogen van bitumineuze materialen variërend van bitumen tot mengsel. Het self healing fenomeen is direct gerelateerd aan een zichtbare scheur. In alle gebruikte testmethoden zijn eerst scheuren op een gecontroleerde manier geproduceerd. Vervolgens is de mate van zelf herstelling van deze scheuren als funktie van o.a. temperatuur en duur van het herstelproces onderzocht. Dit is op de volgende wijze gedaan.

- Allereerst is de zgn TPH (two-piece healing = TPH) test uitgevoerd om het zelfherstellend gedrag van bitumen in een Dynamic Shear Rheometer (DSR) te onderzoeken. Tijdens de TPH proef wordt het healingsproces onderzocht door twee lagen bitumen in een parallelle plaat systeem samen te persen. De ontwikkeling van de complex modulus tijdens en na

het sluiten van de spleet tussen de twee lagen en tijdens rustperiodes werd gebruikt als healing indicator.

- Vervolgens zijn directe trekproef uitgevoerd om het healing gedrag van bitumineuze mastiek te beoordelen. Scheuren zijn op gecontroleerde manier geïntroduceerd via mechanische belasting en het proefstuk, met de weer samengebrachte breukvlakken, is onderzocht na rustperiodes. Deze test kan worden gebruikt om het zelfherstellend vermogen van een volledige breuk, resulterend in twee geheel gescheiden oppervlakken en van meso scheuren te onderzoeken.

- Daarna zijn proeven uitgevoerd op elastisch ondersteunde asfaltbalken (beam on elastic foundation = BOEF). Deze zijn uitgevoerd om het healing gedrag van asfaltmengsels te onderzoeken. Hierbij is een asfalt balk met een kleine, kunstmatig aangebrachte, initiële scheur, gelijmd op een onderlaag van rubber met een lage stijfheid. De BOEF opstelling maakt het mogelijk om een tijdens belasting gegroeide scheur weer volledig te sluiten na ontlasten als gevolg van de "opsluiting" die door de terugverende rubberfundering wordt geleverd. Na een healing periode werden de balken opnieuw belast en het herstel van de stijfheid en de sterkte zijn gebruikt als healingindicatoren.

- Duidelijk is geworden dat het zelfherstellend proces van schade in bitumineuze materialen uit twee fasen bestaat, namelijk het sluiten van de scheur en het weer opbouwen van sterkte. De "aanjagers" voor deze fases kunnen zowel thermisch (temperatuur) als mechanisch (opsluiting, druk) zijn. Het healing proces is gerelateerd aan de viscositeit van het bitumen, die weer sterk afhankelijk is van de healing temperatuur, duur van de rusttijd, de omvang van de schade en bitumen type. Het zelfherstellend vermogen neemt toe met toenemende rusttijd, temperatuur en als de scheur klein is.

Met behulp van de onderzoeksresultaten is het zelfherstellend vermogen van bitumineuze materialen met behulp van de eindige elementen methode gemodelleerd. Het self healing fenomeen is gemodelleerd met behulp van het zogenaamde "smeared type cohesive zone" model door het definiëren van het herstel van de stijfheid en de sterkte.

Het uitgevoerde onderzoek heeft geleid tot een beter begrip van het zelfherstellend vermogen van asfaltmengsels. Het proefschrift sluit af met een bespreking van de mogelijkheden om de bijdrage te maximaliseren van het zelf herstellend vermogen van asfaltmengsels in het realiseren van duurzame asfaltverhardingen. Het zelfherstellend vermogen van asfalt mengsels kan worden geoptimaliseerd wat zal resulteren in een verbeterde duurzaamheid van asfaltverhardingen.

Used Abbreviations

ABAQUS	A finite element package
BOEF	Beam on Elastic Foundation Set-up
CDM	Continuum Damage Mechanics
COD	Crack Opening Displacement
CP	Schapery's extended elastic-viscoelastic correspondence principle
CZM	Cohesive Zone Model
DCSE	Dissipated Creep Strain Energy
DMA	Dynamic Mechanical Analysis
DMT	Displacement controlled monotonic test
DN	Double notched shaped specimen
DP	Double parabolic shaped specimen
DSR	Dynamic Shear Rheometer
DTT	Direct Tension Test
FEMMASSE	A finite element package
FH	Fatigue related healing tests
FHI	Fatigue related healing tests with intermittent loading
FHR	Fracture-healing-re-fracture test procedure
FHS	Fatigue related healing tests with storage periods
FRAH	Fracture related healing tests
FT-IR	Fourier Transform Infrared Spectroscopy
FWD	Falling Weight Deflectometer
GC	Gap constant controlled test
HB	Hard bitumen with penetration grade of 5
ITT	Indirect Tension Test
LC	Load-crack opening displacement curve
LHR	Loading-healing-re-loading procedure
MBT	Monotonic beam on elastic foundation test
MMHC	Ratio of Methyl plus Methylene Hydrogen to Carbon
NF	Normal force constant controlled test
NPCC	Nano Precipitated Calcium Carbonate
NSIO	Nano Silica Oxide
PANDA	Pavement Analysis Using Nonlinear Damage Approach, a finite element analysis program
PB	Pure 70/100 penetration grade bitumen
PBmas	Bituminous mastics with 70/100 penetration grade bitumen
PMB	Styrene Butadiene Styrene polymer modified bitumen
PH	Partial Healing Model, an analytical model
PV	Plateau Value
RDEC	Ratio of Dissipated Energy Change

SBS	Styrene Butadiene Styrene
SBSmas	Bituminous mastics with Styrene Butadiene Styrene modified bitumen
SCW	Single crack width
SD	Side displacement
SEM	Scanning Electron Microscopy
SP	Silly Putty
SURLYN	Surlyn 8940
TPH	Two-piece healing test using the Dynamic Shear Rheometer
UC	Ultrafine Carbon Black
UPP	Uniaxial Push-Pull test
UPV	Ultrasound Pulse Velocity
UR	Ultrafine rubber particles
UT	Uniaxial Tensile Test
UV	Ultraviolet light
VD	Vertical displacement
VE	Visco-elastic
VECD	Visco-elastic Continuum Damage Model
VED	Visco-elastic coupled damage
WPT	Schapery's Work Potential Theory
2D	Two dimensional
3D	Three dimensional
2PB	Two-Point Bending Test
3PB	Three-Point Bending Test
4PB	Four-Point Bending Test

Table of Contents

x

1
Introduction

Abstract

Self healing of asphalt mixtures is known for many years by road engineers. It implies that the asphalt pavement is expected to repair itself during hot summers and long rest periods. The healing factor is also used as one of the important lab-to-field shift factors in mechanistic design methods for asphalt pavements. Healing has a great potential to extend the service life of an asphalt pavement. However, the underlying mechanism is not well understood yet. Research questions are: what is the self healing phenomenon, how to measure it efficiently and how to upgrade it if possible. In order to answer these questions, investigations were carried out which are reported in this thesis. This dissertation is designed in such a way that a better understanding of this phenomenon is obtained. It contains eight chapters, including the research that was done in a preliminary phase (Chapter 1 to Chapter 3), healing assessments (Chapter 4 to Chapter 6), modelling (Chapter 7) and conclusions and recommendations (Chapter 8).

Asphalt concrete is one of the most widely used road building materials all over the world. In the Netherlands, asphalt concrete covers more than 90% of the surface layers of motorways. The structural life of an asphalt pavement is normally around 20 years. However, asphalt concrete is sensitive to the damaging action of heavy traffic and the environment (aging, water ingression). Distresses like ravelling, potholes, cracking and so on can develop which will deteriorate the pavement's service condition.

In asphalt concrete, a process called healing is competing with the deterioration process. Healing is an intrinsic property of bitumen. Bituminous materials are expected to heal themselves during hot summers and long rest periods, which will result in an extension of the service life of the asphalt pavement. Unfortunately, this healing property degrades due to ageing and load repetitions. As a result, understanding and improving the self healing mechanism is important for service life extension.

This chapter introduces the self healing phenomenon both observed in practice and used in pavement design. The research objectives and the organization of this dissertation are also presented.

1.1 Healing in Practice

Cracking is one of the main types of distresses of asphalt pavements. As shown in Figure 1-1, different types of cracks can be observed in bituminous materials, ranging from macro level to meso/micro level:

- o At the level of asphalt pavements, cracks which are observed at the pavement surface can be either bottom-up cracks which develop due to tensile strains at the bottom of the asphalt layers or top-down cracks at the pavement surface due to tensile and shear stresses, climatic effects and ageing.

- o In asphalt concrete specimens, cracks are observed in specimens as a result of load repetitions.

- o At the level of the mortar, cracks are observed either as cohesive type inside the mortar or adhesive type between binder and aggregates.

Healing, as one of the unique properties of bituminous materials, is able to reverse the cracking process:

- o At macro level, healing is thought to occur in two ways. One way is that some of the microcracks can be healed during the rest periods between two axle passages. Another possibility is that microcrack healing happens during summer when the temperature is high. This implies that microcracks developing during the winter can be healed during a hot summer.

o At meso level, healing can be observed both in the cohesive and adhesive regions of asphalt mixtures. Healing is considered to be cohesive when occurring in the bitumen or mastic and to be adhesive when occurring at the bitumen-aggregate interface.
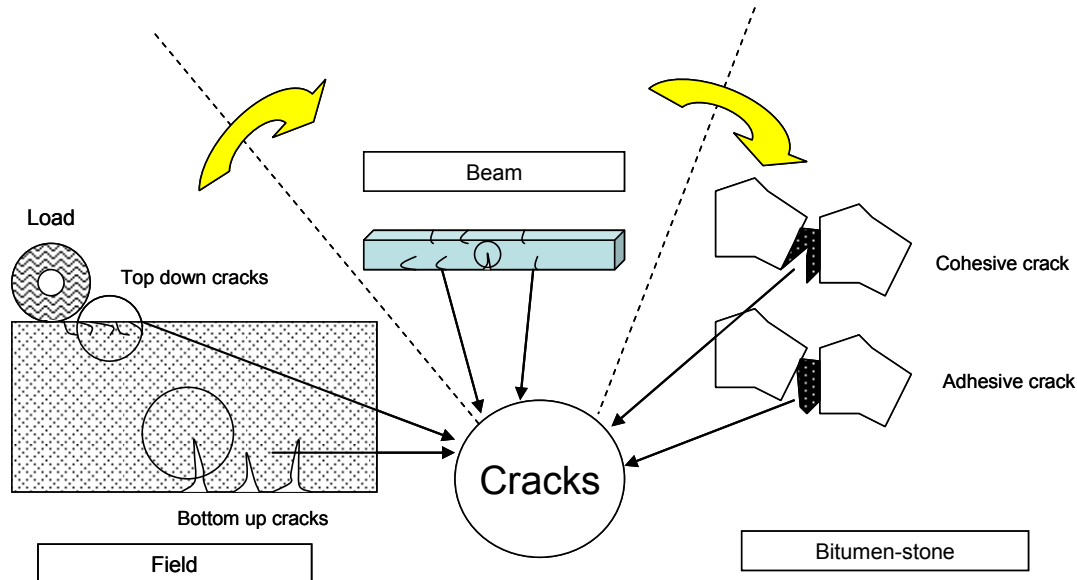
Figure 1-1 Illustrations of different types of cracks at multi-scales of bituminous materials

1.2 Healing in Pavement Design

Fatigue based mechanistic pavement design methods are commonly used in the Netherlands and other countries for the thickness design of asphalt pavements. As shown in Figure 1-2, the input for these methods is the tensile strain ε calculated at the bottom of the asphalt layer due to traffic loadings. This tensile strain is calculated using a multi-layer analysis. The required input consists of the loading F, the elastic modulus and Poisson's ratio of each layer as well as the thickness of each layer. The calculated tensile strain is used as input in a fatigue relation to calculate the number of load repetitions to failure. Laboratory fatigue tests are performed to obtain a fatigue relation. If the calculated number of load repetitions is less than the design number of load repetitions, a larger thickness needs to be applied to reduce the strain level ε and to increase the pavement life.

In this procedure, a number of correction factors need to be applied because of the difference between the real pavement fatigue and the laboratory fatigue test.

In the Shell Pavement Design Manual, a shift factor is proposed to take into account the contribution of healing and the lateral wander of traffic (not each wheel is driving in the same track) [1]. The asphalt fatigue life to be used in practice ("in the field") then can be determined as follows:

$$N_{field} = N_{lab} \times H \times V \qquad\qquad 1\text{-}1$$

where,

        H   = healing factor;

        V   = lateral wander factor.

Lytton proposed to estimate the shift factor using the increase of the dissipated energy of a load cycle after a rest period [2]. The relation between the laboratory and field fatigue life is given by shift factors with a value of 1 or higher.

$$N_{field} = N_{lab} \times SF_h \times SF_r \times SF_d \qquad\qquad 1\text{-}2$$

where,

      SF_h = the shift factor due to healing;

      SF_r = the shift factor due to residual stresses;

      SF_d = the shift factor due to resilient dilation.
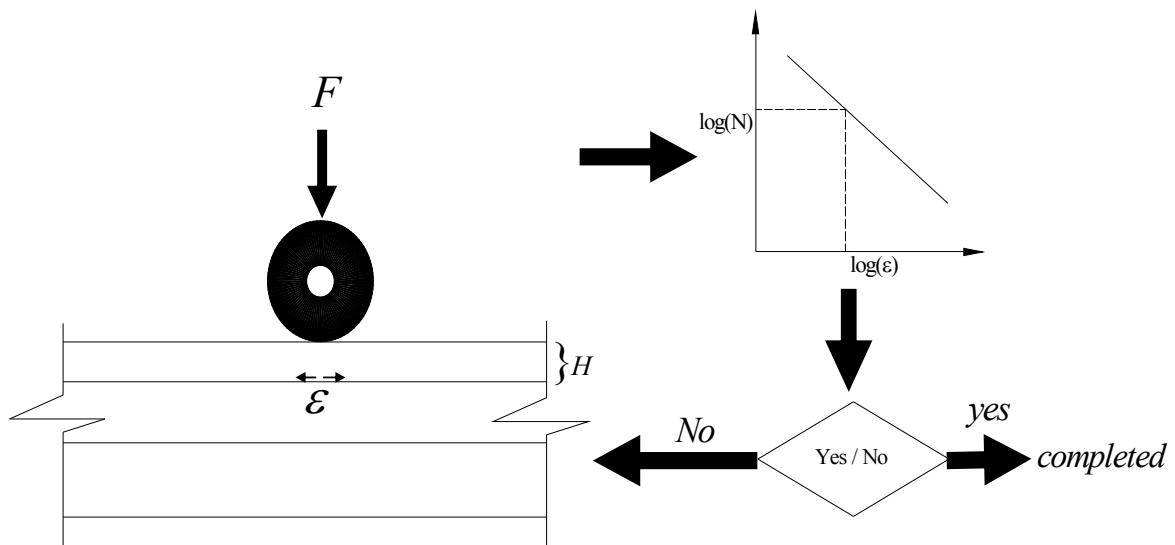
Figure 1-2 Fatigue based thickness design method

Unfortunately, many different shift factors are used and there is no unique relationship. Table 1-1 gives some shift factors used in the literature [3]. The values appear to be dependent on the test types, the test conditions, the test configurations and the mode of loading in the lab tests, and the field conditions. In addition, they may also be dependent on the bitumen characteristics. Shift factors proposed by various researchers vary from slightly more than 1 to 400. Healing, as one of the biggest unknown factors, varies between 1.5 and 20. Normally, a healing factor of 4 is adopted for standard mixtures in the Netherlands with a 70/100 penetration grade bitumen.

Table 1-1 Overview of shift factors [3]

Countries	References	Type of test	Fatigue shift factors				
			Mode	Healing	Crack propagation	Traffic wander	Total
USA	Asphalt Institute						13
UK	Nottingham Pell	Rotating Bending	F	5	20	1	100
UK	Nottingham Brown	Rotating Bending	F	20	20	1.1	440
Ireland	NRA-Dublin Golden 1988	Rotating Bending	F				230
-	Shell SPDM 1978	Variable	D	5	1	2	10
France	LCPC	2 point Bending	D				1.6 -3.7
USA	SHRP A-003 Von Quintus 1994						10-13
Belgium	BRRC Verstraeten 1974	2 point Bending	F	7.1	3	1-2.5	7.1
The Netherlands	DWW Groenendijk 1998	4 point Bending	D	4			

Footnote: F stands for force controlled, D stands for displacement controlled

1.3 Research Objectives

It is clear that the self healing capability of bituminous materials is helpful for service life extension of asphalt pavements. However, there are still a number of research questions to be answered which are as follows:

⇒ What is the self healing phenomenon of bituminous materials and how can we measure it effectively?

Much research could be found in the literature referring to the self healing phenomenon of bituminous materials. However, the underlying mechanism is not explained, and a proper way to measure it is not mentioned. It is noticed that most of the tests are empirical and the research results vary a lot.

⇒ How can we improve the self healing capability of bituminous materials?

The self healing property of asphalt mixtures decreases sharply when bitumen is highly aged (i.e. in recycled asphalt mixtures and the surface of porous asphalt). Based on the knowledge of healing of asphalt mixtures, possibilities to improve the self healing capability of asphalt mixtures can be defined. Inspired by novel self healing materials, several chemical and biological treatments could possibly improve the healing capability of asphalt mixtures [4].

⇒ How can the self healing capability be helpful for durable asphalt pavement?

Upon understanding the self healing phenomenon, the possibility of implementing the self healing ideas for durable asphalt pavement design is discussed. This can be either in structural perspective or in material perspective.

The main goal of this study is to investigate the self healing phenomenon of bituminous materials. In order to achieve this goal, the following objectives were defined:

✓ **Develop effective methods to evaluate the self healing capability of bituminous materials (including bituminous binders, mastics and asphalt mixtures).**

✓ **Explore possible novel self healing modifiers for upgrading the self healing capability of bituminous materials.**

✓ **Understand the self healing phenomenon through numerical modelling.**

1.4 Organization of the Dissertation

Figure 1-3 gives an overview of the structure of this dissertation. This dissertation is divided into eight chapters.

Chapter 1 gives a general introduction about the presence of the self healing phenomenon in asphalt pavements. It also defines the research problems and the research objectives of this dissertation.

Chapter 2 presents an extensive literature review. Investigations on the self healing phenomenon of bituminous materials as described in the literature are summarised. These include the characterization methods, influencing factors and modelling of the self healing phenomenon of bituminous materials. In addition, new emerging novel self healing material systems are also reviewed.

Chapter 3 gives the research approach and methodology. A two-phase research approach is followed being the research exploration phase and the final research phase. With the lessons learned from the literature review, a research exploration phase is introduced to explore the potential benefits of possible self healing characterization methods and possible novel self healing modifiers. With the conclusions and the recommendations from the research exploration phase, the final research phase is designed to further understand the self healing capability of bituminous materials through mechanical assessment and modelling.

In Chapter 4, the assessment of the self healing capability of pure bitumen is conducted using the Dynamic Shear Rheometer. Special attention is paid to separating the real self healing phenomenon from its artefacts.

In Chapter 5, the assessment of the self healing capability of bituminous mastics is conducted using the Direct Tension Test. The self healing capabilities are assessed on open cracks and on meso cracks.

Chapter 6 presents an assessment method for the self healing capability of asphalt mixtures using the Beam on Elastic Foundation Set-up. With an asphalt mixture beam glued on a rubber foundation, the self healing capability of asphalt mixture was investigated.

In Chapter 7, a fracture mechanics based finite element modelling approach was adopted to model the self healing phenomenon of bituminous mastics occurring in the Direct Tension Test and the self healing phenomenon of asphalt mixtures occurring in the Beam on Elastic Foundation test.

Chapter 8 presents the conclusions and recommendations with regard to this dissertation.
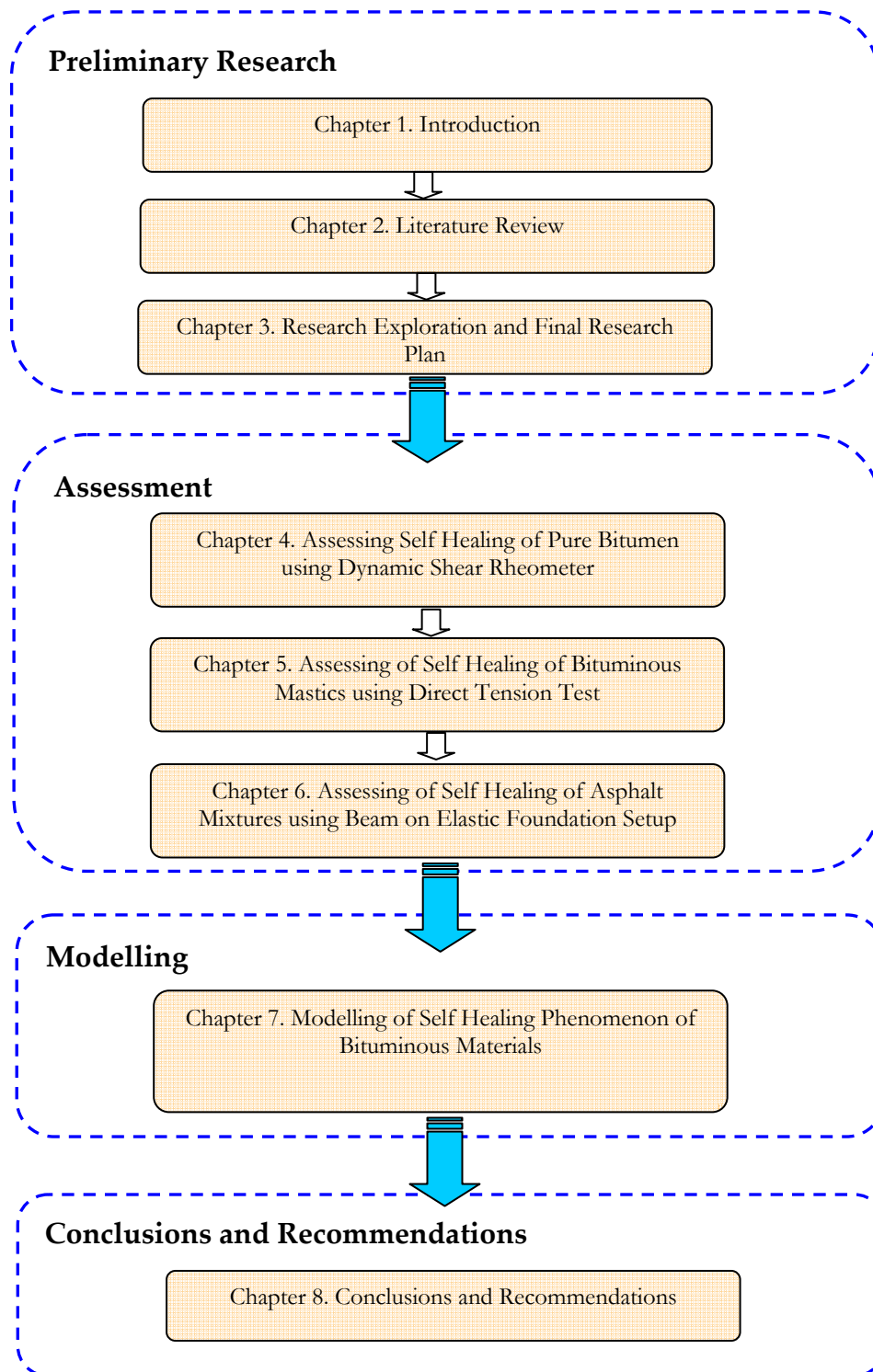
Figure 1-3 Structure of the dissertation

References

[1] Shell. Shell pavement design manual - asphalt pavement and overlays for road traffic. London, UK: Shell International Petroleum Company Limited; 1978.

[2] Lytton RL, Uzan J, Fernando E, Roque R, Hiltunen D, and Stoffels S. Development and validation of performance prediction models and specifications for asphalt binders and mixes. Strategic Highway Research Program SHRP-A-357. Washington DC; 1993.

[3] COST333. European Commission-Directory of Transport COST333: Development of new bituminous pavement design method, Luxemburg,1999.

[4] Van der Zwaag S. Self healing materials: an alternative approach to 20 centuries of materials science. Dordrecht: Springer Verlag; 2007.

2
Literature Review

Abstract

Since 1960s, researchers in road engineering started to pay attention to the self healing phenomenon of bituminous materials. If bituminous materials heal significantly then this phenomenon is beneficial for the service life extension of asphalt pavements. This chapter reviews the state-of-the-art of the self healing investigations ranging from bituminous binders to asphalt pavements, from mechanical experiments to material modelling. In addition, newly developed novel self healing material systems are also reviewed.

This Chapter is partly based on

1. Qiu J. Self healing of asphalt mixtures: literature review. Report 7-08-183-1, Delft University of Technology;

2. Qiu J, van de Ven MFC, Wu SP, Yu JY, and Molenaar AAA. Self healing of bituminous materials: state-of-the-art. Submitted to Construction and Building Materials

Self healing of bituminous materials has been a hot topic for more than 50 years. Since 1960s, researchers in road engineering started to pay attention to this phenomenon. Research was mainly focused on charactering the self healing phenomenon at different scales ranging from bituminous binders to asphalt pavements, from mechanical experiments to material modelling. A state of the art overview of self healing investigations of asphalt mixtures can be found in the following sections.

Section 2.1 gives basic definitions of self healing concepts. Section 2.2 reviews the characterization methods which indicate self healing capability of bituminous materials. Section 2.3 reviews the factors influencing the self healing capability of bituminous materials. Section 2.4 shows possible theories and models which explain the self healing phenomenon. Section 2.5 reviews novel self healing material systems shown to be effective in the other materials.

2.1 Self Healing Definition

2.1.1 Concept of self healing materials

Usually material properties degrade over time due to the initiation of damage (like micro-cracking) on a microscopic scale that tends to grow and will ultimately lead to failure of the material. A self healing material is a material which has a built-in ability to (partially) repair damage occurring during its service life [1].

2.1.2 Concept of self healing of bituminous materials

The stiffness and strength of bituminous materials decrease when bituminous materials are exposed to load repetitions. The processes of micro-cracking initiation, propagation and macro-cracking during cyclic loading were investigated by many researchers [2, 3]. The recovery of material stiffness, the extension of fatigue life and the recovery of strength were for the first time experimentally observed in the 1960s under a fatigue test with rest periods [2-5]. This was from then on defined as the self healing phenomenon of bituminous materials, being the recovery of material properties and diminishing of cracking.

2.1.3 Concept of novel self healing materials

From the biological world the self healing mechanisms of the organisms are well known to continuously sense damage and repair it. Researchers are now trying to engineer this self healing behaviour into man-made materials, to develop self healing materials. Scientists intended to introduce self healing components to normal materials to create a self healing system, and in this way to improve the service life of normal materials. This concept was first defined by White when he introduced micro-encapsulation self healing systems into an

epoxy matrix [6]. Until now, many new self healing materials to be used in concrete, polymers, composites, coatings, metals, etc are under investigations [1]. Successful self healing material systems are developed such as: encapsulations, polymer diffusion, thermo-reversible polymers, etc.

2.2 Characterization of Self Healing of Bituminous Materials

Table 2-1 lists the characterization methods as used for self healing investigations of bituminous materials. Studies are focusing on different levels, dependent on the subject. They include bituminous binders, mastics (bitumen-filler system) and mortars (bitumen-filler-fine sand system), asphalt mixtures and the asphalt pavement itself.

Table 2-1 Methods on characterization of self healing of bituminous materials

		Binders, mastics and mortar	Asphalt mixtures	Asphalt pavement
Fatigue related healing tests (FH)	Fatigue related healing with intermittent loading (FHI)	Dynamic Shear Rheometer (DSR), Dynamic Mechanical Analysis (DMA)	Two-Point Bending Test (2PB), Three-Point Bending Test (3PB), Four-Point Bending Test (4PB), Uniaxial Push-Pull (UPP)	
	Fatigue related healing with storage periods (FHS)	DSR	2PB, 4PB, Indirect Tension Test (ITT)	
Fracture related healing tests (FRAH)		DSR, DMA	Uniaxial Tension Test (UT), Flexural Test	
Other test methods		Scanning Electron Microscopy (SEM), Surface Energy, etc.		
Field healing tests				Falling Weight Deflectometer (FWD), Stress Waves

Most of the characterization methods are related to mechanical tests. In principle, healing is investigated by inserting a series of rest periods between two loadings. The effect of healing is then characterized by comparing the response of the material tested with and without rest periods. Two main categories of test methods are used, namely fatigue related healing tests and fracture related healing tests:

- o **Fatigue related healing tests (FH)**

  - o **Fatigue related healing with intermittent loading (FHI):** Apply intermittent load repetitions to the test specimen. That is, each loading cycle is followed by a rest period.

  - o **Fatigue related healing with storage periods (FHS):** Subject the specimen to continuous load repetitions (as in a conventional fatigue test) for certain periods. Interrupt the continuous load repetitions with certain storage periods during which the specimen is kept under given conditions without loading.

- o **Fracture related healing tests (FRAH):** Apply healing periods between two fracture tests.

Section 2.1.1 reviews the test methods on self healing of bituminous binders and mastics. Section 2.1.2 reviews the test methods on self healing of asphalt mixtures. Section 2.1.3 reviews the test methods on self healing of asphalt pavements.

2.2.1   Self healing of bituminous binders and mastics

Table 2-2 gives an overview of the test methods used for research on self healing of bituminous binders and mastics. From the table it can be observed that the Dynamic Shear Rheometer (DSR), which is widely used for rheological and fatigue investigations of bituminous materials, is also the most commonly used equipment for investigating the self healing capability of bituminous binders and mastics. Detailed information on these approaches can be found hereafter.

Table 2-2 Test methods on self healing of bituminous binders and mastics

Test types	Samples	Tempera-tures (°C)	Control	Systems	Freq-uency (Hz)	Stress /strain levels	Healing procedures	Refs
FHI	Bitumen with sand	25	Strain	DSR Column	10	0.35% and 0.9%	Two-minute rest periods were applied 10 times during the tests	[7, 8]
FHI	Bitumen	15	Stress	DSR Parallel plate	25	184kPa-237kPa	20s loading/10s rest - 20s loading /400s rest	[9]
FHI	Bitumen	15, 25	Stress	DSR Parallel plate (8mm)	10	60kPa - 230kPa	1s loading/0s rest-1s loading/6sec rest	[10]
FHI	Bitumen with filler and sand with maximum particle size of 0.5mm	15	Stress	DSR Column	10	0.025- 0.1 Nm	3s loading/9s rest	[11]
FHS	Bitumen	10	Strain	DSR Parallel plate	41	1.6%	Strain level of 0.02% for 0-5000s	[12]
FHS	Bitumen with filler	10	Strain	DSR Parallel plate	40	0.3%	Strain level of 0.003% for 2h	[13]
FHS	Bitumen	20	Strain	DSR Parallel plate	1.6	20%	After 5000 cycles, specimen rested for periods of 0.5, 1, 3, and 12 hours, then test again	[14]
FHS	Bitumen	25, 20	Stress	DSR Parallel plate (8mm)	10	400kPa	Complex viscosity $|\eta^*|$ was equal to 50% of the $|\eta^*|$ at cycle 10; test was stopped for a rest period ranging from 0 to 48h, then test started again	[15]
FHS	Bitumen	15	Strain	DSR Parallel plate	25	1.6%	4hours for the first rest; 17hours for the second rest	[9]
FHS	Bitumen	5-9	Strain	DSR Parallel plate (8mm)	1.59	1%	Strain level of 0.01% for 2 hours	[16]
FHS	Bitumen	15	Strain	DSR Parallel plate (8mm)	25	1.8%	Strain level of 0.05% for 500 rest (500loading/500rest cycles)	[17]
Local fracture	Bitumen	0	-	DMA hemispheric protuberances	-	-	Rest for 2 minutes to 4 hours	[18, 19]
TPH	Bitumen	25	Strain	DSR Parallel plate (25mm)	-	-	A constant normal force of 0.4 N, strain amplitude of 0.001% and at 10 rad/sec for 1 hour	[20-22]
TPH	Bitumen	20	Strain	DSR Parallel plate (25mm)	-	-	A constant gap thickness of 7.8mm, strain level of 0.00625% at 10 Hz for 2 hours	[23]
Izod with SEM	Bitumen with sand	20	-	Izod	-	-	Rest for 5 minutes to 20 minutes	[24]

2.2.1.1 Fatigue related healing tests with intermittent loading (FHI)

Kim and his colleagues applied strain controlled FHI tests to investigate the fatigue and healing properties of sand asphalt mixtures with/without rest periods [7, 8]. The results showed that the introduction of rest periods during the early phase of the fatigue test extended the fatigue life significantly, which indicated the fast healing of micro-damage during rest periods.
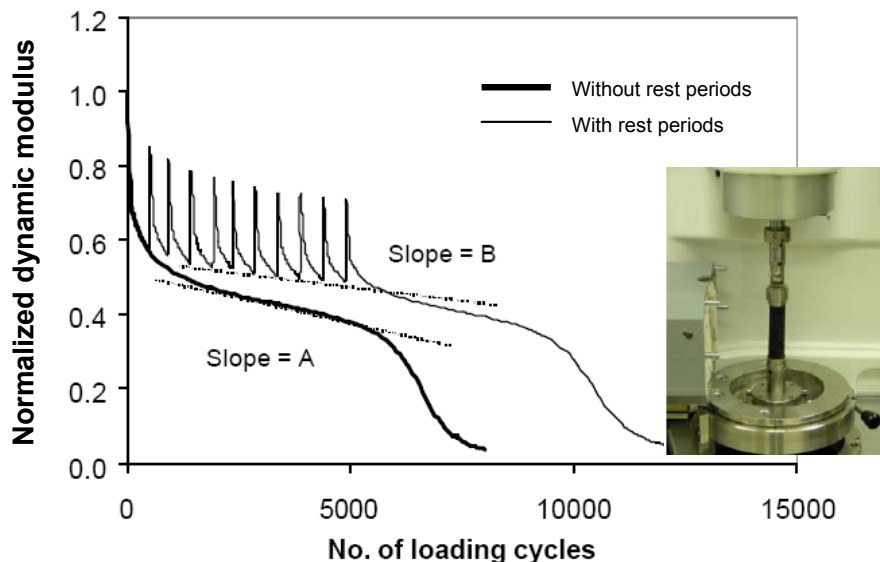

Figure 2-1 Comparison of the test results with and without rest periods [7]

Lu conducted stress-controlled FHI tests with different rest /load period ratios [9]. The tests were carried out under the following conditions: 15°C, 25 Hz, and a constant stress (varied from 184kPa to 237kPa) corresponding to an initial strain level of 1%. Different combinations of loading and rest duration for each cycle were applied in the tests, such as 20s load/10s rest, 20s load/20s rest and 20s load /400s rest. The results indicated that the contribution of rest periods on the fatigue life extension was largely dependent on the type of bituminous binders.

Van den bergh used constant torque controlled FHI tests on cylindrical specimens with 3s load/9s rest for each cycle [11]. The tests were done on both new and recycled bituminous mastics and mortars at a temperature of 15°C and a frequency of 10 Hz. A so-called healing factor was introduced in this research, which was defined as the ratio of cycles to total failure of samples which were subjected to 3s load/9s rest loadings and the cycles to failure of samples which were subjected to only continuous loadings without rest periods. The results indicated that mortar samples clearly showed healing with the introduction of rest periods between loading cycles.

Shen applied the FHI tests in the stress controlled mode to investigate the healing capability of two types of binders, PG64-28 (a neat binder) and PG70-28 (a polymer modified binder) [10]. The load period/rest period settings for each cycle introduced in this test were varied from 1s load/0s rest to 1s load/6s rest.

The results indicated that the type of bituminous binder, healing temperature and stress level applied were all influencing the observed healing capability.

2.2.1.2 Fatigue-healing test with storage periods (FHS)

The FHS tests were proposed to investigate healing after long storage periods. The healing efficiency was then quantified by means of the modulus recovery and/or the extension of cycles (load repetitions) to failure in a re-fatigue test.

Phillips used the FHS test procedure to study the fatigue and healing behaviour during fatigue-healing cycles [12]. As shown in Figure 2-2, the test was conducted in a strain controlled mode. A healing period of 5000s was applied between two fatigue tests during which the samples were subjected to a small strain of 0.02%. The loss and recovery of the complex modulus was used to quantify the fatigue and healing capacity of different types of bituminous binders. The strain levels and the level of damage were also influencing the healing capability.
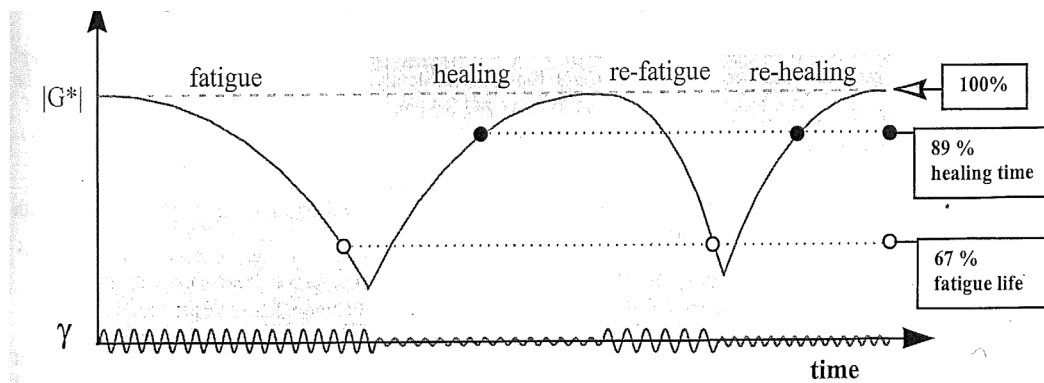
Effect of strain level on bitumen fatigue and cracking (at 10°C after 1 hour, 40 Hz)						
command strain, γ	1%	1.2%	1.5%	1.8%	2.0%	2.5%
fatigue observed ?	no	little	yes	yes, >50%	yes, major	rapid
macro-cracks observed ?	no	no	no	yes	yes	major
healing ?	n.a.	yes, 100%	yes, 100%	partial	partial	no

Figure 2-2 Illustration of FHS test after Phillips [12]

Smith and his colleagues used a strain controlled FHS test to investigate the effects of coarse and fine fillers on the healing properties of bituminous mastics [13]. The tests were conducted at a temperature of 10°C and at a frequency of 40Hz. Each test was performed in two stages. In the first stage, a strain level of 0.3% was applied to introduce fatigue damage. After the stiffness had reduced to 50% of its initial value, the second stage was started with a much lower strain level of 0.003% for a period of two hours. During this stage it was expected that some healing effects could be observed. The healing effect was then defined as the recovery of the stiffness compared to the original stiffness. The test results showed that the mastic with a coarse filler exhibited a better recovery compared to the mastic with a fine filler.

Bahia investigated the healing properties of modified bituminous binders by means of the FHS test procedure [14]. Strain controlled FHS tests were performed at a temperature of 20°C and a frequency of 1.6Hz. In each test, the sample was first subjected to 5000 load cycles at a strain level of 20%. And then the test was stopped for a rest period ranging from 0.5h to 12h. After this rest period the fatigue test was restarted until failure occurred. The test results showed that the introduction of a rest period extended the total number of cycles to failure. After a rest period of 12h, the healing effect became more significant, which was indicated by larger recovery of the stiffness and a longer extension of the re-fatigue life.

Shan and her colleagues conducted stress controlled FHS tests with a 10Hz continuous sinusoidal loading at temperatures of 20°C and 25°C [15]. First, a fatigue test was performed using a stress level of 400kPa until the complex viscosity value $|\eta^*|$ was equal to 50% of the $|\eta^*|$ at cycle 10. Then the test was stopped for a rest period ranging from 0 to 48h. After this rest period, the re-fatigue test was started till total failure. The test results were analyzed according to the thixotropy theory implying that: (a), the fatigue life (Nf_{50}, cycles to 50% of the complex viscosity in the fatigue test) could be related to a break-down coefficient; (b), the healing capability (the recovery of the slope of the re-fatigue curve after 48 hours of rest) could be related to a build-up coefficient. More information about the thixotropic healing theory can be found in Section 2.4.1.2.

Lu also conducted strain-controlled FHS tests [9]. All fatigue tests were performed at a strain level of 1.6%, at 25 Hz and 15°C. Rest periods used were 4h for the first rest duration, and 17h for the second rest duration. The results indicated that the recovery of the complex modulus was not necessarily related to the extension of the fatigue life.

Santagata related the fatigue and healing behaviour observed during FHS tests to the chemical composition of six types of 70/100 penetration grade bituminous binders [16]. The fatigue and healing tests were carried out using equi-stiffness temperatures with a target stiffness of 25MPa. The test temperatures were 5 to 9°C depending on the type of binder. The fatigue and re-fatigue tests were conducted in the strain controlled mode with a frequency of 1.59 Hz and a strain level of 1%. During the healing time of 2 hours, a small strain oscillation at an amplitude of 0.01% was applied to the specimen in order to measure the recovery of the stiffness. The number of loading cycles to failure ($NDER_{max}$) and the Relative Healing Index (RHI) in relation to re-fatigue cycles were compared with the chemical composition indexes of bituminous binders such as the Colloidal Instability Index (CII) and the saturates-to-aromatics ratio (S/Ar). The results supported the idea that bitumen with more components with low molecular weight had a better healing potential.

Bodin proposed a thermo-mechanical model to evaluate the thermal effects induced by the dissipated energy during the FHS tests on bituminous binders [17]. The fatigue tests were carried out in the strain controlled mode with a strain level of 0.18% at 15°C. A test procedure was developed with several load-rest cycles using loading periods of 500s followed by rest periods of 500s. The results indicated that a part of the modulus recovery, which was defined as healing, could be the result of temperature cooling effects.

2.2.1.3 Fracture related healing test (FRAH)

A repeated local fracture test was proposed by Hammoum and Millard to investigate the healing properties of pure bitumen [18, 19]. Figure 2-3 shows that in this test the bitumen binder is held between two hemispheric protuberances simulating two aggregate particles in the asphalt mixture.

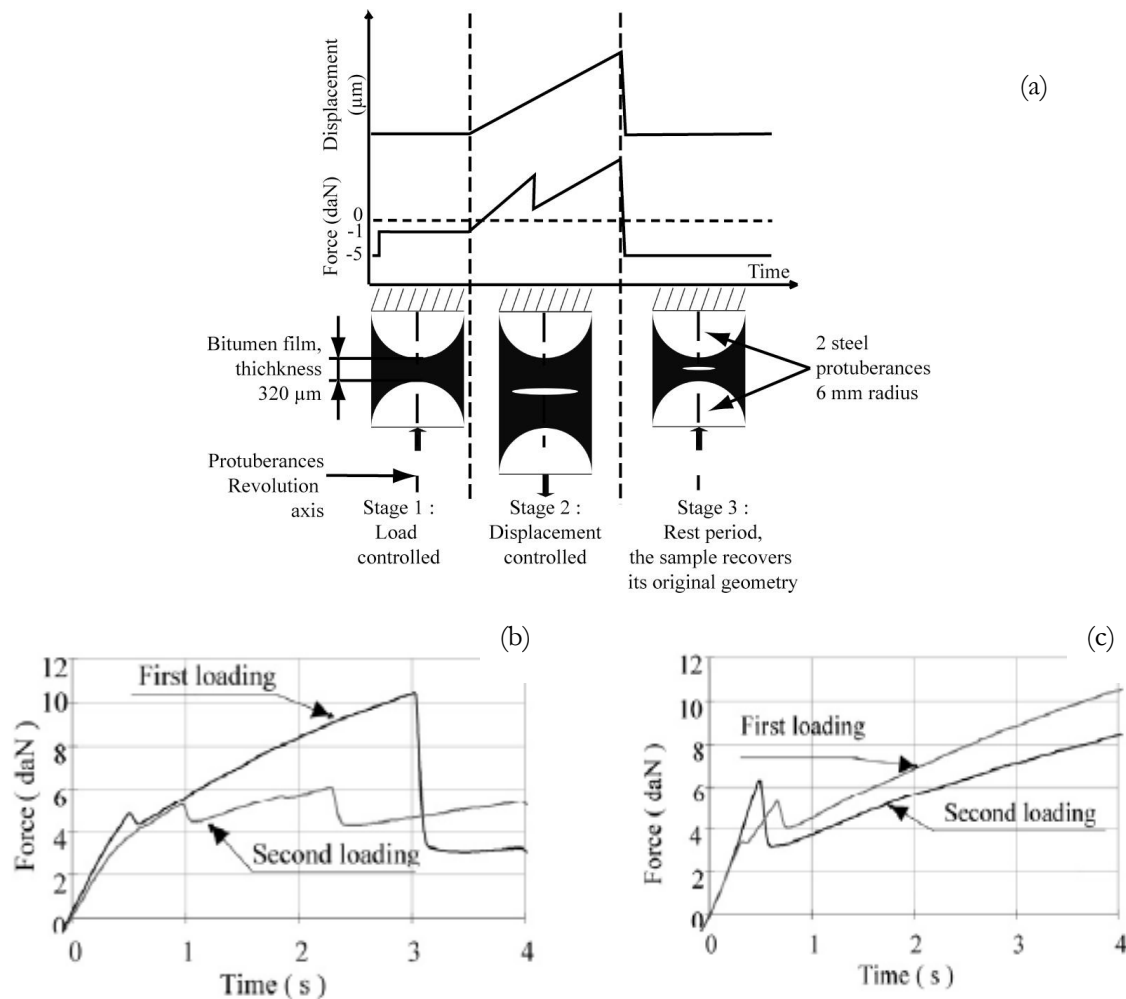Figure 2-3 Illustration of local fracture tests [18, 19]: (a) test procedure; (b) rest period of 2 minutes; (c) rest period of 4 hours

A displacement controlled tension loading was applied to the system with a speed of 12.5mm/s for 4s. After loading, the system returned to the initial gap-width between the spheres. Then healing rest periods were applied with durations of 2 minutes and 2 hours. During the healing period, a slight

compression load of 50N was applied on the sample holder. In addition, all the tests were carried out at 0°C. After the healing period, the loading was applied again. After 2 hours healing, the bitumen had almost recovered its original fracture properties.

Bhasin and his colleagues developed the first intrinsic two-piece healing (TPH) test in order to simulate the crack healing process directly [20-22]. As it is shown in Figure 2-4, two pieces of bitumen were placed on the upper and the bottom plate of the DSR. Then the DSR pressed the two pieces of bitumen together to mimic the crack healing process. The change of the shear modulus was measured with a strain level of 0.001%. During the test, a constant compression normal force of 0.4N was applied. The results indicated that the initial healing values obtained by means of gap closure showed a good agreement with the surface free energy values of the five different types of bitumen tested. This test is also supporting the multi-step healing model about which more information is given in Section 2.4.1.1.

a) Two bitumen specimens affixed to the two end plates of the DSR

b) Bitumen specimen after being brought into contact with each other to measure change in composite G* over time

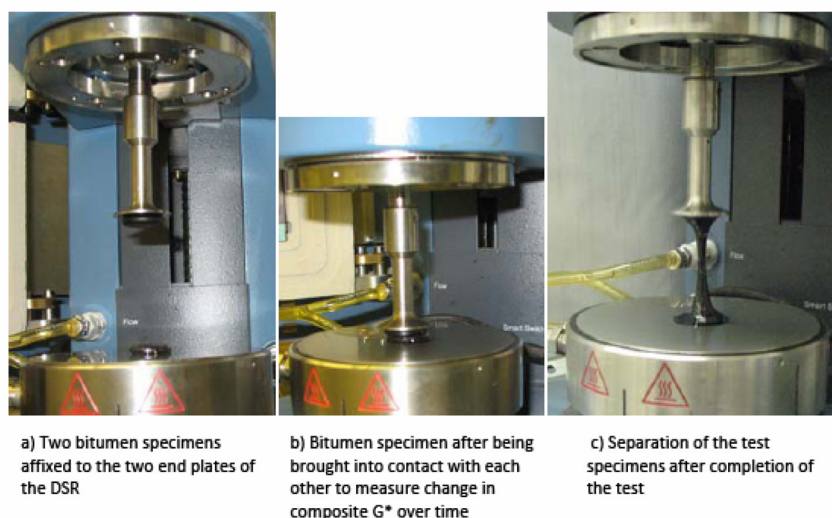c) Separation of the test specimens after completion of the test

Figure 2-4 Illustration of TPH tests [22]

Kim used the scanning electron microscopy (SEM) to investigate the healing properties of bitumen specimens [24]. The bitumen specimens were made of Ottawa sand with 13% (by mass) of bituminous binder. After curing, the specimens were fractured with the Izod impact test machine with a 0.225N impact hammer. The two fractured surfaces of the fractured specimens were brought back into contact with each other. Then these specimens were placed vertically and left undisturbed for varying periods of time at 20°C. Following healing periods of varying lengths, the samples were again fractured by the Izod impact test machine to provide fracture surfaces. Afterwards, all of the fracture surfaces were studied using the SEM. The observations recorded suggested two stages in the healing mechanism including interpenetration and bonding. When bituminous binders from two surfaces were brought into contact with each other, the interface would disappear as a function of time.

Then, the bonding energy developed also as a function of time and contributed the most to the healing in terms of strength of the bitumen.

2.2.2 Self healing of asphalt mixtures

Table 2-3 gives an overview of the test methods shown in literature on self healing of asphalt mixtures. Detailed information of these methods can be found hereafter.

Table 2-3 Test methods on self healing of asphalt mixtures

Categories	Test Name	Temperature (°C)	Control mode	Frequency	Stress /strain level	Brief test method	Healing method	Refs
FHI	Uniaxial Push Pull Test	10, 25	stress			0.02s loading with different rest periods (TR/TW=1 and 6) for a cycle		[3]
FHI	Uniaxial Push Pull Test	15		55.6Hz		18 ms loading with rest period with TR/TW= 0,1,2,6,10,20 for a cycle		[2]
FHI	Three-point Bending Fatigue Test	20	strain	1Hz	200-400 micro strain	sinusoidal loading wave of 0.1 s and a rest time of 1 s for a cycle		[25]
FHI	Four-point Bending Fatigue Test	20	strain	10Hz	500 micro strain	0 to 9 seconds		[26]
FHS	Repeated Cyclic Uniaxial Fatigue Test	25	strain		200, 350 micro strain	0.1s load and 0.9s rest for a cycle, for 10000 cycles, then series of rest periods at 1,000 cycle intervals carried out. The test was terminated at 24,000 load cycles	rest periods of 2, 5, 10, and 30 min after 10,000 loading cycles	[27]
FHS	Uniaxial Tension Test	25	strain			haversine wave with 0.2s	Five different rest durations (20, 40, 80, 320, and 1280 seconds) were introduced between repetitive loading groups	[28]
FHS	Indirect Tensile test	10, 15, 20	stress		700-1300lb, 55, 75psi	Apply 1000 cyclic loads with haversine load of 0.1 second and rest periods of 0.9 seconds	Perform resilient modulus tests at 2, 4, 6, 10, 20, 40 and 60 minutes after discontinuing the loading 20°C and 60°C, for 4 h	[29, 30]
FHS	Three-point Bending with Impact Resonance	20				3000 cycles at 1.7 Hz and rest, then applied again to 10,000 cycles, rest again, applied to 20,000 cycles		[31]
FHS	Indirect Tensile Fatigue Test with Ultrasound Wave Velocity	25	stress		3.5 kN	0.1 s period followed by a 0.4 s rest period for a cycle. Stopped at 3/4 of the initial stiffness and rest, then applied load to failure.	Five different rest periods were under investigation (1 and 3h, 3, 7 and 14 days) at five different temperatures (0, 15, 30, 45 and 60°C).	[32]
FRAH	Flexural Test	5					three outdoor exposure times (1, 3, 6 and 12 months), three traverse temperatures (20, 40 and 60°C)	[33]

2.2.2.1 FHI

From 1960s to 1980s, the fatigue related approaches were used to identify the healing phenomenon under intermittent loading [2, 3, 5, 34, 35]. In this way, the relationship between fatigue life extensions and rest periods could be determined. The ratio between the fatigue life with rest periods and the fatigue life in the continuous fatigue test (no rest periods) was called the healing factor. This term is still widely used in experimental studies and mechanistic flexible pavement design.

Figure 2-5 summarizes relationships of the fatigue life extension vs. rest periods as shown in the literature. In this figure, T_R/T_W= ratio of rest periods to loading periods, and N_R/N_W= ratio of fatigue life with rest periods to fatigue life without rest periods.
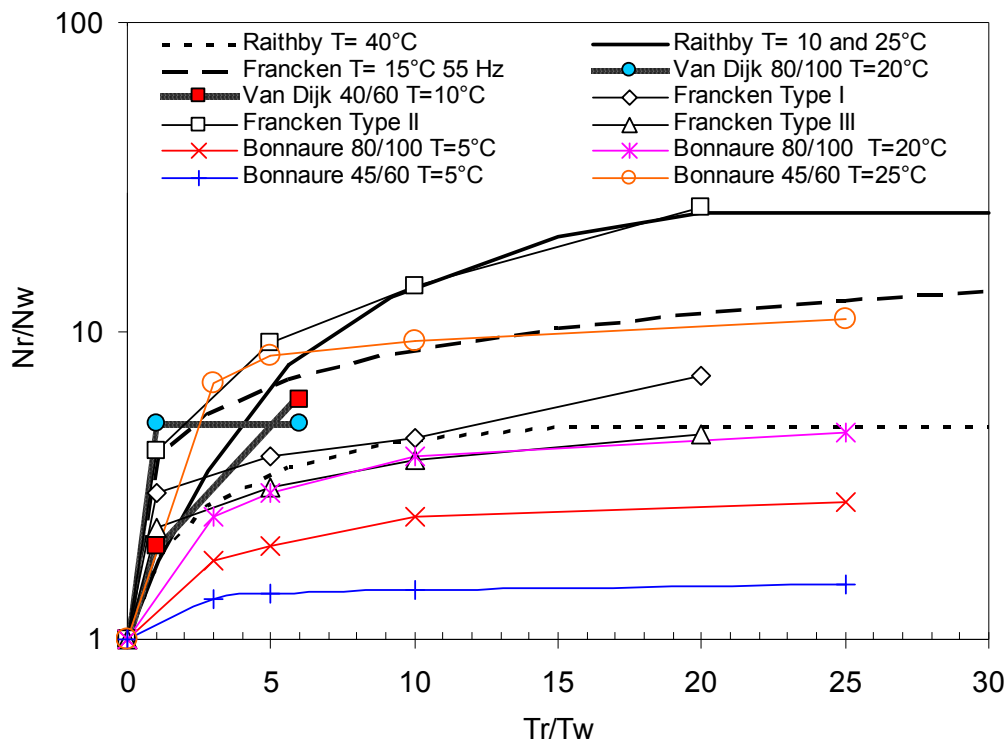

Figure 2-5 Overview of fatigue life extensions due to rest periods [2, 3, 5, 34, 35]

Francken proposed a power equation to simulate the relationship between the fatigue life extension and the ratio of load to rest periods [2, 35].

$$N_R / N_W = 1 + c_1 (T_R / T_W)^{c_2}$$

2-1

It can also be observed that the fatigue life extension reaches a maximum when the ratio of rest period over load period is larger than about 25. This healing factor however is very dependent on healing time, healing temperature, material composition, test methods, etc.

Castro performed strain controlled three point flexural fatigue tests to investigate the healing properties of a dense asphalt concrete [25]. Different strain amplitudes ranging from 200 to 400 microstrain at 20°C were applied with a fixed rest/load period ratio of 10.

Westera conducted a strain controlled four point bending fatigue test with a fixed rest/load period ratio of 10 [36-38]. The strain amplitude was ranging between 100 to 400 microstrain and all tests were done at a temperature of 15°C.

Both Castro's and Westera's results are shown in Figure 2-6, a decrease of the healing factor is observed with increasing strain amplitude.
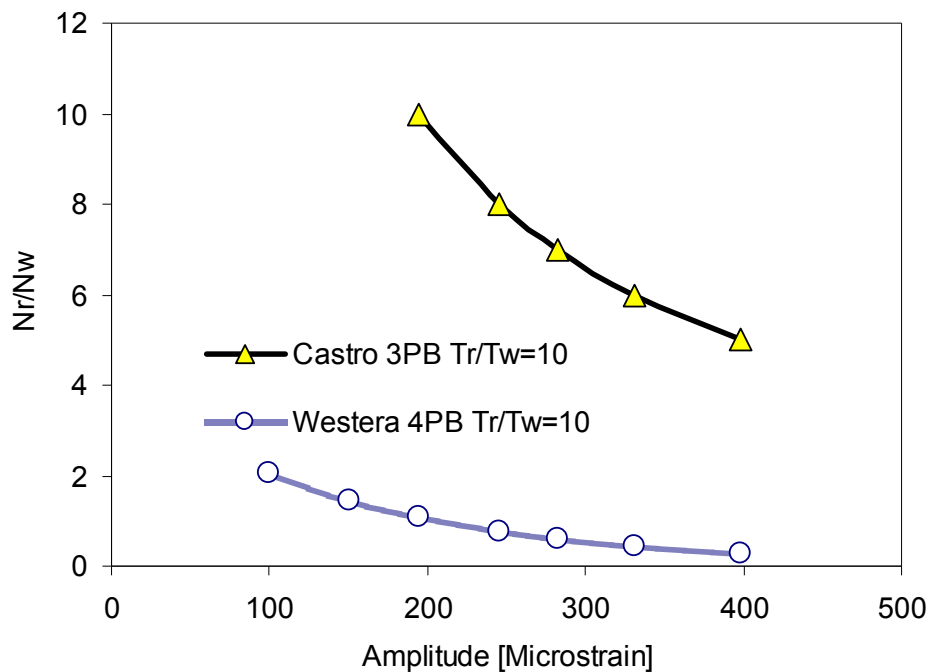

Figure 2-6 Influence of strain levels on fatigue life extension [25, 38]

Carpenter and his colleagues conducted four point bending FHI tests to investigate the healing capability of asphalt concrete based on energy principles [26, 39, 40]. A strain level of 500 microstrain, frequency of 10 Hz and temperature of 20°C were used in this test. The rest periods were selected as 0, 1, 3 and 9 seconds. The Plateau Value (PV) was based on the development of the Ratio of Dissipated Energy Change (RDEC) as shown in Figure 2-7. The development of the RDEC during the fatigue process has three distinct phases. Phase II shows an extended plateau level in the data plot. The PV is defined as the RDEC value at the 50% stiffness reduction failure point (NF_{50}), and this value appears to be related to the mixture composition and the stress and strain condition. A lower PV corresponds to a longer fatigue life. The PV recovery per second of rest period was defined as an indication of the healing capacity. The PV versus (RP+1) (Rest Period plus 1) curve given in Figure 2-8 is indicative for the healing effect based on energy principles. With the increase of the duration

of the rest period from 0 to 9 seconds, the PV is decreasing, which uniquely corresponds to an extended fatigue life.
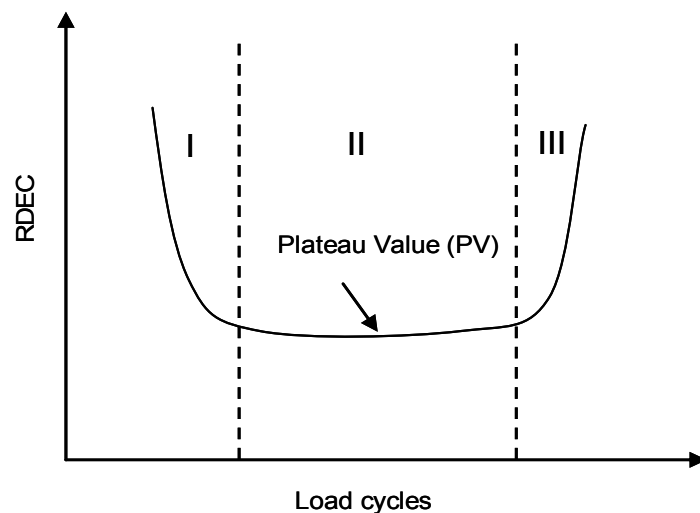

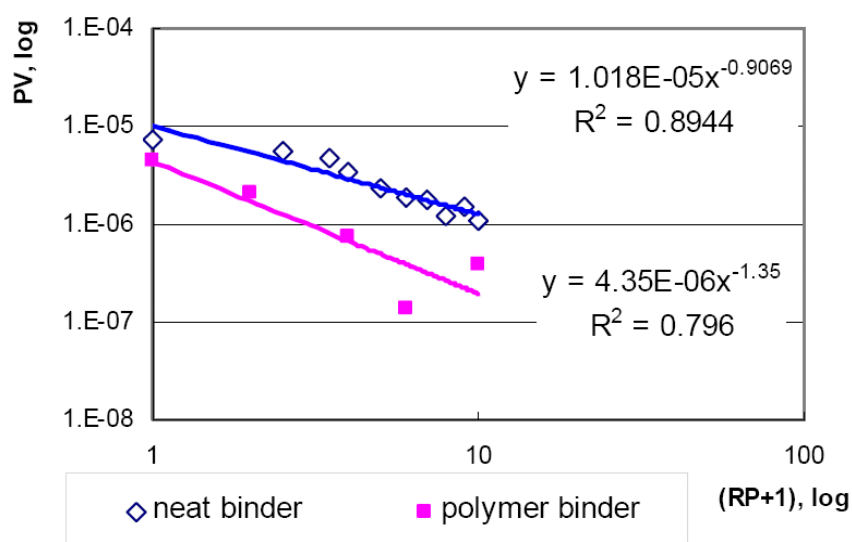Figure 2-7 Typical RDEC plot with three behaviour zones [39]

Figure 2-8 PV vs. (RP+1) Relations for Two IDOT Asphalt Mixtures [40]

2.2.2.2 FHS

Bazin carried out a FHS test procedure with a stress controlled two point bending fatigue test [4]. The specimens were trapezoidal sized and the fatigue tests were done at a frequency of 50Hz and a temperature of 10°C. The tests were stopped just before rupture using a safety device. Then the test specimens were left to rest at the same temperature for periods ranging from several hours to 100 days. During the rest periods, the test bars were placed either flat or in a vertical position. At the end of the rest period, the test bars were fatigued at the same condition as in the first test.

As shown in Figure 2-9, the samples rested vertically obtained an increase in fatigue life. The samples rested horizontally showed almost no improvement in

fatigue life. This result implies that a small compressive stress which is permanently acting on the asphalt mixture is not only promoting but is also needed to ensure a rapid and total healing.
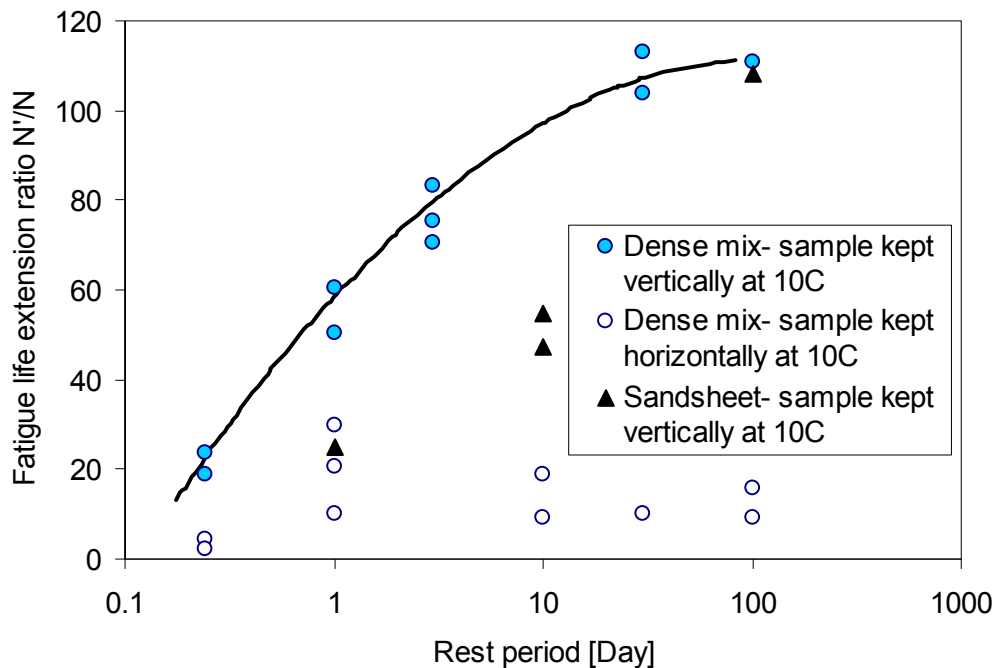

Figure 2-9 Fatigue life extension of asphalt mixtures after healing [4]

Daniel conducted a three point bending test with an impact resonance device [31]. Series of loading and healing cycles were applied in this test. First, 3000 load cycles at 1.7 Hz were applied to the specimens. Then the fatigued asphalt beams were exposed to two different healing temperatures, one at 20°C and the other at 60°C, for 4 hours. After healing, the beams were then conditioned at 20°C for at least 6 hours. The same healing process was conducted at 10000 cycles and 20000 cycles, and then the beams were fatigued till failure. The impact resonance device was used to monitor the change of the dynamic modulus of elasticity of the specimen. The results indicated that the dynamic modulus of elasticity decreased with increasing load repetitions but increased with increasing rest periods.

Pronk applied the FHS test procedure using a strain controlled four point bending test [41]. The strain amplitude was around 160 microstrains and the test temperature was 20°C. The load/rest period was 40000/400000 cycles at 5 Hz. After each load period and before the next load period started, the (beam) stiffness was also measured acoustically with an ultrasonic device. The results indicated the recovery of the stiffness both directly measured from the four point bending tests and back-calculated from the ultrasonic measurements. It was also shown that a nearly complete recovery in the stiffness modulus did not guarantee an elongation of the fatigue life.

Grant and Kim investigated the fatigue and healing properties of asphalt mixtures using the indirect tensile fatigue and resilient modulus tests [29, 30]. Indirect tensile fatigue tests were performed at 10°C, 15°C and 20°C. First, a discontinuous haversine load with a load period of 0.1 second and rest period of 0.9 seconds in one cycle were applied during 1000 cycles on the specimens. Then a number of resilient modulus tests were performed at 2, 4, 6, 10, 20, 40 and 60 minutes after the load was removed. A factor called dissipated creep strain energy (DCSE) was used to quantify the damage and healing capabilities (shown in Figure 2-10). The DCSE was defined as the fracture energy (FE) minus the elastic energy (EE) which is the result of the resilient modulus (M_R). As shown in Figure 2-11, the DCSE accumulates during loading and decreases during unloading, which indicates healing.
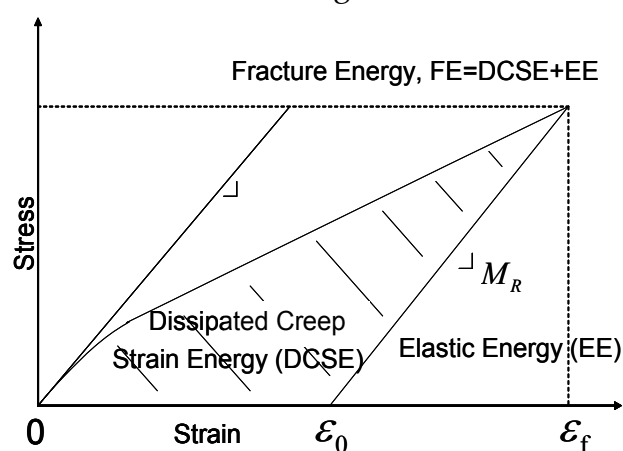

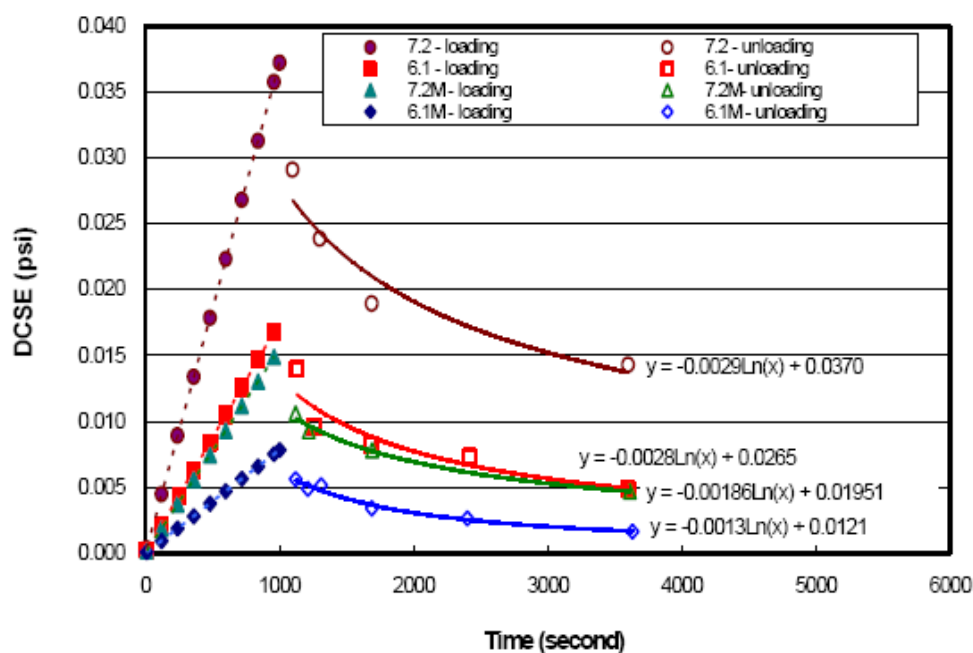Figure 2-10 Definition of dissipated creep strain energy [29]

Figure 2-11 Test results with 1000 load cycles of 75psi and healing to 1 hour at 15°C [30]

26

Abo-Qudais investigated the fatigue and healing properties of asphalt mixtures using stress controlled indirect tensile fatigue tests together with ultrasound pulse velocity (UPV) measurements [32]. The fatigue test was conducted with a cyclic load of 3.5 kN, a load period of 0.1s and a rest period of 0.4s for a cycle. The test temperature was equal to 25°C. The fatigue test was terminated as soon as the stiffness reduced to 3/4 of the initial stiffness. After that, the asphalt specimens were exposed to a rest period. Five different rest periods (1h, 3h, 3, 7 and 14 days) were used at five different temperatures (0, 15, 30, 45 and 60°C). After the rest period, the specimens were tested again by the indirect tensile fatigue test to determine the extended fatigue life due to the rest period (number of additional loading cycles to reduce the stiffness of the asphalt specimen to the same stiffness value where the first stage fatigue test was terminated). In addition, the UPV was measured with a frequency of 54 kHz before and after the application of the first stage fatigue test, after each rest period and after the second stage fatigue test. The results indicated that the UPV decreased with an increasing number of load repetitions and increased with increasing rest periods/temperatures. The change of the UPV values due to healing was also found to be sensitive to the aggregate gradation, rest period length and temperature.

2.2.2.3 FRAH

Bazin applied the FRAH test procedure in a tensile test [4]. Specimens with dimensions of 4*3*10cm were made. The specimens were fractured with a constant displacement speed of 120mm/min. Immediately after fracture, the two parts were put in contact again and were left to rest at temperatures of 10, 18, 25°C and different rest periods ranging from 1 day to 300 days. During the rest periods, the specimens were kept vertically thus they were permanently subjected to a compressive stress of 20 Pa at the rupture interfaces due to own weight. At the end of the rest period, the specimens were fractured again under conditions identical to the first test.

As shown in Figure 2-12, the recovery of the fracture strength (R'T/RT) as a result of healing can be observed. The type of mixture and the healing temperature are shown to play a role in healing. Identical tests were carried out on samples kept horizontally during the rest periods and the results were widely scattered. This implies that a permanent compressive stress, even a very small one, is promoting healing.
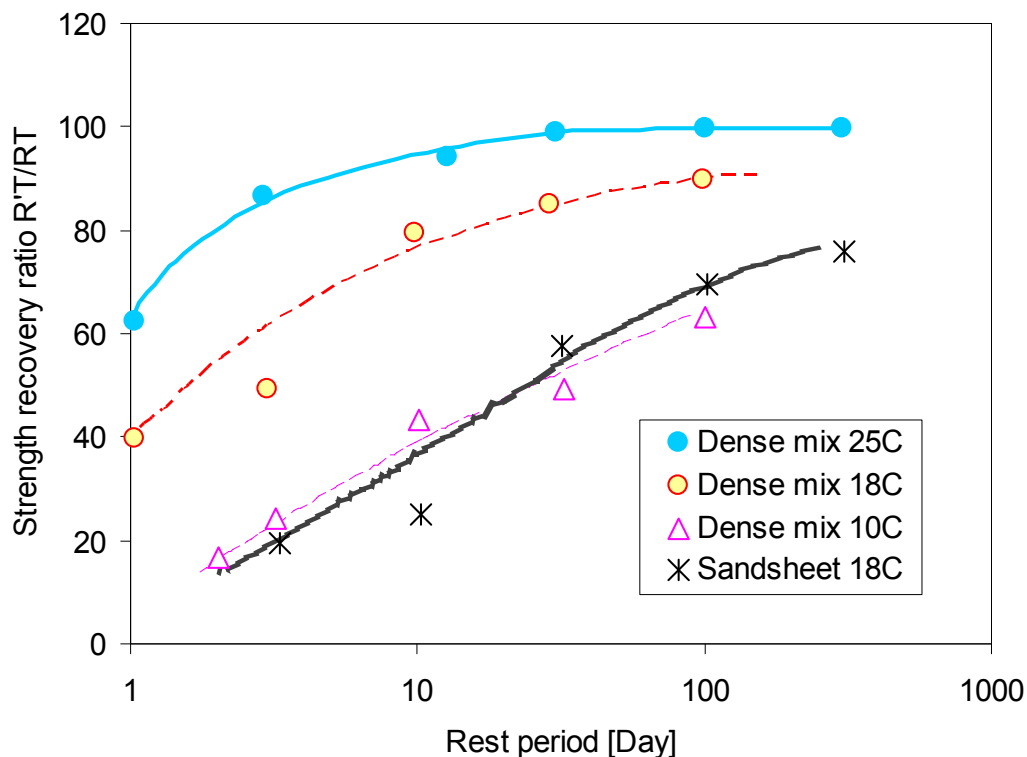
Figure 2-12 Fracture strength recovery of asphalt mixtures after healing [4]

Uchida developed a flexural test to determine the healing properties of an asphalt mixture [33]. In this test, cracks were induced in a wheel tracking test specimen by bending the slab with a steel bar placed at the bottom of the slab. The cracks were closed by pushing the slab into its original shape. Then the specimen was exposed to the sunlight for a number of days. After that, the slabs were subjected to a passing wheel load, which was intended to simulate the kneading action of the tires of vehicles to cause possible healing at the top. Afterwards, beams for the flexural test were sawn from the slab and the flexural strength of the specimens was measured at a temperature of 5°C with a loading rate of 50 mm/min. The test conditions were combinations of three outdoor exposure times (1, 3, 6 and 12 months) and three kneading temperatures (20, 40 and 60°C). The results shown in Figure 2-13 indicate increasing healing potential by increasing kneading temperatures. But the effect of exposure time on healing is not clear.
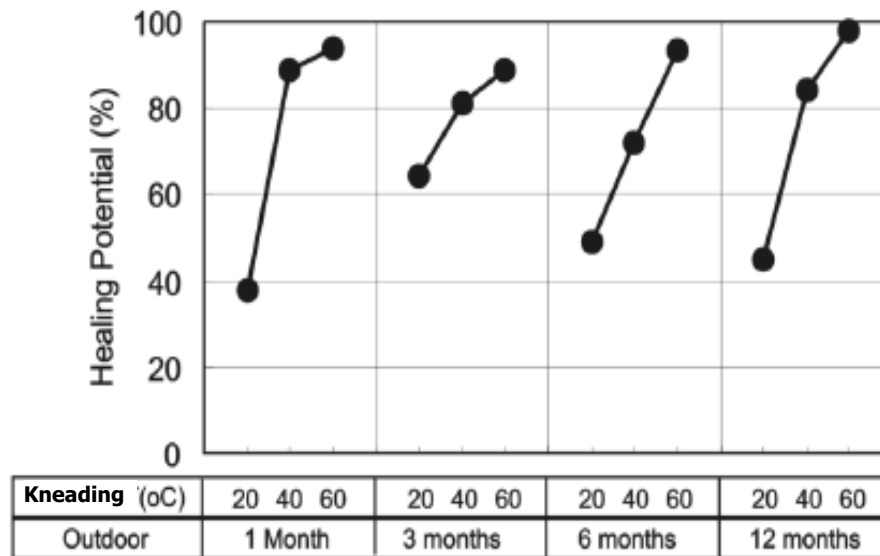
Figure 2-13 Effects of kneading temperature and outdoor exposure time on the healing potential [33]

2.2.3 Self healing of an asphalt pavement

Groenendijk conducted Falling Weight Deflectometer (FWD) measurements during accelerated pavement testing using the Delft University Linear Tracking Apparatus (Lintrack) [42]. In this test, 4 million repetitions of a 75 kN load with a wide base single tyre were applied in bi-directional traffic over a length of 12 m and a trafficked width of 1.6 m. The pavement temperature varied between 0 and 30°C, depending on the ambient conditions. During testing, the continuous load repetitions were stopped from every Friday afternoon to the next Monday morning as a rest period. The FWD was conducted each time before the rest period on Friday and after the rest period on Monday. The basic principle of a FWD measurement is shown in Figure 2-14. An FWD introduces a impulse load by dropping a weight from a given height onto rubber buffers, then the deflections of the pavement surfaces caused by the impulse load are measured by several deflection sensors. From the deflections the stiffness moduli of the constituent layers of the pavement are back-calculated and corrected to the same temperature.

The results are shown in Figure 2-15. The Monday data are observed to be higher than the Friday data. This indicates that the pavement recovered its stiffness during the rest period in the weekend, probably due to healing of the asphalt concrete.
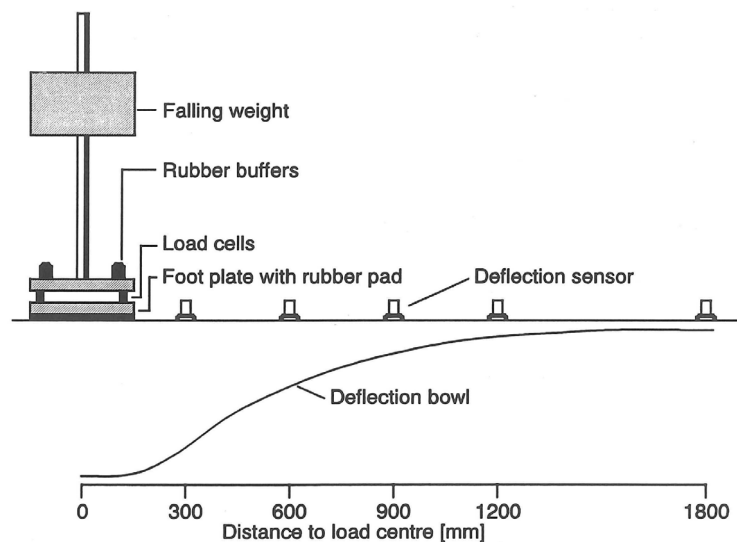
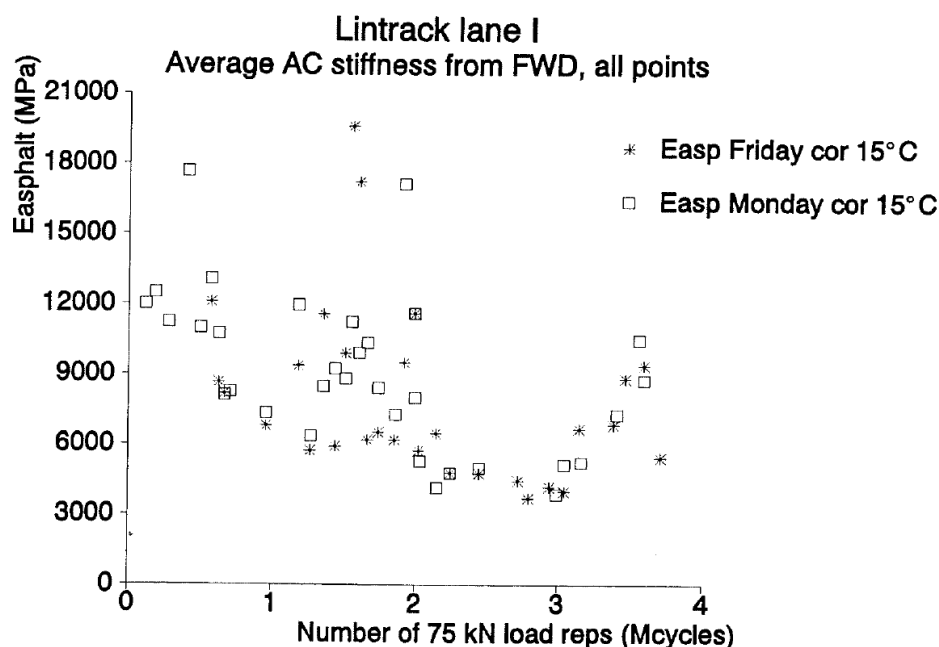Figure 2-14 Basic principle of a Falling Weight Deflectometer [42]

Figure 2-15 Change of back-calculated stiffness of asphalt concrete due to rest periods [42]

Williams and his colleagues conducted an in-situ non-destructive test to determine the self healing capabilities of asphalt pavements using the accelerated pavement testing facility at FHWA Turner-Fairbank Highway Research Centre [43]. This method is named the stress wave method, which involves the excitation of the pavement by means of a suitable impact source and measurement of the response of the structure to this loading. This method makes use of surface wave transients created by an impulse load applied on the pavement surface to determine the wave speed in each layer, which is related to layer material properties. Prior to any loading on the pavement, hexhead nuts were glued to the pavement surface at locations 152 mm, 305 mm, 457 mm and 610 mm away from the designated impact locations. The sensors were attached

on the nuts using magnetic bases. A lightweight hammer of 257 g was used to generate an impact, which contains the most energy at the high frequencies. The wave velocity of the impact surface waves was monitored as an indicator of the elastic modulus.

A combination of loading and stress wave tests were used on four types of asphalt pavements during their entire fatigue lives. The accelerated loading facility applied cyclic loadings at 10 seconds per cycle. The wheel used in this study was 318 mm wide with a load of 53.4 kN and tire pressure of 689.5 kPa. The position of the wheel load was controlled to produce normally distributed wandering transverse to the trafftc direction. The resulting width of the wheel path was 1.07 m. The pavement temperature was maintained at 20°C. The pavements were subjected to repetitions of a group of loading cycles followed by a 24 hours rest period. The number of loading cycles in each group of loading changed from 8000 cycles in the early days of testing to 25,000 cycles in the latter part of testing.
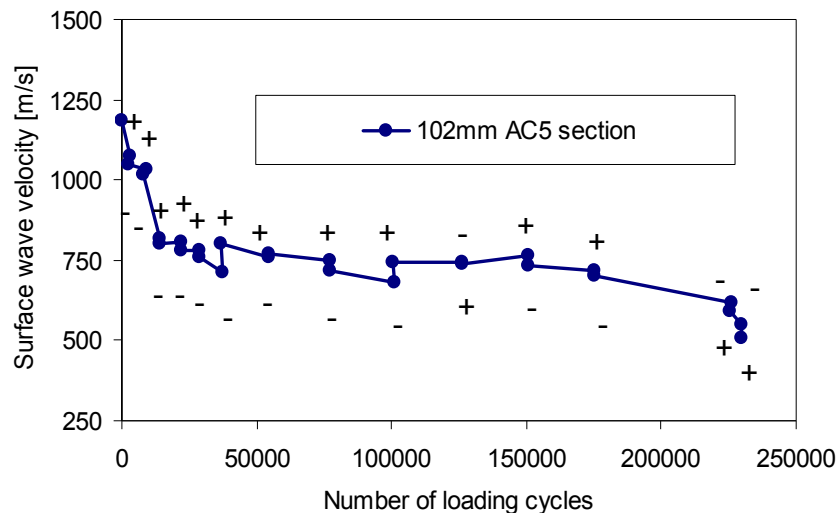

Figure 2-16 Changes in surface wave velocity during fatigue loading and rest periods (102 mm AC 5 section) [43]

Surface wave tests were performed at the following times: before any loads were applied, immediately after each group of loadings, and at the end of the 24 hours rest periods. Figure 2-16 illustrates the changes in wave velocity during fatigue loading and rest periods. Points with "-" symbol in these figures represent the data collected immediately after a group of loading cycles (i.e., at the beginning of each rest period) and those with "+" symbol indicate the data obtained at the end of a 24-hours rest period (i.e., immediately before another group of loading starts). It can be observed that the velocity increased after the 24 hour rest period. This increase is directly related to an increase in elastic modulus of the asphalt pavement, which is thought to be because of micro-damage healing [43, 44].

2.3   Influence Factors on Self Healing of Bituminous Materials

2.3.1   Internal factors

2.3.1.1   Physical property

Penetration values and softening point values are usually used to characterize the physical properties of bitumen. Many researchers indicate that a soft bitumen with a higher penetration grade and a lower softening point has a higher healing capability than a hard bitumen [3, 34, 45].

2.3.1.2   Chemical composition

Williams concluded that the chemical composition has a strong influence on the healing potential of bitumen [43]. Five bitumens ranging widely in aromatic, amphoteric, and wax contents were considered, and bitumens with low amphoteric and high aromatic contents were found to be better healers. In addition, the heteroatom content promotes healing because sulfur, oxygen and nitrogen promote the polarity of bitumen.

Kim related the methyl plus methylene hydrogen to carbon (MMHC) ratio to the healing potential of bitumen (in Figure 2-17) [46]. The MMHC ratio is the number of methyl and methylene hydrogen atoms to methyl and methylene carbon atoms in independent aliphatic molecules or aliphatic chains attached to cycloalkanes or aromatic centres. This ratio can be determined through Fourier Transform-Infrared spectroscopy (FT-IR) and Nuclear Magnetic Resonance (NMR) measurements. It was shown that a higher MMHC ratio corresponds to a lower healing capability.
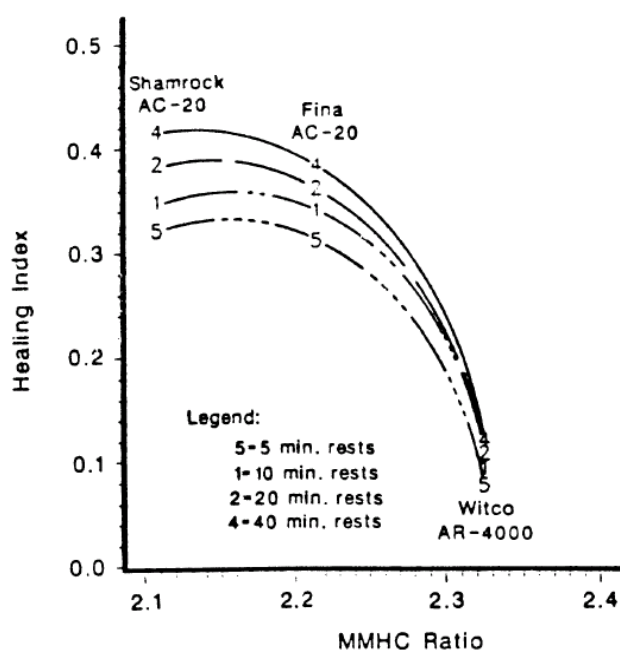

Figure 2-17 Healing index vs. MMHC ratios for bitumens, strain amplitude of 0.674% [46]

Santagata concluded from tests on the healing capabilities of six types of 70/100 penetration grade bituminous binders that bitumen with more low molecular weight (aromatics) components has a better healing capability [16].

2.3.1.3 Surface free energy

Lytton related the surface free energy to the healing potential of bituminous materials [47]. Based on the healing index models proposed by Lytton, the surface free energy can be divided into two parts being the Lifshitz-Van der Waals component and the Lewis acid-base component. As shown in Figure 2-18, the Lifshitz-Van der Waals component has a negative effect on the short term healing, whereas the Lewis acid-base component shows a positive effect on the long term healing. Details of the surface free energy healing index model can be found in Section 2.4.1.1.
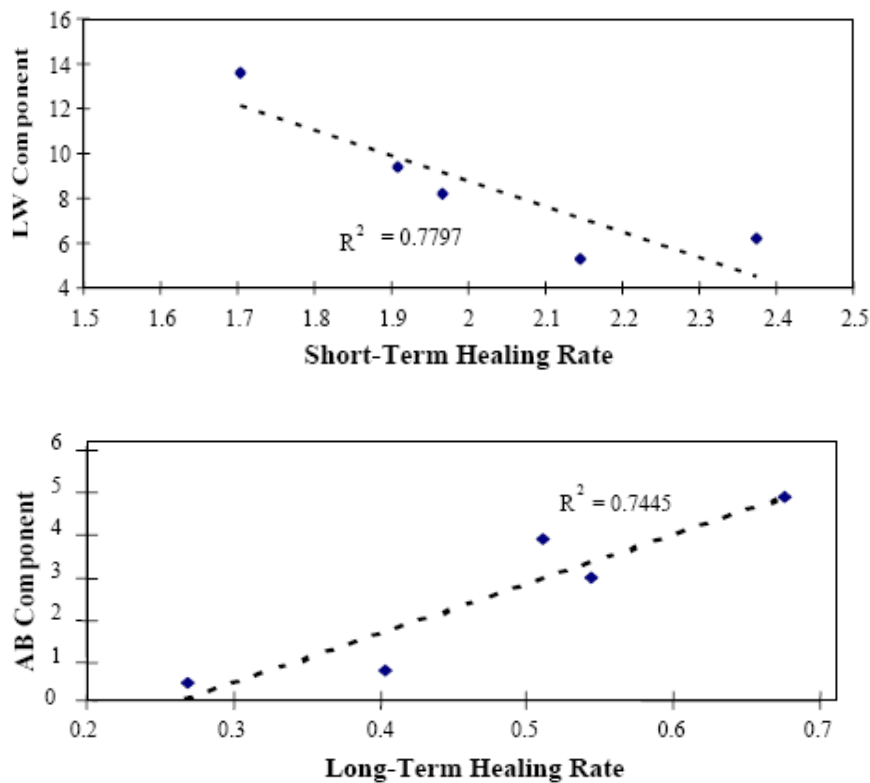
Figure 2-18 Relationship between the Lifshitz-Van der Waals component (LW) and short term healing rate (upper), the Lewis acid-base component (AB) and long term healing rate (lower) [47]

2.3.1.4 Volumetric properties

For an asphalt mixture, a high healing potential is found to be related to a high bitumen content [45]. In addition, healing also increases with an increase of the voids filled with bitumen (VFA), a decrease of the voids in mineral aggregate skeleton (VMA) and a decrease of the volume of air voids (VA) [35].

Grant and Kim concluded that the healing properties of asphalt mixtures are more affected by composition characteristics (which affect the aggregate interlock, the film thickness, etc.) than by polymer modifications [29, 30]. Lee found that stone matrix asphalt (SMA) shows the highest healing capacity compared to other types of asphalt mixtures [48].

2.3.1.5 Modifiers

The influence of modifiers on the self healing capability of bituminous materials as reported in the literature is very confusing.

Bahia tested two unmodified bitumens, two binders modified with plastomers, two modified with elastomers, and two modified by oxidation [14]. He concluded that the modified binder shows a better healing potential than the base bitumen. The results indicated that modification techniques can alter the healing performance.

Lee compared the healing of asphalt mixtures with different modifications like Styrene Butadiene Styrene (SBS), Styrene Butadiene Rubber (SBR) and Gilsonite (GIL) [48]. He concluded that an asphalt mix with the SBS modifier showed the best performance with regard to fatigue, rutting and healing.

Carpenter concluded that the healing/recovery rate of polymer modified binders (PG 70-22) is significantly better than that of the neat binders (PG 64-22) [26].

However, investigations by Kim on the effect of SBS modification on cracking and healing properties showed that the SBS modification has a relatively small effect on the healing rate of asphalt mixtures [30].

Moreover, Little concluded that the addition of SBS and low density polyethylene (LDPE) act as a filler system to interrupt the ability of pure bitumen healing [27]. An explanation of the negative impact of polymer additives on healing may rest in the effect of the polymer on the compositional make-up of the bitumen. Polymer networks in bitumen are swollen by the bitumen as the more compatible components of the bitumen are partially absorbed into the polymer causing it to swell. The rest of the bitumen is left with a higher asphaltene (highly interactive) component. The bitumen with a higher asphaltene concentration is less likely to flow and heal.

Little also explored the possible effect of hydrated lime (HL) on the healing capability of bitumen [27]. Adding HL to bitumen AAM (a highly aromatic bitumen with a very low asphaltene content) was shown to diminish the healing capability as the other additives did. However, the addition of HL to bitumen AAD (a highly associated bitumen and one with a high asphaltene fraction) enhanced the healing capability. This could be because the HL adsorbs or interacts with some of the more polar asphaltene fractions in the bitumen AAD which may enhance flow and healing properties.

2.3.2 External factors

2.3.2.1 Rest periods

The positive effect of rest periods on healing has been widely accepted by many researchers [3, 4, 7, 14, 34, 43]. Both short rest periods in the FHI test procedure and long rest periods in the FHS test procedure and the FRAH test procedure indicated improvement in healing when the duration of the rest periods increases. It is also observed that the rest periods needed for healing are ranging from less than a second in the intermittent loading related healing test for bitumen to up to 100 days in the fracture related healing test for asphalt mixtures.

2.3.2.2 Temperature

Temperature is another important factor which influences healing. It is shown that at high enough temperatures, healing occurs rapidly [3, 5, 10, 27]. Kim supported the idea that the temperature sensitivity of the healing rate is highly non-linear [30]. Uchida also observed that a high temperature had a positive effect on healing [33]. The positive effect of temperature on healing implies that healing may happen in asphalt pavements in a hot summer to close the micro-cracks produced in the winter.

2.3.2.3 Loading methodology

As was shown in section 2.2, the loading methodology is also influencing the observed healing capability, including different procedures like the FHI, FHS or FRAH and different control modes like stress control mode or strain control mode.

2.3.2.4 Load level

The influence of the load level on healing is widely observed in the FHI tests [3, 25, 36-38]. It is shown that a higher tensile stress/strain level has a negative effect on the relative fatigue life extension caused by healing.

2.3.2.5 Damage level

It is shown that the damage level or the loading history has an influence on the healing of asphalt mixtures [7, 49]. The healing is substantially greater when the damage is small (micro-cracks are small). The healing capacity is minimal when loaded beyond the failure point [49]. And healing is not easily to occur during the phase of macro-cracking [50].

2.3.2.6 Compressive stress

Bazin indicated that applying a little compressive stress on the fractured or fatigued specimen during a healing period is necessary for rapid healing [4].

This compressive stress is also adopted in other researches during a healing period to ensure full contact of broken surfaces [18, 20].

2.3.2.7 Ageing

Little found a negative effect of ageing on the healing capability of a laboratory aged sand mixture specimen [27]. He also indicated that the addition of hydrated lime can significantly improve the healing capability of an aged specimen.

Van de bergh found a distinctive difference between the healing capability of a laboratory aged and a field aged mortar sample [51]. The laboratory aged mortar shows a higher healing capability compared to the virgin mortar in a stress-controlled FHI test. However, the field aged mortar, which had the same rheological and chemical properties as the laboratory aged mortar, shows a lower healing capability compared to the virgin mortar.

At mixture level, Liu found that laboratory simulated aging slightly decreases the healing capability of a porous asphalt mixture [52].

2.3.2.8 Moisture

To the knowledge of the author, there is no relevant healing test which well addresses the influence of moisture on the healing capability of bituminous materials. However, some conclusions were drawn from the surface free energy related healing model. Zollinger showed that water has a negative effect on healing of the adhesive bond [53].

2.4 Modelling of Self Healing of Bituminous Materials

Two types of models can be summarised from the literature with regard to the self healing phenomenon of bituminous materials. One type is called the physical-chemical based healing model, which is a somewhat conceptual model to explain the healing phenomenon using physical-chemical theories. The other type is called the mechanical based healing model, which is basically a regression model to model the healing phenomenon in a macroscopic continuum damage state. Details of these two models can be found hereafter.

2.4.1 Physical-chemical based healing model

2.4.1.1 Multi-step healing model

Crack healing of thermoplastic polymers has been the subject of extensive research in the 1980s. It has been discovered that when two pieces of the same polymer are brought into contact at a temperature above its glass transition temperature (T_g), the interface gradually disappears and the mechanical strength at the polymer–polymer interface increases as the crack heals across the interface.

As shown in Figure 2-19, Wool and his colleagues suggested a five stages model to explain the crack healing process in terms of surface rearrangement, surface approach, wetting, diffusion and randomization [54-56].
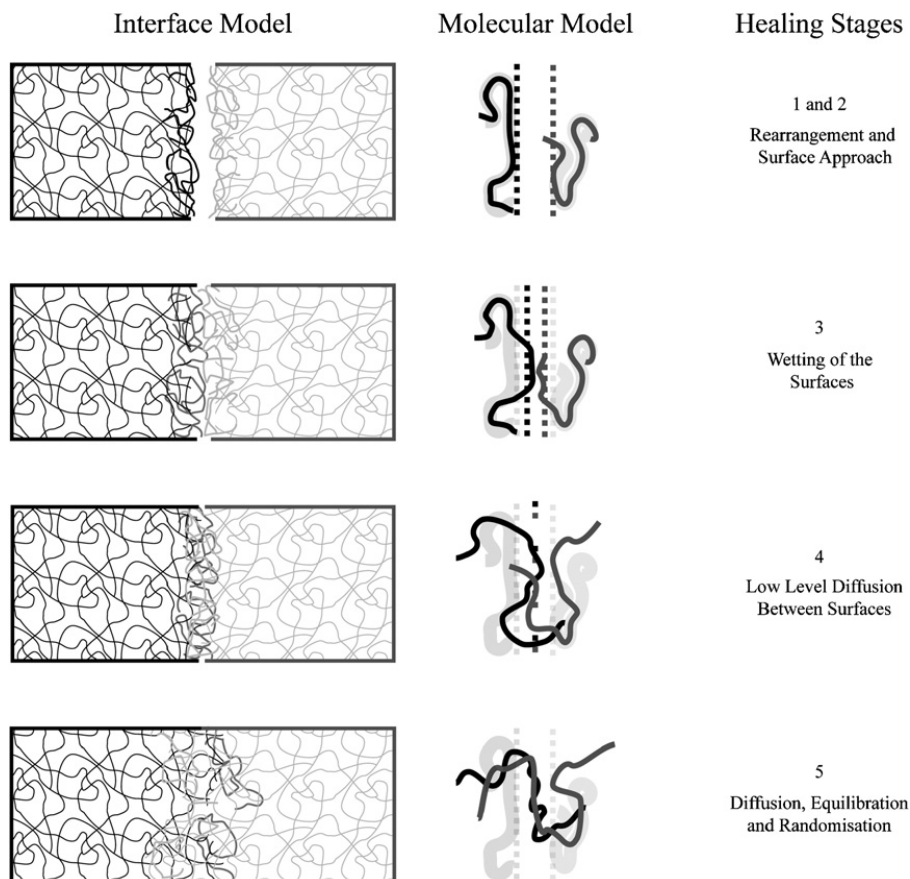

Figure 2-19 Schematic diagram showing the five steps of crack healing [56, 57]

They concluded that the stages of wetting and diffusion are responsible for the majority of the recovery of mechanical properties or healing, and control the intrinsic healing function $R_h(t)$. The observed macroscopic recovery R is a convolution product as shown in Equation 2-2.

$$R = \int_{-\infty}^{t} R_h(t-\tau)\frac{d\phi(\tau)}{d\tau}d\tau$$

2-2

where,

$R_h(t)$ = an intrinsic healing function of time t;

$\phi(t)$ = a wetting distribution function of time t;

τ = a time variable.

Intrinsic healing functions for strength, elongation at break, impact energy, and fracture parameters were obtained as a function of time, molecular weight, temperature, pressure, and processing conditions, which showed excellent agreement with the theory.
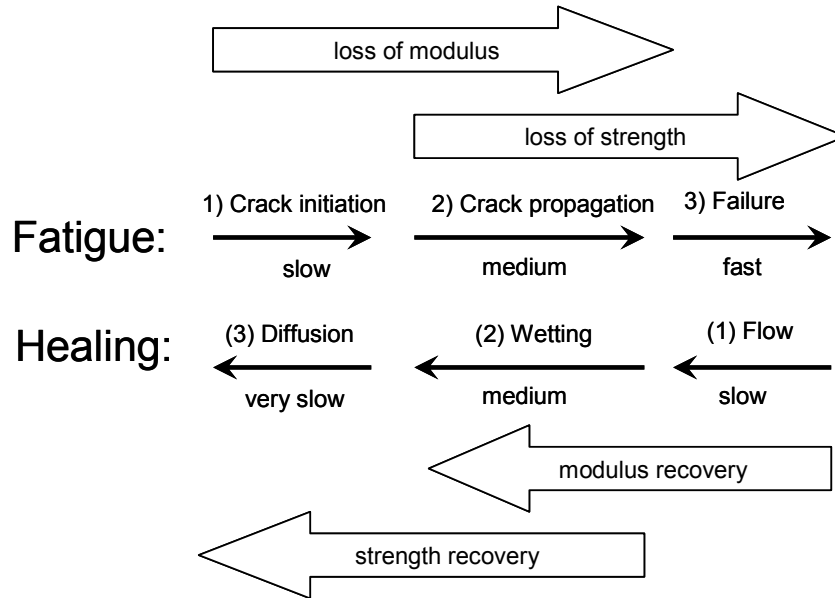

Figure 2-20 Multi-step fatigue and healing model [12]

Because of the similarity of the healing process of bituminous materials with the healing process as described above, this five stages model has been adopted by Phillips to describe the fatigue and healing capability of bituminous materials [12]. Figure 2-20 shows that not only the fatigue can be described using a three-step model (namely crack initiation, crack propagation and failure), but also the self healing process of bituminous material is believed to be a three-step process. This three-step healing process consists of: Step (1), the closure of macrocracks due to consolidating stresses and flow; Step (2), the closure of microcracks due to wetting (adhesion of two crack surfaces driven together by surface energy); and Step (3), the complete recovery of mechanical properties due to diffusion. Step (1) is believed to be the fastest, resulting only in the recovery of stiffness,

while steps (2) and (3) are thought to occur much slower but to improve both stiffness and strength of the material such that it exhibits mechanical properties similar to the virgin material. It should be noted that the order of losing strength and modulus during a fatigue process as observed in the original figure produced by Phillips was incorrect.

Lytton and his colleagues investigated the wetting process extensively using the surface free energy concept [47, 53, 58]. The surface free energy of a solid or a liquid is the energy needed to make a new element surface area under vacuum conditions. This surface energy, Γ, is a combination of a non-polar and an acid-base component. The non-polar component, Γ^{LW}, represents the physical bonds, the Lifshitz-van der Waals forces. The acid-base component, Γ^{AB}, is the representation of the chemical bonds, the electron exchange action. Written as Equation 2-3:

$$\Gamma = \Gamma^{LW} + \Gamma^{AB} \qquad \text{2-3}$$

The surface free energy of bitumen can be determined using the Sessile Drop Device and the Wilhelmy Plate Device [59, 60]. The surface free energy of aggregate can be determined with the universal sorption device [53].

Lytton developed a method to calculate the healing index [47]. This approach allows the calculation of the healing capability using surface energy data and data from the relaxation modulus master curve of the asphalt mixture. The approach can be described with the equations 2-4 to 2-7:

$$\dot{h} = \dot{h}_2 + \left(\frac{\dot{h}_1 - \dot{h}_2}{1 + \left[\left(\frac{\dot{h}_1 - \dot{h}_2}{h_\beta} \right) \left(\frac{\Delta t \cdot C_{sr}}{a_{TSF}} \right) \right]} \right) \qquad \text{2-4}$$

$$\dot{h}_1 = \frac{C_1}{\left[\Delta G_h^{LW} \cdot E_c \right]^{\frac{1}{m_c}}} \qquad \text{2-5}$$

$$\dot{h}_2 = \left[C_2 \cdot \left(\frac{\Delta G_h^{AB}}{E_c} \right) \right]^{\frac{1}{m_c}} + C_3 \qquad \text{2-6}$$

$$h_\beta = C_4 \cdot \left(\frac{\Delta G_h^{AB}}{\Delta G_h^{LW}} \right) \cdot \left(\frac{C_5}{m_c} \right) \qquad \text{2-7}$$

where,

$\dot{h}$	= actual healing rate;
$\dot{h}_{1-2}$	= healing rates generated by the nonpolar (Γ_{LW}) and polar (Γ_{AB}) surface energies;
h_β	= a factor that varies between 0 and 1 and represents the maximum degree of healing that can be achieved by the asphalt binder;
Δt	= loading time (s);
a_{TSF}	= temperature shift factor for field conditions (~1.0);
C_{sr}	= squared rest period factor (~1.0);
C_{1-5}	= healing constants (~105, 0.0039, 0.25, 0.0181, 1.97);
E_c	= elastic relaxation modulus from a relaxation modulus master curve (MPa) in a compressive mode;
m_c	= exponent from the compression relaxation modulus master curve;
ΔG_{hi}	= surface energy due to healing/wetting (ergs/cm^2).

Bhasin and his colleagues further developed the work by Wool and Lytton by proposing a simplified intrinsic healing function which is given by Equation 2-8 [20-22].

$$R_h(t) = R_0 + p(1 - e^{-qt^r})$$

2-8

The healing function represents the sum effect of: i) instantaneous strength gain due to interfacial cohesion (wetting) at the crack interface, represented by the parameter R_0, and ii) time dependent strength gain due to inter-diffusion of molecules between the crack surfaces by the parameter $p(1 - e^{-qt^r})$, which can be obtained by fitting the experimental data.

The intrinsic healing function was determined with an innovative two-piece healing test set-up using the DSR. Three different types of binders were investigated. It was shown that the R_0 obtained from the experiment agrees with the work of cohesion obtained from the surface energy measurements.

2.4.1.2 Thixotropy model

In Figure 2-21, it is shown that bitumen is traditionally regarded as a colloidal system consisting of high molecular weight asphaltene micelles dispersed or dissolved in a lower molecular weight oily medium (maltenes) [61]. The micelles are considered to be asphaltene clusters together with an absorbed layer of high molecular weight aromatic resins which act as a stabilizing

solvating medium. Away from the centre of the micelle there is a gradual transition to less polar aromatic resin layers which extend outwards to the less aromatic oily dispersion medium.

According to the colloidal nature of the bitumen, the bitumen can be divided into three categories: Sol bitumen, Gel bitumen and Sol-gel bitumen. The Sol bitumen has a sufficient amount of resins and aromatics, with enough solvating power to fully peptize the asphaltenes. Therefore, the resulting micelles have a good mobility in the bitumen. The Gel bitumen has not enough aromatic/resin fractions to peptize the micelles. The asphaltenes can associate further in a Gel type bitumen. This can lead to an irregular open packed structure of linked micelles. The rest of the space is filled with an intermicellar fluid of mixed constitution. In practice, most bitumens show an intermediate colloidal character, called Sol-Gel bitumen.
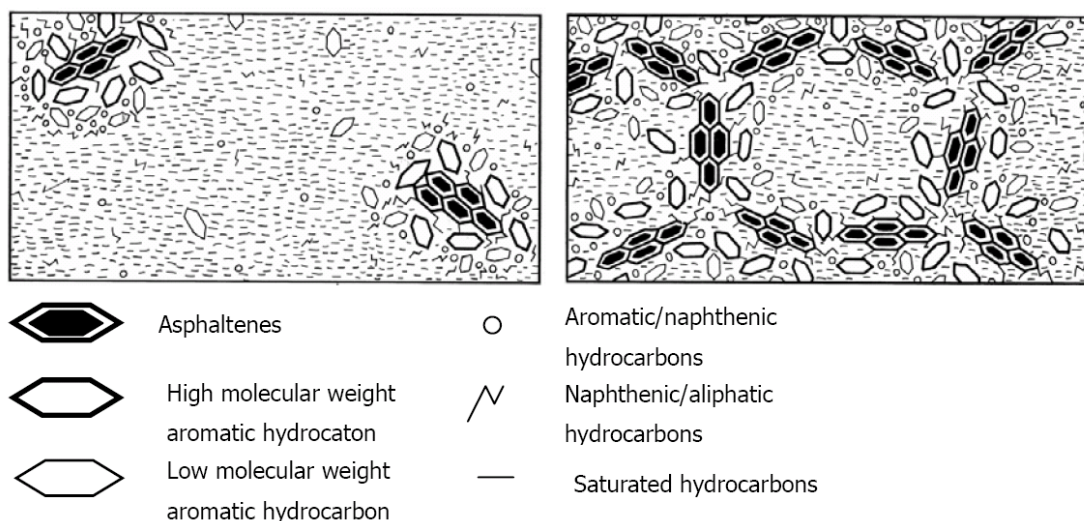

Figure 2-21 Schematic representation of Sol (left) and Gel (right) type bitumen [61]

It has been noticed since 1930s that bitumen exhibits a so-called thixotropic behaviour [62-64], which is also widely observed in many colloidal systems. Thixotropy is defined as the tendency of a material's viscosity to decrease with time when subjected to flow/stress, and to recover with time when the flow/stress is stopped [65]. It is shown that thixotropy is an inherent material property of bitumen and has been shown to have a significant effect on the rheological properties of bitumen [63]. In addition, thixotropy is highly related to the colloidal nature of bitumen, which depends on the source of the bitumen, the degree of processing, and the temperatures.

Thixotropy is also thought to be related to the changes in a material's microstructure [65]. The microstructure of the material breaks down and its viscosity decreases by applying stress/flow. After a period of rest, the material regains the broken-down structure and its viscosity increases to the initial value due to the movement of the molecules.

Verstraeten related the thixotropic effect to the stiffness decrease during fatigue tests and its recovery during rest periods [25, 66]. Based on the results of the fatigue tests on bituminous mixtures carried out at the Belgium Road Research Centre, he proposed that at temperatures higher than 15 ℃, the fatigue of bituminous mixtures is mainly caused by the thixotropic effect in the bitumen. During the load repetitions, bitumen changes progressively from a gel to a sol type structure. And bitumen returns from a sol to a gel structure during rest periods. If the rest time is sufficiently long, the recovery would be almost total. However, at low temperatures (less than 5℃), the fatigue due to the load repetitions is due to structural damage, and recovery of the structural damage at low temperatures would be only partial.

This proposition has been proven by many researchers. Soltani and Anderson concluded that the loss in modulus during a fatigue test and the gain in modulus during rest periods are the result of thixotropy [67]. Di Benedetto concluded that thixotropy is one of the artefacts which influences the real fatigue performance of asphalt concrete and it can be modelled using an equivalent temperature increase [68]. Shan and her colleagues introduced the Cox-Merz relationship of the thixotropy model to characterize the fatigue and healing behaviour using the break-down and build-up coefficients of the microstructure. It is observed that thixotropy does play a role in the fatigue and healing characteristics of bituminous binders [15].

When comparing the thixotropic model with the multi-step healing model, both models explain the recovery process during rest periods. However, the multi-step healing model explains the healing process in case of damage (micro-cracks, macro-cracks), while the thixotropy model explains the recovery process in case of molecular motion and the rebuilt of the microstructure, which is not necessarily related to a crack.

2.4.2   Mechanical based healing model

2.4.2.1   VECD model

For a visoelastic material, the significant rheological change of bituminous materials during a test, such as creep at a constant loading and relaxation due to an imposed straining should be considered [69]. It implies that during a simple displacement controlled direct tension test, the obtained stress-strain relationship combines two major effects: the damage development and relaxation due to viscoelasticity. As a result, for a true material model it is necessary to eliminate the influence of rheological changes because of time/temperature dependency and loading methodology dependency.

Schapery proposed the extended elastic-viscoelastic correspondence principle (CP) by using so-called pseudo strain variables which can be applicable to both linear and nonlinear viscoelastic materials [70]. According to Schapery, the

constitutive equations for certain viscoelastic media are identical to those for elastic cases, but stresses and strains are not necessarily physical quantities in the viscoelastic body but pseudo variables in the form of convolution integrals. As a result, a uniaxial stress-strain relationship can be formed as linear elastic stress- pseudo strain relationship shown in equation 2-9 to 2-11:

- o Stress:

$$\sigma = \int_0^t E(t-\tau)\frac{d\varepsilon}{d\tau}d\tau \qquad \text{2-9}$$

- o Pseudo strain:

$$\varepsilon^R = \frac{1}{E_R}\int_0^t E(t-\tau)\frac{\partial\varepsilon(\tau)}{\partial\tau}d\tau \qquad \text{2-10}$$

- o Stress- pseudo strain relationship:

$$\sigma = E_R\varepsilon^R \qquad \text{2-11}$$

where,

ε	= uniaxial strain;
ε^R	= uniaxial pseudo strain;
E_R	= arbitrary constant (usually equal to 1);
$E(t)$	= uniaxial relaxation modulus as a function of time;
t	= elapsed time;
τ	= integration variable ranging from 0 to t.

Following the correspondence principle, Schapery applied thermodynamics irreversible processes to develop a so-called work potential theory (WPT) [71]. The WPT theory is applicable to describe the mechanical behaviour of elastic media with growing damage and other structural changes. Then damage is defined as all structural changes in the material (except linear viscoelasticity), that result in a reduction in stiffness or strength during loading.

The work potential theory uses the following three fundamental elements:

- o Pseudo strain energy density function:

$$W^R = W^R(\varepsilon^R, S_m) \qquad \text{2-12}$$

- o Stress-strain relationship:

$$\sigma = \frac{\partial W^R}{\partial \varepsilon^R} \qquad \text{2-13}$$

- o Damage evolution law:

$$\dot{S}_1 = \left(-\frac{\partial W^R}{\partial S_m}\right)^{\alpha_m} \qquad \text{2-14}$$

where,

W^R = pseudostrain energy density function;

S_m = internal state variables (or damage parameters), which represents the structural changes in the material (e.g., damage, healing, etc.), and can be estimated using physical strains, material's viscoelastic properties and loading time;

$\dot{S}_1$ = damage evolution rate;

α_m = material constant; $\alpha_m = (1 + 1/m)$ and $\alpha_m = 1/m$ are suggested for the controlled strain mode and the controlled stress mode, respectively, and m is the slope of the relaxation master curve.

In case of a uniaxial loading at a constant temperature, the stress in bituminous materials follows the following constitutive relationship:

$$\sigma = IC_1(S_1)\varepsilon^R \qquad \text{2-15}$$

Where, $C_1(S_1)$ indicates that C_1 is a function of internal state variables (or damage parameters) S_1. The function $C_1(S_1)$ represents the changing stiffness of the material due to changes in microstructure of the material, e.g., growing damage or healing.

The damage parameter S_1 can be obtained through the following equations in the monotonic load (Equation 2-16) and/or in the cyclic load (Equation 2-17).

$$S_1 \cong \sum_{i=1}^{N} \left[\frac{1}{2}(\varepsilon^R)^2(C_{i-1} - C_i) \right]^{\frac{\alpha}{1+\alpha}} (t_i - t_{i-1})^{\frac{1}{1+\alpha}} \qquad \text{2-16}$$

$$S_1 \cong \sum_{i=1}^{N} \left[\frac{1}{2}(\varepsilon^R)^2(C_{i-1} - C_i) \right]^{\frac{\alpha}{1+\alpha}} (\frac{t_i - t_{i-1}}{4})^{\frac{1}{1+\alpha}} \qquad \text{2-17}$$

The use of the C-S relationship on damage and healing characterization of bituminous materials during monotonic and fatigue tests was reported by many researchers [8, 72-75]. During fatigue testing, the slope of the stress-pseudo strain loop is observed to decrease. This represents the reduction in stiffness of the material as damage is accumulating, which is the development of the function $C_1(S_1)$ as mentioned above. A parameter called pseudo stiffness S^R, was defined as the slope of the stress-pseudo strain loop.

$$S^R = \frac{\sigma_{max}}{\varepsilon^R_{max}} \qquad \text{2-18}$$

where,

ε_{max}^{R} = peak pseudo strain in each stress-pseudo strain cycle;

σ_{max} = corresponding stress.

As shown in Figure 2-22, the description of changes in S^R during and after rest periods requires two internal state variables: one for the increase of S^R during rest periods due to microdamage healing (S_2) and another for the reduction in S^R after rest periods due to damage evolution (S_3). The microdamage healing function H is then calculated as:

When $S^R > S_{B,j}^{R}$ (region I):

$$H = \left[S_{B,i}^{R} + C_2(S_2) \right] C_3(S_3) - C_1(S_1) - \sum_{j=1}^{i-1} (S_{B,j}^{R} - S_{C,j}^{R})$$

2-19

When $S^R < S_{B,j}^{R}$ (region II):

$$H = \sum_{j=1}^{i} (S_{B,j}^{R} - S_{C,j}^{R})$$

2-20

where,

$S_{B,i}^{R}$ = S^R before the ith rest period;

$S_{C,i}^{R}$ = S^R without rest period at the point when S^R is equal to S_B^R for the case with a rest period;

$C_2(S_2)$ = a function representing the increase of S^R during rest periods due to micordamage healing;

$C_3(S_3)$ = a function representing the reduction in S^R after rest periods due to damage evolution.

To simplify the representation of damage and healing, a modified model is proposed as shown schematically in Figure 2-23 [76]. The points evenly labeled (0, 2, and 4) represent the pseudo stiffness values at the beginning of load pulses 1, 2 and 3. The points labelled with the odd numbers (1, 3, and 5) represent the pseudo stiffness values at the end of load pulses 1, 2 and 3. It is then expected that a single damage function, $C_1(S_1)$, can be used to compute the whole damage and healing process.
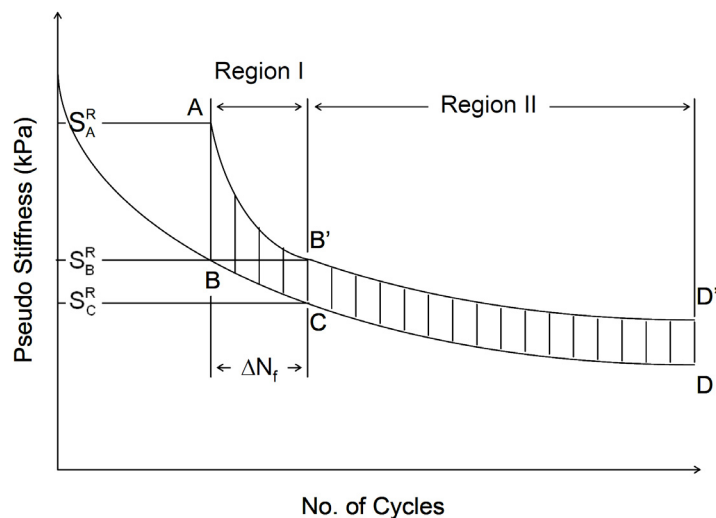
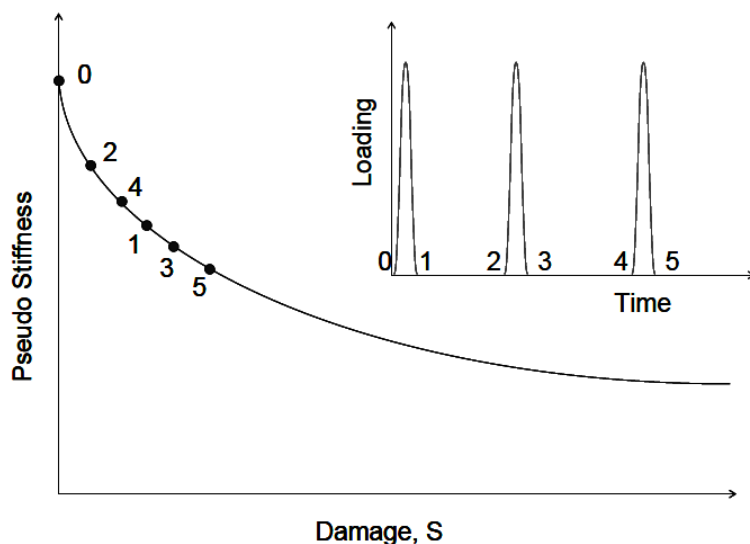Figure 2-22 Change in pseudo stiffness before and after rest period [73]

Figure 2-23 Conceptual schematic diagram for damage and healing [76]

2.4.2.2 PANDA model

Abu Al-Rub and his colleagues proposed a three-dimensional computational code called the Pavement Analysis Using Nonlinear Damage Approach (abbreviation, PANDA) [77]. The code is programmed using a user material subroutine under a commercial finite element code ABAQUS. This PANDA model incorporates almost all the pavement nonlinear behaviours including visco-elastic, visco-plastic, visco-damage and healing. Within the damage-healing model, the effective stress concept was employed as shown in Figure 2-24 and given in Equation 2-21.
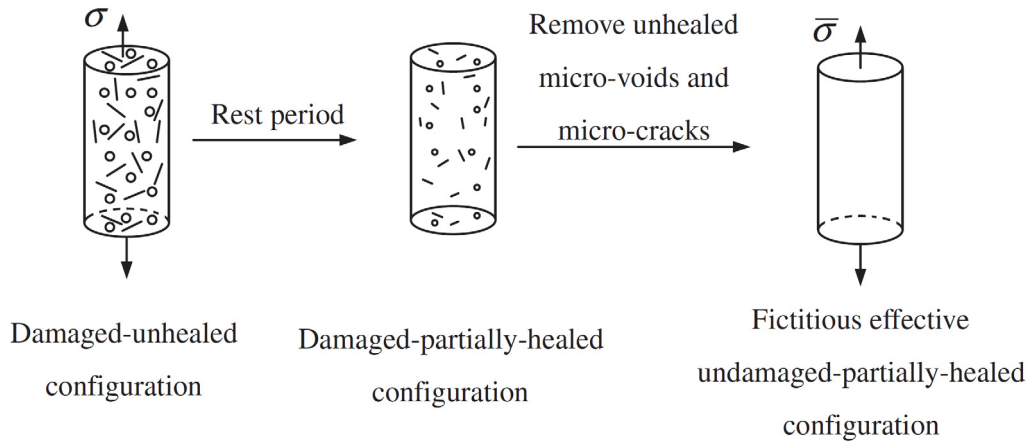
Figure 2-24 Application of effective stress concept to damaged-healed materials [77]

$$\bar{\sigma}_{ij} = \frac{\sigma_{ij}}{1-\bar{\phi}} = \frac{\sigma_{ij}}{1-\phi(1-h)}$$
2-21

where,

$\bar{\sigma}_{ij}$ = stress tensor in the undamaged-healed (effective) configuration;

σ_{ij} = stress tensor in the damaged-unhealed configuration;

$\bar{\phi}$ = effective damage density;

ϕ = damage variable or damage density;

h = healing variable ranging from 0 (no healing) to 1 (completely healed).

Abu Al-Rub and his colleagues indicated that the healing variable h should be a function of the duration of the rest period (or healing time), temperature, level of damage, and the history of healing. Hence, one can incorporate all these effects into the following postulated phenomenological-based healing evolution Equation 2-22:

$$\dot{h} = (1-\bar{\phi})^{b_1}(1-h)^{b_2}\,\Gamma_0^h\,\exp\left[-\delta_3(1-\frac{T}{T_0})\right]$$
2-22

where,

$\dot{h} = \dfrac{dh}{dt}$ = rate of healing;

Γ_0^h = healing viscosity parameter that determines how fast the material heals at a reference temperature of T_0;

δ_3 = healing temperature coupling parameter;

47

T = healing temperature;

b_1, b_2 = material constants.

In practice, the material parameters which are responsible for the healing variable can be calibrated and obtained by modelling a repeated creep-recovery test as it is shown in Figure 2-25. Detail information of this mechanical based damage modelling approach can be found in [78].
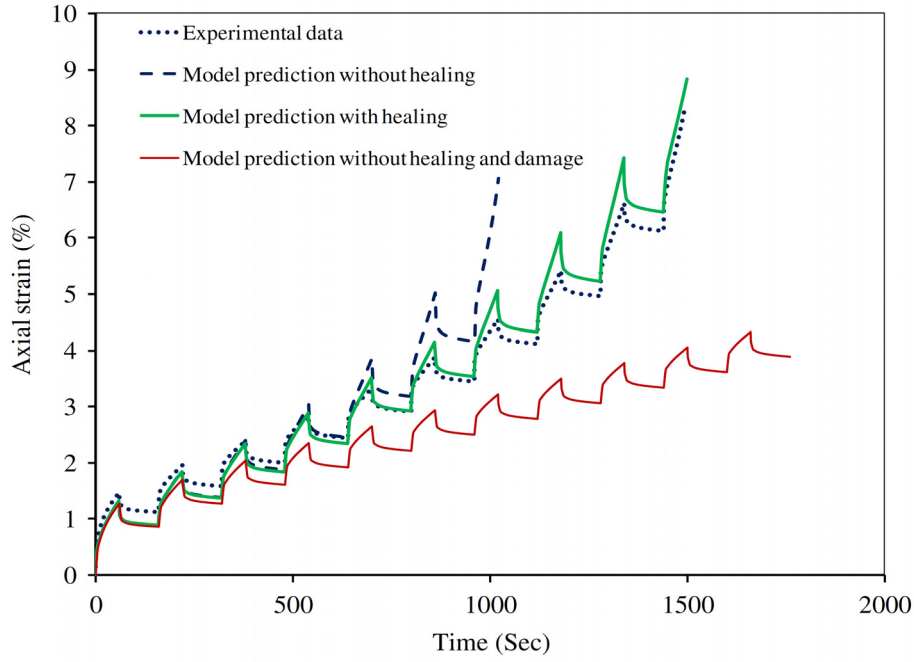

Figure 2-25 Modelling of repeated creep-recovery test in compression with 60 s loading time and 100 s resting period [77]

2.4.2.3 PH model

Pronk proposed a so-called partial healing (PH) model to describe the evolution of the complex stiffness modulus (loss and storage modulus) due to reversible and irreversible damage in a fatigue (bending) test [41, 79]. The model assumed that the damage is related to the dissipated energy per cycle. He also assumed that an asphalt mixture can heal itself not only during rest periods, but also during loading periods.

The PH model is mainly based on two equations:

Loss modulus:

$$S_{mix} \sin(\varphi) = F\{t\} = F_0 - \int_0^t \left[F\{\tau\}\left(\alpha_1 e^{-\beta(t-\tau)} + \gamma_1 \right) \right] d\tau$$

2-23

Storage modulus:

$$S_{mix} \cos(\varphi) = G\{t\} = G_0 - \int_0^t \left[F\{\tau\}\left(\alpha_2 e^{-\beta(t-\tau)} + \gamma_2 \right) \right] d\tau$$

2-24

The parameters α_1, α_2, γ_1, γ_2 and β are the products of material constants times the occurring strain squared (ε^2). The values α and γ also depend on the applied frequency.

Because no energy will be dissipated during a rest period, the function $F\{\tau\}$ in the integral equals zero during the rest period. When after a time t_1 no loading is applied (rest period) the following equation is valid for the loss modulus.

$$F\{t\} = F_0 - e^{-\beta t} \int_0^{t_1} \alpha_1 F\{\tau\} e^{+\beta \tau} \, d\tau - \int_0^{t_1} \gamma_1 F\{\tau\} \, d\tau \qquad \text{2-25}$$

The second term on the right hand represents the reversible damage and the third term the non recoverable (irreversible) damage P_{L1}, which is equal to the accumulation of the permanent damage in the load period. The reversible damage is subjected to the exponential time function at the end of the load period, which will vanish in time. The evolution of the loss modulus during the rest period is described by Equation 2-26. Similarly, we can obtain the development of the storage modulus during the healing time given in Equation 2-27.

$$F\{t\} = F_0 - R_{L1} e^{-\beta(t-t_1)} - P_{L1} \qquad \text{for } t \geq t_1 \qquad \text{2-26}$$

$$G\{t\} = G_0 - R_{S1} e^{-\beta(t-t_1)} - P_{S1} \qquad \text{for } t \geq t_1 \qquad \text{2-27}$$

After the first rest period a second load period starts at $t = t_2$ and will end at $t = t_2 + t_1 = t_2 + \Delta t_L$. The evolutions of the loss modulus and the storage modulus are given by equations 2-28 and 2-29.

$$F\{t\} = F\{t_2\} - \int_{t_2}^{t} \left[F\{\tau\} \left(\alpha_1 e^{-\beta(t-\tau)} + \gamma_1 \right) \right] d\tau \quad \text{for } t_2 < t < t_2 + \Delta t_L \qquad \text{2-28}$$

$$G\{t\} = G\{t_2\} - \int_{t_2}^{t} \left[F\{\tau\} \left(\alpha_2 e^{-\beta(t-\tau)} + \gamma_2 \right) \right] d\tau \quad \text{for } t_2 < t < t_2 + \Delta t_L \qquad \text{2-29}$$

By moving the origin of the time scale to $t = t_2$ the same equations are obtained as for the first load period ($t^* = t - t_2$) as indicated by equations 2-30 and 2-31.

$$F\{t^*\} = F_0^* - \int_0^{t^*} \left[F\{\tau\} \left(\alpha_1 e^{-\beta(t^*-\tau)} + \gamma_1 \right) \right] d\tau \quad \text{for } 0 < t^* < \Delta t_L (= t_1) \qquad \text{2-30}$$

$$G\{t^*\} = G_0^* - \int_0^{t^*} \left[F\{\tau\} . \left(\alpha_2 e^{-\beta(t^*-\tau)} + \gamma_2 \right) \right] . d\tau \quad \text{for } 0 < t^* < \Delta t_L \qquad \text{2-31}$$

The only differences between the first loading and the loading after healing are the start values for the loss modulus $F\{t\}$ and the storage modulus $G\{t\}$ at the beginning of the (second) load period. Therefore the same solutions with shifted time scales can be used for all the load and rest periods.

Figure 2-26 and Figure 2-27 show the examples of the simulation of a continuous fatigue test and a FHS test, respectively. It should be noted that for the FHS simulation, the material parameters were chosen by fitting the first two cycles of loading instead of only one cycle of loading. Pronk claimed that this could be related to the real healing, which cannot be fully explained by the current PH model which is based on the development of the stiffness modulus. He believes that there is a distinction between the stiffness recovery and the fatigue strength recovery (fatigue life recovery) [41].
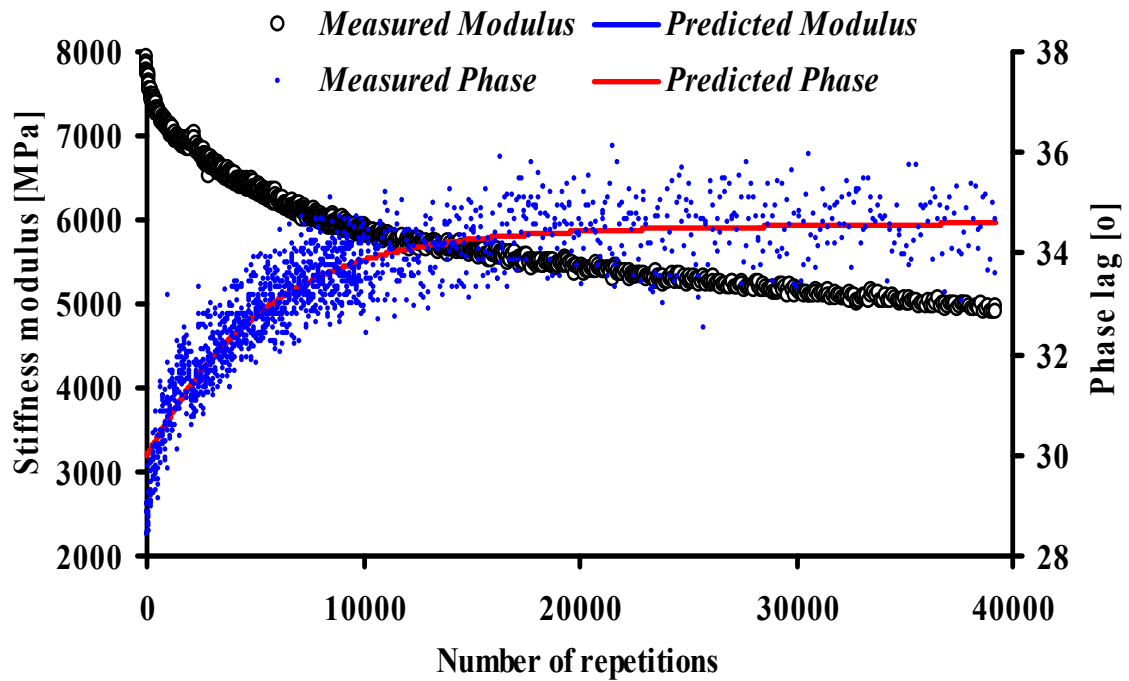
Figure 2-26 Simulation of stiffness and phase lag development for a continuous fatigue test using the PH model [80]
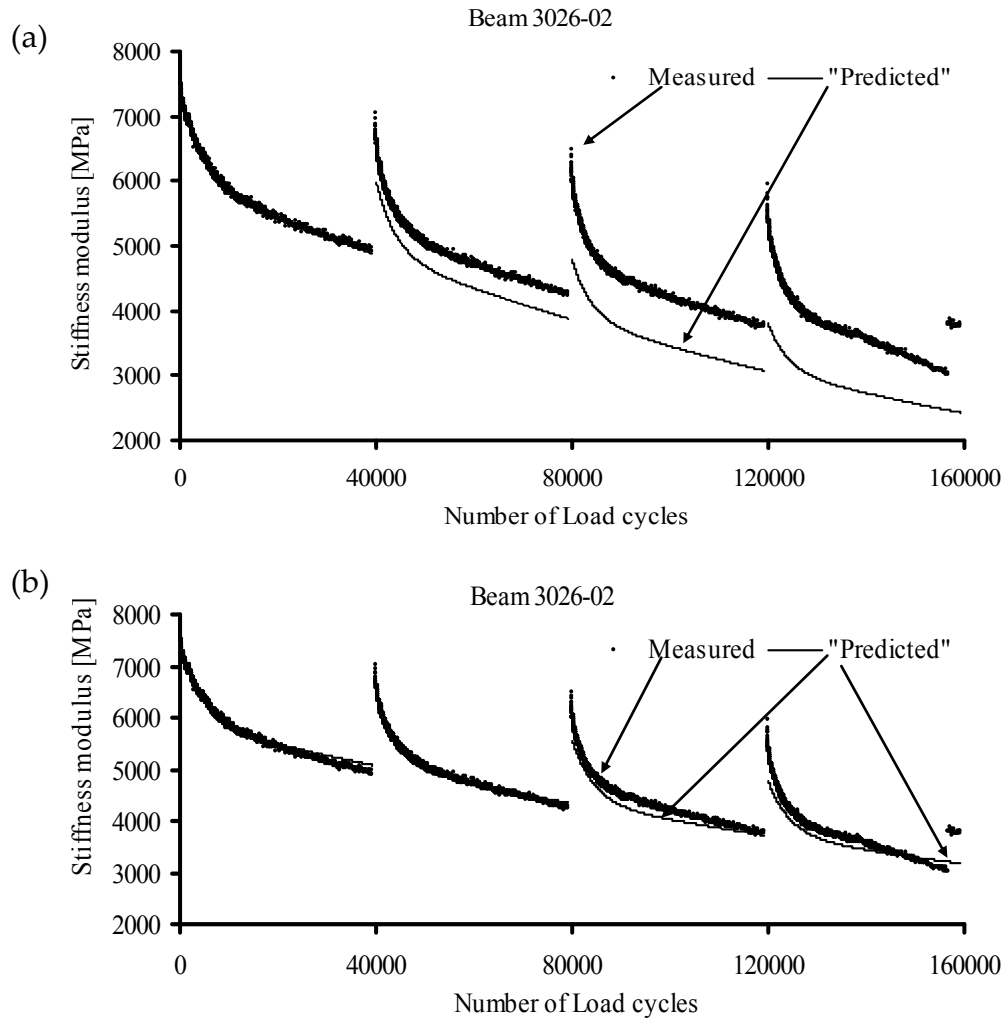
Figure 2-27 Simulation of stiffness development for a FHS test (a) using the parameters determined from the first load period only; (b) using the parameters determined from the first two load periods [41]

2.5   Novel Self Healing Material Systems

The self healing concept is developed from biological and natural phenomena, which help organisms to recover, repair cracks and to extend the life span. Similarly, ideas are explored by the material scientists to develop many kinds of novel self healing materials. Table 2-4 lists novel self healing mechanisms used in advanced composite structures from mimicking nature [81]. There are mainly two types of novel self healing material systems, namely liquid based and solid based self healing systems. Detailed information on these two types of systems can be found hereafter.

Table 2-4 Biomimetic self-healing inspiration in novel self healing materials [81]

Biological attribute	Composite/polymer engineering	Systems	Biomimetic self-healing or repair strategy
Bleeding	Capsules	Liquid based	Action of bleeding from a storage medium housed within the structure, 2-phase polymeric cure process rather than enzyme "waterfall" reaction
Bleeding	Hollow fibres	Liquid based	Action of bleeding from a storage medium housed within the structure, 2-phase polymeric cure process rather than enzyme "waterfall" reaction
Blood flow vascular network	Hollow fibres	Liquid based	2D or 3D network would permit the healing agent to be replenished and renewed during the life of structure
Blood clotting	Healing resin	Liquid based	Synthetic self-healing resin systems designed to clot locally to the damage site. Remote from the damage site clotting is inhibited and the network remains flowing
Concept of self healing	Remendable polymers	Solid based	Bio-inspired healing requiring external intervention to initiate repair
Blood cells	Nano-particles	Solid based	Artificial cells that deposit nano-particles into regions of damage
Skeleton/bone healing	Reinforcing fibres	Solid based	Deposition, resorption, and remodelling of fractured reinforcing fibres
Elastic/plastic behaviour in reinforcing fibres	Reinforcing fibres	Solid based	Repair strategy, similar to byssal thread, where repeated breaking and reforming of sacrificial bonds can occur for multiple loading cycles
Tree bark healing compartmentalization	-	Solid based	Formation of internal impervious boundary walls to protect the damaged structure from environmental attack

2.5.1 Liquid based self healing material systems

2.5.1.1 Microcapsules

White and his co-workers developed the autonomic healing concept and reported the idea of micro-capsulation self healing [6]. A monomer, dicyclopentadiene, stored in microcapsules with an average size of 220μm, and a transition metal catalyst (Grubbs' catalyst) was reported by White [6]. A urea-formaldehyde shell is used to protect the capsule.

The self healing concept is realized by incorporating a micro-encapsulated healing agent and a catalytic chemical trigger within an epoxy matrix [82-84]. The whole process of microcapsule healing is shown in Figure 2-28: (a), cracks form in the matrix wherever damage occurs; (b), the crack breaks the microcapsules, releasing the healing agent into the crack plane through capillary action; (c), the healing agent contacts the catalyst, triggering polymerization that bonds the crack faces together.
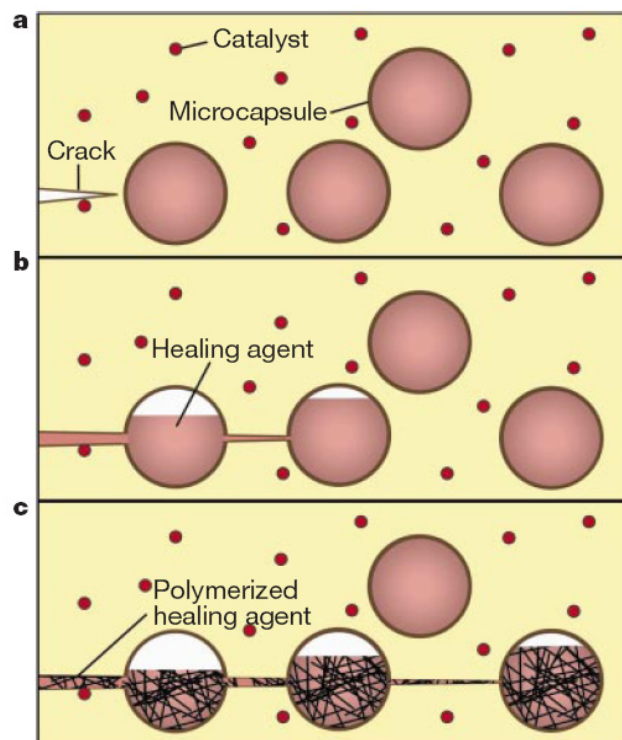

Figure 2-28 Microcapsule healing [6]

Later on, optimizations of this microcapsule self healing system were developed by many other researchers. Dependent on different areas of applications, the research focuses are on the optimizations of the capsule sizes, shapes, shell materials, healing agents and catalysts [85-88].

As shown in Figure 2-29, Brown and his co-workers investigated the effectiveness of these self healing systems by means of fracture tests and fatigue tests with a tapered double cantilever beam specimen [89, 90]. Monotonic displacement controlled tests were performed using a displacement speed of

5mm/s. Fatigue tests were conducted with a triangular waveform with a frequency of 5 Hz applied with a load ratio ($R = K_{min}/K_{max}$) of 0.1. The test results clearly indicate the beneficial effect of the self healing system.
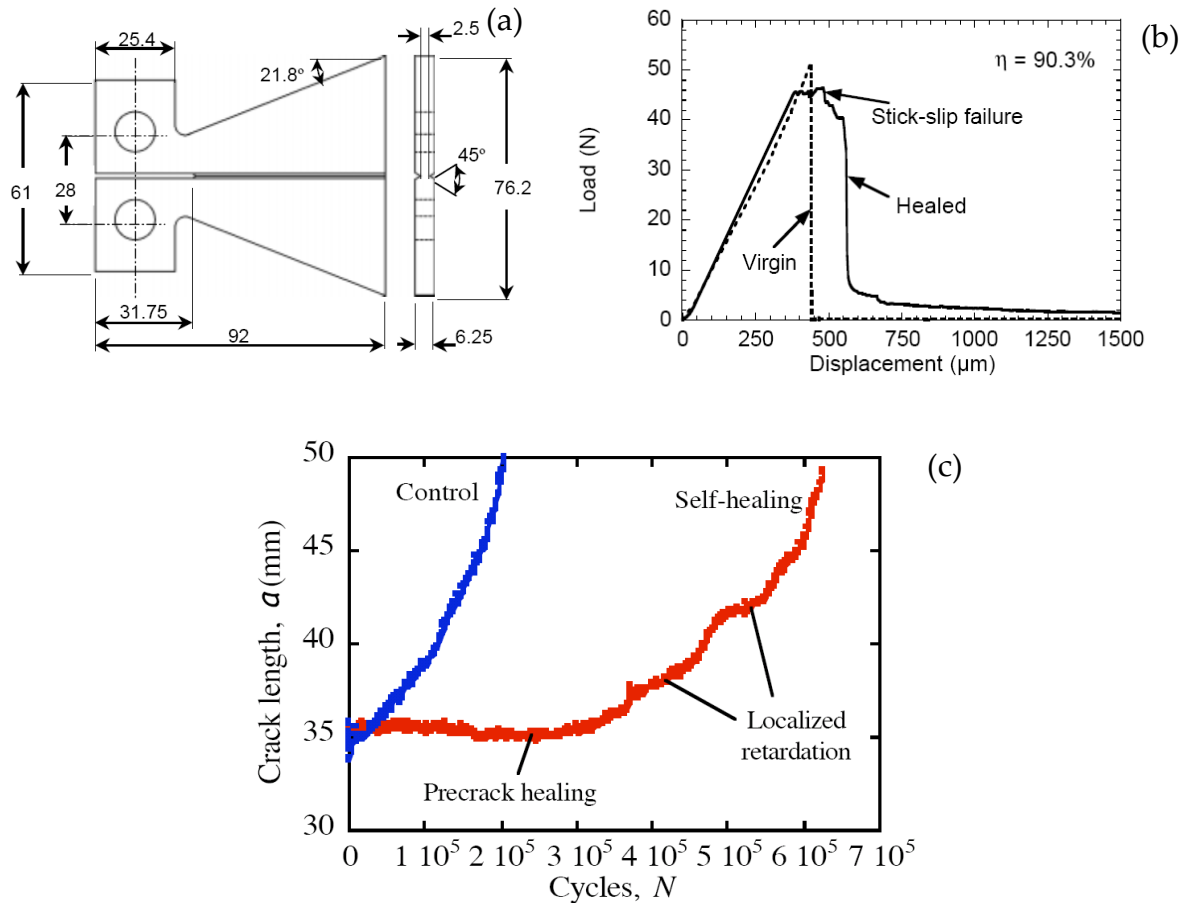

Figure 2-29 Mechanical tests on self healing epoxy with dicyclopentadiene capsules and Grubbs' catalyst: (a) Tapered double-cantilever beam geometry (dimensions in mm); (b) Monotonic test; (c) Fatigue test

[89, 90]

Trask summarised the advantages and disadvantages of the microcapsule self healing system [91].

The key advantages of the microcapsule self-healing method are:

o   good for the repair of resin-only systems,

o   good strength recovery has been reported in self-healing of resin systems (not composite systems).

The disadvantages of the microcapsule self-healing method are:

o   microcapsule fracture is required to release the repair resin,

o   the resin microcapsules must be close to the catalyst,

o the size of the microcapsule will disrupt the fibre profile – fibre waviness and fibre volume fraction,

o an even dispersion of the catalyst and microcapsules is required to match the damage location,

o the resin reservoir to heal damage is limited,

o an inherent void is created in the matrix after consumption of the healing resin.

2.5.1.2   Hollow fibres

Pond and co-workers developed a hollow fibre self healing system for composite laminates [92-94]. A typical self-healing hollow fibre used in composite laminates is illustrated in Figure 2-30. Three types of hollow fibre self healing systems can be discriminated: 1. hollow fibres containing a one-part resin; 2. hollow fibres containing a resin and hardener; 3. hollow fibres containing the resin system with the catalyst or hardener contained within the matrix material.
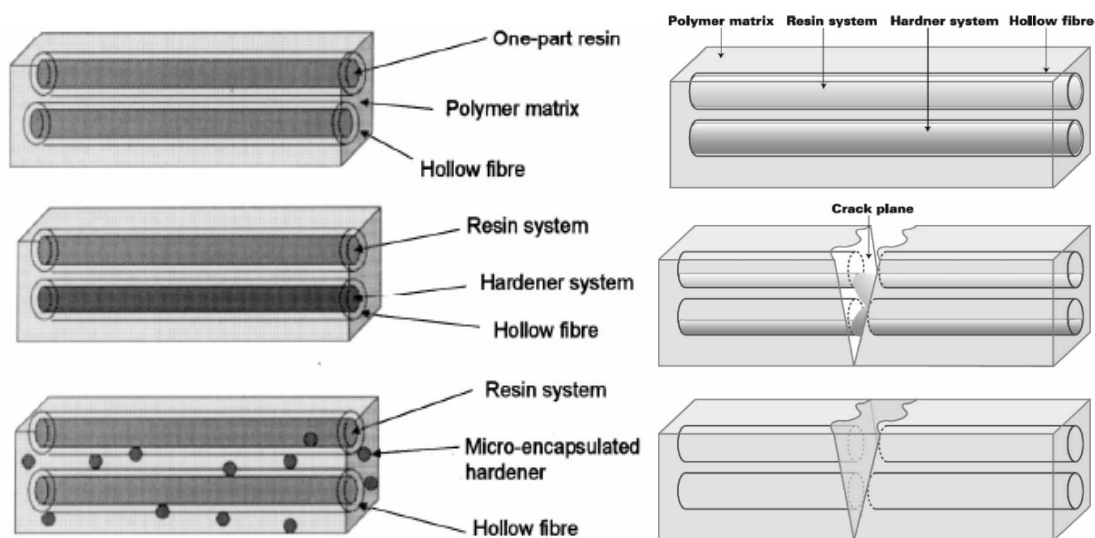

Figure 2-30 Typical hollow fibre self healing on polymer matrix (left) and schematic of self healing concept (right) [91]

It is shown that the hollow fibres can range in diameter from 30-100μm with a hollowness up to 65% in volume. The successful use of self healing hollow glass fibres on an epoxy and carbon fibre reinforced polymer system were reported [81, 95].

Trask concluded that the key advantages of the hollow fibre self-healing concept are [91]:

o the fibres can be tailored to match the orientation of the structural fibres,

o the fibres can be placed within the stacking sequence to address specific failure threats,

- o different healing resins can be used depending on the operational requirements,

- o different activation methods can be used to cure the resin,

- o compared to the microcapsule route, potentially a considerably higher volume of liquid resin is available to heal the damage.

The disadvantages of the hollow fibres are:

- o fibre fracture is required to release the repair resin,

- o low viscosity resin systems must be used to facilitate the fibre infiltration,

- o self-healing resins must be infused as an additional processing method,

- o the hollow fibre diameter is typically larger than conventional reinforcing fibres.

2.5.1.3 Microvascular networks

Toohey reported a self healing material system with 3D microvascular networks as shown in Figure 2-31 [96].
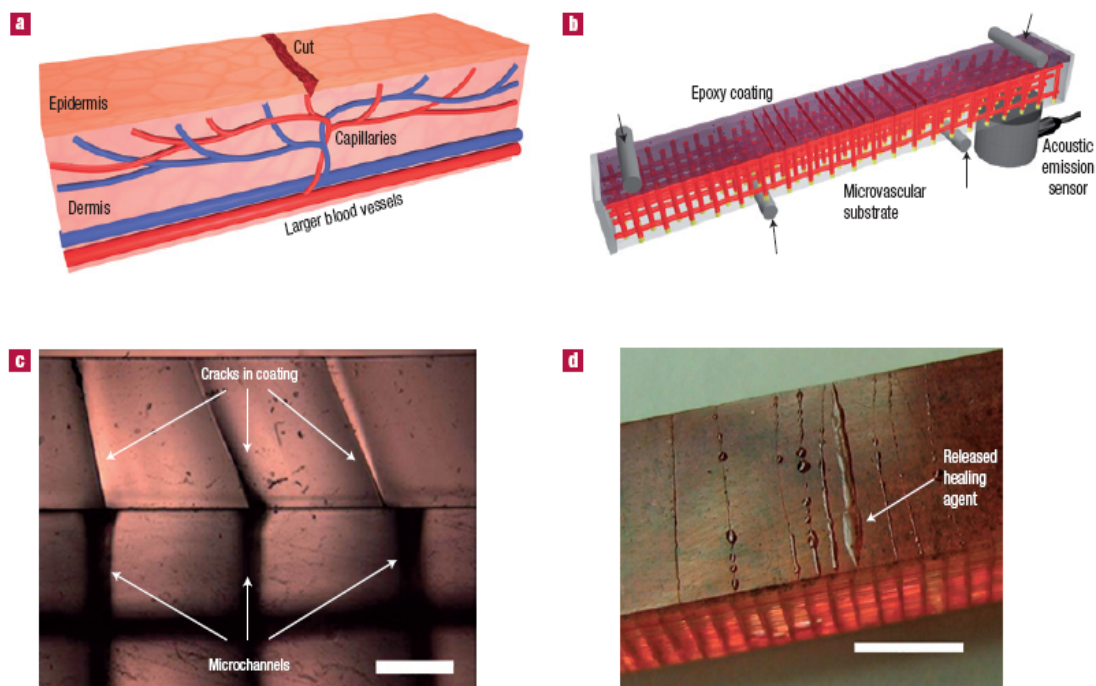

Figure 2-31 Self-healing materials with 3D microvascular networks [96]

Figure 2-31a gives a schematic diagram of a capillary network in the dermis layer of the skin with a cut in the epidermis layer. Figure 2-31b gives a schematic diagram of the self-healing structure composed of a microvascular substrate and a brittle epoxy coating containing an embedded catalyst in a four-point bending configuration monitored with an acoustic-emission sensor. Figure 2-31c shows a high-magnification cross-sectional image of the coating showing that cracks, which initiate at the surface, propagate towards the

microchannel openings at the interface (scale bar = 0.5 mm). Figure 2-31d is an optical image of the self-healing structure after cracks are formed in the coating (with 2.5% (by mass) catalyst), revealing the presence of excess healing fluid on the coating surface (scale bar = 5 mm).

In addition, Bejan compared different loops of the microvascular networks and he concluded that triangular loops on the network structures of vascular perform the best when compared with square, hexagon loops [97].

2.5.2 Solid based self healing material systems

2.5.2.1 Remendable cross-linked polymers

Chen developed a different approach for healing crosslinked polymers where no catalyst or embedded liquid healing agent was required [98]. In his research, a specially designed matrix containing a weak chemical bond which will preferentially break during damage initiation and reform on heating was developed. This matrix, which was produced by a thermally reversible Diels-Alder (DA) cyclo-addition of multi-furan (F) and multi-maleimide (M), 3M4F, has tensile and compressive properties comparable with epoxies and unsaturated polyesters. The brittle, crosslinked polymer can be fractured, clamped together, and heated to reform DA adducts across the crack face.

As shown in Figure 2-32, the compact tension test was used to analyze the healing of a thermally remendable self healing material. This process was shown to be fully reversible and could be used to restore the fractured part multiple times. After structural failure, the two pieces are matched as closely as possible and were held together with a clamp. Specimens are treated at 120°C to 150°C under nitrogen for about 2 hours, and then cooled to room temperature. After thermal treatment, only a slight interface mismatch is observable, indicating mending (healing) of the interface. The re-fracture result indicated that the specimen recovered about 57% of the original fracture load after healing.
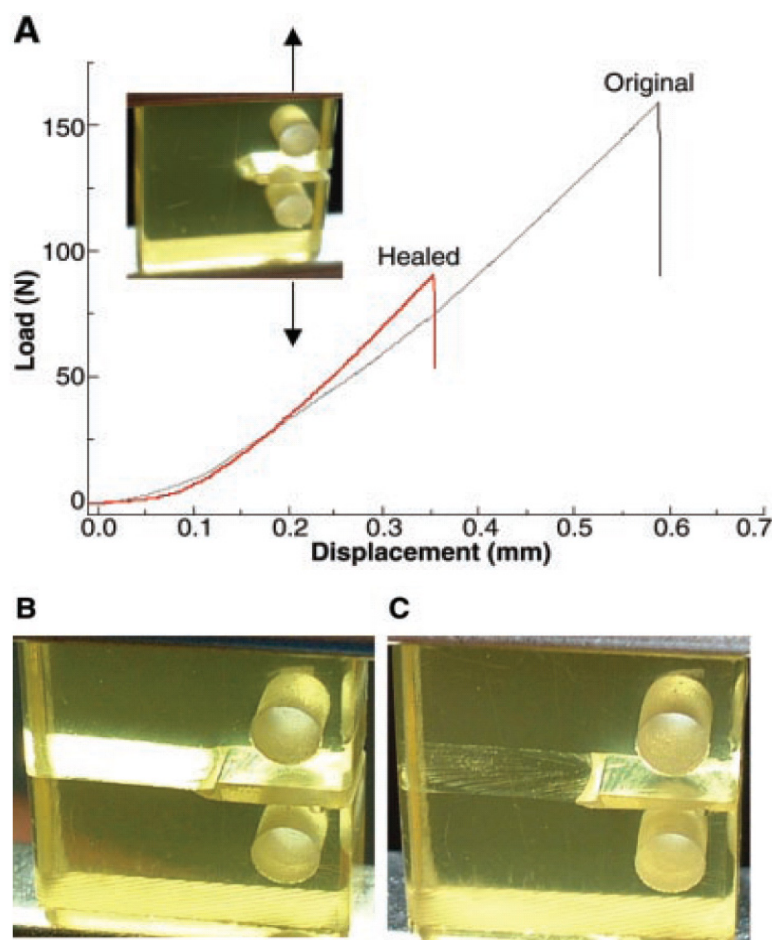
Figure 2-32 Thermal remendable polymer based on Diels-Alder reactions (A) Fracture test results; (B) Broken specimen before thermal treatment; (C) Broken specimen after thermal treatment [98]

2.5.2.2 Inonomers

Ionomer systems are a class of polymers which employs reactive bonds within the skeleton of ionics. Ionomer bonds are formed between inorganic elements M^+ and a carboxyl group R-COOH. M^+ can be Mg^{2+}, Zn^{2+} or Na^+. Thus, low molecular weight polymers can react together to form longer chains with ionic reversible bonds.

This reversible bond can be used for healing [99-102]. A high-speed impact test or puncture test was used to investigate the self-healing behaviour. Under a high-speed impact test, the material was damaged locally but also heated due to the impact energy.

As shown in Figure 2-33, the self-healing response is related to ionic aggregation and melts flow behaviour of these copolymers. Healing is expected to occur if sufficient energy is transferred to the polymer upon impact; this results in heating of the material above its order–disorder transition and results in disordering of the aggregates. During the post-puncture period, the ionic aggregates have the tendency to reorder and patch the hole. It is observed that

the healing driving forces are the puncture event which produces a local melt state in the polymer and the flow of the molten material to snap back and to close the hole.
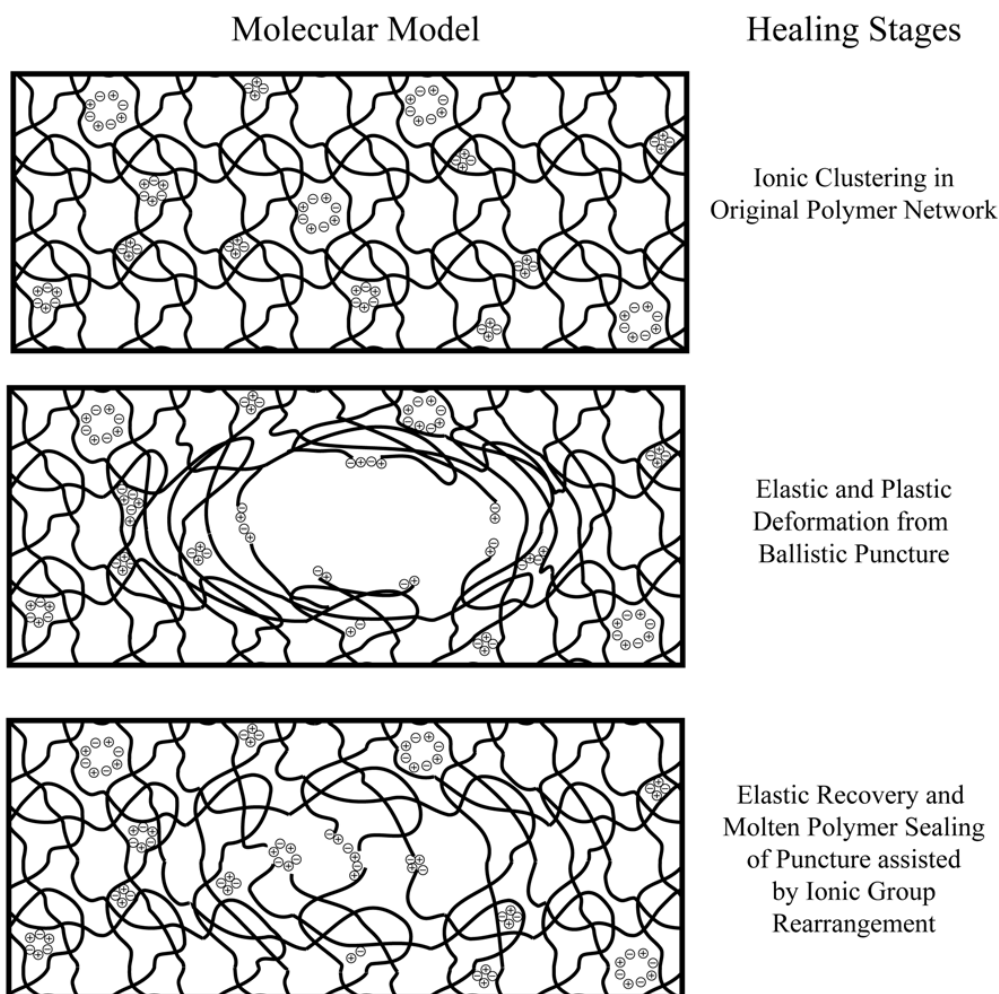

Figure 2-33 Theoretical healing mechanism in ionomers [57]

2.5.2.3 Supramolecular rubbers

Cordier and his co-workers reported a self healing rubber produced via a supramolecular assembly method [103]. Figure 2-34 gives a schematic view of a reversible supramolecular network formed by mixtures of ditopic (blue) and tritopic (red) molecules associated by directional interactions (represented by dotted lines). The carboxylic-acid ends were used to attach functional groups that are able to form multiple hydrogen bonds. Infrared spectroscopy shows the presence of multiple hydrogen bonds between N-H (1544 cm^{-1}) and C=O (1697 cm^{-1}) groups . Two-step synthetic pathway introduces three types of functional groups able to strongly associate via multiple hydrogen bonds, namely amidoethyl imidazolidone, di(amido ethyl) urea and diamido tetraethyl triurea. In the first step, acid groups were condensed with a controlled excess of

diethylene triamine. In the second step, the obtained product reacted with urea. The glass transition temperature of this rubber is 28°C.

In contrast to the conventional cross-linked or thermo-reversible rubbers made of macromolecules, the self healing rubber, when broken or cut, can be simply repaired by bringing together fractured surfaces to self-heal at room temperature. Repaired samples recuperate their enormous extensibility. The process of breaking and healing can be repeated many times.
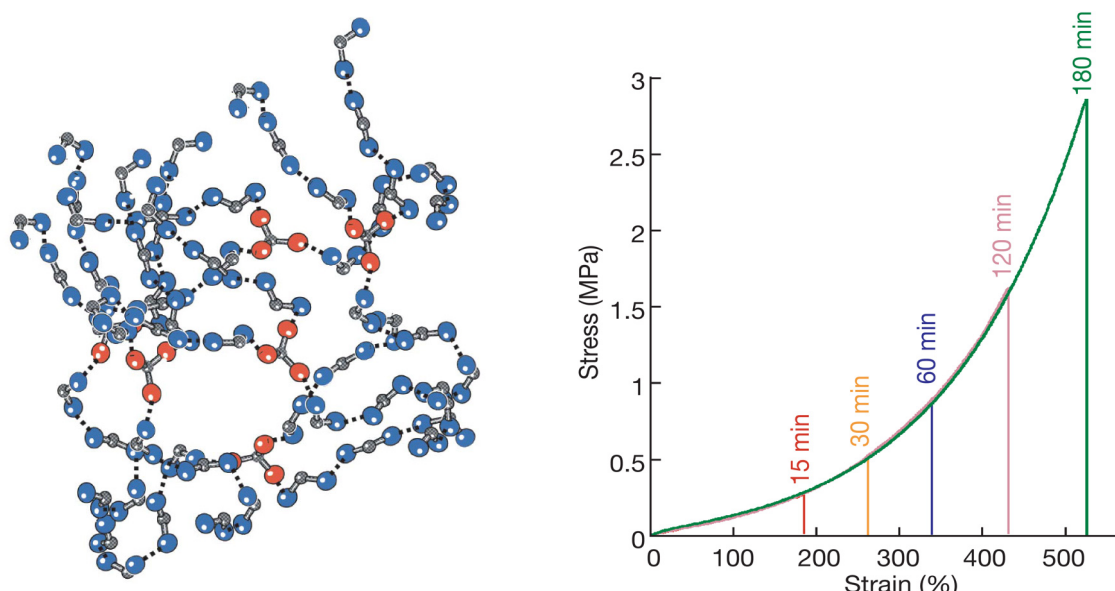

Figure 2-34 Self-healing supramolecular rubber: (a) Supramolecular network; (b) healing efficiency of the cut parts which are brought into contact at 20°C immediately after being cut (waiting time less than 5 minutes) [103]

2.5.2.4 Nanoparticles

Balazs and co-workers [104, 105] investigated the capabilities of nanoparticles with numerical methods for self healing of composites, especially in coatings. The results indicate that the stress concentration at the tip of a notch is significantly reduced due to the presence of the nanoparticles.

As shown in Figure 2-35, the polymer chains close to the nanoparticles are stretched and extended. Then the nanoparticles segregate in the crack and pre-crack regions driven by the tendency to minimize nanoparticles-polymer interactions hence to provide self healing capability [57].

Gupta experimentally demonstrated migration and clustering of embedded nanoparticles around the cracks in a multilayered composite structure due to entropy driven process [106]. He also suggested that the nanoparticles are more effective than the larger particles for healing because they diffuse faster than the larger ones.
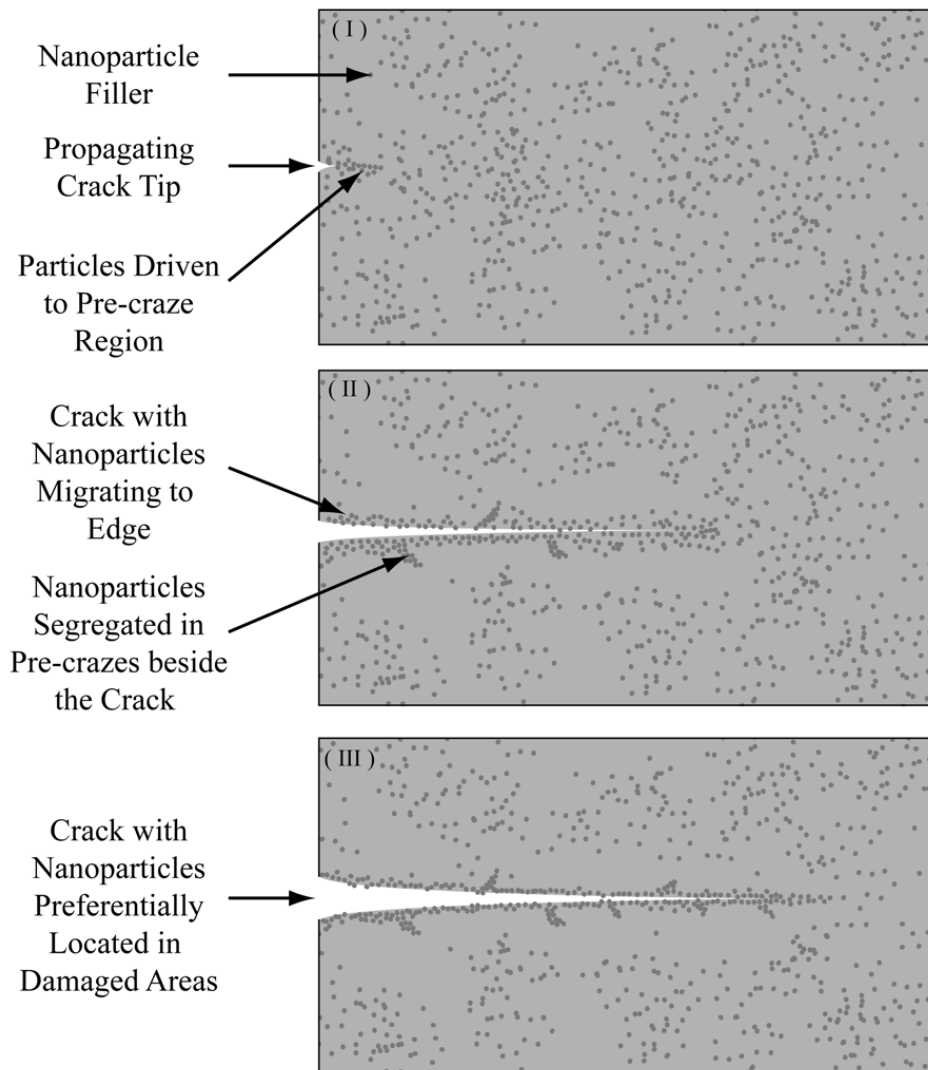
Figure 2-35 Schematic diagram of nanoparticle movement during crack growth in thermoplastics [57]

2.6 Summary

Based on the extensive literature review, the following can be summarised:

- o **Characterization of self healing materials**

  - ➢ Healing of bituminous materials exists and is observed by many researchers. Most of the characterization methods are mechanical related tests. Three types of self healing characterization methods are widely reported in literature, namely, the fatigue-healing test with intermittent loading (FHI), the fatigue-healing test with storage periods (FHS) and the fracture-healing test (FRAH). The investigation scales are ranging from bituminous binders at micro level, to bituminous mastics/mortars at meso level, up to asphalt mixtures and asphalt pavements at macro level. Due to the different approaches used by researchers, the results vary from one to another. Nevertheless some general observations can still be made and will be reported hereafter.

  - ➢ It is observed from the FHI tests that the fatigue life of bituminous materials can significantly be improved by applying an intermittent loading. However, the fatigue life is not increasing anymore when the rest/load period ratio exceeds 25. The self healing behaviour observed in the FHI tests is also sensitive to the type of loading, the strain/stress control mode and the strain/stress levels applied.

  - ➢ It is observed from the FHS tests that the observed recovery in stiffness modulus and the extension of the fatigue life are different indicators. The stiffness modulus can recover very fast after a short rest period and can recover completely to almost 100% of the initial stiffness modulus. However, the extension of the fatigue life can only develop slowly in time. In addition, it is shown that the self healing behaviour in the FHS test is sensitive to the level of damage at which the healing experiment was carried out.

  - ➢ Self healing can explain the improvement of the strength of bituminous materials observed from the FRAH test. Different from the fatigue related healing test, the FRAH test conducts healing investigations on a specimen which is fractured with noticeable cracks. It is also shown that a small permanent compressive stress on the cracked surfaces, sometime just the weight of the specimen around 20 Pa, is promoting healing.

  - ➢ From non-destructive in-situ tests on asphalt pavements it is observed that an asphalt pavement which is subjected to realistic

loads can restore its stiffness modulus during rest periods. This is believed to be because of healing.

➢ When comparing the types of the tests, the FHI test shows the fastest healing and the FRAH test shows the slowest healing.

➢ When comparing how healing influences the recovery in stiffness, fatigue resistance and strength, then one can conclude that the stiffness modulus shows the fastest recovery (healing), followed by the fatigue life extension. The strength recovery is the slowest.

➢ When comparing the scales, full healing observed in bituminous binders and mastics is very fast, ranging from seconds to hours. Full healing observed in an asphalt mixture and an asphalt pavement is slow, ranging from hours to days.

o **Influence factors on self healing of bituminous materials**

➢ The self healing behaviour of bituminous materials is shown to be a complex phenomenon and is very sensitive to many factors. Both internal (material) and external (temperature etc.) factors are of importance.

➢ Factors which influence the self healing behaviour are the rheological properties, chemical composition, surface energy, volumetrics and modifications.

▪ A soft bitumen with a high penetration grade and a high percentage of aromatic components is a good healer.

▪ Relatively spoken, an asphalt mixture which has a dense structure, a higher bitumen content, thicker bitumen films and a lower air voids content has a better healing capability.

▪ Polymer modification is shown to be an adverse influencing factor, which can decrease the healing capability. But the addition of hydrated lime is favourable for healing.

➢ The external factors consist of number and duration of the rest periods, temperature, way of loading, load level, damage level, presence of a compressive stress, ageing and moisture.

▪ A higher temperature and a longer rest period are favourable for healing.

▪ The healing observed in an experiment is not a true material behaviour, but very much dependent on how the load is applied, including different test procedures as the FHI, FHS or FRAH, different control modes as stress control mode or strain control mode.

- A higher level of damage can reduce the healing capability. Once marcocracks are formed from microcracks, the healing capability will be limited.

- A compressive stress on the cracked surfaces can improve healing considerably.

- Ageing and moisture will decrease the healing capability.

o **Modelling of self healing of bituminous materials**

➢ Two types of models are considered in the literature for self healing investigations, namely the physical-chemical based healing model and the mechanical based healing model.

➢ The physical-chemical based healing model is intended to explain the self healing phenomenon via physical-chemical effects.

- The multi-step healing model describes the self healing phenomenon of a crack with several steps. They mainly consist of flowing, surface approaching and inter-diffusion. The first two steps are necessary for the recovery of the stiffness modulus. Inter-diffusion is the main reason of the strength regain during the healing process.

- The thixotropy model relates the damage and recovery phenomenon during load repetitions and rest periods to a thixotropic behaviour of bituminous materials. The recovery process is believed to be due to molecular motion and rebuilt of the microstructure, which is not related to a crack healing process.

➢ The mechanical based healing models explain the observed self healing phenomenon through non-linear material mechanics.

- The VECD model simulates the self healing phenomenon using non-linear visco-elastic continuum damage theory. A unique C-S relationship is used to represent the damage behaviour of bituminous materials under both monotonic and fatigue loading. Healing is then the recovery of the damage parameter C over time.

- The PANDA model simulates the self healing behaviour using the effective stress concept. Healing is defined to be the reverse of the damage, which is dependent on healing time, temperature and damage.

- The PH model simulates the self healing behaviour during a fatigue process. Through simulation of the evolution of the loss modulus and the storage modulus of the

fatigue/healing process using mathematical equations, the fatigue/healing process in terms of development of stiffness modulus and phase angle can be modelled successfully using a shifted time scale.

o **Novel self healing material systems**

➢ Novel self healing material systems can be divided in two groups, namely liquid and solid based self healing systems.

➢ The liquid based self healing systems consist of a shell material, which can be a microcapsule, hollow fibre or microvascular network, and the embedded liquid, which can be a solvent, monomer and/or catalyst or polymer and/or hardener. When a crack is passing through the shell of the self healing system, the shell breaks and the embedded liquid flows out to fill the crack and then repair the crack with further reactions. This system is good for strength recovery of the material. However, the self healing process of the system is complex, the mechanical properties can be influenced by addition of the liquid based self healing system and the capability of multi-time self healing is limited.

➢ The solid based self healing system mainly consists of polymers with reversible reactions. This can be the reversible cross-link reaction like DA reaction, the reversible ionic bonds or the reversible hydrogen bonds. In addition, the nanoparticles with a special migration and diffusion effect due to their size effect also contribute to the self healing capability. Such a system has a multi-time healing capability. However, a trigger, mostly heat, is often needed for the self healing system due to the nature of the reversible reaction.

References

[1] Van der Zwaag S. Self healing materials: an alternative approach to 20 centuries of materials science. Dordrecht: Springer Verlag; 2007.

[2] Francken L. Fatigue performance of a bituminous road mix under realistic best conditions. Transportation Research Record 1979;712:30-4.

[3] Van Dijk W, Moreaud H, Quedeville A, and Uge P. The fatigue of bitumen and bituminous mixes. 3rd int. Conference on the Structural Design of Asphalt Pavements. Ann Arbor, Michigan, USA; 1972.

[4] Bazin P and Saunier JB. Deformability, fatigue and healing properties of asphalt mixes. Proceedings of the Second International Conference on the Structural Design of Asphalt Pavements. Ann Arbor, Michigan, USA; 1967, p. 553-69.

[5] Raithby KD and Sterling AB. The effect of rest periods on the fatigue performance of a hot-rolled asphalt under repeated loading. Journal of Association of Asphalt Paving Technologists 1970;39:134-52.

[6] White SR, Sottos NR, Geubelle PH, Moore JS, Kessler MR, Sriram SR, et al. Autonomic healing of polymer composites. Nature 2001;409:794-7.

[7] Kim YR, Little DN, and Lytton RL. Use of dynamic mechanical analysis (DMA) to evaluate the fatigue and healing potential of asphalt binders in sand asphalt mixtures. Journal of Association of Asphalt Paving Technologist 2002;71:176-99.

[8] Kim YR, Little DN, and Lytton RL. Fatigue and healing characterization of asphalt mixtures. J Mater Civil Eng 2003;15:75-83.

[9] Lu X, Soenen, H., Redelius, P. Fatigue and healing characteristics of bitumens studied using dynamic shear rheometer. 6th RILEM Symposium PTEBM'03. Zurich; 2003, p. 408-15.

[10] Shen S, Chiu H-M, and Huang H. Characterization of fatigue and healing in asphalt binders. J Mater Civil Eng 2010;22:846-52.

[11] Van den bergh W, Molenaar AAA, van de Ven MFC, and De Jonghe TC. The influence of aged binder on the healing factor of asphalt mixtures. AES - ATEMA' 2009 Third International Conference on Advances and Trends in Engineering Materials and their Applications. Montreal, Canada; 2009.

[12] Phillips MC. Multi-step models for fatigue and healing, and binder properties involved in healing. Eurobitume Workshop on Performance Related Properties for Bituminous Binders. Luxembourg; 1998, p. 115.

[13] Smith BJ and Hesp SAM. Crack pinning in asphalt mastic and concrete: effect of rest periods and polymer modifiers on the fatigue life. 2nd Eurasphalt & Eurobitume Congress. Barcelona; 2000, p. 539-46.

[14] Bahia H, Zhai H, Bonnetti K, and Kose S. Non-linear viscoelastic and fatigue properties of asphalt binders. Journal of Assoc. Asphalt Paving. Technol. 1999;69:1-34.

[15] Shan L, Tan Y, Underwood S, and Kim YR. Application of thixotropy to analyze fatigue and healing characteristics of asphalt binder. 2010 Annual Meeting of the Transportation Research Board; 2010.

[16] Santagata E, Baglieri O, Dalmazzo D, and Tsantilis L. Rheological and chemical investigation on the damage and healing properties of bituminous binders. Journal of Assoc. Asphalt Paving. Technol. 2009;78:567-96.

[17] Bodin D, Soenen H, and De la Roche C. Temperature effects in binder fatigue and healing tests. 3rd Eurasphalt & Eurobitume Congress. Vienna; 2004.

[18] Hammoum F, de La Roche C, and Piau JM. Experimental investigation of fracture and healing of bitumen at pseudo-contact of two aggregates. 9th International Conference on Asphalt Pavements; 2002.

[19] Maillard S, De La Roche C, Hammoum F, Gaillet L, and Such C. Experimental investigation of fracture and healing of bitumen at pseudo-contact of two aggregates. 3rd Eurasphalt & Eurobitume Congress. Vienna; 2004, p. paper No. 266.

[20] Bhasin A, Little DN, Bommavaram R, and Vasconcelos K. A framework to quantify the effect of healing in bituminous materials using material properties. Road Material and Pavement Design 2008;EATA2008:219-42.

[21] Bommavaram R. Evaluation of healing in asphalt binders using dynamic shear rheometer and molecular modeling techniques: Texas A&M University, 2008.

[22] Bommavaram R, Bhasin A, and Little DN. Determining intrinsic healing properties of asphalt binders: role of dynamic shear rheometer. Transportation Research Record 2009;2126:47-54.

[23] Qiu J, Van de Ven MFC, Wu SP, Yu JY, and Molenaar AAA. Investigating the self healing capability of bituminous binders. Road Material and Pavement Design 2009;10:81-94.

[24] Kim YR, Little DN, and Burghardt RC. SEM Analysis on Fracture and Healing of Sand-Asphalt Mixtures. Journal of Materials in Civil Engineering 1991;3:140-53.

[25] Castro M. Fatigue and healing of asphalt mixtures: discriminate analysis of fatigue curves. J. Transp. Eng. 2006;132:168-74.

[26] Carpenter SH and Shen S. A dissipated energy approach to study HMA healing in fatigue. 2006 Annual Meeting of Transportation Researh Board Washington D.C.; 2006.

[27] Little DN, Lytton RL, Williams DA, and Kim YR. An analysis of the mechanism of microdamage healing based on the application of micromechanics first principles of fracture and healing. Journal of Assoc. Asphalt Paving. Technol. 1999;68:501-42.

[28] Lee H-J, Daniel JS, and Kim YR. Laboratory performance evaluation of modified asphalt mixtures for Inchon airport pavements. International Journal of Pavement Engineering 2000;1:151-69.

[29] Grant TP. Determination of asphalt mixture healing rate using the Superpave indirect tensile test: University of Florida, Master Thesis, 2001.

[30] Kim B and Roque R. Evaluation of healing property of asphalt mixture. 2006 Annual Meeting of Transportation Research Board. Washington, D.C.; 2006.

[31] Daniel JS and Kim YR. Laboratory evaluation of fatigue damage and healing of asphalt mixtures. Journal of Materials in Civil Engineering 2001;13:434-40.

[32] Abo-Qudais S and Suleiman A. Monitoring fatigue damage and crack healing by ultrasound wave velocity. Nondestructive Testing and Evaluation 2005;20:125-45.

[33] Uchida K, Kurokawa T, Himeno K, and Nishizawa T. Healing characteristics of asphalt mixture under high temperature conditions. 9th International Conference on Asphalt Pavements; 2002.

[34] Bonnaure FP, Huibers AHJJ, and Boonders A. A laboratory investigation of the influence of rest periods on the fatigue characteristics of bituminous mixes. Journal of Assoc. Asphalt Paving. Technol. 1982;51:104-28.

[35] Francken L and Clauwaert C. Characterization and structural assessment of bound materials for flexible road structures. 6th int. Conference on the Structural Design of Pavements. Ann Arbor; 1987, p. 130-44.

[36] Westera GE and Bouman SR. Healingonderzoek deelrapport 1 evaluatie van zeven healing onderzoeken. KOAC/WMD-Research and Development; 1993.

[37] Westera GE and Bouman SR. Healingonderzoek deelrapport 2 nadere beschouwing van het fenomeen healing bij asfalt. KOAC/WMD-Research and Development; 1994.

[38] Westera GE and Pelgrom LJW. Review healing. CROW wegbouwkundige Werkdagen 2002 2002, p. 87-98.

[39] Carpenter SH, Ghuzlan K, and Shen S. Fatigue endurance limit for highway and airport pavements. Transportation Research Record 2003;1832:131-8.

[40] Shen S and Carpenter SH. Development of an asphalt fatigue model based on energy principles. Journal of Assoc. Asphalt Paving. Technol. 2007;76:525-74.

[41] Pronk A and Cocurullo A. Investigation of the PH model as a prediction tool in fatigue bending tests with rest periods. Advanced Testing and Characterization of Bituminous Materials: CRC Press; 2009.

[42] Groenendijk J. Accelerated testing and surface cracking of asphalt concrete pavements, Delft: Delft University of Technology, 1998.

[43] Williams D, Little DN, Lytton RL, Kim YR, and Kim Y. Microdamage healing in asphalt and asphalt concrete; volume II: laboratory and field testing to assess and evaluate microdamage and microdamage healing. Federal Highway Administration; 2001.

[44] Kim YR, Whitmoyer SL, and Little DN. Healing in asphalt concrete pavements: is it real? Transportation Research Record 1994;1454:89-96.

[45] Molenaar AAA. Design of flexible pavement. Delft University of Technology.

[46] Kim YR, Little DN, and Benson FC. Chemical and mechanical evaluation of healing mechanism of asphalt concrete. Journal of Assoc. Asphalt Paving. Technol. 1990;59:240-75.

[47] Lytton RL. Characterizing asphalt pavements for performance. Transportation Research Record 2000;1723:5-16.

[48] Lee NK, Morrison GR, and Hesp SAM. Low temperature fracture of polyethylene-modified asphalt binders and asphalt concrete mixes. Journal of the Association of Asphalt Paving Technologists 1995;64:534-74.

[49] Song I, Little DN, Masad E, and Lytton RL. Comprehensive evaluation of damage in asphalt mastics using X-ray CT, continuum mechanics, and micromechanics. Journal of Assoc. Asphalt Paving. Technol. 2005;74:885-920.

[50] Molenaar AAA. APT as a tool for the development of design and performance models. 10th International Conference on Asphalt Pavements; 2006.

[51] Van den bergh W. The effect of ageing on the fatigue and healing properties of bituminous mortars: Delft University of Technology, PhD thesis, 2011.

[52] Liu Q, Schlangen E, van de Ven MFC, van Bochove G, and van Montfort J. Predicting the performance of the self healing porous asphalt test section. Submitted to 7th RILEM International Conference on Cracking in Pavements. Delft; 2012.

[53] Zollinger CJ. Application of surface energy measurements to evaluate moisture susceptibility of asphalt and aggregates: Texas A&M University, Master thesis, 2005.

[54] Kim YH and Wool RP. A theory of healing at a polymer-polymer interface. Macromolecules 1983;16:1115-20.

[55] Wool R and O'Connor K. A theory crack healing in polymers. J. Appl. Phys. 1981;52:5953.

[56] Wool RP and O'Connor KM. Time dependence of crack healing. Journal of Polymer Science: Polymer Letters Edition 1982;20:7-16.

[57] Wu DY, Meure S, and Solomon D. Self-healing polymeric materials: a review of recent developments. Progress in Polymer Science 2008;33:479-522.

[58] Hefer AW, Little DN, and Lytton RL. A synthesis of theories and mechanisms of bitumen-aggregate adhesion including recent advances in quantifying the effects of water. 74th Annual Meeting of the Association of Asphalt Paving Technologists; 2005.

[59] van Lent D. Aggregate characterisation in relation to bitumen-aggregate adhesion: Delft University of Technology, Master thesis, 2008.

[60] Cheng DX. Surface free energy of asphalt-aggregate system and performance analysis of asphalt concrete based on surface free energy: Texas A&M University, 2002.

[61] Read J and Whiteoak D. The Shell Bitumen Handbook, 5th edition: Thomas Telford Ltd, 2003.

[62] Saal RNJ and Labout JWA. Rheological properties of asphaltic bitumen. The Journal of Physical Chemistry 1940;44:149-65.

[63] Traxler RN and Coombs CE. The colloidal nature of asphalt as shown by its flow properties. The Journal of Physical Chemistry 1935;40:1133-47.

[64] Mouillet V, de La Roche C, Chailleux E, and Coussot P. Thixotropic behaviour of paving grade bitumens under dynamic shear. Journal of Materials in Civil Engineering 2011.

[65] Tan Y, Shan L, Underwood BS, and Kim YR. Thixotropic characteristics of asphalt binder Journal of Materials in Civil Engineering 2011.

[66] Verstraeten J. Fatigue of bituminous mixes and bitumen thixotropy. XIXth World Road Congress, AIPCR. Marrakech; 1991, p. 766-9.

[67] Soltani A and Anderson DA. New test protocol to measure fatigue damage in asphalt mixtures. Road Materials and Pavement Design 2005;6:485-514.

[68] Di Benedetto H, Quang TN, and Sauzeat C. Nonlinearity, heating, fatigue and thixotropy during cyclic loading of asphalt mixtures. Road Materials and Pavement Design 2011;12:129-58.

[69] Kim YR, Lee HJ, and Little DN. Fatigue characterization of asphalt concrete using viscoelasticity and continuum damage theory. Journal of Assoc. Asphalt Paving. Technol. 1997;66:520-69.

[70] Schapery RA. Correspondence principles and a generalized J- integral for large deformation and fracture analysis of viscoelastic media. International Journal of Fracture 1984;25:195-223.

[71] Schapery RA. A theory of mechanical behavior of elastic media with growing damage and other changes in structure. Journal of the Mechanics and Physics of Solids 1990;38:215-53.

[72] Daniel JS and Kim YR. Development of a simplified fatigue test and analysis procedure using a viscoelastic, continuum damage model. Journal of Assoc. Asphalt Paving. Technol. 2002;71:619-50.

[73] Lee H and Kim Y. Viscoelastic continuum damage model of asphalt concrete with healing. J. Eng. Mech. 1998;124:1224.

[74] Lundstrom R. On rheological testing and modelling of asphalt mixtures with emphasis on fatigue characterization: KTH Royal Institute of Technology, PhD thesis, 2004.

[75] Lundstrom R and Isacsson U. Characterization of asphalt concrete deterioration using monotonic and cyclic tests. International Journal of Pavement Engineering 2003;4:143-53.

[76] Roque R, Zou J, Kim YR, Baek C, Thirunavukkarasu S, Underwood BS, et al. NCHRP Web-only Document 162: Top-down cracking of hot-mix asphalt layers: models for initiation and propagation. National Cooperative Highway Research Program; 2010.

[77] Abu Al-Rub RK, Darabi MK, Little DN, and Masad EA. A micro-damage healing model that improves prediction of fatigue life in asphalt mixes. International Journal of Engineering Science 2010;48:966-90.

[78] Darabi MK, Abu Al-Rub RK, and Little DN. A continuum damage mechanics framework for modeling micro-damage healing. International Journal of Solids and Structures 2012;49:492-513.

[79] Pronk AC. Partial healing model - curve fitting. Report WDWW- 2000-047. Delft: DWW; 2000.

[80] Pronk A. PH model in 4PB test with rest periods. Road Materials and Pavement Design 2009;10:417-26.

[81] Trask RS, Williams HR, and Bond IP. Self-healing polymer composites: mimicking nature to enhance performance. Bioinspiration & Biomimetics 2007;2:P1-P9.

[82] Sottos N, White S, and Bond I. Introduction: self-healing polymers and composites. Journal of The Royal Society Interface 2007;4:347-8.

[83] Brown EN, White SR, and Sottos NR. Retardation and repair of fatigue cracks in a microcapsule toughened epoxy composite-Part I: Manual infiltration. Composites Science and Technology 2005;65:2466-73.

[84] Brown EN, White SR, and Sottos NR. Retardation and repair of fatigue cracks in a microcapsule toughened epoxy composite-Part II: In situ self-healing. Composites Science and Technology 2005;65:2474-80.

[85] Blaiszik BJ, Sottos NR, and White SR. Nanocapsules for self-healing materials. Composites Science and Technology 2008;68:978-86.

[86] Shansky E. Synthesis and characterization of microcapsules for self-healing materials. C500 Final Report: Indiana University; 2006.

[87] Yin T, Rong MZ, Zhang MQ, and Yang GC. Self-healing epoxy composites - Preparation and effect of the healant consisting of microencapsulated epoxy and latent curing agent. Composites Science and Technology 2007;67:201-12.

[88] Mookhoek SD. Novel routes to liquid-based self-healing polymer systems: Delft University of Technology, PhD thesis, 2010.

[89] Brown E, Sottos N, and White S. Fracture testing of a self-healing polymer composite. Experimental Mechanics 2002;42:372-9.

[90] Brown EN, Jones AS, White SR, and Sottos NR. Self-healing polymer composites for extended fatigue life. Mechanics of 21st Centry-ICTAM04; 2004.

[91] Trask RS and Bond IP. Enabling self-healing capabilities - a small step to bio-mimetic materials. Materials Report Number: 4476; 2006.

[92] Trask RS and Bond IP. Biomimetic self-healing of advanced composite structures using hollow glass fibres. Smart Materials and Structures 2006;15:704.

[93] Pang JWC and Bond IP. Bleeding composites, Damage detection and self-repair using a biomimetic approach. Composites Part A: Applied Science and Manufacturing 2005;36:183-8.

[94] Pang JWC and Bond IP. A hollow fibre reinforced polymer composite encompassing self-healing and enhanced damage visibility. Composites Science and Technology 2005;65:1791-9.

[95] Williams G, Trask R, and Bond I. A self-healing carbon fibre reinforced polymer for aerospace applications. Composites Part A: Applied Science and Manufacturing 2007;38:1525-32.

[96] Toohey KS, Sottos NR, Lewis JA, Moore JS, and White SR. Self-healing materials with microvascular networks. Nat Mater 2007;6:581-5.

[97] Bejan A. Networks of channels for self-healing composite materials. J. Appl. Phys. 2006;100:033528.

[98] Chen X, Dam MA, Ono K, Mal A, Shen H, Nutt SR, et al. A thermally re-mendable cross-linked polymeric material. Science 2002;295:1698-702.

[99] Kalista SJ. Self-healing of thermoplastic poly(ethylene-co-methacrylic acid) copolymers following projectile puncture: Virginia Polytechnic Institute and State University, 2003.

[100] Varley R. Ionomers as self healing polymers. In: S van de Zwaag editor. Self Healing Materials: Springer Netherlands; 2008, p. 95-114.

[101] Varley RJ, Shen S, and van der Zwaag S. The effect of cluster plasticisation on the self healing behaviour of ionomers. Polymer 2010;51:679-86.

[102] Varley RJ and van der Zwaag S. Towards an understanding of thermally activated self-healing of an ionomer system during ballistic penetration. Acta Materialia 2008;56:5737-50.

[103] Cordier P, Tournilhac F, Soulie-Ziakovic C, and Leibler L. Self-healing and thermoreversible rubber from supramolecular assembly. Nature 2008;451:977-80.

[104] Lee J, Buxton G, and Balazs A. Using nanoparticles to create self-healing composites. J. Chem. Phys. 2004;121:5531.

[105] Smith KA, Tyagi S, and Balazs AC. Healing surface defects with nanoparticle-filled polymer coatings: effect of particle geometry. Macromolecules 2005;38:10138-47.

[106] Gupta S, Zhang Q, Emrick T, Balazs AC, and Russell TP. Entropy-driven segregation of nanoparticles to cracks in multilayered composite polymer structures. Nat Mater 2006;5:229-33.

3

Research Exploration and Final Research Plan

Abstract

This chapter contains the research approach and the research methodology. Three parts of the self healing phenomenon of asphalt mixtures are of interest namely the material, mechanical and modelling part. A two-phase research approach was anticipated starting with a research exploration phase before defining the final research phase. In the exploration phase, research was initiated based on the critical review from the literature. In this phase the focus was on exploring self healing methods and exploring possible novel self healing modifiers. Based on the experimental results from the exploration phase, it was observed, however, that all the novel modifications used in this research are not quite beneficial. The pure bitumen was observed to be the best healer among all the modified bitumens tested. With this conclusion, the final research phase was planned to further understand the self healing phenomenon of pure bituminous materials ranging from bitumen level up to asphalt mixture and pavement level through mechanical testing and modelling.

It is known that the self healing phenomenon of bituminous materials is complex and depends on many influencing factors. Even the self healing mechanism itself is not clear so far. In order to fully understand this phenomenon, a well defined and systematic research approach and methodology are needed. Therefore a literature review was done first of all and section 3.1 shows the lessons learned from this review. Following this, section 3.2 gives the research approach and research methodology defined on the basis of the literature review. Section 3.3 shows the research exploration phase and in section 3.4 the final research plan is given.

3.1 Lessons from Literature

From the literature review on the researches that were performed to investigate the self healing phenomenon of bituminous materials and on the novel self healing material systems, the following points are regarded as important to be taken into account in the research approach and methodology to be adopted.

o   The self healing phenomenon itself is complex and is dependent on many influencing factors. Internal influencing factors which are related to the material itself include the composition of materials, physical-chemical properties, modifications, etc. External influencing factors are duration of rest periods, temperature, presence of confinement, ageing, moisture, etc.

⇒ **In practice, the most important factors which should be considered are the rheological properties of the bitumen, the duration of the healing (rest) period, the healing temperature and the level of damage at the moment when healing is starting .**

o   Healing is a material property but in reality the method used to characterize the self healing capability influences the result. For example healing of asphalt mixtures is quite often characterized using fatigue tests with and without rest periods. Due to the complexity of such tests, the observed healing capability is not a true material property, but is strongly dependent on the mode of loading (stress control or strain control mode), the used test procedures such as the fatigue related healing test procedure with intermittent loading (FHI), the fatigue related healing test procedure with storage periods (FHS) or the fracture related healing test procedure (FRAH), etc.

⇒ **An efficient way of determining the self healing capability free of artefacts is highly needed.**

o   The current approaches to healing can roughly be divided into two groups. The first group is based on a physical-chemical approach, which is a conceptual model which largely relies on assumptions. The second group is based on a mechanical approach. It is a phenomenological model which describes the phenomenon but does not explain it.

⇒ **An effective model approach which links the physical-chemical based healing model to the mechanical based healing model is needed. In addition, an experimental self healing approach which mimics the self healing process as it occurs in practice is also necessary.**

o From the literature review, it becomes clear that novel self healing material systems provide a new emerging scientific field. These novel materials are widely investigated and from the point of view of a pavement engineer, the possibility of applying such novel self healing systems to upgrade the self healing capability of bituminous materials should be explored.

⇒ **Possibilities of upgrading the self healing capability of bituminous materials using novel self healing material systems should be investigated.**

3.2 Research Approach and Methodology

Based on the literature review, a triangle research approach on self healing of asphalt mixtures was developed.

Figure 3-1 shows the conceptual representation of this approach. Three main parts of the self healing phenomenon are considered including the mechanical, material and modelling part. The following explains the three parts in detail:
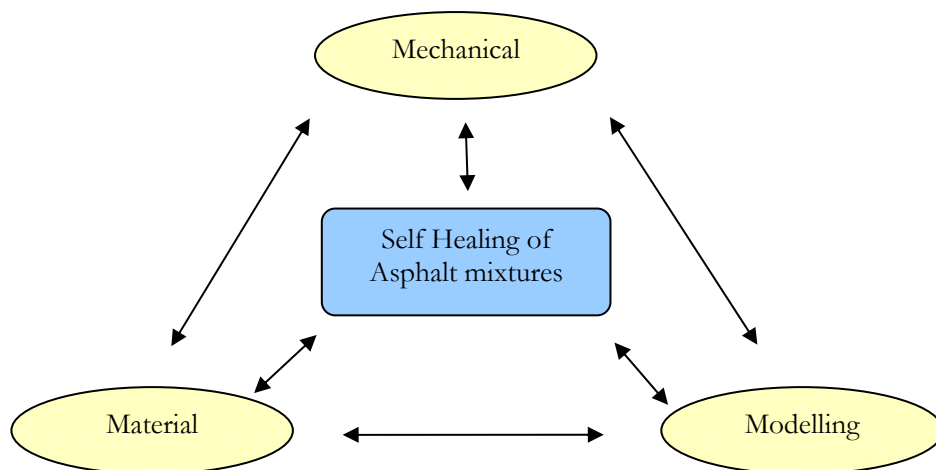
Figure 3-1 Conceptual representation of the research approach

o **Mechanical Part**

▪ This part focuses on the development of an effective test method for quantifying the self healing capability of bituminous materials. This test method should closely mimic the self healing process which is occurring in practice. Furthermore, the effect of influencing factors such as temperature, duration of healing

75

period and level of damage where healing is starting should also be taken into account.

o **Material Part**

- This part focuses on improving the self healing capability of bituminous materials using novel self healing components. The novel self healing modifiers shown in the literature review should be selected through certain criteria. The fundamental properties and the self healing capability should be investigated.

o **Modelling Part**

- This part focuses on explaining the self healing phenomenon using numerical modelling. An effective model approach which links the physical-chemical based healing model to the mechanical based healing model is needed.

In this thesis, all these three parts will be explored to understand the self healing phenomenon. A two-phase research methodology is adapted to conquer this challenging topic, namely the research exploration phase and the final research phase.

o **The research exploration phase:** In this phase, the possible novel self healing modifiers will be investigated. The potential self healing test methods will also be explored.

o **The finial research phase:** In this phase, the self healing behaviour of bituminous materials ranging from bituminous binder to bituminous mastics to asphalt mixtures will be characterized. This is followed by the modelling approach to gain further understanding of the self healing phenomenon. Based on the research findings, recommendations are also given for durable asphalt pavement using self healing technologies.

3.3   Research Exploration Phase

3.3.1   Research diagram

Figure 3-2 shows the research approach used for the exploration phase. Two main targets are set:

1) finding novel self healing modifiers;

2) exploring potential self healing test methods.

The research process is explained as follows:

o Firstly, potential novel self healing modifiers for bitumen are selected from the literature review. The modifiers are mixed with pure bitumen to produce novel self healing bitumens.

o Secondly, material properties of the novel self healing bitumens are characterized in terms of chemical structural, morphological and rheological properties.

o Thirdly, potential self healing test methods are explored and the self healing capabilities of the novel self healing bitumens are assessed.
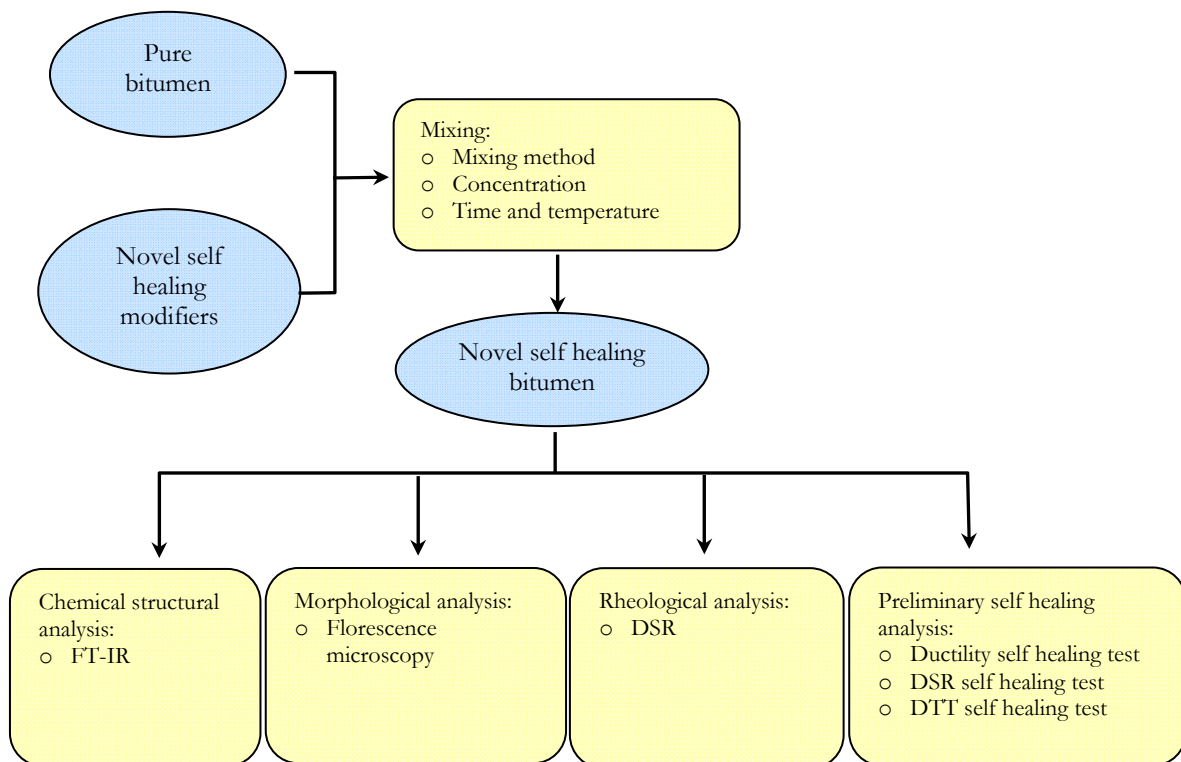
Figure 3-2 Research diagram for exploration phase

3.3.2 Materials and methods

3.3.2.1 Materials

Similar to healing concepts observed in nature, the healing performance of an asphalt mixture can be upgraded. Some additives can be introduced to achieve this.

One should keep in mind however that self healing systems should not only be effective under laboratory conditions. This implies that any self healing technique to be applied in practice should survive the harsh conditions which prevail during mixing, laying and compaction as well as those during the service life when the pavement is used by traffic. Several requirements should therefore be met.

o The possible candidates should have good thermal stability even at asphalt mixing temperatures of 150-200°C.

o They should also show excellent mechanical damage resistance during mixing, laying and compaction of the asphalt mixture.

o They should show good compatibility with bitumen.

o Most of all, the candidates must be or become active when the pavement is used by traffic to provide self healing capability to the pavement. This means that they should be active at temperatures ranging from -30°C to 70°C.

o Multi-time healing of the self healing material system is to be preferred rather than healing in one time.

Modifications of bitumen at molecular level could be the best choice to develop an asphalt mixture with a strong self healing capability. Table 3-1 gives an overview of self healing material systems and their mechanisms. Among these, ionomers, supramolecular rubbers and nanoparticles are believed to be able to fulfil the requirements. This can be explained with the following reasons.

o The reversible ionic bonding inside ionomers makes them capable to heal multi-times, which could be a possible solution for bitumen. In fact, ionomers have been used to improve the high temperature stability of bitumen and a good compatibility between ionomers and bitumen has been reported [1, 2].

o The reversible hydrogen bonding is the main design idea behind supramolecular rubber. The modification of hydrogen bonding of bitumen could also be a possibility to upgrade the self healing capability of asphalt mixtures.

o Nanoclay particles have shown to be able to modify and improve the rheological characteristics and aging resistance of bitumen and asphalt mixtures [3-5]. Nanoparticles also seem to have an excellent potential to

repair microcracks. The mechanism is that when microcracks develop, the nanoparticles tend to move to the tip of the crack driven by the high surface energy. In this way they are able to stop the crack propagation and to heal it.

Table 3-1 Possibilities of self healing systems for asphalt mixtures

Self healing systems	Mechanism	Effective temperature range for healing	Advantages	Disadvantages	Requirement for hot mix asphalt
Microcapsules	Healing agent and catalyst	Ambient or 48hours at 80°C	Good strength recovery	Works only once	A. Good compatibility with bitumen;
Hollow fibers	Healing agent and catalyst	24 hours at Ambient		Works only once	
Microvascular networks	Healing agent and catalyst	Ambient		Complex	B. high temperature stability of 150-180°C;
Remendable cross-linked polymer	Reversible chemical reaction	30min at 115°C then 6hours at 40°C	Multi-time healing	High healing temperature	C. Severe construction and laying conditions;
Ionomers	Reversible ionic bonding	Ambient	Multi-time healing	Blend	
Nanoparticles	Nano effect	Ambient	Prevent crack growth	Distribution	D. Healing temperature should be around -30 to 70°C;
Supramolecular rubber	Reversible hydrogen bonding	Ambient	Multi-time healing	Aging	E. Multi-time healing
Molecular interdiffusion (thermal)	Wetting and diffusion	7-8min at 115°C	Multi-time healing	Aging	

In this exploration phase, due to limited time, only commercially available novel self healing modifiers were considered and are shown in Table 3-2.

Table 3-2 List of selected novel self healing modifiers

Group	Selected novel self healing modifiers	Abbreviation
Inonomers	Surlyn 8940 from DuPont	SURLYN
Supramolecular rubbers	Silly Putty Molykote R° X-3180 dilatant from Dow Corning	SP
Nanoparticles	Narpow utrafine rubber particles from Sinopec Beijing Research Institute of Chemical Industry	UR
Nanoparticles	Utrafine carbon black	UC
Nanoparticles	Nano Precipitated Calcium Carbonate from Minerals Technologies Inc.	NPCC
Nanoparticles	Nano Silica Oxide	NSIO

o **SURLYN:** Figure 3-3 shows the production process of the ionomers Surlyn® series from Dupont. First, copolymers are made by the reactions of small molecules, and then NaOH is added into the copolymers to introduce ionic groups with Na^+. Finally, ionomers are obtained as polymers with ionic groups of Na^+. Also Ca^{2+}, Zn^{2+} and Mg^{2+} are possible ionic groups in ionomers. The selected Surlyn 8940, which is a 30% Na^+ neutralized inonomer resin, is the most promising self healing ionomer according to the literature [6].
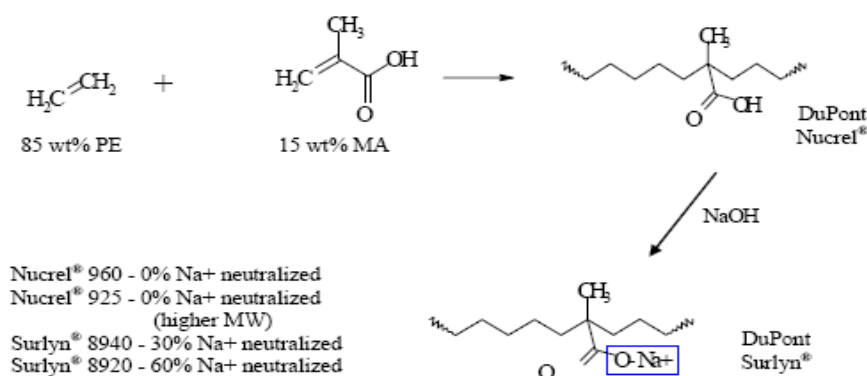
Figure 3-3 Surlyn® ionomer resins [6]

o **SP:** The commercialized Silly Putty (abbreviation, SP) made by Dow Corning is a dilatant, or shear thickening material, which is widely used in toys and bullet proof applications. The basic Silly Putty is made from the reaction of silicone oil with boric acid. A unique reversible network is

then formed with the hydrogen bond O-H. Silly putty is also a visco-elastic material, which behaves ductile under slow loading speed and brittle under fast loading speed [7].

o **UR, UC, NPCC and NSIO:** A number of ultrafine particles are selected for investigations. The particle sizes are ranging from several micrometer of ultrafine carbon black (abbreviation, UC), full-vulcanized ultrafine rubber particles (abbreviation, UR), 100 nm of nano precipitated calcium carbonate (abbreviation, NPCC) and 10-20 nm of nano silica oxide (abbreviation, NSIO).

o **BITUMEN:**

   ▪ The pure bitumen (abbreviation, PB) used for modification is a 70/100 penetration grade bitumen obtained from Kuwait Petroleum. This type of bitumen is commonly used in the Netherlands. It has a penetration of 93 (0.1mm) at 25°C, and a softening point of 45°C.

   ▪ A Styrene-Butadiene-Styrene polymer modified bitumen (abbreviation, PMB) with a penetration of 65 (0.1mm) at 25°C and a softening point of 70°C [8]

   ▪ A very hard penetration grade bitumen (abbreviation, HB) with a penetration of 5 (0.1mm) at 25°C, and a softening point of 84°C.

Bituminous mastics were also used for some preliminary self healing analysis. The mastics were made by mixing bitumen with filler using a ratio of 1:1 by mass. The used filler was a Wigro filler with the characteristics shown in Table 3-3.

Table 3-3 Characteristics of Wigro limestone filler [9]

Density [kg/cm³]	Bitumen number [ml/100g]	Gradation passing the sieve [%]	Voids [vol. %]
2.68-2.88	42-48	0.125mm: 87-97 0.063mm: 77-87	37-41

3.3.2.2 Sample preparation

The selected self healing modifiers are either powders or polymers. To ensure a very good dispersion of the self healing modifiers in the pure bitumen, a Silverson L5M high shear mixer was used (see Figure 3-4). A certain amount of modifier was added to hot bitumen (150 °C) during continuous stirring with a speed of around 3000rpm for 1 hour. After mixing, samples were taken for further analysis.

Figure 3-4 Silverson L5M high shear mixer

3.3.2.3 Characterization methods

3.3.2.3.1 Material analysis

> **Structural analysis**

Figure 3-5 shows the PerkinElmer Spectrum 100 FT-IR Spectrometer which was used for the structural analysis of the novel self healing bitumens. The analysis was done in the attenuated total reflectance (ATR) mode. First, a thin film of bitumen was pasted on the diamond crystal at room temperature. Then the measurement was conducted in the mid-infrared region (600 - 4000 cm^{-1}) in a layer thickness of around 5µm of bitumen. An absorption spectrum diagram through a Fourier transformation function was obtained using the available computer program.
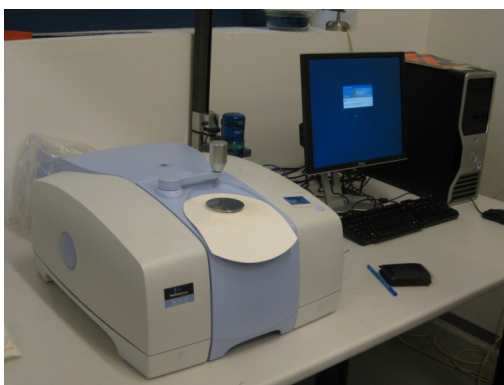
Figure 3-5 PerkinElmer Spectrum 100 FT-IR Spectrometer

> **Morphological analysis**

Figure 3-6 shows the Olympus Fluorescence Microscope, which was used for morphological analysis of the novel self healing bitumens. A droplet of the bitumen sample was taken right after mixing and placed on a glass plate. After it was cooled down to the room temperature, the measurement was conducted.

Through the ultra-violet light from the beam, a fluorescence reaction light from the bitumen sample was captured by the microscope. This picture was transformed into a digital photograph using a computer program provided by Olympus.
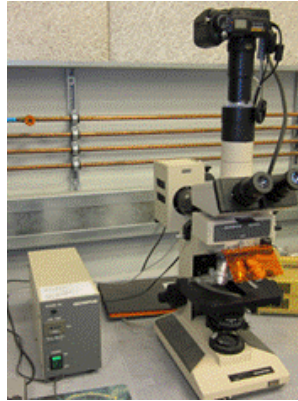
Figure 3-6 Olympus Fluorescence Microscope

> **Rheological analysis**

As shown in Figure 3-7, the Dynamic Shear Rheometer (DSR) measurements were conducted to determine rheological properties of the bitumens with novel self healing modifiers such as the complex shear modulus and phase angle as function of frequency at different temperatures. Two test procedures were used.

o **Temperature sweep:** Temperature sweep measurements were carried out at a constant strain level within the linear elastic range and a fixed frequency of 1Hz. The temperature at which the tests were conducted ranged from -50°C to 60°C. The 8mm diameter parallel plate geometry was used with a sample thickness of 2mm.

o **Frequency sweep:** Frequency sweep measurements were carried out at a strain level within the linear elastic range to obtain G* and δ as a function of temperature and frequency. Measurements were performed at temperatures ranging from -10°C to 40°C and frequencies ranging from 0.01Hz to 50Hz. The 8mm diameter parallel plate geometry was used with a sample thickness of 2mm.
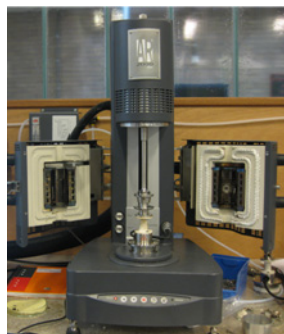
Figure 3-7 Dynamic Shear Rheometer TA AR2000

3.3.2.3.2 Self healing analysis

From the literature review it was concluded that the existing self healing test methods for bituminous materials are too empirical and too complex. An exploration on more appropriate self healing test methods was thus necessary. The new test method should be simple and closely mimic the self healing process. As a result, three potential self healing test methods were developed including the self healing test using the Dynamic Shear Rheometer (DSR), the ductility self healing test and the self healing test using the Direct Tension Test (DTT). The self healing capabilities of the novel self healing bitumens were evaluated by means of these tests. Detailed information can be found in Section 3.3.7 and Section 3.3.8.

3.3.3 Material analysis

3.3.3.1 Chemical structural analysis

The FT-IR spectrums of the novel self healing bitumen (pure bitumen with a percentage of novel self healing modifiers) are shown in Figure 3-8 to Figure 3-16. The following statements can be made from the FT-IR spectra.

- o **SURLYN:** The addition of SURLYN does not change the FT-IR spectrum of bitumen (Figure 3-8). The reason can be that the SURLYN is a C-H back-bonded copolymer, which has similar -CH_2, -CH_3 functional groups like bitumen. Another possibility can be that the addition of SURLYN is not well dispersed due to compatibility problems with bitumen and the measurement is only made through the bitumen phase. This was checked later with a morphological analysis using a fluorescence microscope.

- o **SP:** As shown in Figure 3-9, the pure SP has a distinct different when compared to the pure bitumen. The peak observed at a wavenumber of 1013 cm^{-1} indicates the Si-O bond. The -OH bond can be observed at wavenumbers around 3200cm^{-1}, which is believed to be the key for the self healing behaviour of the SP. When comparing the pure bitumen with the SP modified bitumen in Figure 3-10, the overlap of the Si-O peak from the SP with the S-O peak from the pure bitumen can be observed. But the change is limited because of the limited dosage. In addition, a limited increase in the -OH peak can also be observed.

- o **UR and UC:** The addition of the UR overlaps the peak visible in the bitumen spectrum at around 1301 cm^{-1} (Figure 3-11). Due to the nature of the carbon black, the addition of the UC increases the base line of the spectrum (Figure 3-12).

- o **NPCC and NSIO:** As shown in Figure 3-13 and Figure 3-14, the addition of the NPCC shows an increase in the peak around

wavenumber 875 cm^{-1}. The peak at wavenumber 1455 cm^{-1} is increased and shifted to a lower wavenumber. Figure 3-15 and Figure 3-16 shows that the addition of the NSIO enlarges the peak at wavenumber 1032 cm^{-1}.
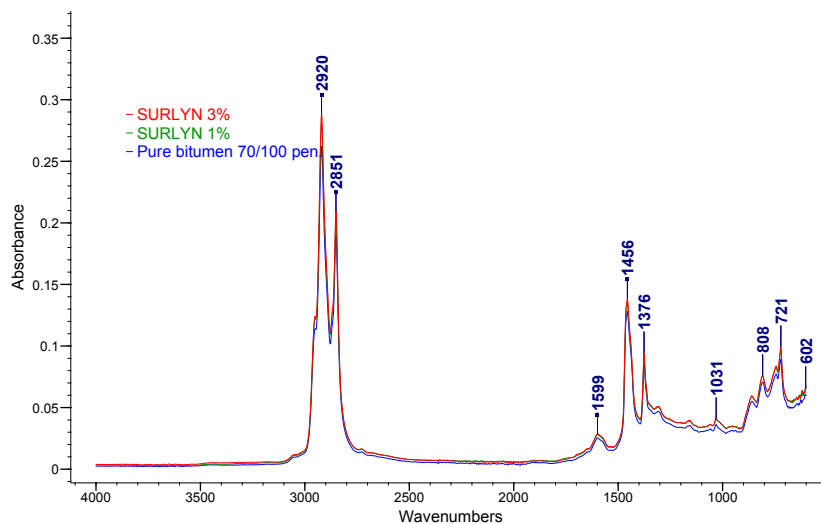
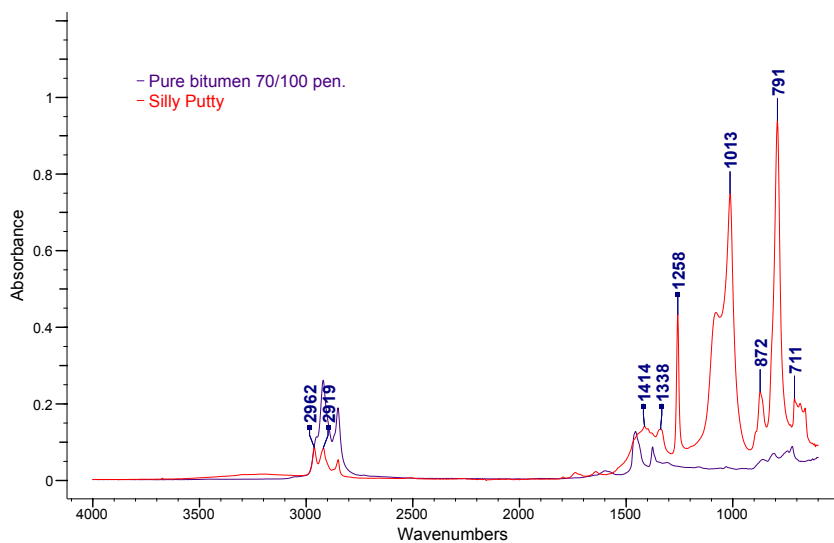Figure 3-8 FT-IR spectrum of pure bitumen, with 1% and 3% of SURLYN

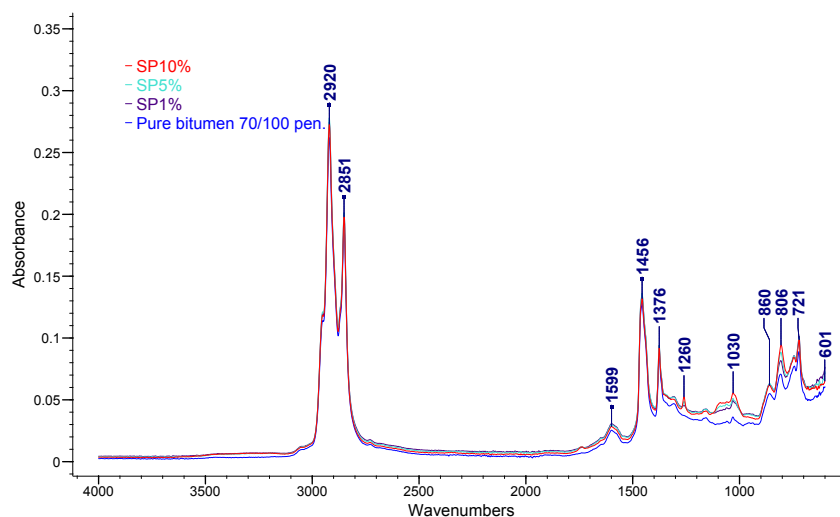Figure 3-9 FT-IR spectrum of pure bitumen and Silly Putty

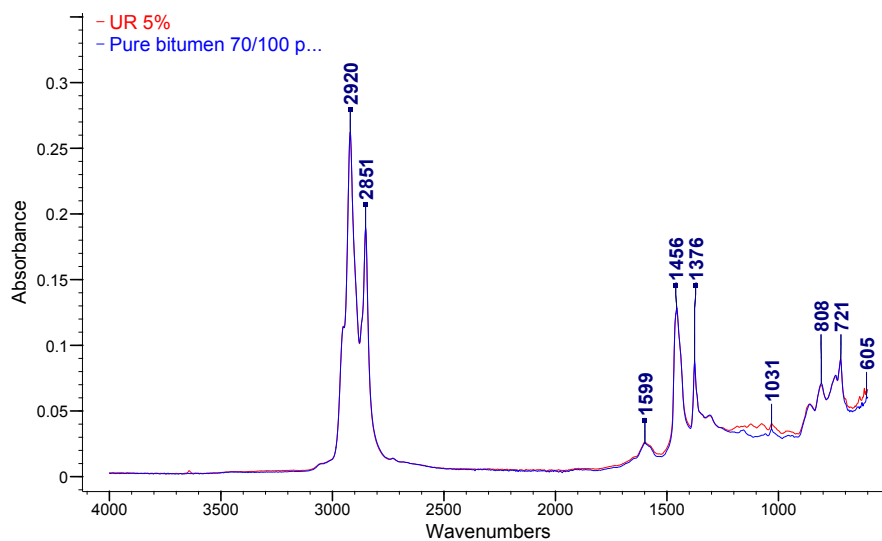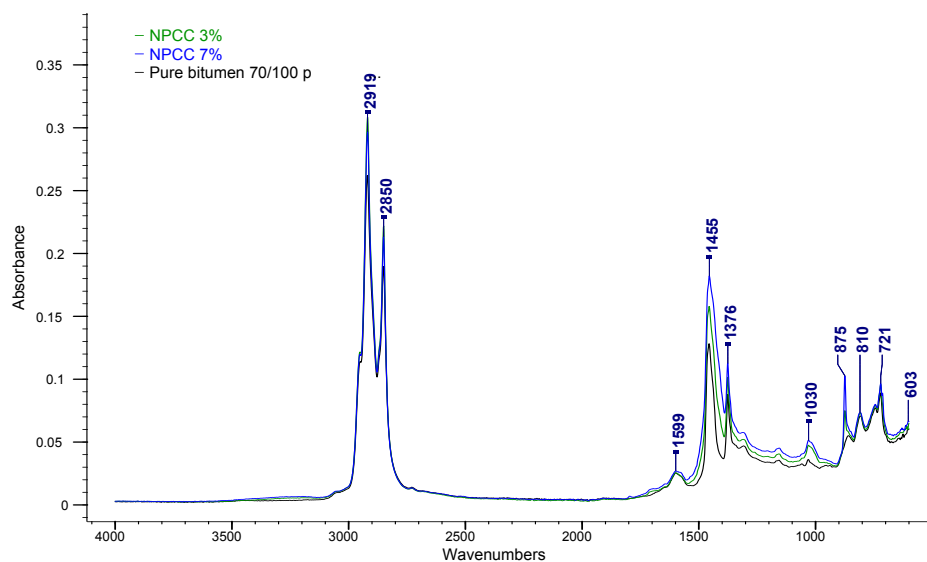Figure 3-10 FT-IR spectrum of pure bitumen, with 1%, 5% and 10% of Silly Putty

Figure 3-11 FT-IR spectrum of pure bitumen, with 5% of UR
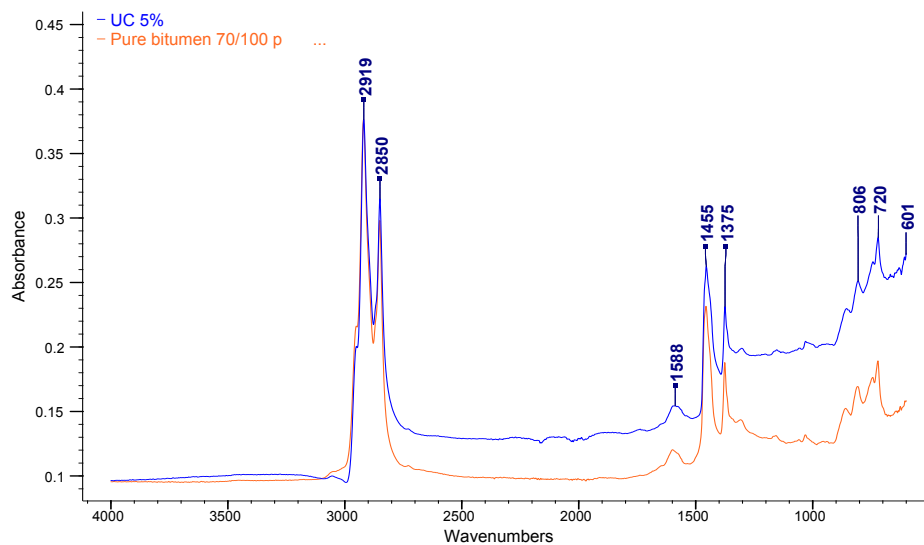
Figure 3-12 FT-IR spectrum of pure bitumen, with 5% of UC
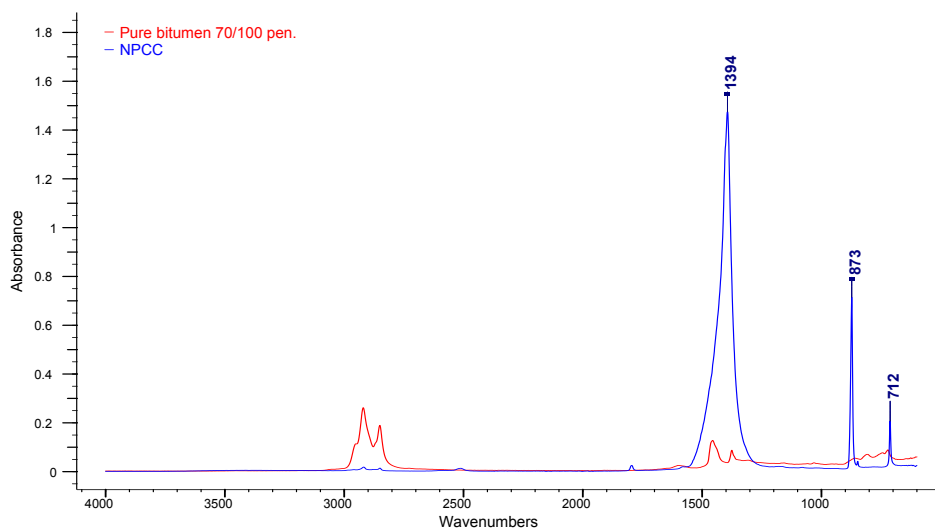
Figure 3-13 FT-IR spectrum of pure bitumen and NPCC

Figure 3-14 FT-IR spectrum of pure bitumen, with 3% and 7% of NPCC
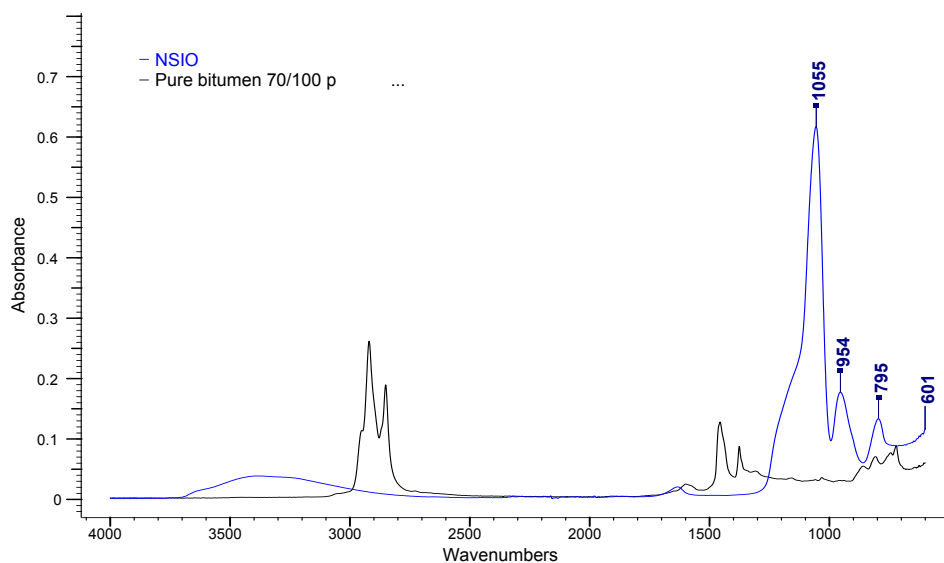
Figure 3-15 FT-IR spectrum of pure bitumen and NSIO
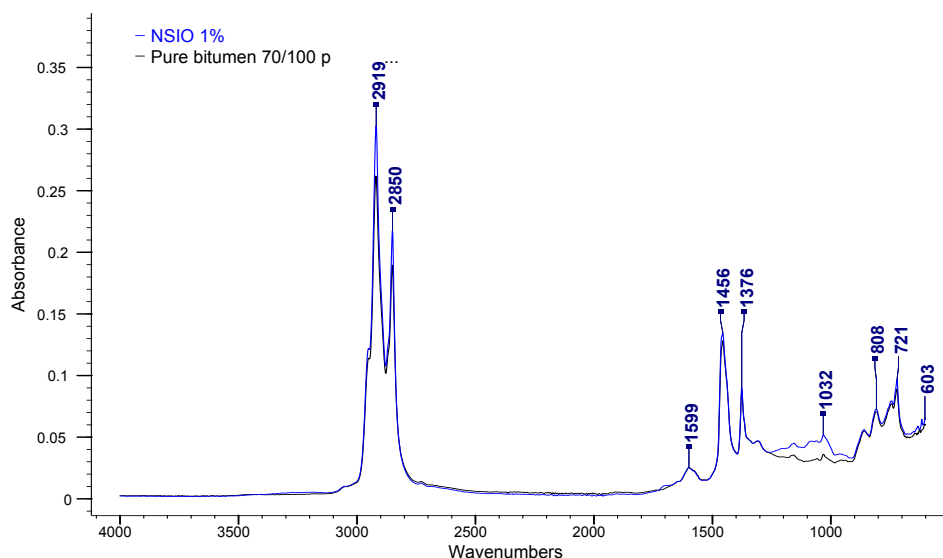
Figure 3-16 FT-IR spectrum of pure bitumen, with 1% of NSIO

3.3.3.2 Morphological analysis

Fluorescence microscope images of the novel self healing bitumen are shown in Figure 3-17 to Figure 3-20. The following statements can be made from the morphological analysis.

o **Pure bitumen and SBS modified bitumen:** In order to verify the effect of the morphological change due to modification, the morphological analysis was first conducted on the pure bitumen and the SBS modified bitumen. The results are shown in Figure 3-17. The figure shows that the morphology of the SBS modified bitumen is distinctively different from the pure bitumen. The observed shinning network is believed to be from the SBS molecules.

o **SURLYN:** As shown in Figure 3-18, the addition of SURLYN can clearly be observed from the fluorescence microscope images. Different from the SBS network like distribution in bitumen, the SURLYN is distributed in the pure bitumen with an average particle size of around 10µm.

o **SP:** As shown in Figure 3-19, the pure SP shows shinning fluorescence light due to its high reactivity with the ultra-violet light. When looking into the morphological change of the pure bitumen due to the SP modification, the SP particles can not be detected easily at dosages of 1% or 5%. Instead, segregation was noticed between the bitumen phase and the SP phase, especially at a dosage of 10%. It seems like the two phases are not compatible. During the experiment, it was also observed that the SP phase tended to float on top of the pure bitumen after storage for some time in an oven. This indicates incompatibility of the two phases. This problem is believed to be

caused by the difference in the C-H backbone materials and the Si-O backbone materials.

o **UR:** When adding 5% of UR to the bitumen, the particles distribute homogenously in the bitumen phase (Figure 3-20). Our observations show that they are dispersed with a diameter of around 10μm.

o Due to the inorganic nature of the UC, NPCC, NSIO particles, they can not be detected by means of fluorescence microscopy. As a result, no morphological observations could be made on these modified bitumens.
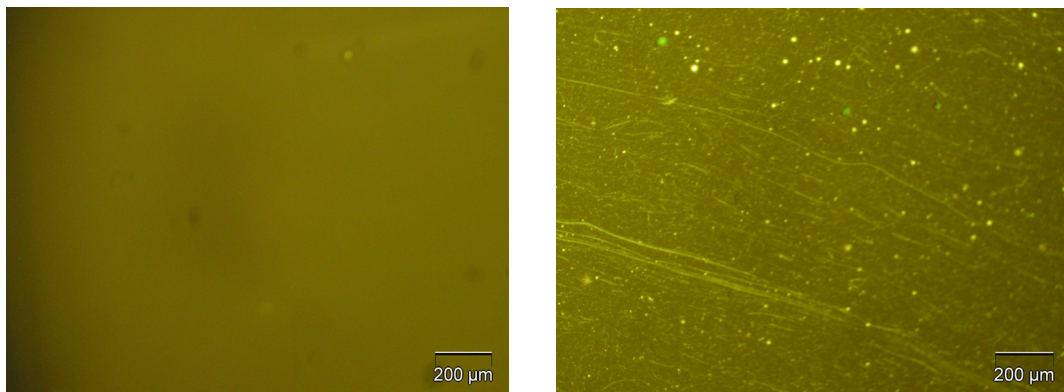

Figure 3-17 Fluorescence microscopy of pure bitumen (left) and SBS modified bitumen (right)
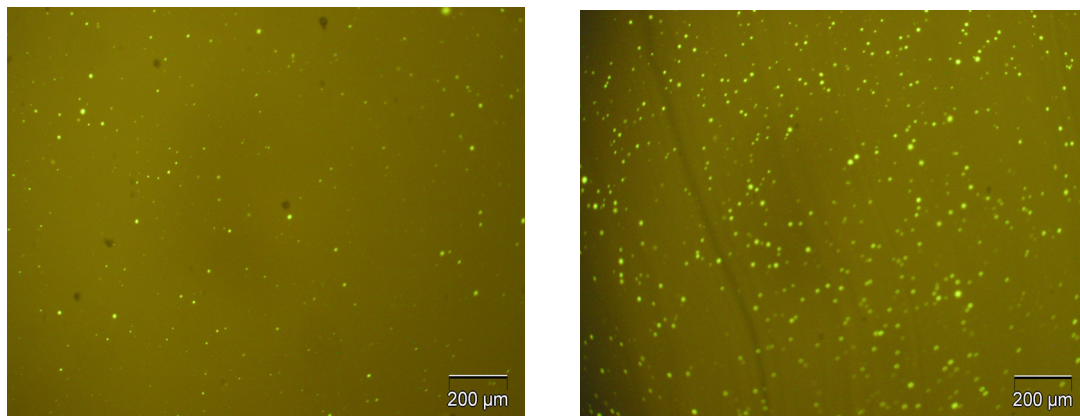
Figure 3-18 Fluorescence microscopy of novel self healing bitumen with 1% of SURLYN (left) and with 3% of SURLYN (right)
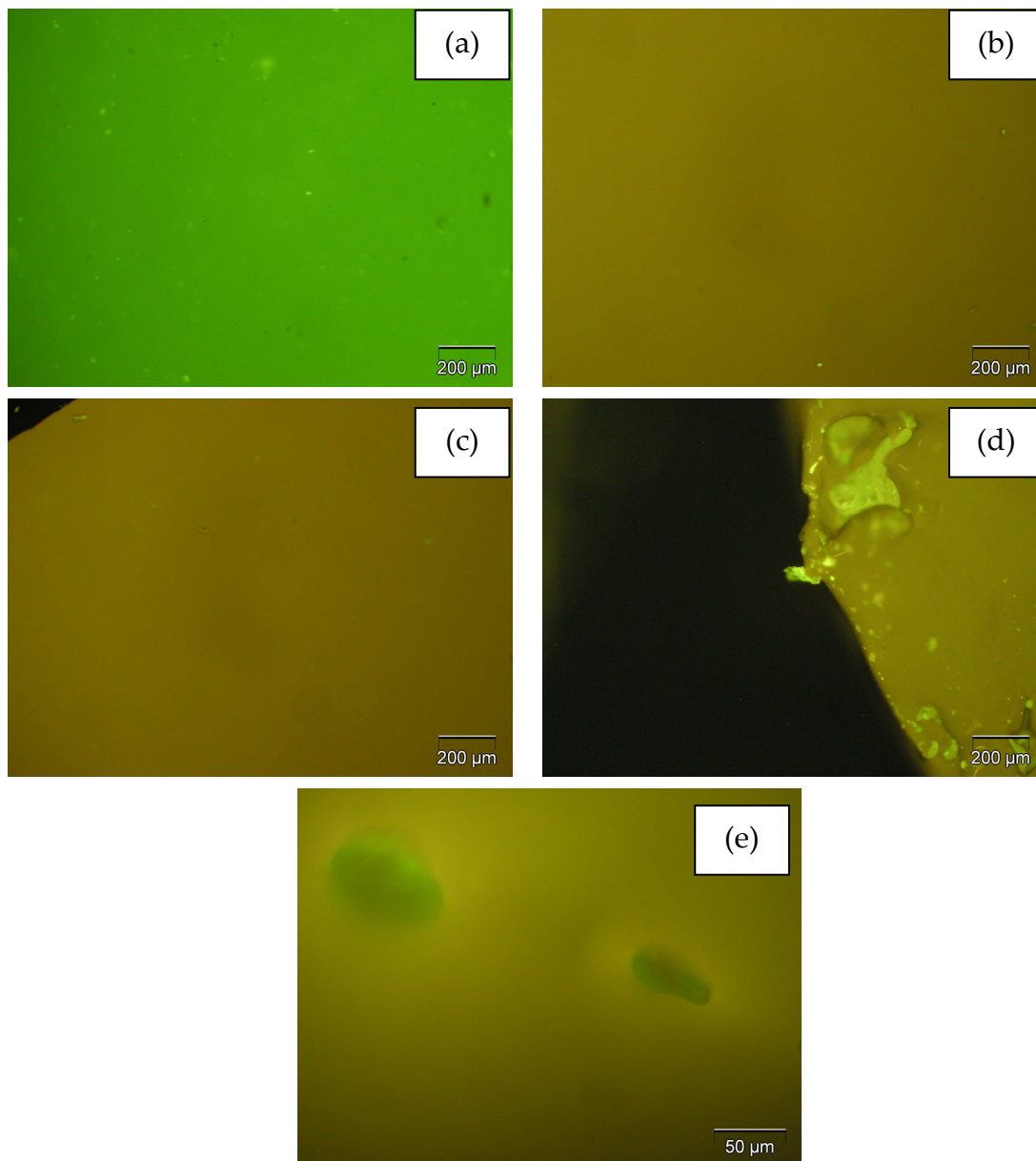
Figure 3-19 Fluorescence microscopy of (a) pure SP, (b) bitumen with 1% SP, (c) 5% SP, (d)10% SP and (e) detail of 5% SP
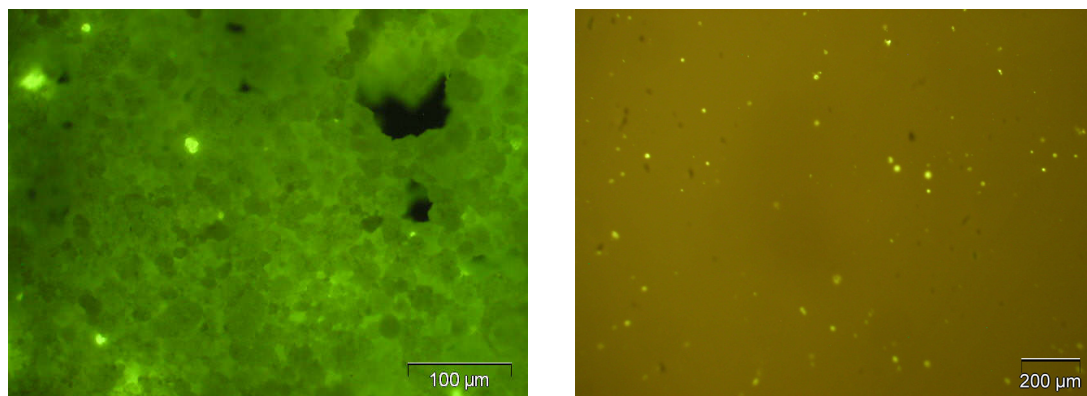
Figure 3-20 Fluorescence microscopy of UR (left), pure bitumen with 5% UR (right)

3.3.3.3 Rheological analysis

Prior to the rheological analysis of the novel self healing bitumen, a preliminary research was conducted on the influence of the test parameters on the rheological behaviour of the pure bitumen.

Figure 3-21 shows the frequency sweep data of the pure bitumen which were obtained at different test temperatures and frequencies. As a visco-elastic material, master curves of the complex shear modulus and the phase angle can be constructed using the Time-Temperature superposition principle. This principle allows shifting the response data obtained at various temperatures with respect to time or frequency to a reference temperature. The amount of shifting required at each temperature can be obtained using Arrhenius equation as shown in Equation 3-1. Apparent activation energy of 488.5 KJ/mol was obtained for pure bitumen to construct its master curves.

$$\log \alpha_T(T) = \frac{\Delta E_a}{2.303R}\left(\frac{1}{T} - \frac{1}{T_0}\right)$$
3-1

where,

T_0 = reference temperature, [K];

T = test temperature, [K];

ΔE_a = apparent activation energy, [J/mol];

R = universal gas constant, 8.314 [$J/(mol \cdot K)$].
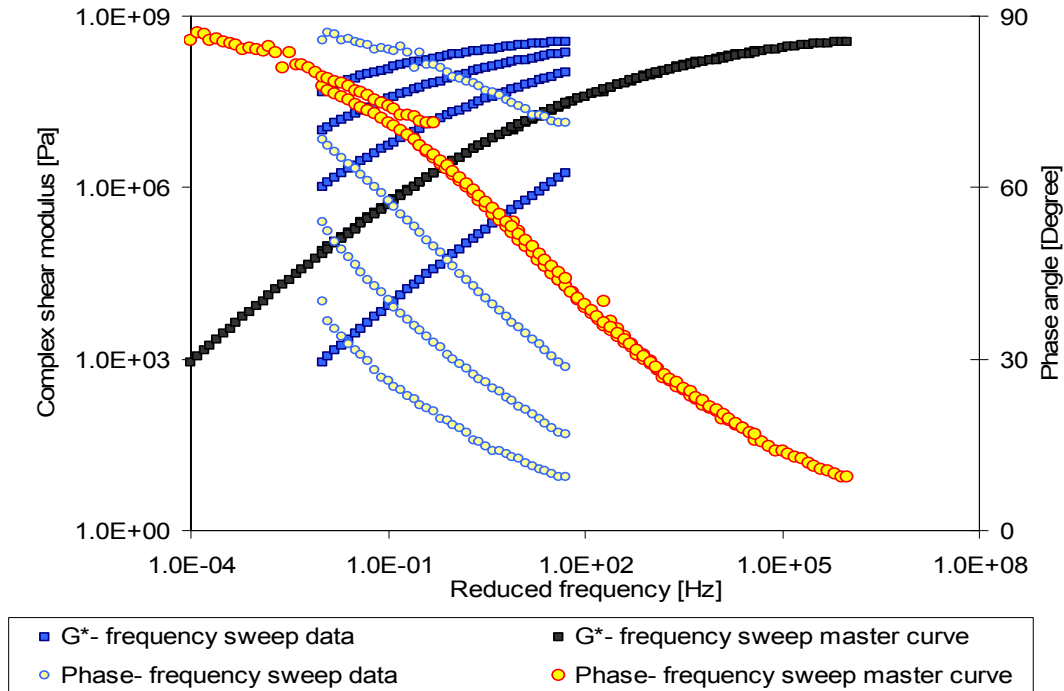
Figure 3-21 Results of the frequency sweep data of pure bitumen and its master curves at a reference temperature of 20ºC

91

Figure 3-22 shows the temperature sweep data of the pure bitumen which were obtained from a temperature ramping program with a fixed measuring frequency of 1Hz. An 8mm parallel-plate system was used during the measurement with different gap widths as 1mm, 2mm and 4mm.
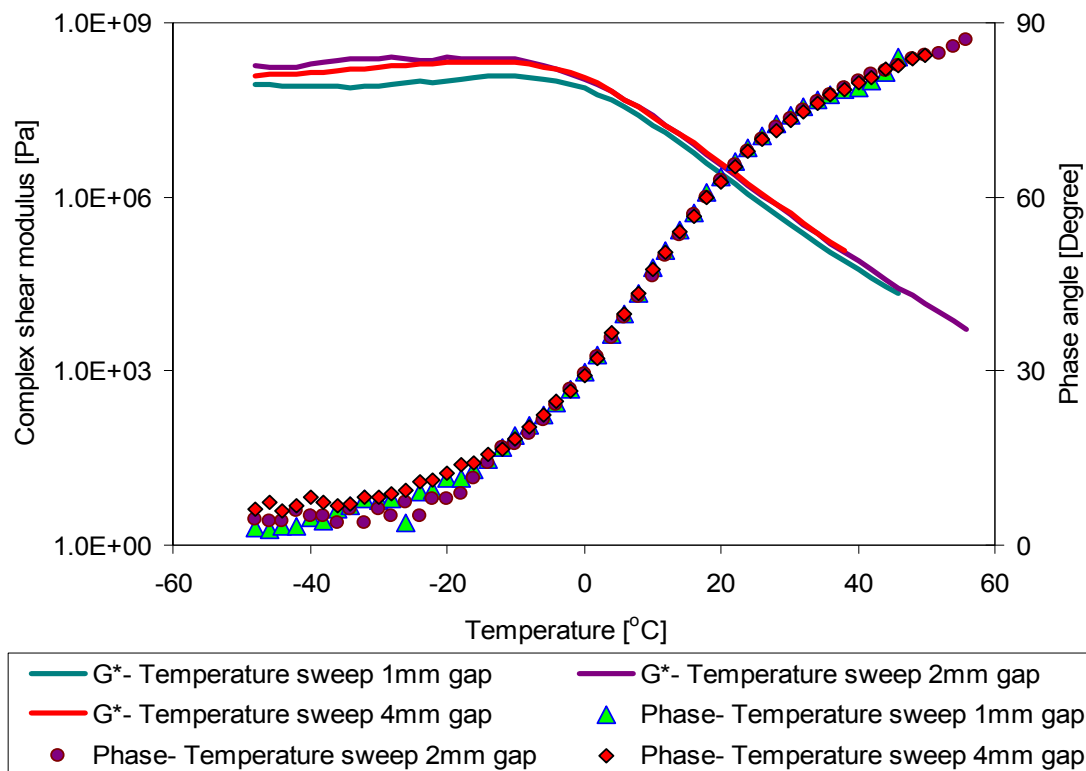

Figure 3-22 Results of the temperature sweep data of pure bitumen at 1Hz

Figure 3-23 compares the frequency sweep master curves with the temperature sweep curves at different gap widths at a reference temperature of 20 °C. In order to compare the frequency sweep data with the temperature sweep data in an efficient way, the time-temperature superposition principle was also applied to the temperature sweep data. The Arrhenius equation with the apparent activation energy of 488.5 KJ/mol was used to shift the temperature sweep data to a reference temperature of 20 °C.

The following statements can be made from the results:

- The plateau value in the low temperature range of the temperature sweep curve represents the glass complex shear modulus [10]. A small gap thickness of 1mm shows a lower complex shear modulus in the glassy range. Using a gap thickness of 2mm and 4mm results in an almost similar complex shear modulus in the glassy range.

- No influence of the gap thickness on the development of the phase angle can be observed during the visco-elastic state. A gap thickness of 4mm shows a slightly higher phase angle in the glassy state.

o When comparing the temperature sweep with the frequency sweep, the glass state of the temperature sweep can not be well captured by simply extrapolation of the frequency sweep master curve. The frequency sweep master curve tends to overestimate the glassy state plateau value.

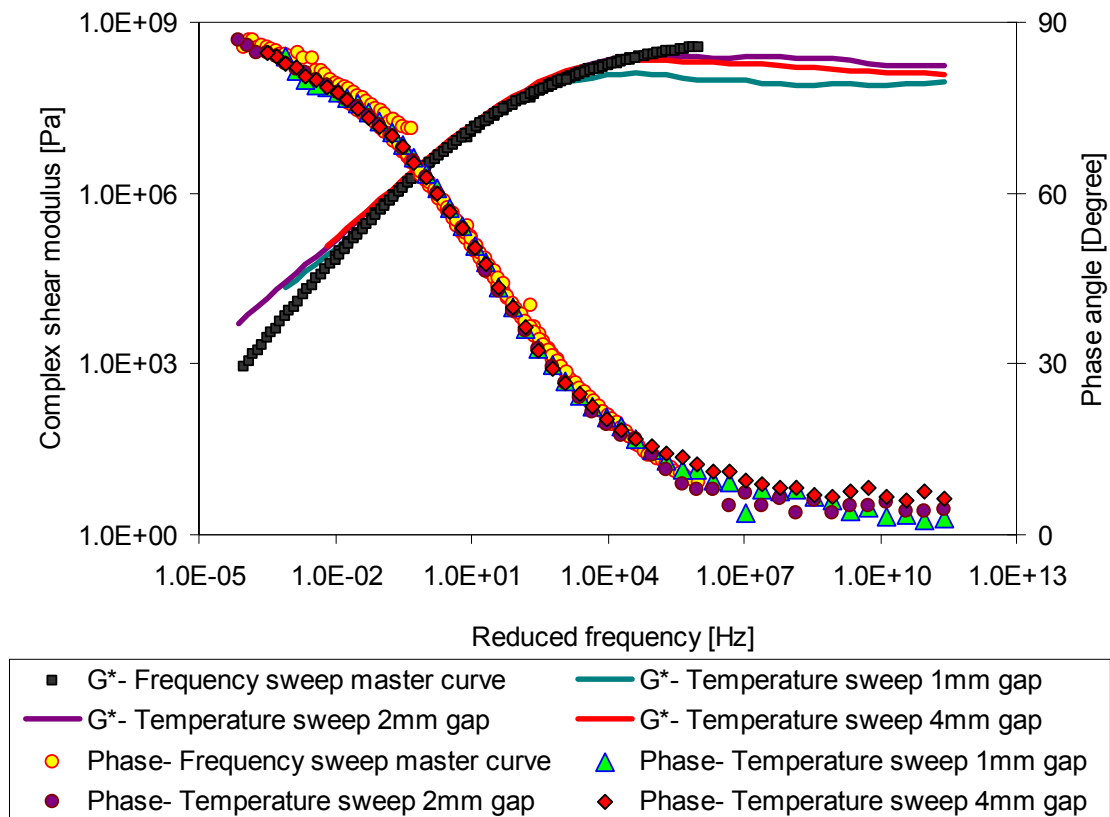o A small gap thickness of 1mm shows a better fit with the frequency sweep data at the high temperature range.

Figure 3-23 Comparison of the frequency sweep master curve with the temperature sweep curve with different gap thickness at reference temperature of 20°C

Table 3-4 Activation energy (ΔEₐ) as determined using the Arrhenius equation for master curve construction

Name	Pure bitumen	SURLYN 1%	SURLYN 3%	SP	SP 1%	SP 5%
ΔE_a [KJ/mol]	488.5	494.9	496.1	73.5	470.5	484.6

Name	SP 10%	UR 5%	UC 5%	NPCC 3%	NPCC 7%	NSIO 1%
ΔE_a [KJ/mol]	475.6	495.1	495.1	495.8	497.2	478.1

The results of the rheological analyses of the novel self healing bitumens are shown in Figure 3-24 to Figure 3-27. Table 3-4 gives all the time-temperature superposition shift factors used for to the master curve construction. The experimental observed data are shifted to construct the master curves. It should be noted that no phenomenological model like the Christensen Anderson Model (CAM) was used.

- o **SURLYN:** As shown in Figure 3-24, the addition of the SURLYN modifier increases the complex shear modulus and decreases the phase angle. However, because of the limited dosage of SURLYN (up to 3%), the change is very limited. The plateau value in the low temperature range of the temperature sweep curve represents the glass complex shear modulus [10]. The addition of SURLYN increases the glass complex shear modulus while a limited decrease in the phase angle can also be observed. The temperature susceptibility of the bitumen does not change due to the addition of SURLYN. This is concluded by comparing the slope of the complex shear modulus vs. temperature curves.

- o **SP:** The rheological properties of SP modified bitumen are shown in Figure 3-25. There is a distinct difference between the master curve of the pure bitumen and the pure SP. The SP is a rubber-like visco-elastic material, which is more sensitive to frequency or loading speed, but not so sensitive to the test temperature. It has a very low activation energy of 73.5 KJ/mol, and its reduced frequency range in the master curve is a lot shorter than that of the pure bitumen. Due to the similarity of the SP and the pure bitumen in modulus, the complex shear modulus and the phase angle of the SP modified bitumen does not change much when the dosage is 1% and 5%. When the dosage is 10%, the high frequency range changes. When looking into the temperature sweep, a slight decrease in the temperature susceptibility can be observed due to the SP modification. It should be noted that the incompatibility between the SP phase and the pure bitumen phase may also play a role in the variation of the rheological properties of the SP modified bitumen.

- o **UR and UC:** Figure 3-26 shows the results of the master curves obtained on the UR and UC modified bitumen. The UR modification shows almost no change in the complex shear modulus and phase angle compared to the pure bitumen. The UC modification increases the complex shear modulus and slightly decreases the phase angle. When comparing with the pure bitumen in the temperature sweep, the UR modified bitumen shows a lower glass complex shear modulus and the UC modified bitumen shows a higher glass complex shear modulus. In addition, both the UR and UC modifiers

decrease the temperature susceptibility of the bitumen. Especially for the UR modification, a rotation in the phase angle development vs. temperature can clearly be observed.

o **NPCC and NSIO:** Figure 3-27 shows the rheological results of the NPCC and the NSIO modified bitumen. Unfortunately, almost no change of the rheological properties can be observed through the master curve.
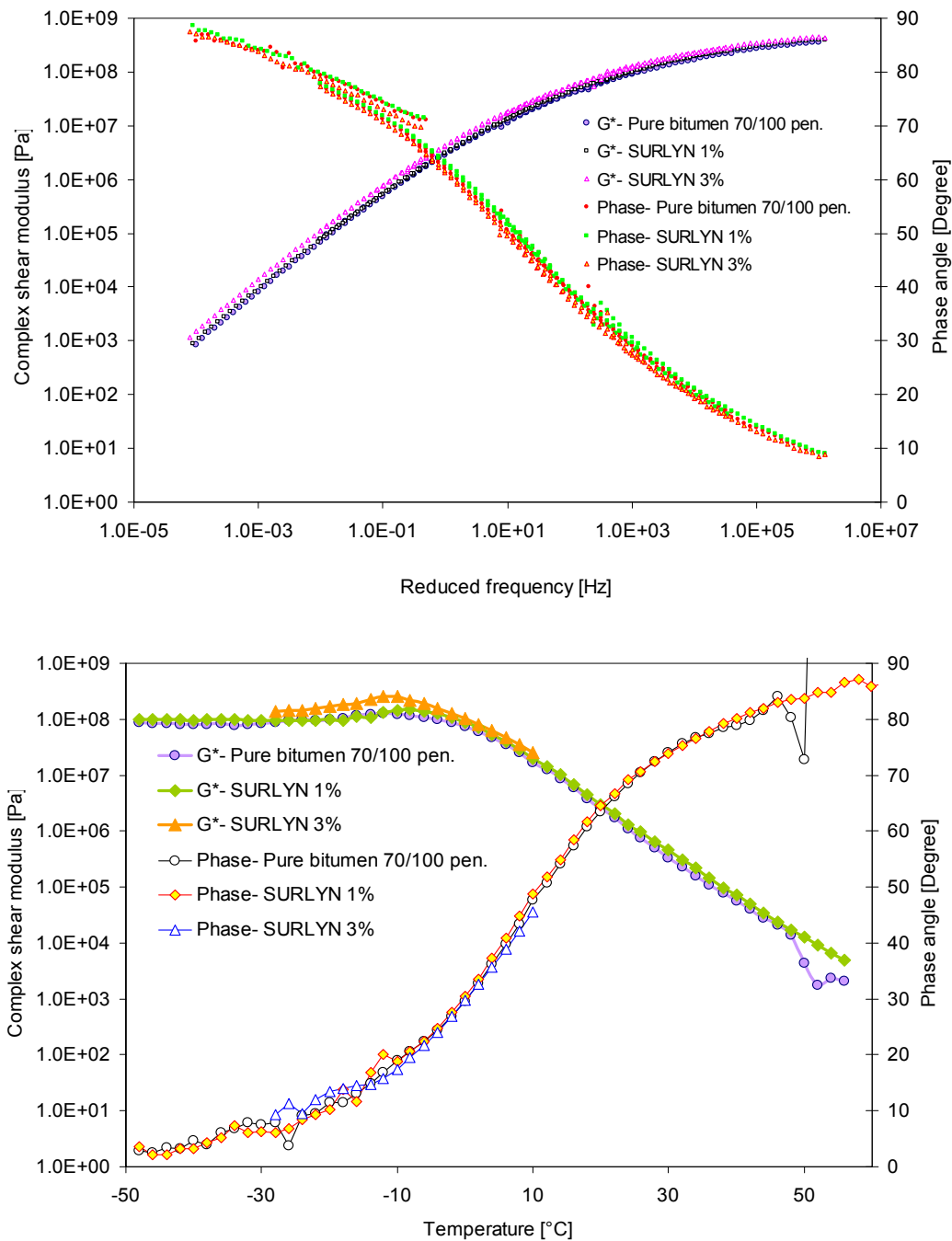

Figure 3-24 Rheological analysis of novel self healing bitumen with SURLYN modifiers: master curves at a reference temperature of 20°C (upper) and temperature sweep results at a frequency of 1Hz (lower)
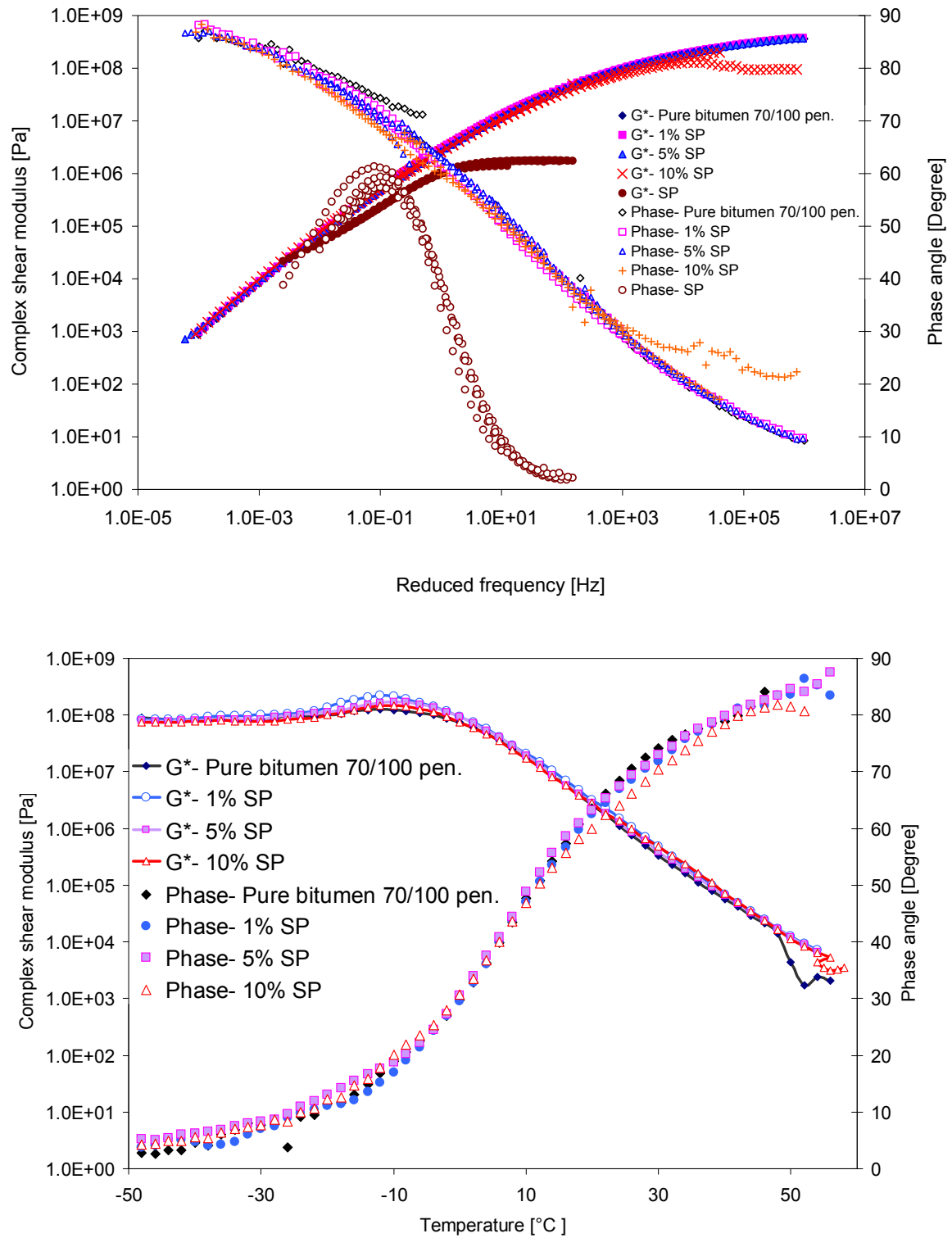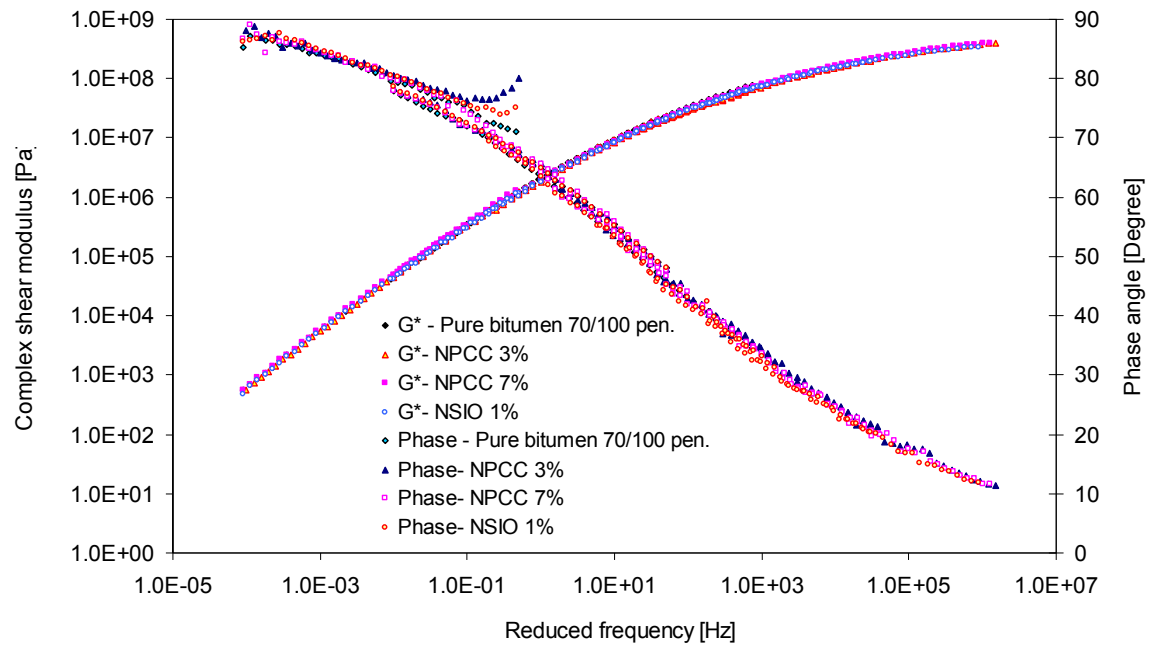
Figure 3-25 Rheological analysis of novel self healing bitumen with SP
modifiers: master curves at a reference temperature of 20°C (upper) and
temperature sweep results at a frequency of 1Hz (lower)
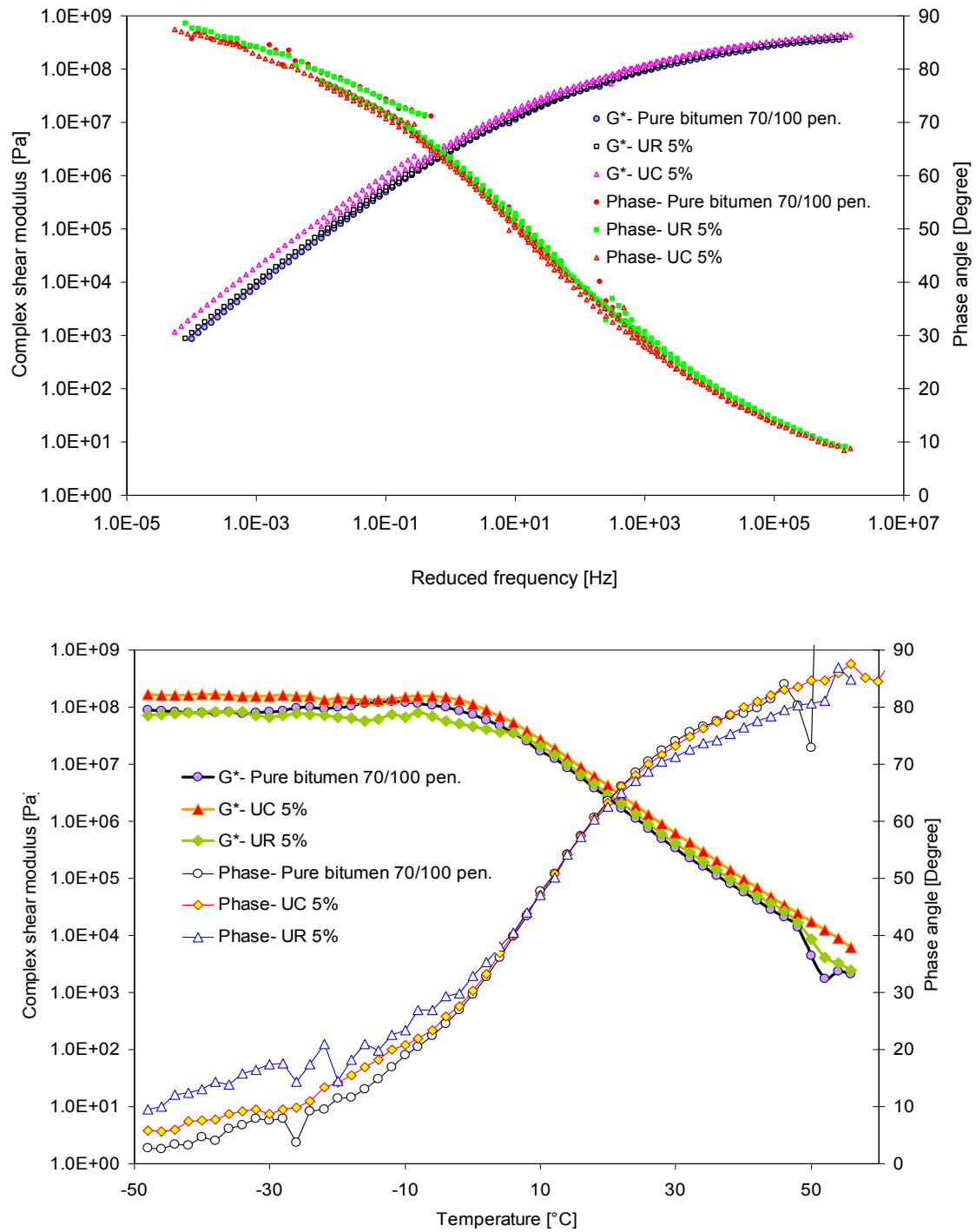
Figure 3-26 Rheological analysis of novel self healing bitumen with UR and UC modifiers: master curves at a reference temperature of 20°C (upper) and temperature sweep results at a frequency of 1Hz (lower)

Figure 3-27 Rheological analysis of novel self healing bitumen with NPCC and NSIO modifiers: master curves at reference temperature of 20°C

3.3.4 Self healing analysis

3.3.4.1 Introduction

In order to quantify the self healing capability of bituminous materials in a simple and effective way, the potential of several self healing test methods was explored. Inspired by the physical-chemical self healing model and the test methods for the novel self healing material systems shown in the literature review, the study of the self healing process was initially simplified to study healing of a single open crack. During this process, the healing time, healing temperature and other influencing factors were taken into account. In this exploration phase, four new self healing test methods were proposed as listed in Table 3-5 namely a ductility self healing test, a self healing test using the DSR, a self healing test using the DTT with standard specimen and a self healing test using the DTT using modified specimen.

Table 3-5 Overview of the self healing test methods

Test methods	Loading methods	Healing methods	Indicators	Materials tested
Ductility self healing test	5cm/min at 5°C	4 hours at 20-22°C	Length at break	Pure bitumen Bitumen modified with 1-5% of NanoA and NanoB
Self healing test using the DSR	Two-piece methods with strain level of 0.00625% at 10 Hz at 20 °C	200 mintures at 20°C	Complex shear modulus	Pure bitumen (PB) Polymer modified bitumen (PMB) Hard bitumen (HB)
Self healing test using the DTT with standard specimen	10 mm/min at 0°C	3, 6, 20 and 48 hours at room temperature about 22°C	Strength	Pure bitumen (PB) Polymer modified bitumen (PMB) Hard bitumen (HB)
Self healing test using the DTT with modified specimen	10mm/min and 100mm/min at 0°C with modified DTT specimen	3, 6, 24 hours at 20°C	Strength	Pure bituminous mastics (PBmas) Novel self healing bituminous mastics

3.3.4.2 The ductility self healing test

The ductility self healing test is shown in Figure 3-28. First, the ductility samples were prepared and then cut into two parts with a sharp knife (Figure 3-28-a); after cutting the specimen, the obtained two parts were placed on a glass plate to ensure alignment. A small force by hand was then applied via the metal mould to make sure that the two cut surfaces of the bitumen briquettes were in full contact with each other. After about 10s, the force was relieved (Figure 3-28-b); finally, the side moulds were fixed and then the samples were allowed to heal at room temperature (about 20-22°C) for a period of 4 hours (Figure 3-28-c). After this healing time, ductility tests were conducted on the self healed samples at 5°C and at a displacement rate of 5cm/min. The tests were performed in a water bath. For comparison purposes, the original samples without any treatment were also tested. These tests were only done with two types of ultrafine rubber particles NanoA and NanoB.

The test results are shown in Figure 3-29. The self healing percentage was calculated as follows:

$$H_{Ductility} = \frac{L_{healed}}{L_{original}} \times 100\%$$

3-2

where,

$H_{Ductility}$ = the self healing percentage observed in the ductility test;

L_{healed} = the length at break of the self healed samples;

$L_{original}$ = the length at break of the original samples.

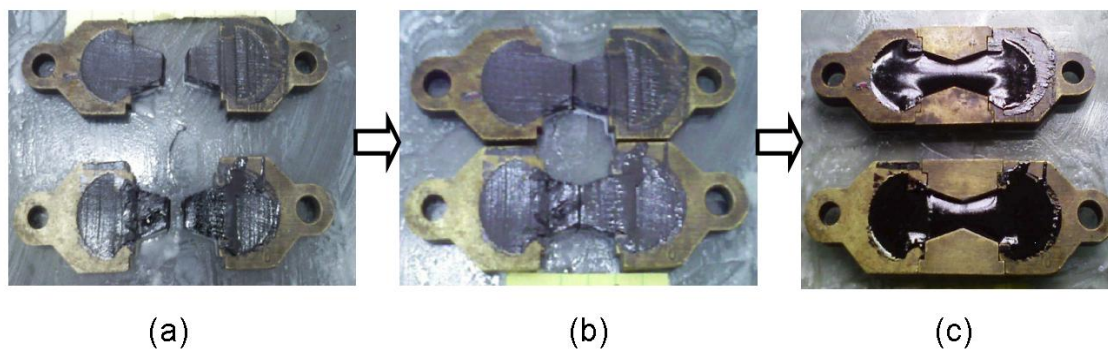(a)   (b)   (c)

Figure 3-28 Illustration of a self healing test with the ductility apparatus

Figure 3-29 shows that both the unmodified pure bitumen and the modified bitumen have self healing properties. After being cured at room temperature for 4 hours, the pure bitumen recovered to 70% of its original ductility. Also the modified bitumen recovered between 15% and 90%, depending on the type of modification and the concentrations used.
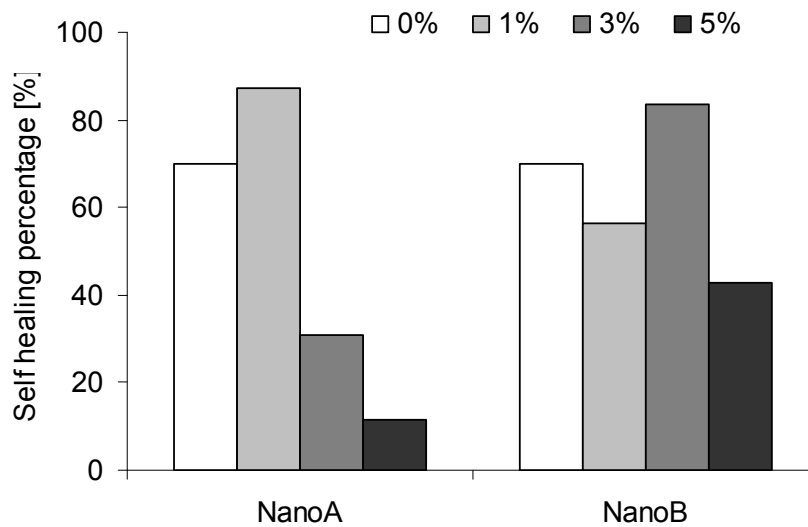
Figure 3-29 Results of ductility self healing tests at 5°C, 5 cm/min for different concentrations of Ultrafine rubber particles NanoA and NanoB on pure bitumen 70/100 pen. (Different concentrations of NanoA and NanoB were mixed with pure bitumen in an ESR-500 high shear mixer at 5000 rpm at 150°C for 1 hour)

However, it is concluded that the ductility self healing test is not very suitable for further self healing investigations. The reason is that a large deformation of the specimen can be expected even when the ductility test is conducted at 5°C and a displacement speed of 5cm/min. This introduces artefacts, e.g. elongation, plastic deformation, etc which are not really related to the self healing.

3.3.4.3 Self healing test using the DSR

The DSR test was used to investigate the self healing capability of the shear modulus of bituminous binders at small strains. This test setup was first used by Bhasin and his co-workers [11]. Two pieces of bitumen are attached to the upper and the bottom plates of a plate-plate DSR configuration. Then the two parts are pressed together with the DSR machine till a certain thickness and the change of the shear modulus over time is measured. A small strain level is used during the testing to avoid any disturbance in the development of self healing between the two bitumen samples.

The following test method is adopted in this research. Two pieces of bitumen, each with a diameter of 25 mm and a thickness of 4 mm, were brought together and pressed to a height of 7.8 mm to make sure that the two surfaces were fully in contact with each other. The reason for the thickness of 4mm is meant to treat the test geometry as bulk material as good as possible. Then the cohesive healing behaviour of the bulk material can be investigated. The test was conducted at a small strain level of 0.00625% at 10 Hz during 2 minutes and

then followed by a rest period of 8 minutes. The total test duration was 200 minutes (20 measurements). Testing was done at a temperature of 20°C.

The percentage recovery is calculated by using the measured shear modulus of the self healing samples divided by the reference modulus as follows:

$$H_{DSR} = \frac{M_{healed}}{M_{original}} \times 100\%$$

3-3

where,

H$_{DSR}$ = the self healing percentage as determined using the DSR test;

M$_{healed}$ = the observed modulus of the self healed samples;

M$_{original}$ = the modulus for the original samples.

Figure 3-30 shows the healing curves of bitumen samples during the tests. The initial healing percentage is quite high, between 30% and 60%. After 1 hour, most curves tend to become stable. It is believed that the initial healing can be related to the wetting mechanism and a further increase in time of the self healing ratio may be attributed to the diffusion mechanism [11].

Among the bitumens tested, the pure bitumen (PB) has the best short term healing effect; 50% recovery was observed in the beginning, and 80% healing after 30 minutes. It took more time for the polymer modified bitumen (PMB) to heal itself compared to PB but it heals to a higher ratio. Reasons are: less wetting for the short term and a longer diffusion time is needed as observed in the tests. PMB heals from 40% at the beginning to 100% after 90 minutes. Hard bitumen (HB) does not show any improvement over time. After the test, the HB sample can easily be removed and separated into two parts. The modulus of HB observed in the beginning is probably largely caused by the friction and hardly by wetting at the surfaces.

The DSR test can be used for a fast check of the modulus healing of bituminous materials. However, this test method is rated as being complex and the results can be influenced by artefacts. The compressive stress to which the binder is subjected was not under control with the DSR machine. The confinement offered by this compressive stress certainly has an effect on the healing process.
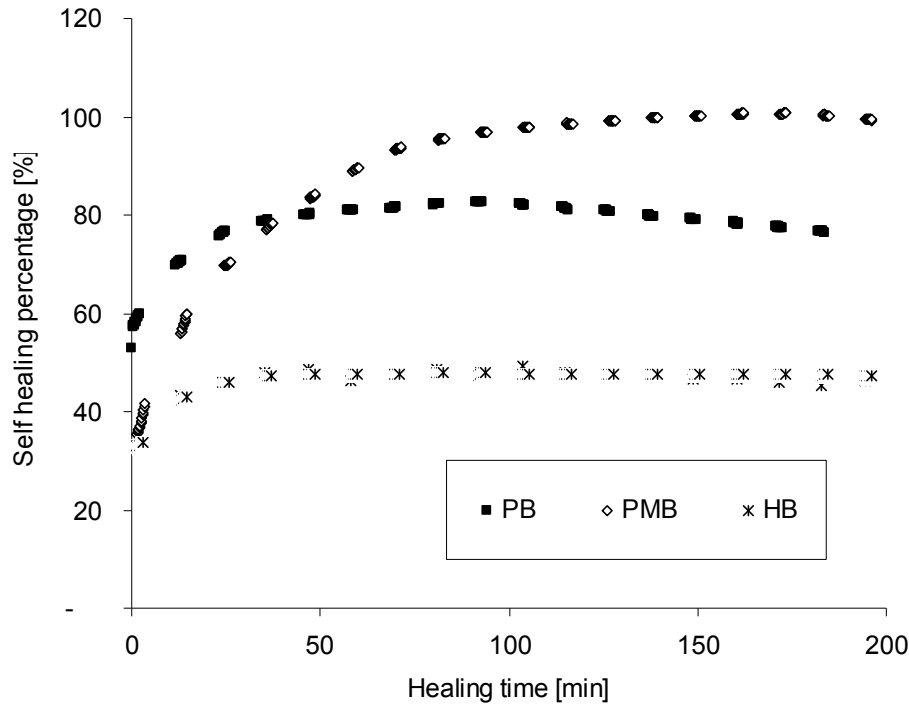
Figure 3-30 Preliminary results from DSR self healing tests (recovery of stiffness) at 20°C (PB, pure bitumen; PMB, polymer modified bitumen; HB, hard bitumen)

3.3.4.4 Self healing test using the DTT with standard specimen

As shown in Figure 3-31, standard dog-bone shape direct tension test samples were used. After production of the samples they were cut into two equal parts with a sharp knife at 5°C to avoid ductile damage (Figure 3-31-a). The two cut surfaces were brought together and then placed into a silicone rubber mould (Figure 3-31-b). The samples were then cured at room temperature (around 22°C) for healing. After curing for 3, 6, 20 and 48 hours (Figure 3-31-c), the DTT tests were performed to determine the stress-strain properties at a temperature of 0°C and a loading speed of 10mm/min.

The percentage recovery is calculated by using the measured strength of the self healing samples divided by the reference strength as follows:

$$H_{DTT} = \frac{S_{healed}}{S_{original}} \times 100\%$$

3-4

where,

H_{DTT}	= self healing percentage as determined by means of the DTT test;
S_{healed}	= strength of the self healed samples;
$S_{original}$	= strength of the original samples.

103

Figure 3-32 shows that the strength increases over time, which indicates the occurrence of healing. After 6 hours curing, the PB shows almost the same strength as original. Sometimes, the samples are broken at a location other than the healing surfaces, which means that the samples are fully healed. The healing capability of PMB samples is second best. The self healing percentage grows to 80% when cured for 6 hours. The strength recovery is still 80% after 48 hours, which indicates that the diffusion of the molecules has almost stopped after 6 hours. The HB shows almost no healing in time.

| (a) | (b) | (c) |
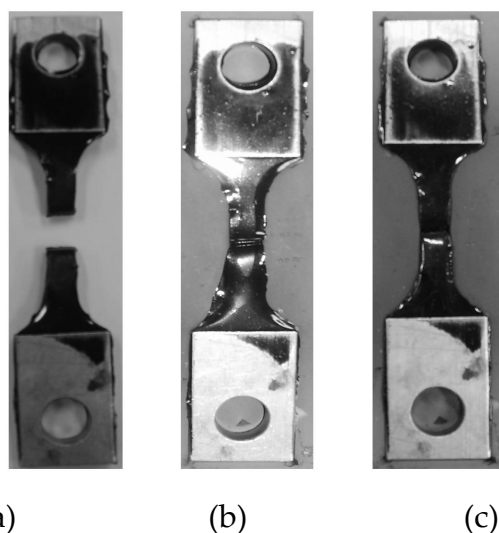
Figure 3-31 Illustration of self healing test using the DTT
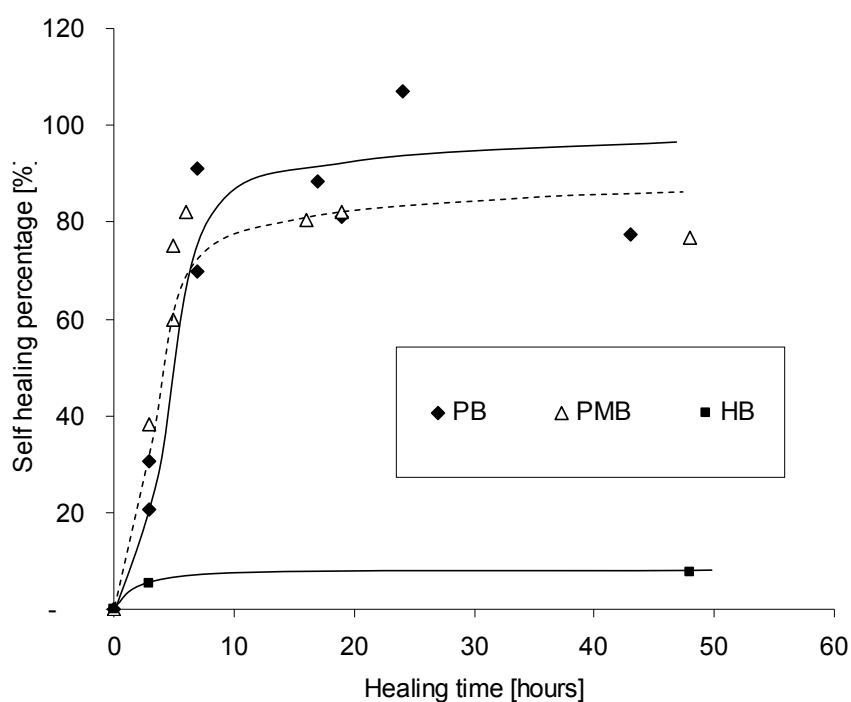
Figure 3-32 DTT self healing test results (recovery of strength) on DTT bitumen specimen at 0 °C and 10 mm/min

The self healing test using the DTT specimen is good for a fast check of the strength healing of bituminous materials. However, the dog-bone shaped sample geometry gives variable results. The arbitrarily chosen loading speed of 10mm/min introduced large elongation to the samples.

In addition, it was concluded that cutting the specimens using a knife is not so desirable because it causes artefacts in the measurements. This process interrupts the morphology of the two broken surfaces and also shortens the specimen. Alternatively, the specimens were first fractured using the DTT machine to produce reliable crack surfaces.

After several trials, it was then observed that these standard DTT specimens were not really suitable because of the following reasons:

o   Firstly, a sudden break of the normal DTT specimens during the fracture test would cause the sample to break into more than two pieces, making further healing and re-fracture testing almost impossible.

o   Secondly, in order to get an indication of the healing of the crack, the re-fracture surface was supposed to be the same as the initial fracture surface. However, sometimes the re-fractured sample did break at a different place than the first fracture surface, which caused variable results.

Hence, there was a need for a special specimen geometry for the self healing investigations.

3.3.4.5 Self healing test using the DTT with modified specimen

Figure 3-33 shows the special specimen geometries developed in this work. Inspired by the fracture-mechanics based fracture tests reported in literature [12-14], specimens were developed with such a shape that stress concentrations would occur. Two types of such specimens were developed namely a double-edge notched shaped specimen (DN) and a double-edge parabolic shaped specimen (DP). A standard dog-bone shaped DTT specimen is shown for comparison.

It should also be noted that, from here on, the specimens used in the DTT test were all made of bituminous mastics (bitumen/filler ratio of 1:1) to taken into account the influence of the filler.

Figure 3-34 shows the results of finite element analyses that were carried out [15]. An elastic modulus of 50MPa and a Possion's ratio of 0.45 were arbitrarily chosen and assigned to the specimen. A tensile load of 100N was applied. The stress concentration in the middle of the DN and DP specimen can be observed clearly. For a standard DTT sample geometry, the stress distribution in the middle part is almost constant, which makes it not possible to predict the breaking point. This can also explain why the standard DTT sample could break into more than two pieces in a fracture test. However, due to the special stress

concentration, it would be very difficult to calculate the stress distribution during a fracture test. Especially for the DN specimen, addition bending during testing could happen if crack propagates faster from one direction than the other direction. In this research, the force-displacement curve is going to use to avoid complications of the stress calculations.
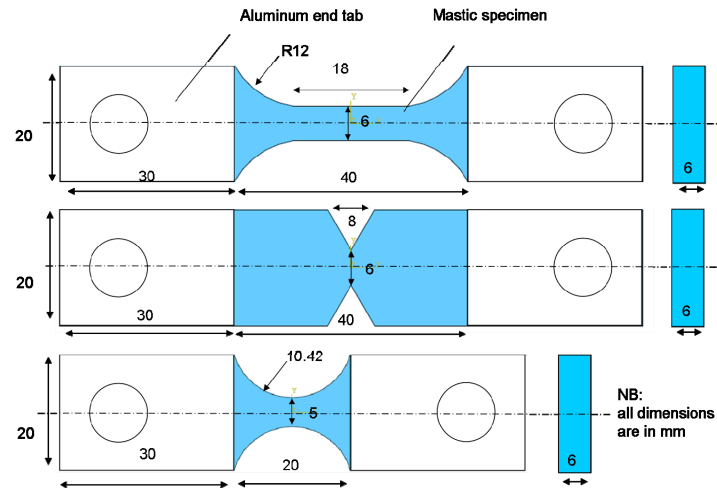

Figure 3-33 Illustration of special specimen geometries (from top to bottom: DTT, DN, DP)

Figure 3-35 shows the fracture curves obtained using the DN and DP geometries at a displacement speed of 100mm/min and a temperature of 0°C. The DN specimen and the DP specimen show a similar fracture behaviour. In practice, the de-moulding of the DN sample from the silicone rubber mould is very difficult. Because of its high stress concentration, it can easily be damaged during de-moulding. The DP specimen was much easier to handle and showed no damage after de-moulding.
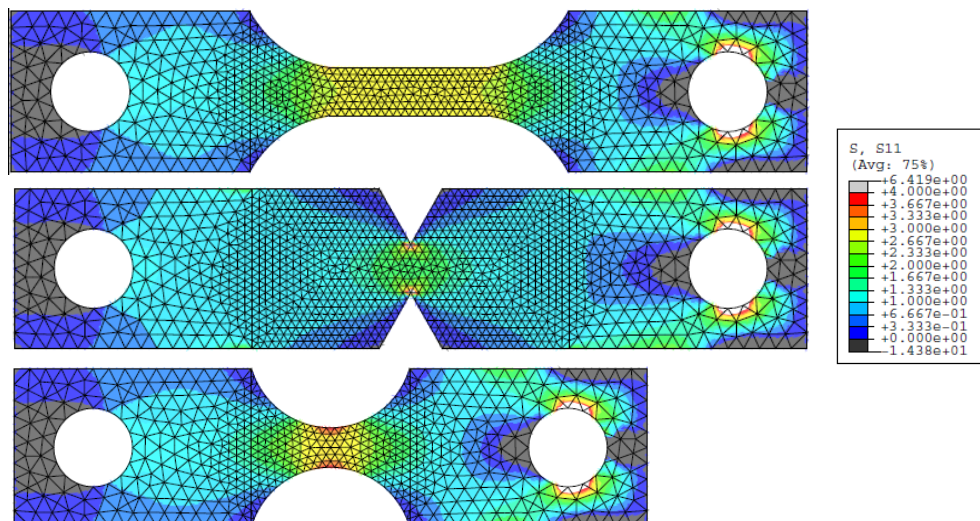
Figure 3-34 ABAQUS simulation of the DTT self healing samples (from top to bottom: DTT, DN, DP) (S11 stands for the horizontal direction perpendicular to the length direction)
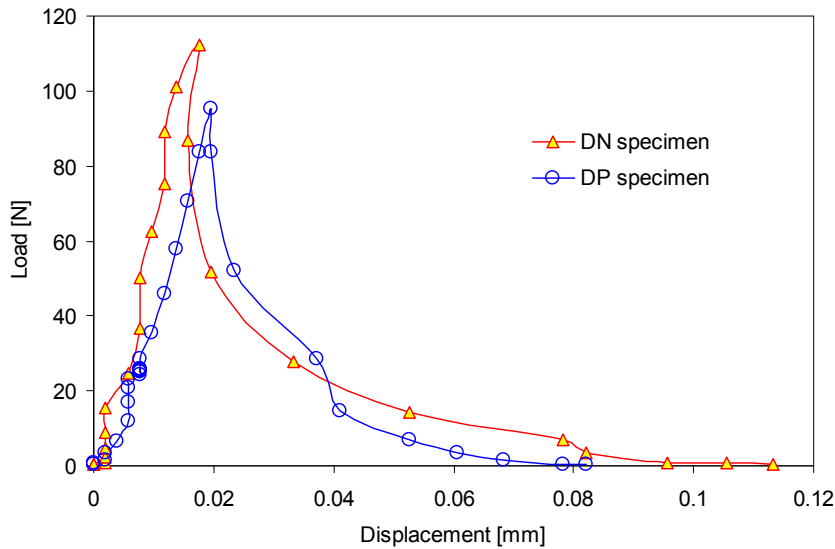
Figure 3-35 Test results of the bituminous mastics specimens

(70/100 pen. bitumen/filler ratio=1) for two geometries DN and DP (a displacement speed of 100mm/min at a temperature of 0ºC)

In addition, the displacement speed also influences the test. As shown in Figure 3-36, the 1mm/min and the 10 mm/min displacement speed results in a ductile failure with elongation of the sample. The 100 mm/min displacement speed shows a sudden break because of the stress concentration and the rapid crack propagation.
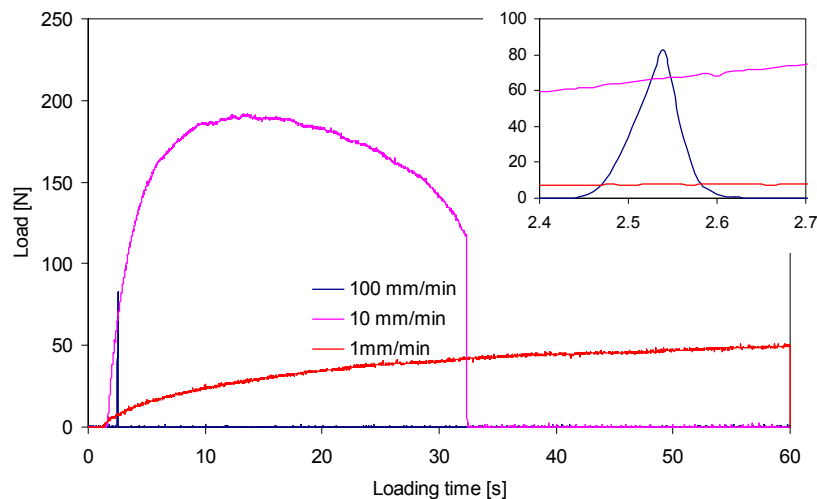
Figure 3-36 Typical test results of PBmas bituminous mastic samples with different displacement speeds

As shown in Figure 3-37, a nice and flat broken surface is obtained at a displacement speed of 100mm/min. While quite a rough surface texture is obtained at a displacement speed of 10mm/min. It seems that the displacement speed of 100mm/min is more promising for the fracture healing test since it

results in a good fracture surface. As a result, the displacement speed of 100mm/min was selected in this study for the fracture tests.
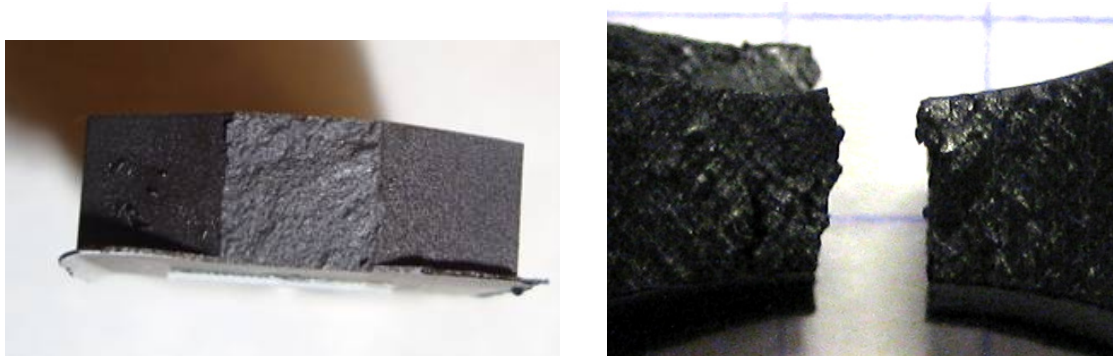

Figure 3-37 Illustration of broken surface of samples after 100mm/min (left) and 10mm/min loading (right)

Figure 3-38 presents the self healing results of all different shapes and loading speeds. It should be noted that all the specimens were first fractured by applying a displacement speed of 100mm/min. Next they were put back into the silicone rubber mould to heal. After healing, the samples were refractured using the DTT equipment at displacement speeds of 100mm/min or 10mm/min. The self healing percentage was calculated by the refractured strength over the fracture strength at the same displacement speed (100mm/min or 10mm/min).
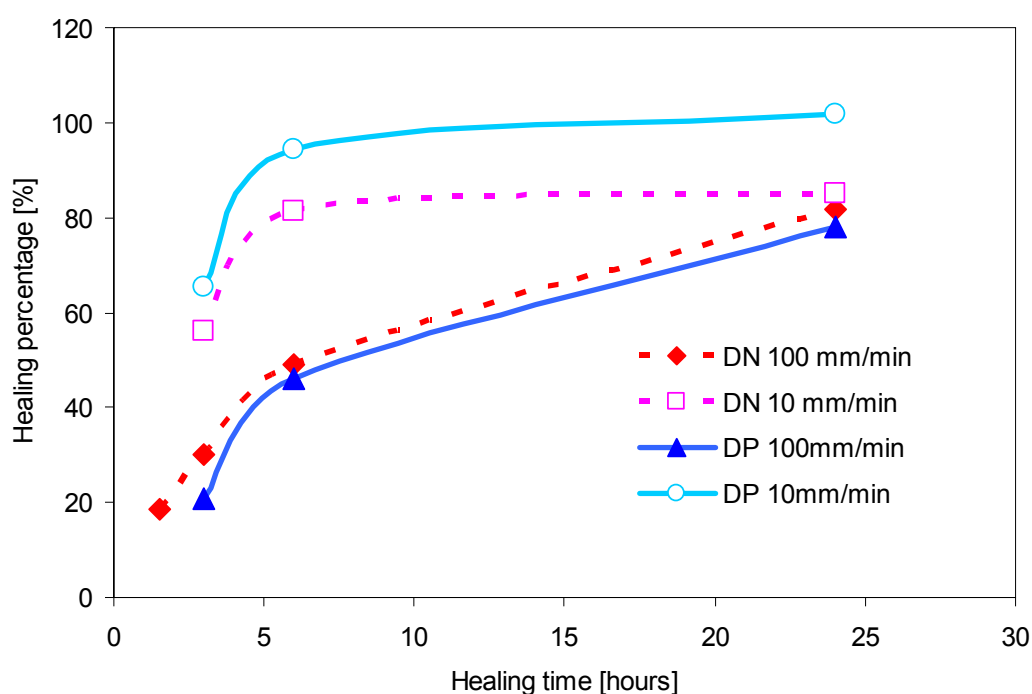

Figure 3-38 Influences of different geometries and loading speeds on self healing results of the PBmas bituminous mastics

When comparing the different geometries used, the results obtained from the DN and DP specimens are similar with each other in all cases. The DP sample fractured under a displacement speed of 10mm/min heals slightly faster than the DN sample, but the trends are the same.

When testing the sample in the refracture test with a displacement speed of 100mm/min, the sample suffers a sudden break in the middle of the specimen at the newly healed surfaces of the sample, which is the weakest point. When a displacement speed of 10mm/min is used, the failure process is related to both crack propagation and elongation. During the refracture test with a displacement speed of 10mm/min, microcracks and macrocracks are initiated and propagated in the entire sample instead of a sudden break on the healed surfaces. As a result, the healing capability was overestimated by using a displacement speed of 10mm/min.

The modified DTT test using a double parabolic shaped specimen gave more reliable results. In addition, the displacement speed used also has an influence on the healing evaluation. As mentioned previously, a displacement speed of 10mm/min may overestimate the healing capability due to the elongation artefact. A displacement speed of 100mm/min at a temperature of 0°C is recommended to analyse the healing capability of an open crack.

Figure 3-39 shows some results of healing tests performed on novel self healing bituminous mastics. The bituminous mastics had a bitumen/filler ratio of 1:1. All the specimens were fractured first with a fast displacement speed of 100mm/min to obtain a nice open crack. Healing was allowed to occur with the healing time of 24 hours at a healing temperature of 24°C. Then the healed DN specimens were tested with a refracture displacement speed of 10mm/min at 0°C.
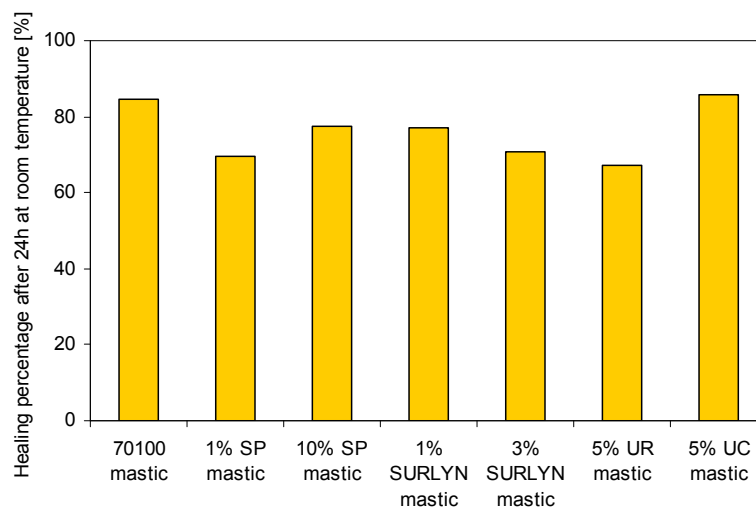

Figure 3-39 First results of novel self healing bituminous mastic using DN specimen (a displacement speed of 10mm/min at a temperature of 0°C)

It can be observed that the healing capability of all the novel self healing bituminous mastics was not as good as expected. All the self healing modifiers tend to decrease the self healing capability of bituminous mastics. The following explains the possible reasons:

- o SURLYN: It is believed that the temperature at which healing of the SURLYN really becomes effective is high. Furthermore, distribution of the SURLYN particles is not favourable for healing improvement. Because of this distribution, the SURLYN network falls apart, and the crack will most likely occur in the bitumen phase. Figure 3-40 shows the influence of elevated temperature on the healing capability of the SURLYN modified bituminous mastics. When the temperature is around 95 °C, the healing capability of the SURLYN modified bitumen increases. However, this temperature too high for asphalt pavement applications.

- o SP: The morphological analysis shows that the SP has a poor compatibility with pure bitumen. Thus the observed reduction in the self healing capability and the variation in the self healing results were expected.

- o Nanoparticles: It seems that the addition of the nanoparticles will not work as expected, that is they do not diffuse to the crack to heal it. The reason could be either the particle size is not small enough, or the nanoparticles are acting as an ultrafine filler. The NPCC with average size of 100nm and the NSIO with the particle size of 10nm were tested and the results are shown in Figure 3-41. Both the NPCC and the NSIO modifications decrease the healing capability at the test conditions considered. It seems that they act as an ultrafine filler in the bitumen, which increases the rigidity of bitumen and decreases the capability for healing. As a result, it can be concluded from our results that the nanoparticles modification is not beneficial for improving the self healing capability of bituminous materials.
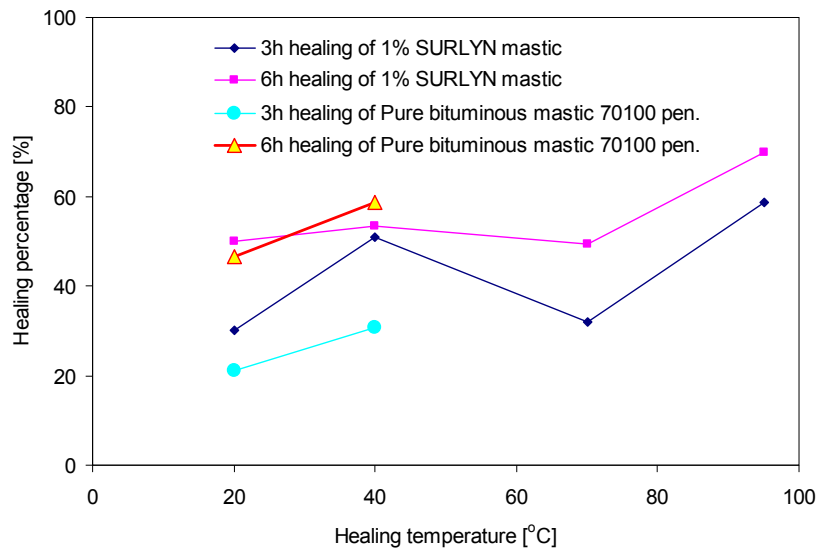
Figure 3-40 Self healing test data of 1% SURLYN modified bitumen using DP specimen (a displacement speed of 100mm/min at a temperature of 0°C)
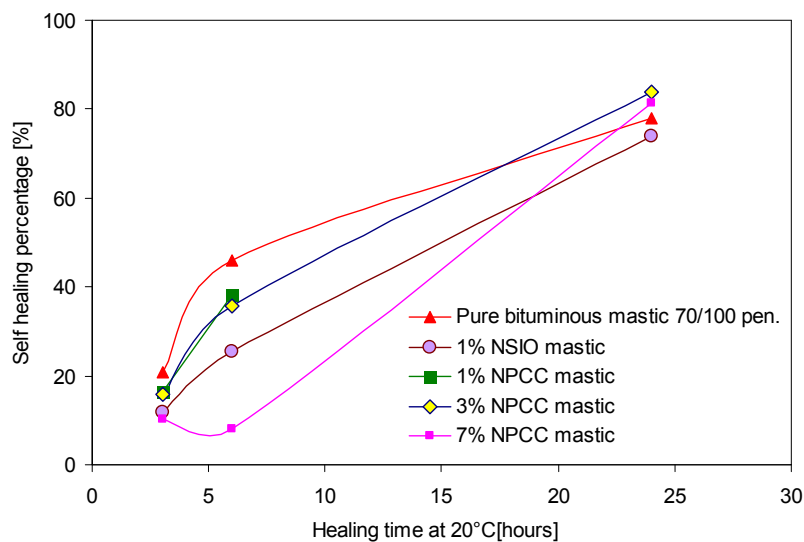

Figure 3-41 Self healing test results for NPCC and NSIO samples using DP specimen (a displacement speed of 100mm/min at a temperature of 0°C)

3.3.5 Summary of research exploration phase

Based on the experimental results from the exploration phase, the following conclusions can be made:

- o **Material analysis**

  - ➢ **Ionomers:** The addition of SURLYN to bitumen was investigated and the possibility of the self healing improvement was also explored. Although the SURLYN cannot be observed in the FT-IR spectrum, it distributes homogenously in the bitumen phase and stiffens the bitumen.

> **Supramolecular rubbers:** The SP modifier was investigated and the possibility for self healing improvement was explored. Due to the difference in back-bone between the SP and the pure bitumen, the SP shows incompatibility with the bitumen phase.

> **Nanoparticles:** The UR, UC, NPCC and NSIO modifiers were investigated. Most of the nanoparticles increase the stiffness modulus of bitumen.

> **Others:** The mixing method used in this phase is the commonly used mixing method for polymer modified bitumen. This mixing method results in a homogenous distribution of the novel self healing modifiers. However, it also appears that with a different mixing method, such as using a Z-blade, the morphology and performance of a polymer modified bitumen such as a SURLYN modified bitumen can be very different [2].

o **Self healing analysis**

> The self healing test using the DTT is not good for measuring healing of bituminous materials. The self healing test using the DSR is good for a fast check of the modulus healing of bituminous materials. However, this test method is observed to be complex and the results can be influenced by artefacts. Further research is needed to have more understanding. The self healing test using the DTT is good for fast check of the strength healing of bituminous materials. The modified DTT test using a double parabolic shaped specimen gives reliable results in the healing evaluation. However, the displacement speed has an influence on the healing evaluation.

> Self healing tests should be improved such that the real self healing capability is evaluated without the influence of any artefacts. Furthermore the improved test method should allow influencing factors like rest periods, temperature, crack sizes and confining stress to be studied.

> It is concluded that the pure soft bitumen is an excellent healer among all the healing systems. All the other self healing systems used in this research are not beneficial for improving self healing of bituminous materials.

> The polymer modified bitumen did not show any additional healing after initial healing. This is probably due to the decrease in the rate of diffusion caused by the existence of the polymer network. A very hard bitumen only shows a limited amount of healing. It is known that aging or low temperatures results in a

harder binder. This thus implies that the healing of bitumen may decrease or become limited after aging or at low temperatures.

➢ The self healing capability of the SURLYN modified bitumen is similar to that of the unmodified bitumen. This could be because of the high reactive temperature of SURLYN and the particle distribution of the SURLYN in the bitumen phase.

➢ A lower self healing capability can also be observed with the SP modification, which is related to the incompatibility between the SP and the bitumen.

➢ The self healing capability of bitumen decreases with the nanoparticle modification. The reason is that the addition of the nanoparticle only acts as filler in the bitumen phase, which also interrupt the real healing process of bitumen itself.

3.4 Final Research Plan

Based on the findings from the research exploration phase, a final research plan was developed to investigate and to further understand the self healing phenomenon of asphalt mixtures. The plan is shown in Figure 3-42 and explained hereafter.

o **Bitumen level (Chapter 4):** the self healing capability of pure bitumen will be investigated further using the DSR. In this part, both the complexity of the healing process and the complexity of the test itself will be explored.

o **Mastic level (Chapter 5):** the self healing capability of bituminous mastics will be investigated further using the DTT. With the test method, two test procedures will be followed: self healing of open cracks and self healing of meso cracks.

o **Mixture level (Chapter 6):** the self healing capability of asphalt mixtures will be investigated using a Beam on Elastic Foundation Setup.

o **Modelling in Mastic/Mixture level (Chapter 7):** finite element modelling will be applied on the self healing tests performed on the mastics and mixture to further understand the healing phenomenon.

o **Conclusions and Recommendations (Chapter 8):** based on the research findings obtained from material behaviours, mechanical assessments and modelling simulations, the conclusions and recommendation will be given and the possibilities of durable asphalt pavement using self healing ideas will be discussed.
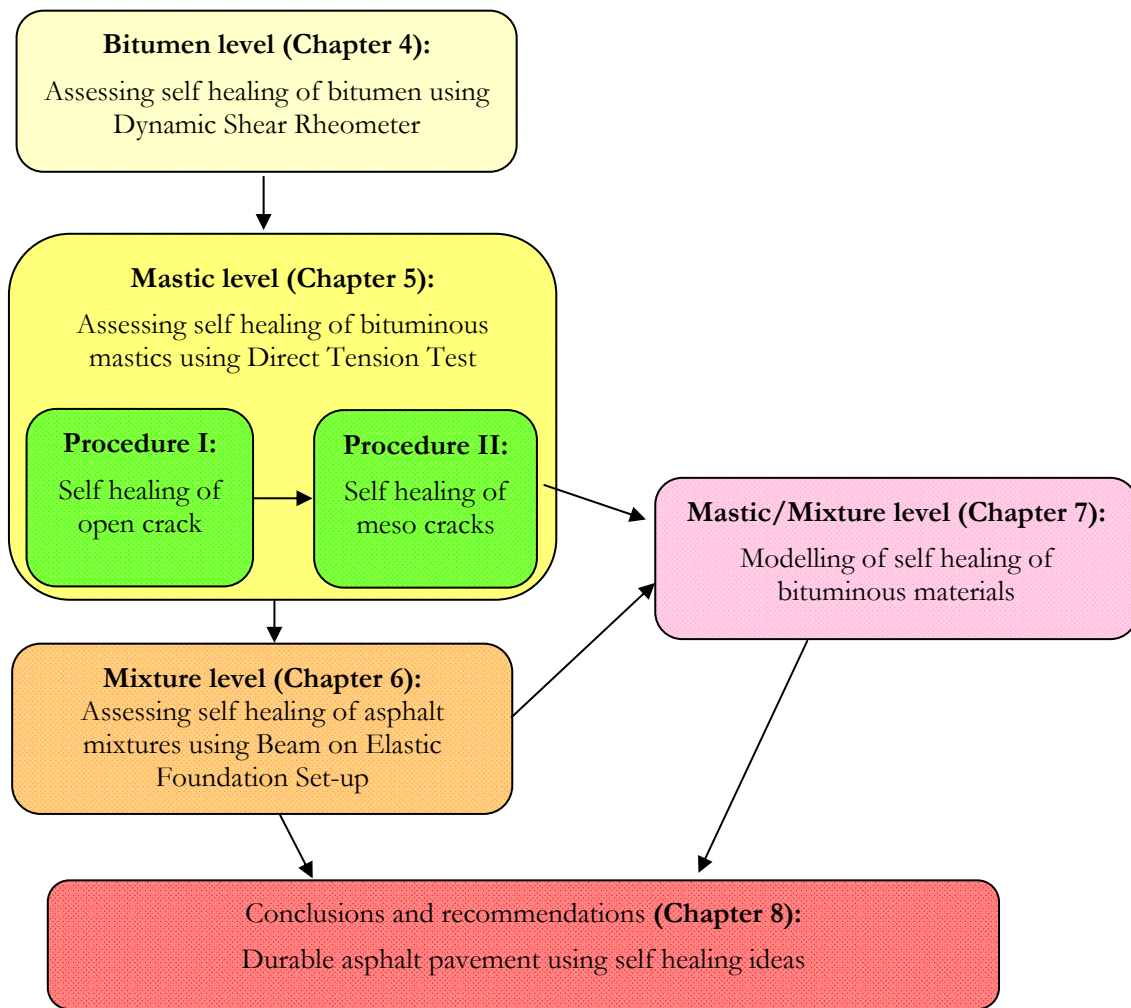
Figure 3-42 Research diagram for final research

References

[1] Engel R, Vidal A, Papirer E, and Grosmangin J. Synthesis and thermal stability of bitumen-polymer. Journal of Applied Polymer Science 1991;43:227-36.

[2] Fawcett AH and McNally T. Studies on blends of acetate and acrylic functional polymers with bitumen. Macromolecular Materials and Engineering 2001;286:126-37.

[3] Ghile DB. Effects of nanoclay modification on rheology of bitumen and on performance of asphalt mixtures: Delft University of Technology, 2006.

[4] Liu G, Wu S, van de Ven M, Yu J, and Molenaar A. Influence of sodium and organo-montmorillonites on the properties of bitumen. Applied Clay Science 2010;49:69-73.

[5] Liu G. Characterization and identification of bituminous materials modified with montmorillonite nanoclay, Delft: Delft University of Technology, PhD Thesis, 2011.

[6] Kalista SJ. Self-healing of thermoplastic poly(ethylene-co-methacrylic acid) copolymers following projectile puncture: Virginia Polytechnic Institute and State University, 2003.

[7] Jansen GW. Development of a damage tolerant composite with deformation rate dependent rigidity: Delft University of Technology, Master Thesis, 2008.

[8] Shell. Productinformatie 1539NL01 Cariphalte XS. Shell Nederland Verkoopmaatschappij B.V.; 2003.

[9] NEVUL. Lijst erkende vulstofmerken (in Dutch): NEVUL - Nederlandse Vereniging van Fabrikanten en Importeurs van Vulstof voor Bitumineuze Werken, 2010.

[10] Woldekidan M, Huurman M, and Mo L. Testing and modeling of bituminous mortar response. Journal of Wuhan University of Technology--Materials Science Edition 2010;25:637-40.

[11] Bhasin A, Little DN, Bommavaram R, and Vasconcelos K. A framework to quantify the effect of healing in bituminous materials using material properties. Road Material and Pavement Design 2008;EATA2008:219-42.

[12] Erkens SMJG. Asphalt concrete response (ACRe)-determination, modeling and prediction: Delft University of Technology, 2002.

[13] Hesp SAM. An improved low-temperature asphalt binder specification method. Final Report, MTO Contract No. 9015-A-000190 and NCHRP-IDEA Contract No. 84. Kingston, Ontario; 2004.

[14] Hesp SAM. Development of an improved asphalt binder specification testing approach. Final Report for Highway IDEA Project 104. Kingston, Ontario; 2006.

[15] ABAQUS. ABAQUS User's Manual, Version 6.6, 2006.

4

Assessing Self Healing of Pure Bitumen Using Dynamic Shear Rheometer

Abstract

Self healing is known as a built-in property of bitumen. It helps bitumen and asphalt concrete to recover its strength after damage has occurred. Healing will therefore extend the service life of asphalt pavements. A two-piece healing (TPH) test was developed to investigate the self healing behaviour of pure bitumen using the Dynamic Shear Rheometer (DSR). During the TPH test, the healing process was achieved by pressing two pieces of bitumen together under a parallel-plate system. Two phases can be distinguished from the TPH test being the initial healing phase due to gap closure, and the time dependent healing phase. The results are summarised as follows. (1) During the initial healing phase there is a three-stage complex shear modulus increase with the closure of the gap width. (2) Next to the initial healing there is a time dependent healing phase. The time dependent healing results show a distinctive difference between the results obtained when the gap between the parallel plates of the DSR was kept constant and the results obtained when the normal force applied was kept constant. It was shown that the compressive normal force strongly promotes the development of healing. (3) It was also demonstrated that many factors can influence the complex shear modulus measurement results by using the DSR parallel-plate geometry.

The so-called self healing capability of asphalt concrete has always been an interesting topic since it was discovered forty years ago [1-3]. The significance of self healing is that an asphalt concrete can repair itself under certain conditions such as hot summers or rest periods. Due to this healing, the service life of an asphalt pavement is extended. Healing is defined as the recovery of mechanical properties like strength, stiffness and an increase of the number of load repetitions to failure in a fatigue test.

In the past, investigations have been carried out to measure the healing phenomenon at the scale of asphalt concrete [3, 4]. It is known that the healing phenomenon of asphalt concrete is highly dependent on the mixture composition as well as the properties of the bituminous binders. Since the bituminous binder is the only part in an asphalt mixture that can heal, knowledge on the healing characteristics of pure bitumen at meso- and micro-scale is important to understand its contribution to the healing capacity of asphalt concrete.

In this chapter, the Dynamic Shear Rheometer (DSR) was used to investigate the self healing capability of pure bitumen with a special two-piece bitumen healing (TPH) setup. The usefulness of the TPH setup to investigate the self healing capability of pure bitumen will be explored. The influence of measuring factors on the experimental results will also be discussed.

4.1   Two-piece Healing Test Setup

Figure 4-1 shows the crack propagation process in pure bitumen under mode I tension loading [5]. Of special interest is the zone at the tip of the crack surface; this zone is called the fracture/healing process zone. This process zone can be considered to be composed of a number of micro cracks, which are gradually developing during loading. When the load is removed, the healing process will be concentrated in this zone.

To investigate the healing process in this zone, The TPH test was proposed to mimic the healing process of the crack surface using the DSR. This setup was first used by Bhasin and his colleagues [5, 6], and later on by the principal author of this work [7]. As shown in Figure 4-2, two pieces of bitumen are placed on the upper and the bottom plates of the DSR. Then the DSR presses the two pieces of bitumen together to stimulate the crack healing process. The change of the shear modulus is measured over time. A small strain level is used during the test to avoid any disturbance in the development of healing between the two bitumen pieces. After testing, it was observed that the two pieces of bitumen were totally connected with each other.
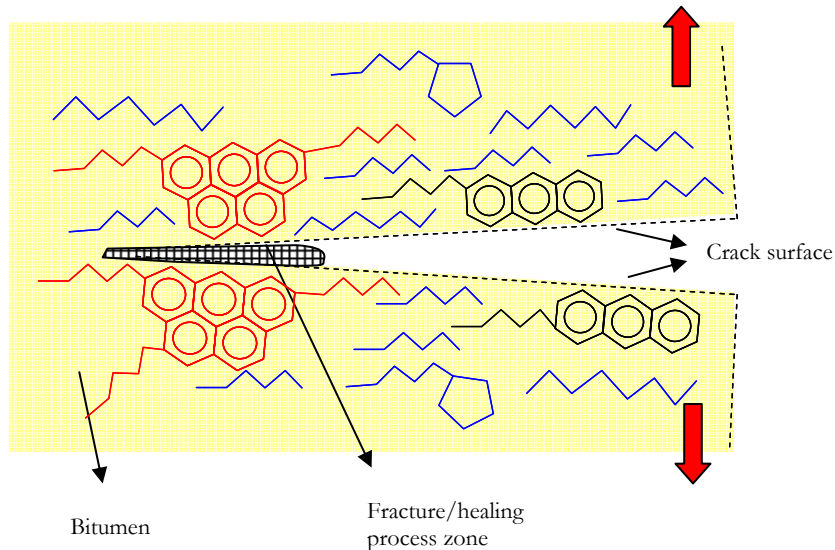
Figure 4-1 Illustration of crack propagation process and the fracture/healing process of pure bitumen in mode I tension loading [5]
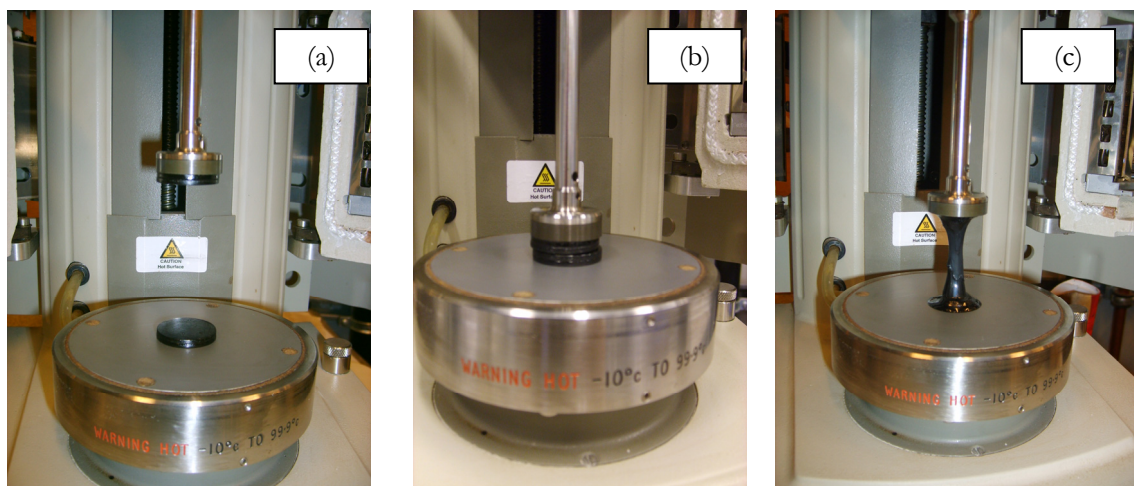

Figure 4-2 Illustration of the TPH setup using Dynamic Shear Rheometer [7], (a) Attaching two pieces of bitumen on top and bottom plates; (b) Decreasing the gap width to allow full contact of the two pieces and measuring the change in complex shear modulus over time; (c) Removing the upper plate after the testing

Figure 4-3 shows a typical test result from the TPH testing. The self healing percentage was defined as the complex shear modulus of the TPH sample divided by the complex shear modulus of a one-piece sample which was used as reference. Two phases can be distinguished from the TPH healing test, the initial healing phase and the time dependent healing phase. This initial healing phase is caused by the gap closure, which accounts for the initial complex shear modulus values of the TPH healing curve. The time dependent healing phase accounts for healing over time. A model was proposed by Bhasin to describe the healing process of bituminous binders based on a convolution of wetting

and inter-diffusion processes [5]. It is believed that the initial healing can be related to the wetting mechanism. A further increase in time of the self healing ratio may be attributed to the diffusion mechanism (in time). This model is in line with the Multi-step healing model proposed by Phillips [8]. In his model Phillips defined three steps being: Step (1) flow, Step (2) wetting and Step (3) inter-diffusion. However in the TPH setup, Step (1) "flow" is replaced by an external pressure to ensure the closure of the artificial crack.
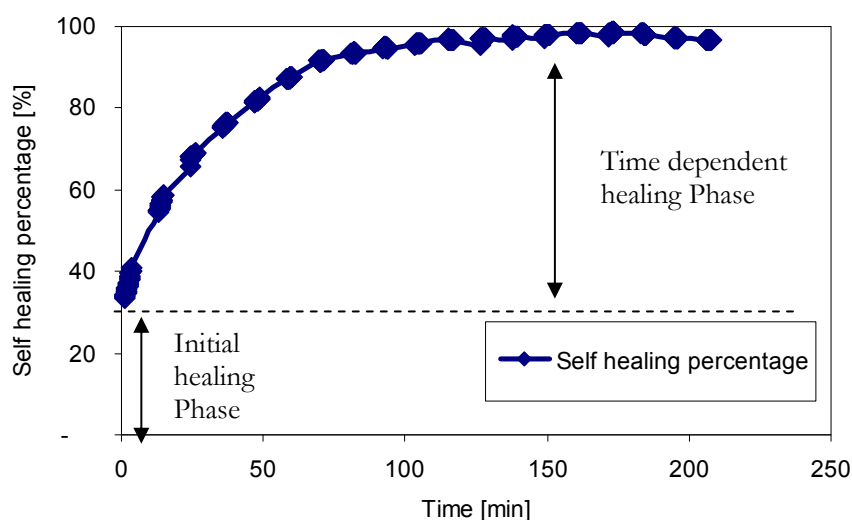
Figure 4-3 Typical TPH results and healing phases at test temperature of 20°C[7]

By mimicking the crack closure using the DSR, the TPH test is believed to provide a direct relation to the fundamental healing process. However, due to limited knowledge of this test setup, a further investigation is needed to evaluate the usefulness of the TPH test and the factors influencing the measurements. To this end, the initial and time dependent phases observed in the TPH test were investigated separately in this work. The factors influencing each phase are also discussed.

4.2 Experiments

4.2.1 Materials

A standard 70/100 penetration grade Kuwait Petroleum bitumen with a penetration of 93 (0.1mm) at 25°C, and a softening point of 45°C was used in this study. This type of bitumen is commonly used in the Netherlands.

4.2.2 Equipment

Figure 4-4 shows the Dynamic Shear Rheometer AR2000ex that was used in this research. A 25mm parallel-plate system was used to conduct the experiments [30]. A normal force sensor was located under the bottom plate. The normal force data were intensively investigated in this paper and special emphasis was placed on (a), monitoring the normal force (vertical force) development with a constant change of the gap width; (b), measuring the generated normal force over time at a constant gap width; (c), controlling the constant normal force testing time by continuously adjusting the gap width.
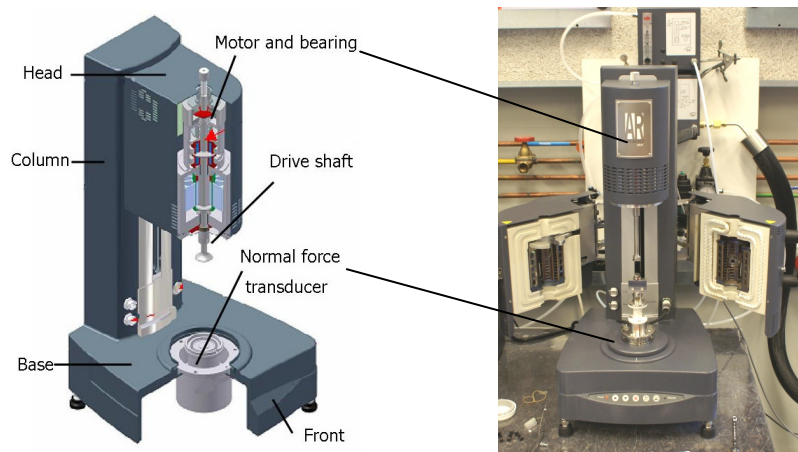

Figure 4-4 Dynamic Shear Rheometer AR2000ex

4.2.3 Test procedure

As it is shown in Figure 4-5, pure bitumen samples were made into a disk shape with a diameter of 25 mm, and the thickness varied between 6-6.5 mm for the one-piece sample, and 3-3.5mm for the two-piece sample. It should be noted that the thickness of the specimen mentioned here is smaller than that was used in the exploration phase (Section 3.3.4.3). As suggested by the DSR equipment, the gap width during the measurement may not be too high, for example, 1-3 mm was recommended in polymer tests. As a result, the sample thickness was decreased to 3-3.5 mm (the total height decreased from 8 mm to about 6 mm) to ensure the effective measurement.

Table 4.1 shows the main test program of the TPH test. Apart from healing measurements on two-piece samples, also measurements on one-piece samples were carried out. This was done in order to allow the characteristics of cracked and healed specimens to be compared with the characteristics of undamaged specimens.

In order to analyze the real healing signal and its influencing factors, the two phases were investigated separately in this research. The results of the initial healing phase and discussions of its influencing factors are presented in Section 4.3. The results of the time dependent healing and discussions of its influencing factors are given in Section 4.4.
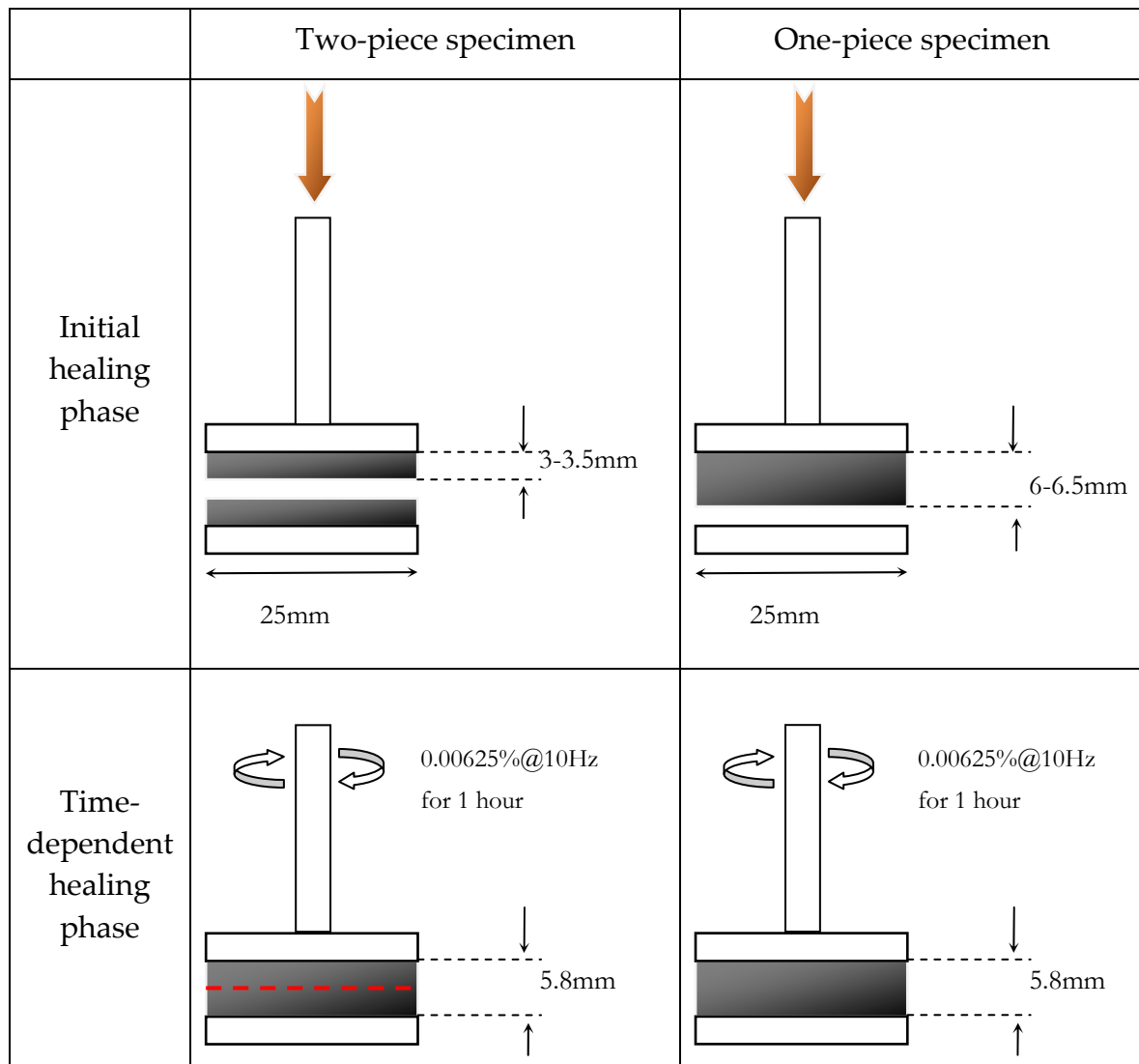
	Two-piece specimen	One-piece specimen
Initial healing phase	3-3.5mm, 25mm	6-6.5mm, 25mm
Time-dependent healing phase	0.00625%@10Hz for 1 hour, 5.8mm	0.00625%@10Hz for 1 hour, 5.8mm

Figure 4-5 The TPH tests test procedure

Table 4.1 TPH test procedures

		Test on two piece samples	Test on one piece samples
Initial healing phase	Initial healing test	**Test samples:** Initial two-piece, Initial two-piece trim **Procedures:** A1. Stick two sample pieces to the top and bottom plates, and keep test temperature at 20 °C; A2. Decrease the gap from 7000μm to such a level that the two pieces come in contact with each other. This is determined by visual inspection and a camera inside of the temperature chamber; A3, Start the complex shear modulus measurement applying a shear strain level of 0.00625% with frequency of 10 Hz for 3min with a constant gap width. The strain level is chosen to be within the linear visco-elastic range and is small enough not to interrupt the healing process; A4, After the test, decrease the gap width step by step from 7000μm to 500μm with 200-500μm for each step and repeat the test procedure A3. Monitor the normal force development during the decrease of the gap. A5 Trim the sample at gap width of 5000μm, 2000μm, 1000μm and 500μm, respectively. Measure the complex shear modulus before and after trimming according to procedure A3.	**Test samples:** Initial one-piece, Initial one-piece trim **Procedures:** B1. Stick one piece of sample on the top plate of the DSR, and keep the temperature constant at 20°C; B2. Decrease the gap such that the sample fully touches the bottom plate; B3. B4, B5 and B6. The same as A3 to A5.
Time dependent healing phase	Time dependent healing test with gap constant control	**Test samples:** TP-GC-a, TP-GC-b, TP-GC-c **Procedures:** C1. Same as A1; C2. Decrease the gap width of the parallel plates to a target gap width of 5.8mm; C3. Start the measurement by applying a small strain level of 0.00625% at 10 Hz during 2 minutes followed by a rest period of 8 minutes; C4. During the test, keep the gap width constant.	**Test samples:** OP-GC **Procedures:** D1. Same as B1; D2. Decrease the gap to a gap width of 5.8mm; D3 and D4. Same as C3 and C4
	Time dependent healing test with normal force constant control	**Test samples:** TP-NF-a, TP-NF-b, TP-NF-c **Procedures:** E1, E2, E3. The same as C1, C2 and C3; E4. During the test, the normal force is kept constant at 0+/-0.1N.	**Test samples:** OP-NF **Procedures:** F1, F2, F3. Same as D1, D2 and D3; F4. Same as E4.

4.3   Initial Healing Phase

4.3.1   Initial healing curve

Figure 4-6 shows the results of the initial healing tests. It can be observed that both the complex shear modulus of the one-piece sample and the two-piece sample increase when the gap width decreases.

The one-piece sample shows a gradual increase of the complex shear modulus. The two-piece sample exhibits a fast initial increase compared with the one-piece sample. It should be noted that during the analysis, the bitumen samples and the steel plates are assumed to be fully bonded. The development of the complex shear modulus is then interpreted as the response of the one-piece or the two-piece bitumen samples.
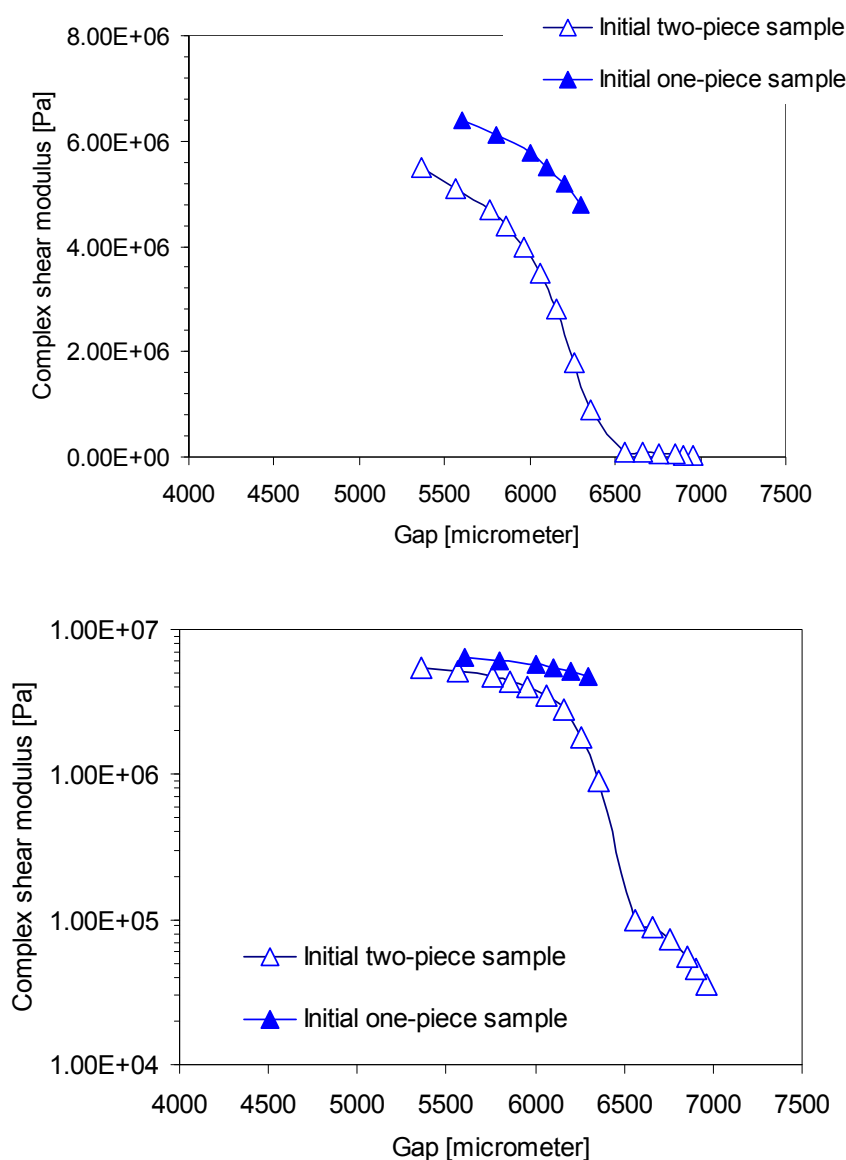
Figure 4-6 Initial healing curves with the decrease of the gap width at 20°C in normal scale (upper) and in semi-log scale (lower)

For the two-piece sample, three stages of the development of the complex shear modulus can be observed.

  o The first stage is when the gap width between the parallel plates decreases from 7000 μm to 6500 μm. In this case, the two pieces of bitumen, which are attached to the top plate and the bottom plate, respectively, are visually in touch with each other. This was observed by the web camera inside of the temperature cabinet. However, the measured complex shear modulus is less than 1MPa, and the decrease of the gap width causes limited improvement of the complex shear modulus. The reason could be that the two pieces of bitumen were not really in touch with each other yet, although visual inspection indicated that they seemed to be pressed together.

  o In the second stage, when the gap width decreases from 6500 μm to around 6000 μm, the complex shear modulus increases strongly, which may be due to the full contact between the two bitumen pieces.

  o In the third stage, when the gap width continuously decreases from 6000 μm to lower, the behaviour of the two-piece sample is almost the same as that of the one-piece sample. Here, the two-piece sample is believed to be fully healed and behaves the same as the one-piece sample.

Considering the uniqueness of the three-stage initial healing curve, the increase of the measured complex shear modulus can be calculated as a function of the gap width decrease. The second stage of the initial healing curve can be used as an indicator of the initial value for the time dependent healing data, which will be discussed later.

4.3.2 Factors influencing initial healing

4.3.2.1 Compressive force and relaxation

Figure 4-7 shows an example of how the normal compressive force developed when the gap width was decreased. From of an energy balance point of view, this compressive force is a major energy input because the temperature is kept constant. Within the setup, the compressive work either transfers into deformation of the samples or causes the closure of the crack. These effects can result in an increase of the complex shear modulus. It is believed that the compressive work is the main driving force for the increase of the complex shear modulus. As shown in the figure, the decrease of the gap width was nonlinear with respect to time. As a result, the normal force first increased to a peak value and then decreased because of relaxation.
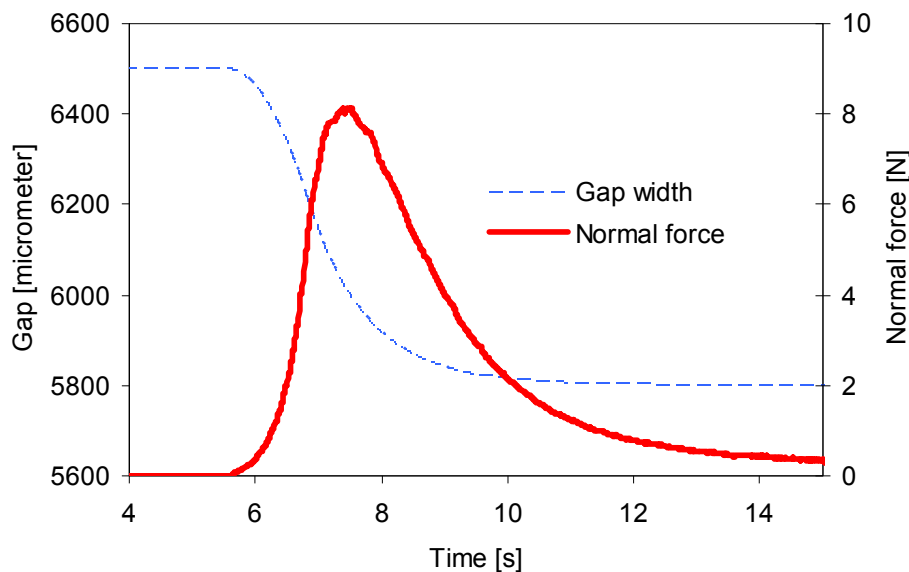
Figure 4-7 Illustration of the compressive force during the decrease of the gap width

Even when the gap width is kept constant, relaxation still occurs inside the sample to release the residual normal compressive force, which might influence the initial healing. For this reason, a healing test with a fully relaxed normal force (till compressive force of 0.1N) was carried out.

Figure 4-8 shows the initial healing curves with relaxation. It is interesting to note that the general trends of the initial healing samples with full relaxation are exactly the same as the samples where no relaxation was allowed, ignoring the height differences due to the variation of the sample thickness.
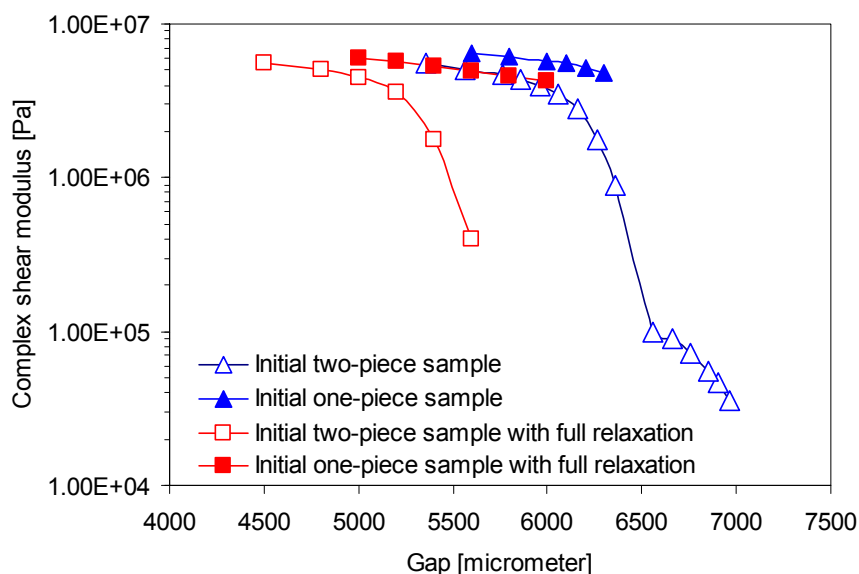
Figure 4-8 Influence of relaxation on the initial healing curves

4.3.2.2 Gap width sensitivity

The dramatic change of the complex shear modulus with a 0.5mm gap width decrease in the second stage of the initial healing curve was not expected. However, it explains why the time dependent healing test results are very sensitive to the sample thickness. This will be discussed in more detail in Section 4.4.

4.3.2.3 Geometry change

In principle, the complex shear modulus of the one-piece sample should be constant during the test. However, the decrease of the gap width resulted in a significant increase of the complex shear modulus. One or more of the following reasons might explain this phenomenon.

  o Orientation of bitumen molecules of the sample due to the applied shear force; this was reported to exist in the low gap width range [9];

  o The measurement itself, which generates more error at a larger gap (normally the recommended gap width is around 1mm to 3mm);

  o Change of the sample geometry.

During the test, the gap decrease could cause the sample geometry to change, and part of the sample could get a larger diameter than the diameter of the plate (25mm in diameter). In order to investigate the influence of the change in sample geometry on the initial healing measurement, the specimens were trimmed as shown in figure 4-9. The difference in complex shear modulus before and after trimming was compared and the difference was referred to the geometry change effect.

Figure 4-9 shows the influence of trimming on the measured complex shear modulus of the one-piece sample. When the gap width decreased from 6000 μm to 5000 μm, the complex shear modulus of the untrimmed sample increased continuously. When trimming was applied on samples with a gap width of 5000 μm, the complex shear modulus of the trimmed sample became less than that of the untrimmed sample. The change in complex shear modulus due to trimming was also observed at the gap widths of 2000 μm, 1000 μm and 500μm respectively, but the difference in modulus between the trimmed and untrimmed samples is smaller at these gap widths.
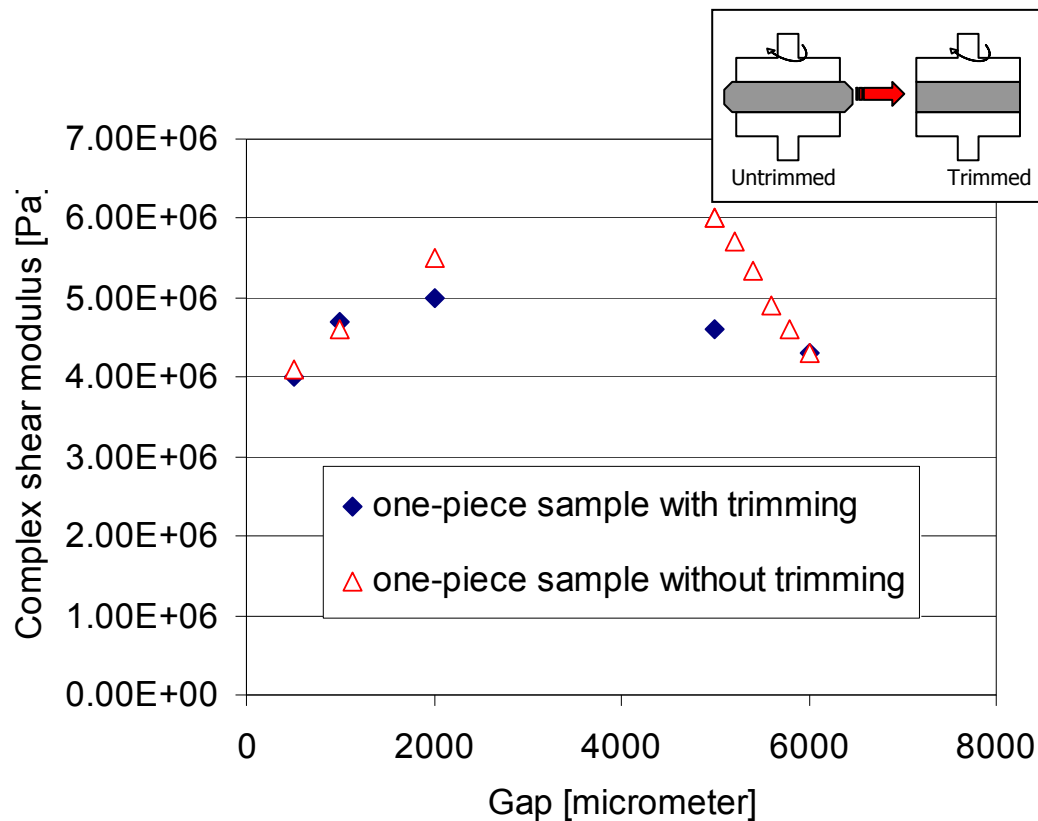
Figure 4-9 Influence of the geometry change on the complex shear modulus of the one-piece sample

Figure 4-10 shows the influence of trimming on the two-piece sample. At gap widths between 6000 μm to 5000 μm, the effect of trimming on the change of the modulus on a two-piece sample is less than for the one-piece sample.

The reason could be:

o   For the one-piece sample, the complex shear modulus measures the response of the whole specimen. The mass surrounded the plate geometry would cause a considerable difference in the complex shear modulus measurement.

o   For the two-piece sample, the complex shear modulus is based on the response of the weakest part, the shear resistance of the artificial crack between the two bitumen pieces. At the beginning of the gap decrease, the artificial crack closes. The deformation is less and the influence of trimming on the complex shear modulus is also less. The response of the weakest part, the artificial crack, rules the whole signal.

However, after the two pieces fully touches each other, the same phenomenon as the one-piece sample can be observed.
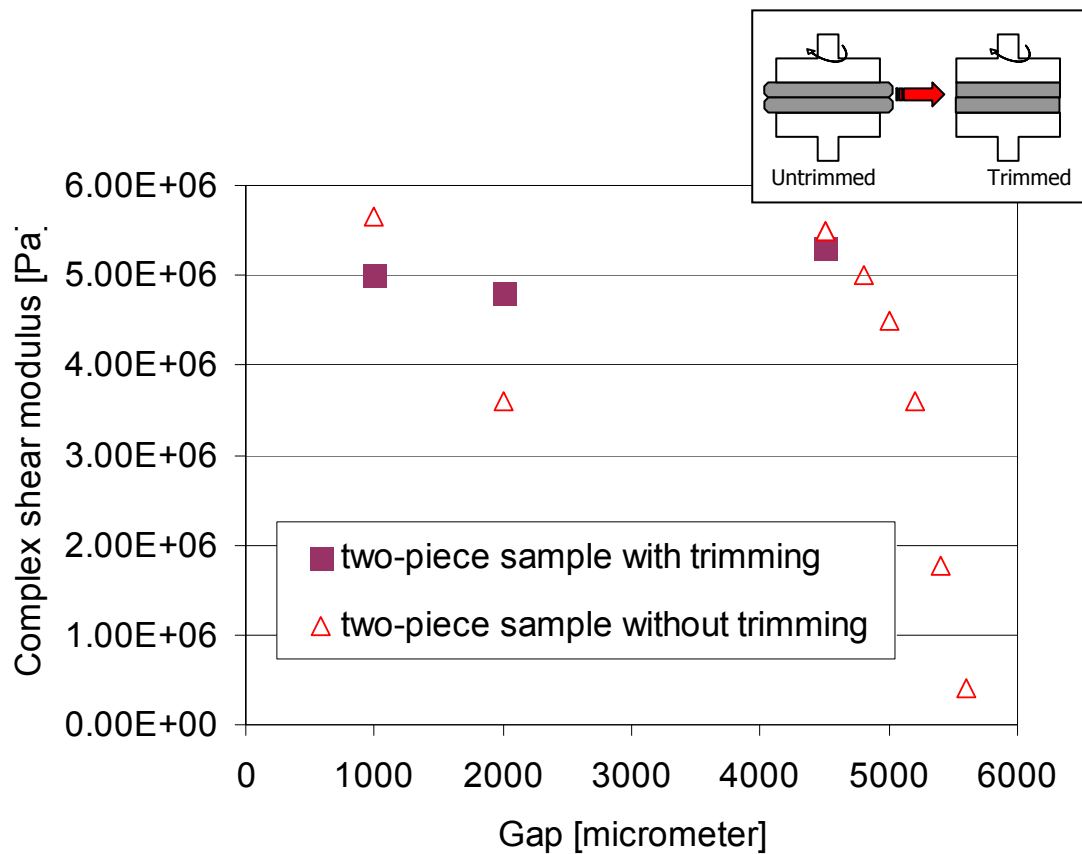
Figure 4-10 Influence of the geometry change on the two-piece sample

Furthermore, the healing percentage, which was defined by the ratio of the complex shear modulus of the two-piece bitumen specimen to that of the one-piece bitumen specimen over any given time point at the measuring gap width of 5800 μm, can be influenced by the geometry artefact on the one-piece sample results.

4.4　Time Dependent Healing Phase

4.4.1　Time dependent healing results

4.4.1.1　Time dependent healing with constant gap width

Figure 4-11 and Figure 4-12 show examples of the time dependent healing test results obtained by keeping the gap width (GC healing) for the two-piece and the one-piece samples constant.

As shown in Figure 4-11, the complex shear modulus of the two-piece sample increases slowly during time. A decrease of the normal force is also monitored throughout the test. This might be due to the relaxation of the residual normal force as shown in Figure 4-7. A more detailed explanation of the decreasing normal force will be given in Section 4.4.2.1. Here, only the relative trends are compared.

Figure 4-12 shows the results of a one-piece sample. The complex shear modulus keeps constant throughout the test. For the one-piece sample, a similar trend of the decreasing normal force is observed compared to the two-piece sample.
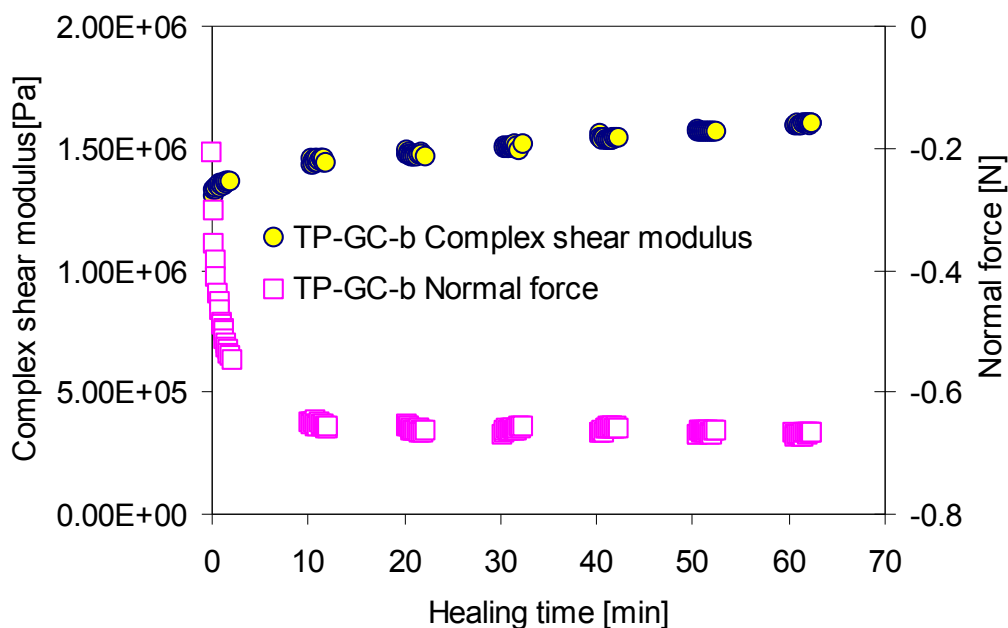

Figure 4-11　Test results of the two-piece GC healing sample TP-GC-b
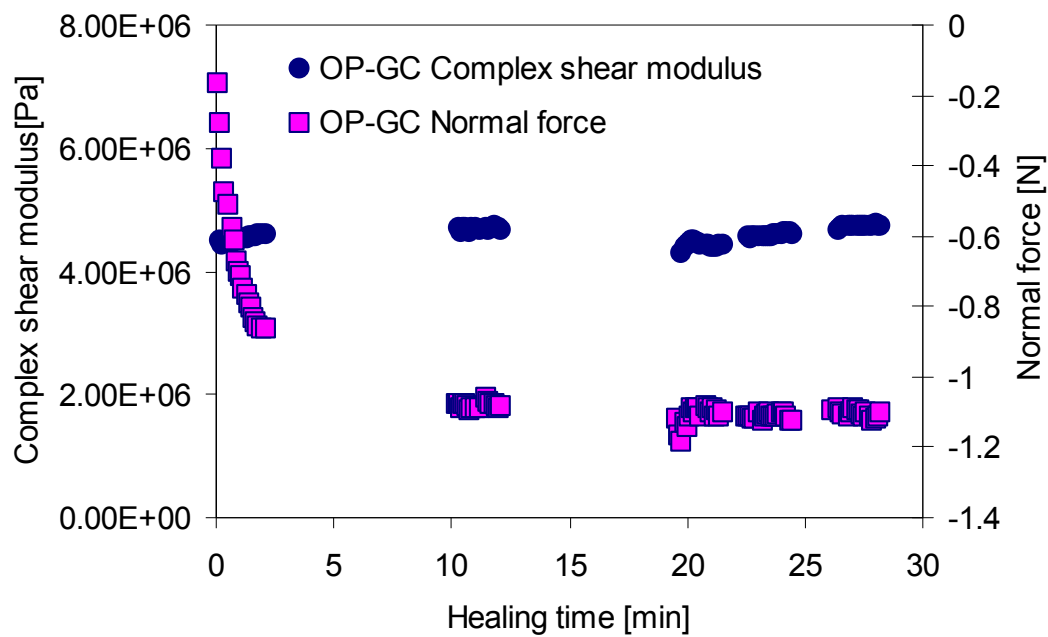
Figure 4-12 Test results of the one-piece GC healing sample OP-GC
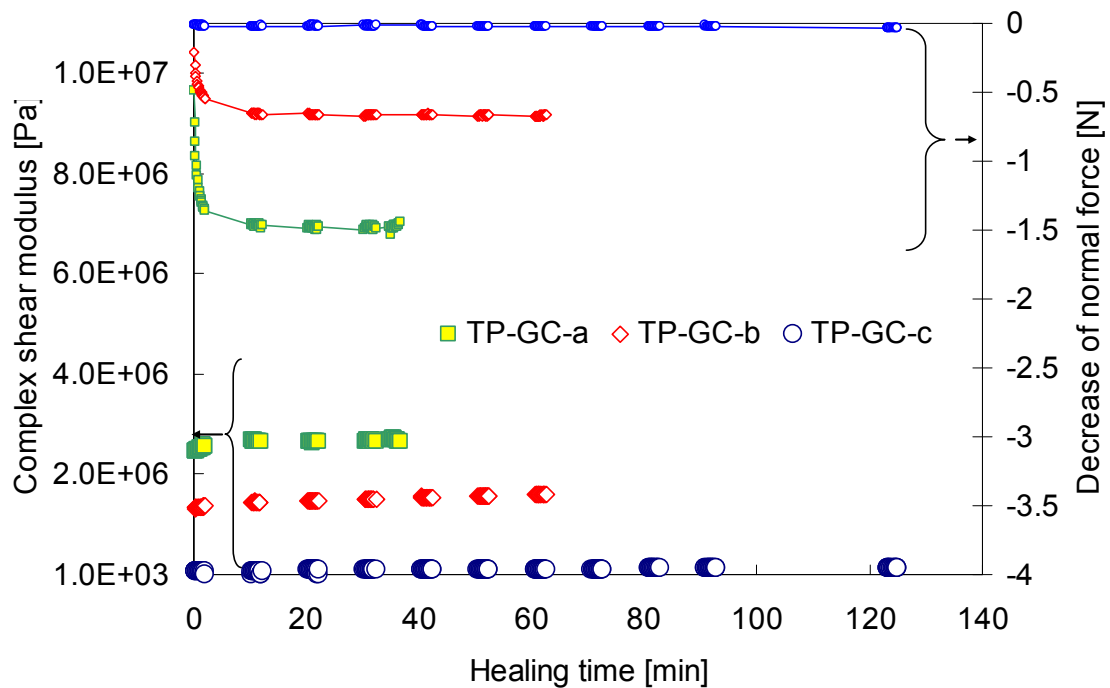

Figure 4-13 Time dependent healing results with gap constant control obtained on two-piece samples

Figure 4-13 shows the results from the GC healing performed on three two-piece samples. The following can be observed:

o   Different tests gave different results. This is mainly due to the fact that the complex shear modulus is depending on the sample thickness.

o In the first 20 minutes, a 5% to 10% increase of the complex shear modulus of the two-piece samples is observed. After that, a slight increase of the complex shear modulus is monitored over time.

o When comparing the normal force with the level of the complex shear modulus, one can notice that a higher complex shear modulus is obtained with a lower normal force.

4.4.1.2 Time dependent healing with constant normal force

A time dependent healing test during which the normal force was kept constant (NF healing) was also performed in this study. During the test, the DSR kept the normal force constant automatically by adjusting the gap width between the upper and bottom plates.

Figure 4-14 and Figure 4-15 show examples of the results of the two-piece sample and the one-piece sample, respectively.

For the two-piece sample, a rapid increase in complex shear modulus can be observed. The controlled normal force is around -0.12N and -0.14N, which is much smaller compared with the GC healing. Consequently, the gap width decreases from 5800 μm to 5500 μm to keep the normal force constant.

A similar trend is observed for the one-piece sample (Figure 4-15). Surprisingly, the gap width decreases from 5800 μm to almost 4000 μm. The increase of the complex shear modulus over time is quite different when compared with the one-piece sample under gap constant mode.
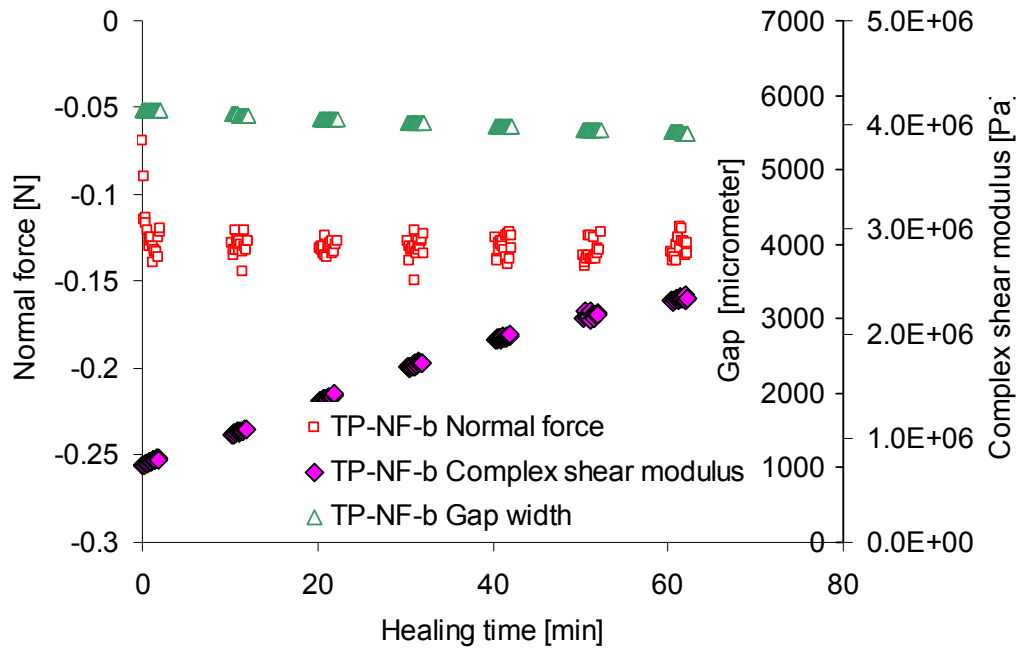

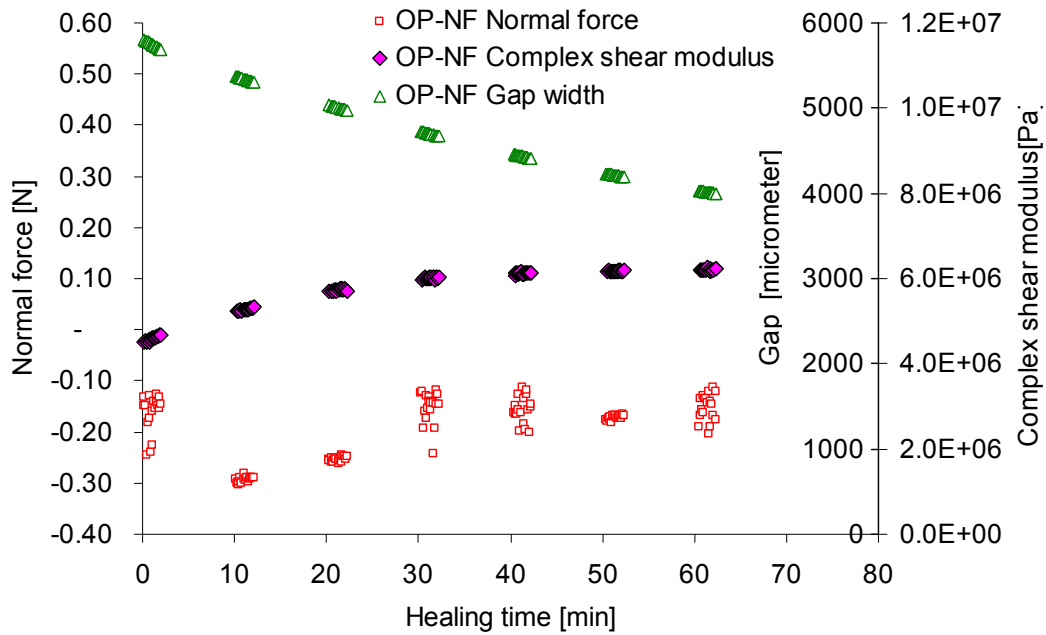Figure 4-14 Test results of the two-piece NF healing sample TP-NF-b

Figure 4-15 Test results of the one-piece NF healing sample OP-NF
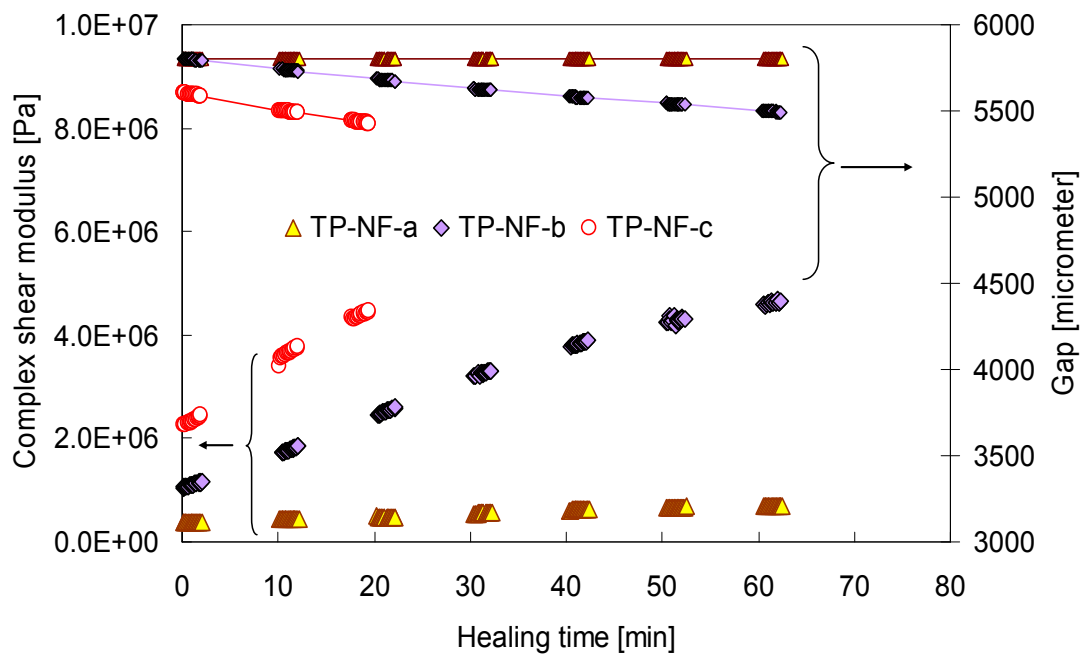

Figure 4-16 Time dependent healing results with normal force constant control obtained on two-piece samples

All NF healing results are shown in Figure 4-16, and the following can be observed:

o Differences between the initial values of the time dependent curves can be observed. These differences are due to the thickness sensitivity effects.

o The increase of the complex shear modulus over time is much faster in the NF healing tests than in the GC healing tests (Figure 4-13).

133

Furthermore the development of the complex shear modulus with time in the NF healing tests is almost constant.

o Different trends in gap decreases are observed. The two-piece sample at a constant normal force of -0.12N shows a lower gap decrease compared to the one-piece sample.

4.4.2 Influence of normal force on time-dependent healing

4.4.2.1 Normal force control mechanism

The time healing test results presented above show a large influence of the normal force. Hence, an equipment-based investigation was carried out to understand the normal force measuring and controlling mechanisms.

According to the control manual of the DSR AR2000ex, the normal force control is realized by controlling the feedback signal from the normal force transducer located under the bottom plate. However, during the test, the normal force working function of the DSR is automatically zeroed when the test is started [10].

Figure 4-17 shows the zeroing mechanism of the normal force of the DSR. After reaching a target gap width, the generated normal force starts to relax over time (also shown in Figure 4-8). If the time is long enough, the normal force will relax to almost zero. If the TPH test starts after full relaxation, shown as start point 1 in Figure 4-17, the program will be zeroed with almost no normal force. If the test starts from the start point 2 (not enough time for relaxation), the normal force will be zeroed at zero line 2. As a result, a decreasing "negative" normal force would be expected during the test because of the remaining relaxation.
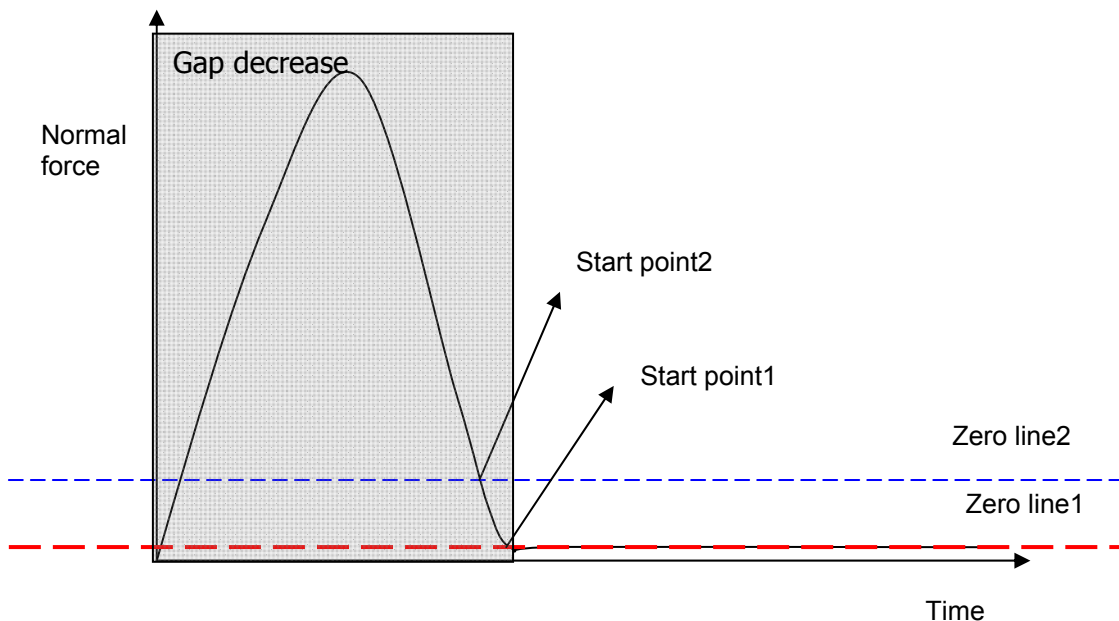

Figure 4-17 Illustration of working mechanism of the normal force

During the self healing test described in this research, the test was started less than 1 minute after pressing the two pieces of samples to a certain target gap width. Similar to starting the test from start point 2, relaxation of the remaining force can be expected. It explains the decrease of the "negative" normal force measured at the beginning of the GC healing test.

However, in the NF healing test, the normal force control is active. After starting the measurement, the DSR machine indicates a decreasing "negative" normal force. Then the gap width is decreased in order to keep the constant normal force.

4.4.2.2 Normal force effect on NF healing results

A decrease of the gap width is observed in the NF healing test in order to keep the normal force constant. As a result, for the NF healing sample, the development of the complex shear modulus over time is composed of two parts: time dependent healing with a constant gap width and additional healing due to gap decrease. This additional gap decrease can be related to the initial healing as described in section 4.3.

Figure 4-18 shows the development of the complex shear modulus in relation to the gap width for both the NF healing and the initial healing results.

The following comments can be made:

- o A three-stage curve can be obtained in the NF healing test.

- o The development of the complex shear modulus of the NF healing two-piece samples follows the second stage of the initial healing curve.

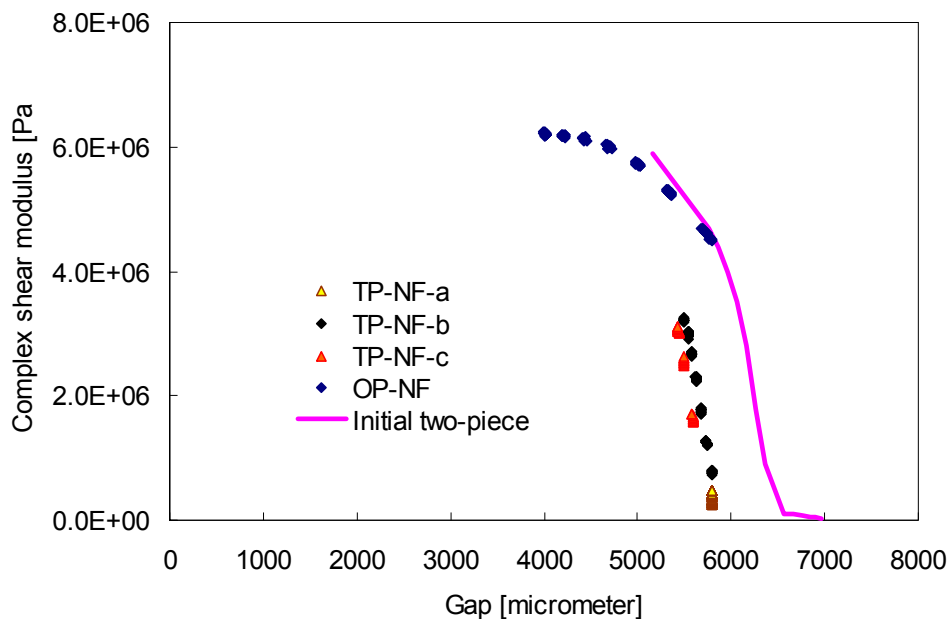- o The one-piece sample follows the third stage of the initial healing curve.

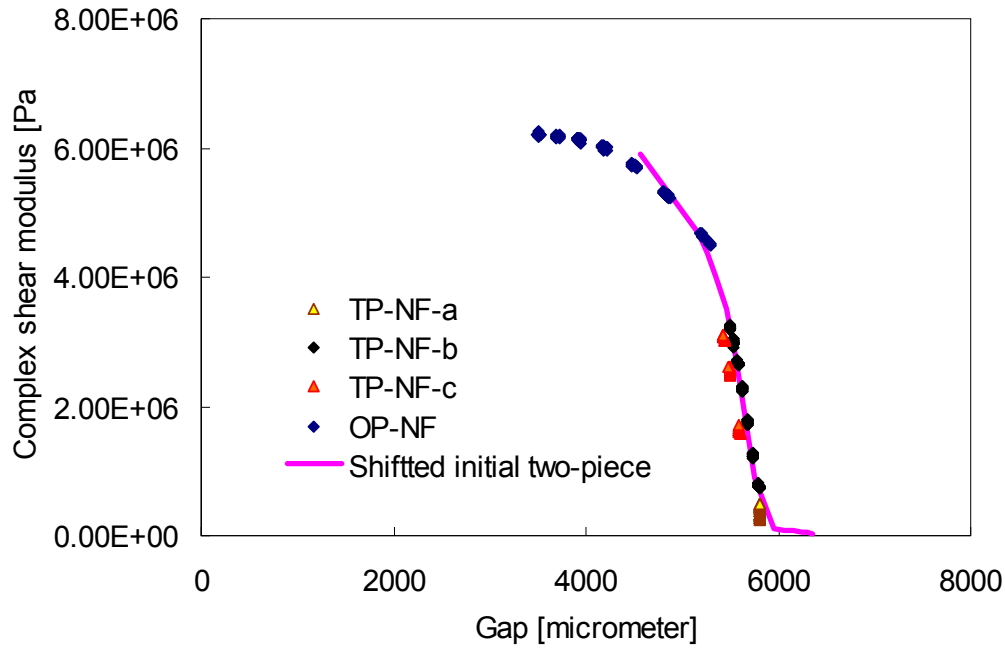Figure 4-18 Development of the complex shear modulus vs. the gap width

Figure 4-19 Normalized three stages of the initial healing and the NF healing

Figure 4-19 shows the normalized three stages of the initial and normal force healing curves. In order to delete the effects of thickness variation, the curve was shifted horizontally. The slope of the second stage of the NF healing in relation to the gap decrease is almost the same as that of the initial healing curve. Hence, it seems that most of the self healing signal through the NF healing is contributed by the gap decrease, which is caused by a compressive force.

As a result, the NF healing can be decomposed into time dependent healing that occurs during the time the gap width is kept constant and additional healing by compression. Since the contribution of the gap decrease part is dominant, it can be concluded that healing benefits much more from compressive forces than from the length of the time period during which healing can occur.

4.5   Summary and conclusions

By means of a Dynamic Shear Rheometer a detailed investigation of the self healing behaviour of pure bitumen has been carried out. Based on the test data and analysis, the following conclusions have been made:

o   The DSR is very useful for complex shear modulus measurements on bitumen. Since healing has an influence on the complex shear modulus of two-piece samples, the DSR can be used to investigate the healing effect by using the development of the complex shear modulus as an indicator.

o   Healing can be divided into an initial healing phase and a time dependent healing phase.

o   During the initial healing phase, a unique three-stage relationship between the initial healing modulus and the gap width decrease was obtained.

o   In the time dependent healing phase, the normal force controlled healing showed a much faster modulus improvement over time compared to gap controlled healing. The normal force controlled healing can be decomposed into the time dependent healing during a gap constant mode and additional healing due to compression. It was also indicated that the compressive normal stress strongly promotes healing development.

Furthermore, it was demonstrated that many factors can influence the complex shear modulus measurement results by using DSR parallel-plate geometry. Special attention must be paid to distinguish the real healing effect from those factors that may not really contribute to bitumen healing.

References

[1] Bazin P and Saunier JB. Deformability, fatigue and healing properties of asphalt mixes. Proceedings of the Second International Conference on the Structural Design of Asphalt Pavements. Ann Arbor, Michigan, USA; 1967, p. 553-69.

[2] Raithby KD and Sterling AB. The effect of rest periods on the fatigue performance of a hot-rolled asphalt under repeated loading. Journal of Association of Asphalt Paving Technologists 1970;39:134-52.

[3] Van Dijk W, Moreaud H, Quedeville A, and Uge P. The fatigue of bitumen and bituminous mixes. 3rd int. Conference on the Structural Design of Asphalt Pavements. Ann Arbor, Michigan, USA; 1972.

[4] Francken L. Fatigue performance of a bituminous road mix under realistic best conditions. Transportation Research Record 1979;712:30-4.

[5] Bhasin A, Little DN, Bommavaram R, and Vasconcelos K. A framework to quantify the effect of healing in bituminous materials using material properties. Road Material and Pavement Design 2008;EATA2008:219-42.

[6] Bommavaram R, Bhasin A, and Little DN. Determining intrinsic healing properties of asphalt binders: role of dynamic shear rheometer. Transportation Research Record 2009;2126:47-54.

[7] Qiu J, Van de Ven MFC, Wu SP, Yu JY, and Molenaar AAA. Investigating the self healing capability of bituminous binders. Road Material and Pavement Design 2009;10:81-94.

[8] Phillips MC. Multi-step models for fatigue and healing, and binder properties involved in healing. Eurobitume Workshop on Performance Related Properties for Bituminous Binders. Luxembourg; 1998, p. 115.

[9] Zhai H, Bahia HU, and Erickson S. Effect of film thickness on rheological behavior of asphalt binders. Transportation Research Record 2000;1728:7-14.

[10] AR-G2 2000ex Rheometers, Operator's manual. TA Instrument; 2006.

5

Assessing Self Healing of Bituminous Mastics Using Direct Tension Test

Abstract

Cracking is one of the main distresses responsible for the service life reduction of asphalt pavements. Self healing of (micro-) cracks will increase the service life. So understanding of the cracking and healing behaviour of bituminous materials is very important for service life predictions. Instead of a complex and time consuming fatigue test, a modified direct tension test was developed to characterize the cracking and healing behaviour of bituminous mastics in a simple and effective manner. Two test procedures were developed including a fracture-healing-re-fracture procedure (FHR) for investigating the self healing capability of an open crack and a loading-healing-reloading procedure (LHR) for investigating the self healing capability of meso cracks. The results indicate that the observed self healing process is a viscosity driven process, consisting of two steps namely crack closure and strength gain. The healing behaviour is very dependent on the healing temperature, duration of the rest period, crack phase and material type. In addition, a clear difference in self healing capabilities between a polymer modified bituminous mastic and a conventional penetration grade bituminous mastic was observed. As a result, the modified direct tension test is believed to be an effective tool for characterizing the self healing capability of bituminous mastics.

T he cracking behaviour of bituminous materials has been widely investigated for many years, and ranges from bituminous binders to asphalt pavements [1-3]. The self healing capability of these materials was also studied since 1960s [4-6]. The significance of the self healing capability is that an asphalt concrete can repair cracks thanks to hot summers and/or rest periods. It is known that self healing is a quite complex phenomenon, which is dependent on different factors including healing time, healing temperature, crack phase, material modifications and confinement.

In the past, numerous studies were carried out to qualify and quantify the self healing capability of bituminous materials. Most of the tests mentioned in the literature, like fatigue tests, are not really suitable for healing investigations because of their complexity and time consuming nature [7, 8]. There is a need for an efficient test method to understand the self healing phenomenon and to distinguish the healing capability between materials.

In this work, the self healing capability of bituminous mastics was investigated with a Direct Tension Test (DTT). Two test procedures were developed to evaluate the self healing capability under different crack phases.

- o Procedure I: a fracture-healing-re-fracture procedure (FHR) to assess the self healing capability of an open crack;

- o Procedure II: a loading-healing-reloading procedure (LHR) for self healing capability of a damaged specimen.

The usefulness of the two procedures to investigate the self healing capability of bituminous mastics is described in this chapter. In addition, influence factors on the self healing capability will also be discussed.

5.1 Experiments

5.1.1 Materials

Two types of commonly used bituminous binders were selected in this research.

- o a standard 70/100 penetration grade Kuwait Petroleum bitumen with a penetration of 93 (0.1mm) at 25°C, and a softening point of 45°C;

- o a Styrene-Butadiene-Styrene (SBS) polymer modified bitumen from Shell with a penetration of 65 (0.1mm) at 25°C, and a softening point of 70°C.

Bituminous mastics were produced by mixing the bituminous binders with a Wigro limestone filler (shown in Table 3-3) with a mass ratio of 1:1. Within this research, the mastic with 70/100 penetration bitumen is called the PBmas, and with SBS polymer modified bitumen is called the SBSmas.

5.1.2 Test procedure

The tests were carried out using a Direct Tension Test Machine (ATS 900DTTS) and in a temperature controlled environment. The parabolic shaped specimen as developed from research exploration phase was adopted in this test (shown in Figure 3-33). The test procedures are shown in Figure 5-1 and explained in detail in Table 5-1.
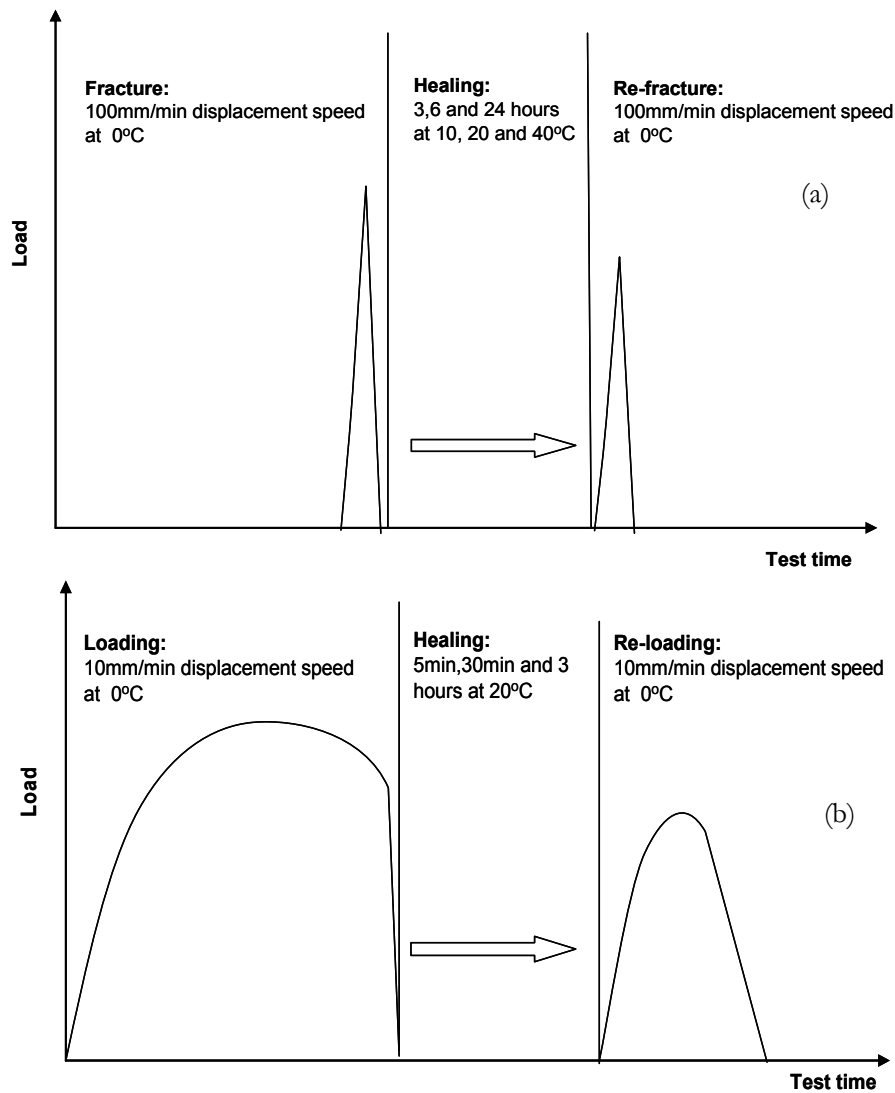
Figure 5-1 The DTT tests: (a) the FHR procedure and (b) the LHR procedure

Table 5-1 the DTT test procedure

Steps	FHR procedure	LHR procedure
1. Sample preparation	The preheated bituminous mastic is poured into a preheated silicon rubber mould, and covered with another piece of silicone rubber in order to get the same texture on each side of the specimen [9]. After natural cooling and conditioning in a refrigerator for 24 hours at -18°C, the specimens were de-moulded and placed in the temperature chamber of the direct tension test (DTT) machine for at least 2 hours at 0°C.	
2. First cycle	The original samples were fractured using a displacement speed of 100mm/min at 0°C.	The specimens were subjected to a direct tension loading with a displacement speed of 10mm/min at 0°C. In order to develop different crack phases in the specimen, various post-peak target elongations (TE_{after}) were set. The DTT machine was programmed to stop at a TE_{after} of 1mm, 2mm, 3mm, 3.5mm and totally broken respectively.
3. Healing	The two broken pieces of the specimen was placed back into the silicone rubber mould to heal. Various healing temperatures of 10°C, 20°C and 40°C and healing periods of 3 hours, 6 hours and 24 hours were applied.	The specimens were unloaded at each TE_{after} and then placed back into the silicon rubber mould in order to heal. Healing times of 5 minutes, 30 minutes and 3 hours in a temperature chamber of 20°C were applied.
4. Second cycle	After the healing periods, the specimens were conditioned back to 0°C for at least 2 hours and then de-moulded. The specimens were re-fractured afterwards with a displacement speed of 100mm/min at 0°C.	After the healing period, the specimens together with the silicon rubber mould were conditioned back at 0°C for at least 2 hours. The reloading was applied with a displacement speed of 10mm/min at 0°C till total failure. For comparison purpose, a reference specimen was directly reloaded without any healing procedure.
5. Microscopy	An Olympus Fluorescence Microscope was used to investigate the morphological change of the sample during the healing period at ambient temperature (around 25°C). Time intervals of 0, 1, 3, 8 and 18hours were applied.	An Olympus Fluorescence Microscope was used to analyze the real crack sizes immediately after unloading from each TE_{after}. The average width of a single crack (single-crack-width, SCW) perpendicular to the elongation direction was used as a parameter to quantify the real crack size at each TE_{after}.

After several trials, displacement speeds of 100mm/min and 10mm/min at a temperature of 0°C were chosen for this work.

- o In the FHR procedure, which is performed at a high displacement rate (100mm/min), the sample suddenly breaks in the middle. Because of that, the broken surfaces can be nicely connected again. This displacement speed was used for the FHR test procedure to investigate the healing capability of an open crack. Detailed information is presented in Section 5.2.

- o In the LHR procedure, the specimens were loaded at a displacement speed of 10mm/min. They showed a complex meso crack pattern at the middle of the specimen (Figure 3-37). The micro cracks and macro cracks are initiated and propagated in the entire sample and a sudden break did not occur. This displacement speed used in the LHR tests allows investigating the healing capability of meso cracks. Detail information can be found in Section 5.3.

5.2 FHR procedure

5.2.1 Strength recovery

Figure 5-2 shows the FHR test results obtained on the PBmas and the SBSmas samples. The self healing percentage was calculated by the re-fracture strength of the healed sample divided by fracture strength of the original sample:

$$H = \frac{S_{refracture}}{S_{fracture}} \times 100\%$$ 5-1

where,

H	= the self healing capability as a percentage of the original fracture strength;
$S_{refracture}$	= the strength of the re-fractured samples;
$S_{fracture}$	= the strength of the original fractured samples.

Bituminous materials are visco-elastic materials, which means that they show time-temperature dependent behaviour. Such a feature can also be observed in the self healing process. The healing percentage increases with increasing healing time and healing temperature. The following observations can be made when comparing the healing speed of the PBmas and the SBSmas (Figure 5-2).

- o The healing percentage of both the PBmas and the SBSmas is only 10% over time at 10°C.

- o The PBmas shows faster healing at temperatures of 20°C and 40°C and the strength recovery approaches nearly 80% after a healing period of 24hours.

o The SBSmas has a limited healing ability at 20°C but a fast healing speed at 40°C.
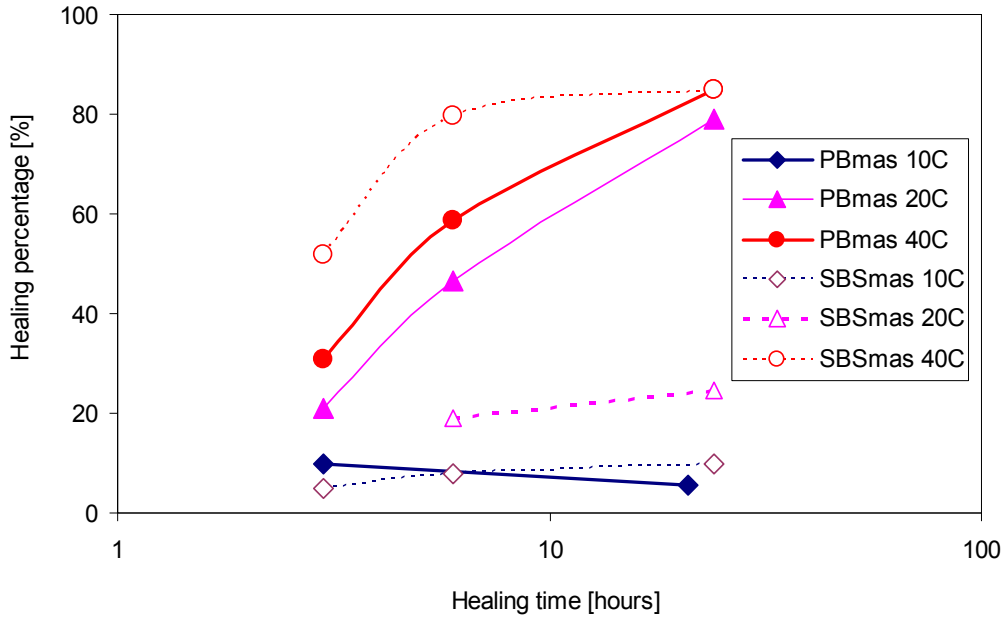

Figure 5-2 FHR Self healing test results of the PBmas and the SBSmas

To model the time-temperature dependency of the self healing process, a strength recovery master curve was constructed using the time-temperature superposition principle. An S shaped equation was used as shown in Equation 5-2, which is similar to the Christensen-Anderson Model for the complex modulus master curves of bituminous binders [10, 11]. The time-temperature superposition shift factor in Equation 5-3 is based on the Arrhenius Equation.

$$H(t,T) = 100 \times \left[1 + \left(\frac{m}{t \times \alpha_T} \right)^{\frac{\log 2}{n}} \right]^{-\frac{n}{\log 2}} \qquad 5\text{-}2$$

$$\log \alpha_T(T) = \frac{\Delta E_a}{2.303R} \left(\frac{1}{T} - \frac{1}{T_0} \right) \qquad 5\text{-}3$$

where,

    m, n = model parameters;

    α_T = time-temperature superposition shift factor;

    ΔE_a = apparent activation energy, J/mol;

    R = universal gas constant, $8.314 \, J/(mol \cdot K)$.

Figure 5-3 shows the strength recovery master curves of both the PBmas and the SBSmas at a reference temperature of 20°C. The related model parameters are shown in Table 5-2. It is shown that the PBmas could approach 100% healing much faster than the SBSmas.
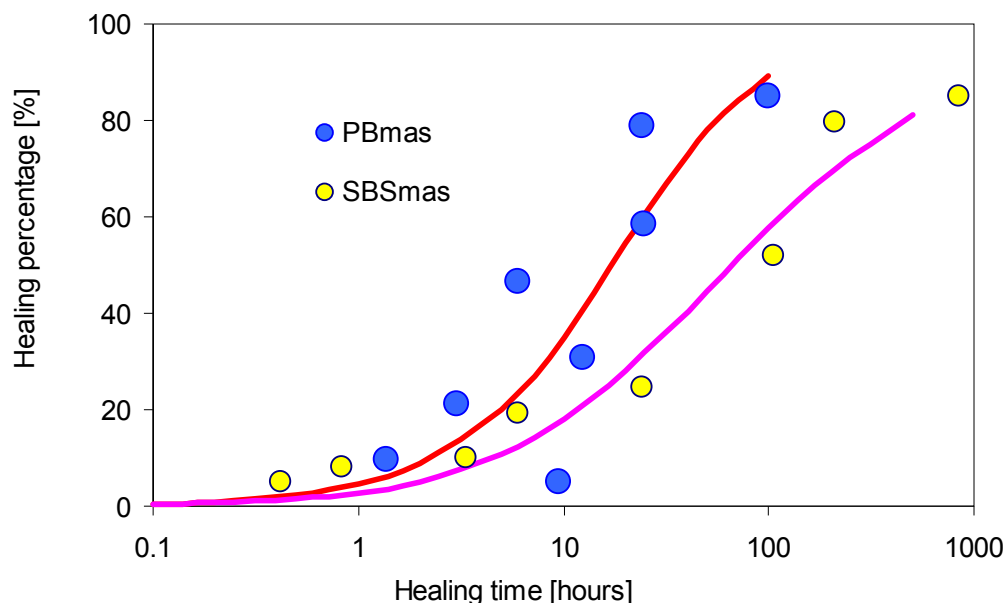

Figure 5-3 Self healing master curves of the re-fracture strength of the bituminous mastics at a reference temperature of 20°C

Table 5-2 List of model parameters

	m	n	ΔEa
	[hours]	[-]	[J/mol]
PBmas	22.22	0.24	124749
SBSmas	32.3	0.44	312195

5.2.2 Crack closure

Figure 5-4 shows the how the two broken pieces of the DP specimen are placed into the silicone rubber mould. Due to limited deformation of the specimen, the two pieces fit nicely into the original silicone rubber mould. A visible crack between the two pieces can be observed.
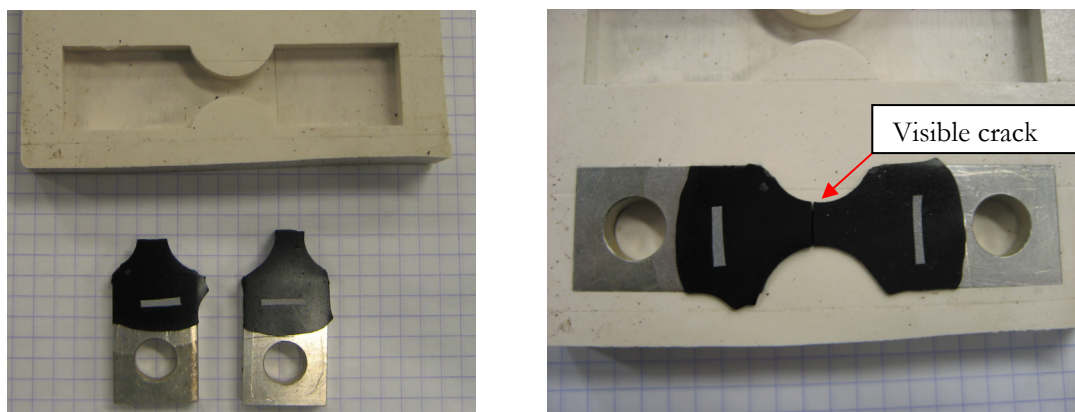
Figure 5-4 Illustration of placing the two broken pieces (left) into the silicone rubber mould (right)

In order to monitor the morphological change of the visible crack during the healing period, an Olympus Fluorescence Microscope was used.

Figure 5-5 shows the cross-section of a PBmas and a SBSmas specimen after fracture. The fracture face of the SBSmas specimen clearly shows shining spots when compared to the fracture face of the PBmas. These are believed to be the broken SBS molecules. The SBS molecules cover about 25% of the surface area according to the statistical analysis of the photo.

Figure 5-6 presents the morphological measurement of the PBmas after different healing times. The crack is about 150μm, and the closure of the crack can clearly be monitored over time. After a healing period of 3 hours, the crack disappears because of full closure of the crack.
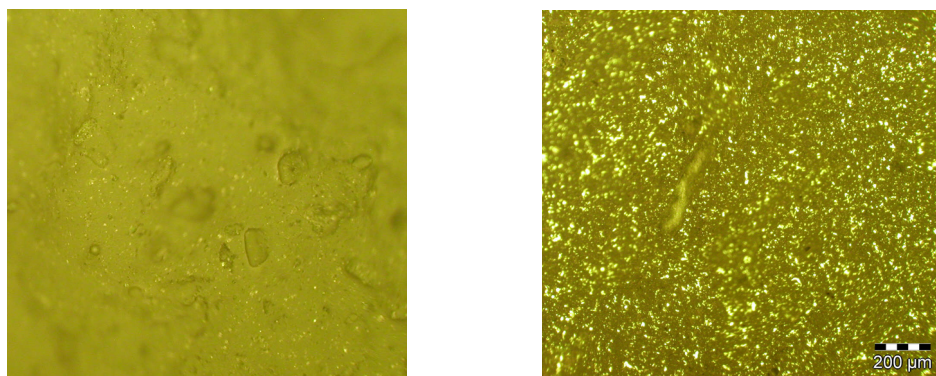

Figure 5-5 Fluorescence microscopic pictures of the cross-section of the PBmas (left) and the SBSmas (right) directly after being broken at $0^{\circ}C$
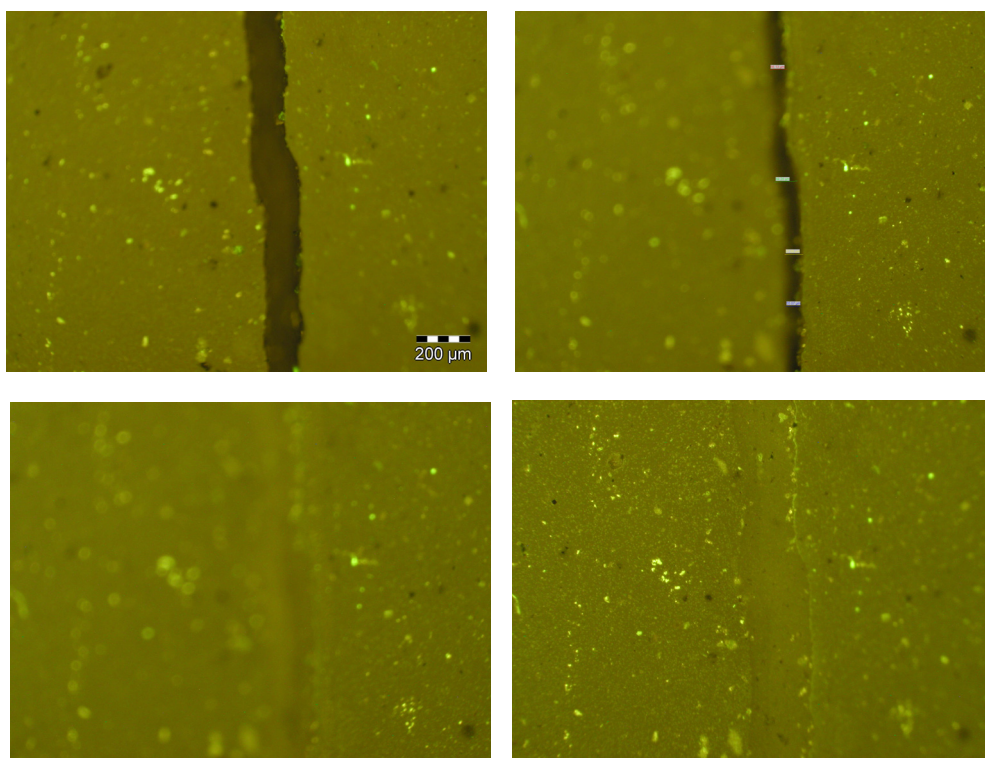
Figure 5-6 Fluorescence microscopic pictures of the PBmas specimen with different healing times (0, 1, 3 and 18hours) at a test temperature of 25°C

Figure 5-7 shows the morphology of the healing process of the SBSmas specimen. The initial crack width is about 100μm. It is interesting to see that the crack closure speed is much less compared to the PBmas sample. After a healing time of 8 hours, the crack can still be observed, but the width, especially in the centre of the picture, is much smaller.
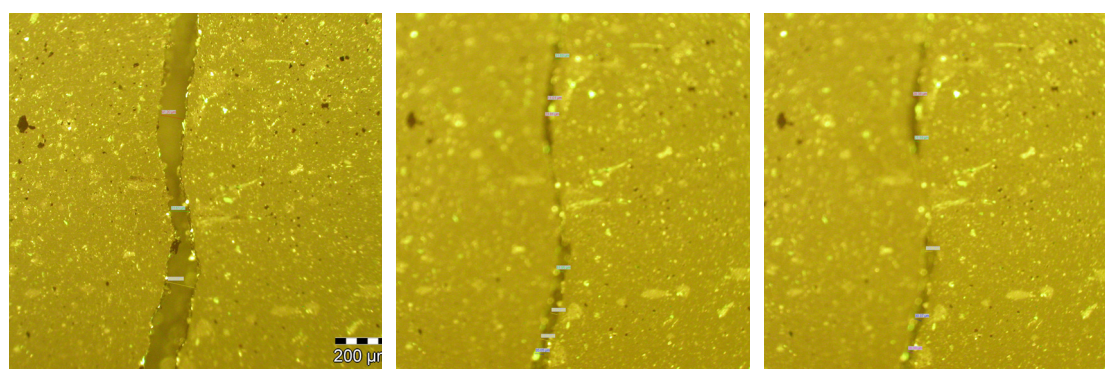

Figure 5-7 Fluorescence microscopy of the SBSmas with different healing times (0, 3 and 8 hours) at a test temperature of 25°C

5.2.3 Discussions

In Figure 5-8 both the decrease of the crack sizes as well as the recovery of the re-fracture strength are shown. Two phases can be observed namely crack closure and strength gain. It can be observed that the full closure of the crack does not mean a total recovery of the re-fracture strength. The strength recovery

curve was shifted to a reference temperature of 25°C. Once the crack is closed, the bituminous samples may still have micro cracks and air bubbles inside the sample which are not easy to detect. A longer healing time is still needed for more gain in strength of the specimen. Hence, the nature of the bituminous binder has a huge influence on the healing process. The healing in this crack phase is believed to be a viscosity driven process.

When comparing the PBmas and the SBSmas used in this research, the PBmas shows an excellent healing capability in both the crack closure and strength gaining phase. In general SBS polymer modifications give a significant improvement of the high and low temperature properties of bituminous binders because of the polymer network. However, the network also absorbs soft components from the bitumen. That results in a bitumen with a higher viscosity. This could be the reason why the SBSmas shows a lower healing speed. In addition, it is known that the SBS molecules are stable at healing temperatures from 10°C to 40°C, implying that no phase change or physical chemical reactions will happen at these temperatures. Hence, the broken SBS molecules can not repair themselves during the healing process at these temperatures, and will act as a "filler" in the bituminous system. Moreover, the broken SBS molecules cause difficulties for wetting and inter-diffusion both of which have a beneficial effect on the healing process. But this influence is lower at a higher temperature. All these reasons added up result in a lower healing speed of the SBSmas.
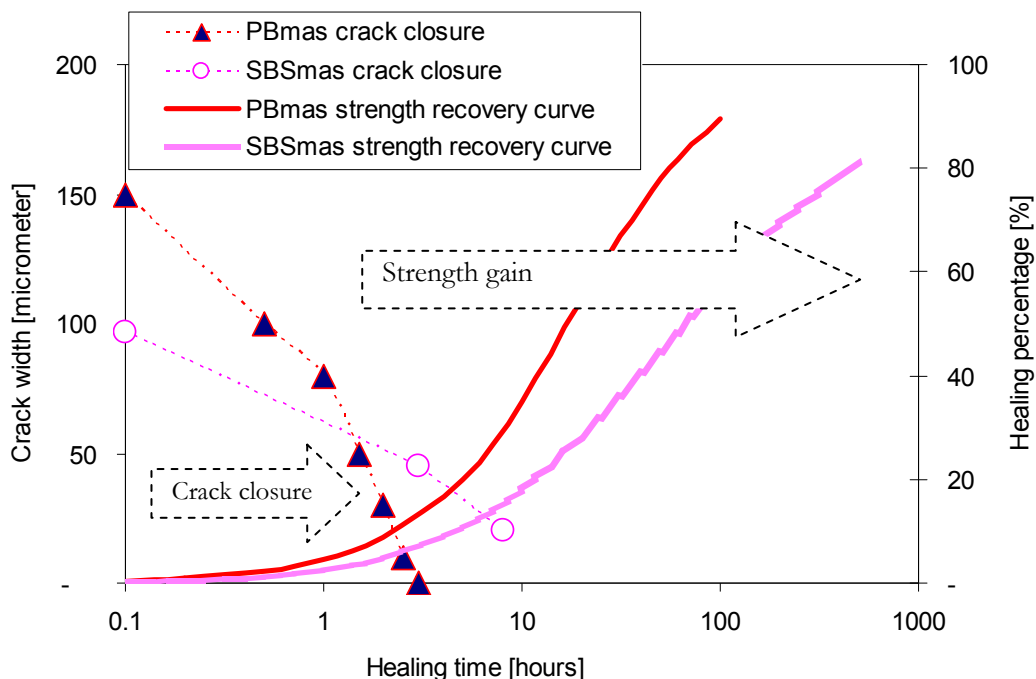

Figure 5-8 Comparison of the crack closure process and the strength recovery process at a temperature of 25°C

5.3 LHR procedure

5.3.1 Introduction to the envelope behaviour

A displacement controlled monotonic tension test (DMT) is widely used to determine the strength of bituminous materials [12, 13]. However, very little attention was paid to the failure envelope behaviour as shown in Figure 5-9. The failure envelope behaviour in a DMT test is extensively investigated in cement concrete research [14-17]. For concrete materials, it was found that the force-displacement curve formed a crack envelope. Furthermore it was shown that post-peak unloading-reloading cycles followed the softening phase of the DMT curve. Based on the fact that the softening phase of the DMT curve can be regarded as the crack evolution phase, it is possible to distinguish and quantify different crack phases on the softening curve using the post-peak unloading-reloading cycles. Nguyen investigated the DMT crack envelope behaviour of asphalt mixtures in a four point bending test using post-peak unloading-reloading cycles [18]. The results indicated that cracking of asphalt mixtures at low temperature resulted in a similar envelope behaviour as for cement concrete. Hence, the DMT crack envelope behaviour seems promising for crack phase quantification, rather than complex and time consuming fatigue tests.
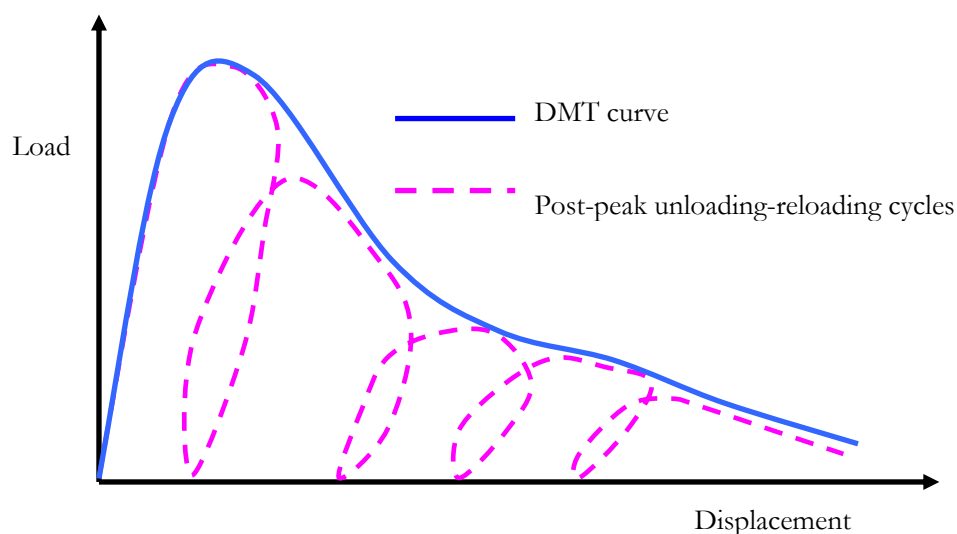

Figure 5-9 Illustration of the DMT envelope behaviour

5.3.2 Cracking behaviour with immediate reloading

A florescence microscope was used to analyze the crack sizes of the PBmas specimens at different elongations which were tested with a displacement speed of 10mm/min at a temperature of 0°C. The results are shown in Figure 5-10. The shinning white lines are the visible cracks that had developed. The average width of a single crack (single-crack-width, SCW in abbreviation) was calculated for each target elongation, TE_{after}.
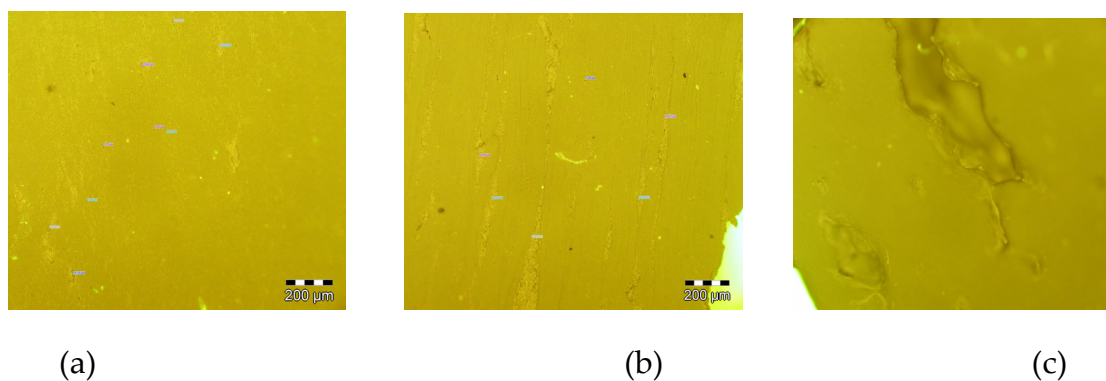
(a)　　　　　　　　　　　(b)　　　　　　　　　　　(c)

Figure 5-10 Microscopic images of crack phases at different post-peak elongations: a. 2mm TE$_{after}$; b. 3mm TE$_{after}$; C. total failure

Figure 5-11 shows in one picture the development of the SCW and the DMT curve. It can be seen that a crack can only be observed visually after a TE$_{after}$ of 1mm. Once a visible crack is obtained, the crack size increases with the elongation of the sample till total failure.
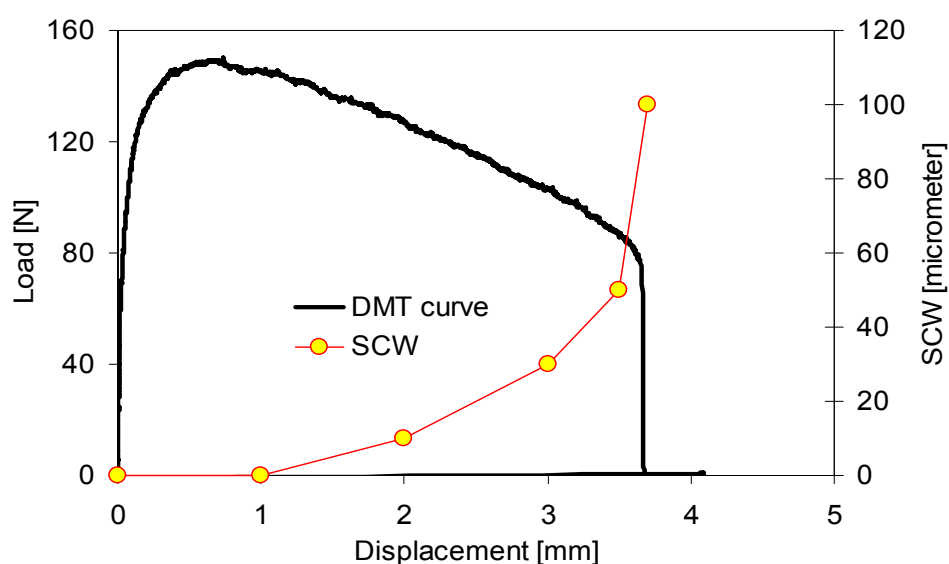

Figure 5-11 Comparison of the DMT curve with single crack width (SCW)

In Figure 5-12, the original DMT curve and the loading-immediate reloading cycle without healing are shown. The curves are normalized to the same peak load to avoid the influence of sample-to-sample variation. It can be seen that all the loading-reloading cycles follow the original DMT curve till failure. This indicates that the original DMT curve can be seen as an envelope [16]. This is to note that the DMT curve of the bituminous mastic is highly influenced by its visco-elastic relaxation behaviour even during post-peak softening, which is quite different when compared to cement concrete materials [11, 13, 19].
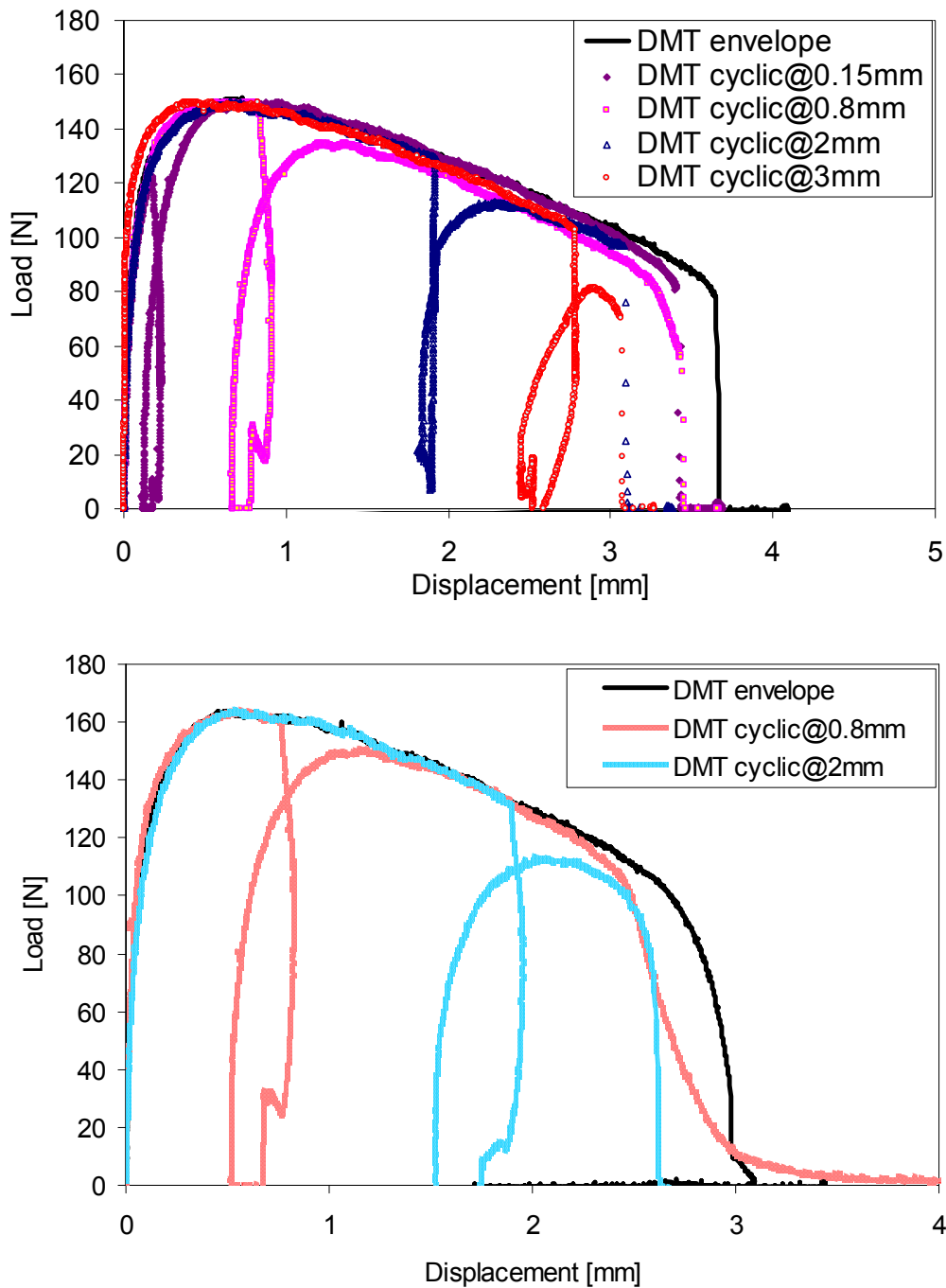
Figure 5-12 Crack envelopes of PBmas specimens (upper) and SBSmas specimens (lower) by normalizing the peak load

In addition, it appears that after immediate reloading, the curve will not return to the same point of the original loading curve but to a point with a lower strength value. This difference increases with the increase of the applied TE_{after}. The total failure displacement for the loading-immediate reloading cycle is smaller than the envelope and it decreases with the increase of the TE_{after}. This phenomenon is caused by the damage occurring during the unloading-reloading cycle [16].

151

Figure 5-13 shows in a graph the percentage of the immediate reloading strength, the immediate reloading energy and the SCW values, respectively. The energy was calculated by the area of the load-displacement curve. The following observations can be made:

o When the loading-immediate reloading cycle is applied before the peak load, the immediate reloading strength is the same as the original strength. After the peak load, the immediate reloading strength is lower than the original strength.

o A continuous dissipation of energy is shown throughout the test, even before the peak load. The development of the energy dissipation of the immediate reloading is similar as for the immediate reloading strength.

o The immediate reloading strength shows a reverse trend compared to the SCW development. But the immediate reloading energy indicates a much sharper decrease when compared to the immediate reloading strength and the SCW.
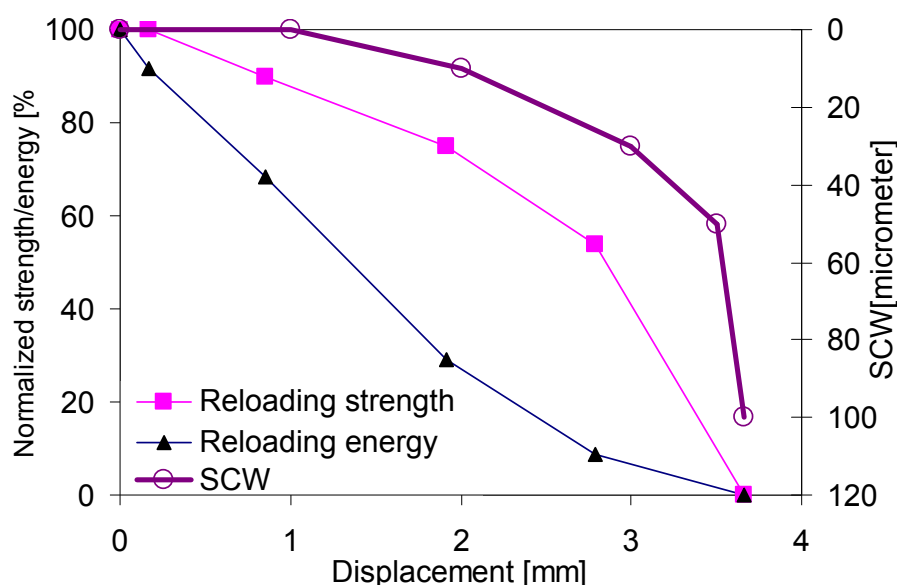

Figure 5-13 Comparison of immediate reloading strength, immediate reloading energy and SCW

5.3.3 Healing behaviour with reloading after rest periods

Figure 5-14 shows the results of the reloading curves of the PBmas and the SBSmas specimens after different healing periods at a temperature of 20°C. When no healing is observed, the reloading curve should remain the same and stay within the envelope. However, an increase of the reloading curve can be observed for bituminous mastics subjected to longer rest periods, which indicates healing.
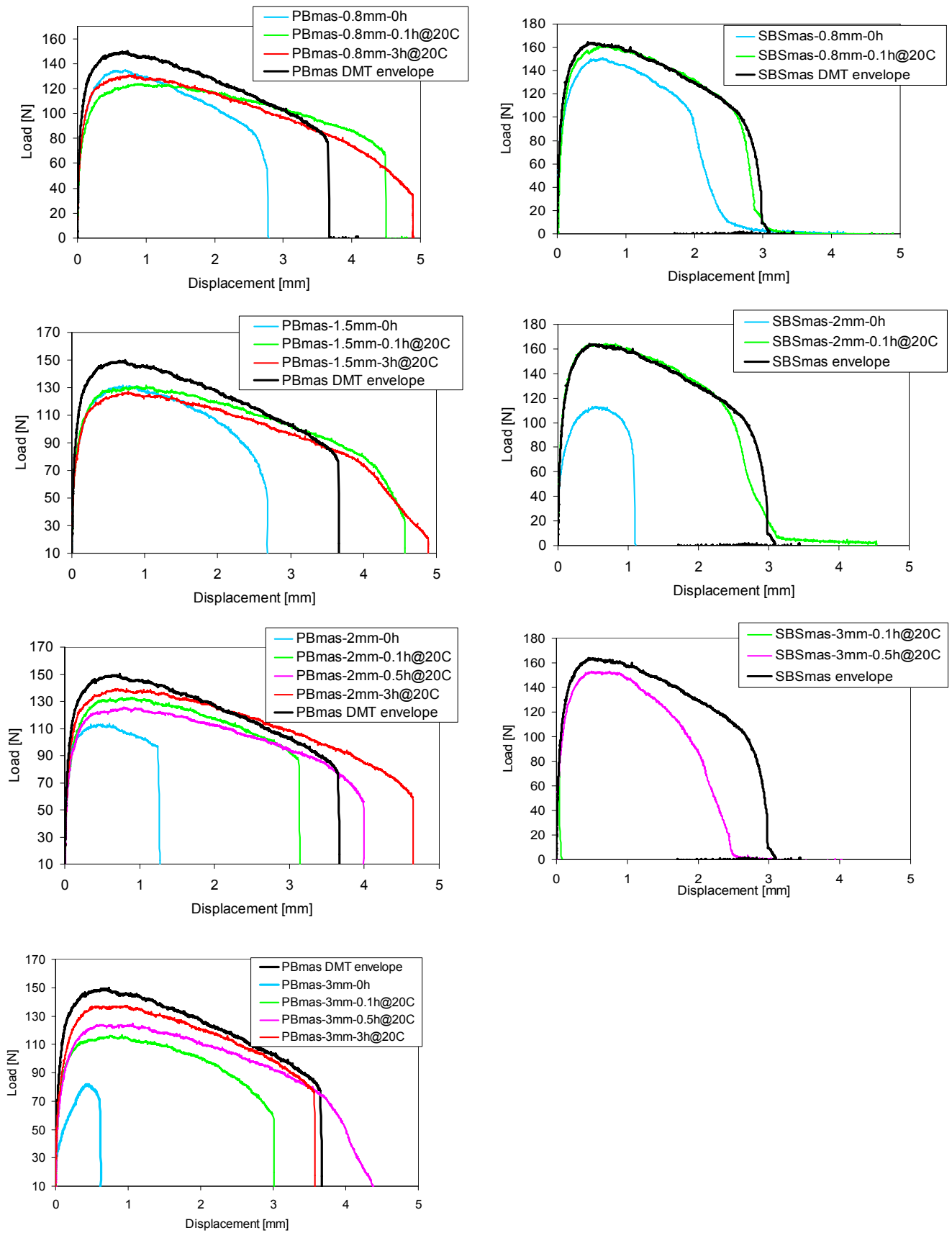
Figure 5-14 Healing results of PBmas (left) and SBSmas (right)

When comparing the reloading curves, the initial slopes of the reloading curves are almost similar to the original curve, which indicates a rapid recovery of the stiffness [11]. This may be due to relaxation of the specimen. However, a gradual increase of the reloading strength and the area under the reloading curve can still be observed over healing time.

The reloading strength, reloading displacement and reloading energy in relation to the duration of the healing periods are shown in Figure 5-15. It can be seen that the healing behaviour is strongly dependent on healing time, crack phase and material type. This will be discussed further in this section.
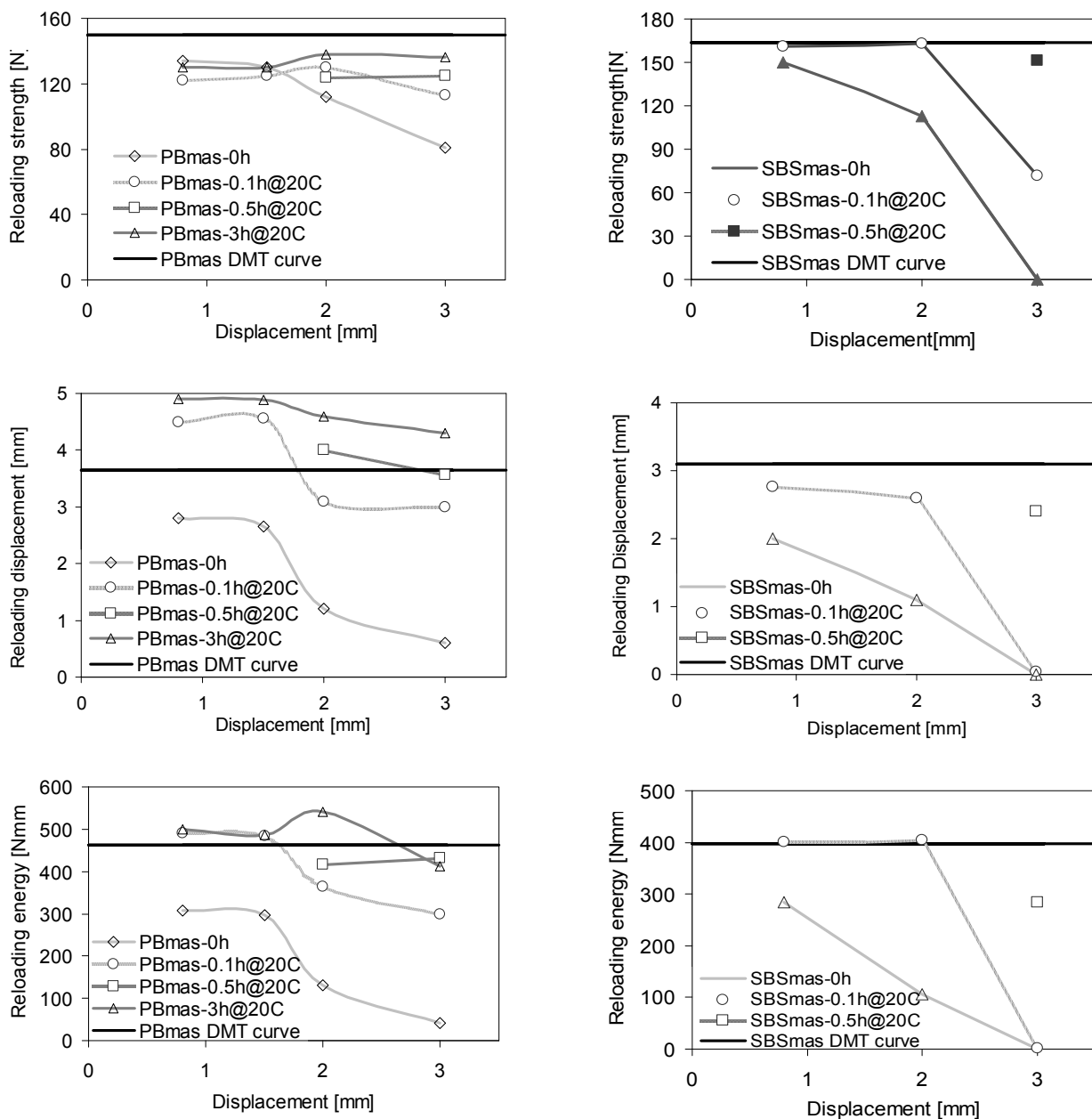

Figure 5-15 The reloading strength, the reloading displacement and the reloading energy of the PBmas and SBSmas

5.3.3.1 Time dependency

It can be seen that the reloading strength, displacement and energy increase with increasing healing time. However, it seems that the increment is not linear with healing time. For example, as shown in Figure 8-a, the reloading strength initially increases rapidly, and then increases slowly. At the TE$_{after}$ of 3mm, a 30% increase of the reloading strength can be observed at a healing time of 0.1h. An increase of another 15% of the reloading strength can be observed when the healing time is extended to 3hours.

The reloading displacement and the reloading energy follow similar trends. Both of them show a rapid increase after a healing time of 0.1h. After that, no clear increment in energy can be observed at a lower TE$_{after}$. However, at a TE$_{after}$ above 2mm, a slow recovery of the energy can still be observed over time after a healing time of 0.5h and 3h.

5.3.3.2 Crack phase dependency

Multi-cracks are accumulating and the crack sizes are increasing with increasing elongation. Hence, the healing of the cracks is probably much faster at a small elongation than at a large elongation. When comparing the different TE$_{after}$, the samples heal immediately at a TE$_{after}$ of 0.8mm and 1.5mm, where no visible or small visible cracks are found. However, when larger cracks are initiated (TE$_{after}$ of 2mm and 3mm), the samples heal slower over time.

5.3.3.3 Material type dependency

At elongations of 0.8mm and 2mm, both the SBSmas and the PBmas specimens show a fast healing. The SBSmas specimens show a better healing than the PBmas ones probably because of the SBS polymer networks. The SBS polymer network within the SBSmas does not break, but undergoes elastic deformation at these elongation levels. After unloading, the deformed network tends to return to its original shape, resulting in a higher healing of the strength.

At the TEafter of 3mm, the healing efficiency of the SBSmas specimens is less compared to the PBmas ones. The healing effect of the PBmas specimens is more significant, and is related to the flow properties of the pure bitumen. Due to the high viscosity of the SBSmas, the binder can not flow easily to heal the crack. In addition, the SBS network starts to break and gets even totally broken. The broken SBS network may also reduce the flow contribution of the binder, especially when part of the soft components of the bitumen phase are absorbed by the SBS network. If the SBS polymer network can not repair itself at the prevailing healing temperature, it will act as a filler at the crack surfaces and slow down the healing process.

5.4   Summary and conclusions

The self healing capability of bituminous mastics has been investigated using a special designed direct tension test. Based on the test data and analysis, the following conclusions can be made:

FHR procedure

- o A strength recovery master curve can be obtained using the time-temperature superposition principle.

- o Healing of an open crack is believed to be a viscosity driven process. The healing process includes two phases: crack closure and strength gain. The completion of the crack closure process does not imply a full recovery of the strength.

- o The negative effect of the polymer modification on self healing capability was clearly observed. An SBS modified bituminous mastic shows less self healing capability than a standard 70/100 penetration bituminous mastic in both the crack closure and strength gain phase.

LHR procedure

- o Multi-cracks can be obtained at a temperature of 0°C and a displacement speed of 10mm/min. The crack envelope behaviour can be obtained with the immediate unloading-reloading cycles and can be used to quantify the crack phases from different target elongations.

- o The healing observed after applying healing rest periods of different duration is dependent on healing times, crack phases and material types. A higher self healing capability can be obtained when the healing time is longer and/or in case of smaller cracks.

- o Due to the unique composition of the polymer modification, the SBS modified bituminous mastics showed a better strength healing capability than the standard bituminous mastics at a smaller crack phase or lower damage level, while the later show better strength healing at a larger crack phase.

- o The self healing capability causes rapid increase of the reloading stiffness and a gradual increase of the reloading strength, the reloading displacement and the reloading energy.

References

[1] Jacobs MMJ. Crack growth in asphaltic mixes, Delft: Delft University of Technology, PhD Thesis, 1995.

[2] Kim YR, de Freitas FAC, and Allen DH. Experimental characterization of ductile fracture-damage properties of asphalt binders and mastics. Annual Meeting of Transportation Research Board; 2008.

[3] Molenaar AAA. Structural performance and design of flexible road constructions and asphalt concrete overlays, Delft: Delft University of Technology, PhD thesis, 1983.

[4] Bazin P and Saunier JB. Deformability, fatigue and healing properties of asphalt mixes. Proceedings of the Second International Conference on the Structural Design of Asphalt Pavements. Ann Arbor, Michigan, USA; 1967, p. 553-69.

[5] Raithby KD and Sterling AB. The effect of rest periods on the fatigue performance of a hot-rolled asphalt under repeated loading. Journal of Association of Asphalt Paving Technologists 1970;39:134-52.

[6] Van Dijk W, Moreaud H, Quedeville A, and Uge P. The fatigue of bitumen and bituminous mixes. 3rd int. Conference on the Structural Design of Asphalt Pavements. Ann Arbor, Michigan, USA; 1972.

[7] Di Benedetto H, Quang TN, and Sauzeat C. Nonlinearity, heating, fatigue and thixotropy during cyclic loading of asphalt mixtures. Road Materials and Pavement Design 2011;12:129-58.

[8] Soltani A and Anderson DA. New test protocol to measure fatigue damage in asphalt mixtures. Road Materials and Pavement Design 2005;6:485-514.

[9] Muraya PM. Permanent deformation of asphalt mixes: Delft University of Technology, PhD thesis, 2007.

[10] Christensen DW and Anderson DA. Interpretation of dynamic mechanical test data for paving grade asphalt caments. Journal of Assoc. Asphalt Paving. Technol. 1992;61:67-116.

[11] Woldekidan M, Huurman M, and Mo L. Testing and modeling of bituminous mortar response. Journal of Wuhan University of Technology--Materials Science Edition 2010;25:637-40.

[12] Erkens SMJG. Asphalt concrete response (ACRe)-determination, modeling and prediction, Delft: Delft University of Technology, 2002.

[13] Lundstrom R. On rheological testing and modelling of asphalt mixtures with emphasis on fatigue characterization: KTH Royal Institute of Technology, 2004.

[14] Hillerborg A, Modeer M, and Petersson PE. Analysis of crack formation and crack growth in concrete by means of fracture mechanics and finite elements. Cement and Concrete Research 1976;6:773-81.

[15] Gaedicke C. Fracture-based method to determine the flexural load capacity of concrete slabs, Urbana-Champaign: University of Illinois, 2009.

[16] Hordijk DA. Local approach to fatigue of concrete, Delft: Delft University of Technology, PhD thesis, 1991.

[17] Roesler J and Gaedicke C. Flexural behavior of concrete specimens on various support conditions. 7th International DUT-Workshop on Design and Performance of Sustainable and Durable Concrete Pavements. Seville, Spain; 2010.

[18] Nguyen ML, Sauzeat C, and DiBenedetto H. Investigation of cracking in bituminous mixtures with a 4 points bending test. In: Al-Qadi, Scarpas, and Loizos editors. The Sixth RILEM International Conference on Cracking in Pavements. Chicago; 2008, p. 283-93.

[19] Lundstrom R and Isacsson U. Characterization of asphalt concrete deterioration using monotonic and cyclic tests. International Journal of Pavement Engineering 2003;4:143-53.

6

Assessing Self Healing of Asphalt Mixtures Using Beam on Elastic Foundation Setup

Abstract

It is a well known fact that asphalt mixtures have self healing capabilities. Most of the self healing investigations are carried out using complex and time consuming fatigue tests. Most of these tests do not give information on the real self healing capability of a cracked surface. In order to investigate the self healing capability of cracks under a well controlled condition, a beam on elastic foundation test setup (BOEF) is proposed. With a notched asphalt concrete beam fully glued on a low modulus rubber foundation, the BOEF setup is able to control the self healing process of a cracked surface autonomously including crack closure and crack healing at different rest periods and temperatures. A load-crack opening displacement (COD) curve was used for characterizing the self healing capability from the response to a loading-healing-reloading sequence. In addition, small numbers of dynamic loads were also applied to the BOEF setup under different cracking and healing conditions to check the recovery of the stiffness. An apparent modulus of the BOEF asphalt beam was obtained based on the dynamic response of the COD. The results indicated that the self healing capability which is observed from the monotonic reloading response is dependent on the healing time and healing temperature. The healing temperature has the largest effect of the two. The largest part of the apparent modulus of the BOEF asphalt beam recovers at the beginning of the self healing process. The influence of the healing time and temperature on the recovery of the apparent modulus is limited.

Self healing of bituminous materials has been investigated for over 40 years. Bituminous materials are believed to heal themselves during rest periods and hot summers. Most of the time, the self healing capability of bituminous materials is investigated in a fatigue test, which is a complex and time consuming process [1, 2]. Limited insight can be gained due to the complexity of the fatigue test itself. Therefore, there is a need for developing a more efficient test method to evaluate the self healing capability of bituminous materials.

A test setup called the Beam on Elastic Foundation (BOEF) has been used to evaluate the crack propagation behaviour through asphalt mixtures for many years [3-5]. This setup, in which an asphalt beam is supported by a rubber foundation, is designed to simulate a real flexible pavement structure. Because of the uniqueness of the rubber foundation, complications like permanent deformation of the simply supported asphalt beam can be neglected [3]. In addition, the rubber foundation can provide confinement to the crack after the load is removed, which is necessary for the first healing step of crack closure from the multi-step healing model [6, 7]. The BOEF test setup is very promising for the self healing investigations of asphalt mixtures and can really show if a crack can be healed by the material under investigation. In this paper, the usefulness of the BOEF setup for evaluating the self healing capability of asphalt mixtures is explored.

6.1 Beam on Elastic Foundation Set-up

Initially, the BOEF setup was developed for fatigue characterisation of asphalt mixtures. By using a soft art gum rubber foundation, Majidzadeh found that the creep effect during bending of an asphalt beam under load repetitions can be neglected [3, 8]. With respect to the fatigue crack growth, the parameter n of Paris's law obtained from the BOEF fatigue test was around 3.7. This was in agreement with what was expected from theory [4].

Molenaar investigated the fatigue behaviour of asphalt beams with full contact between the asphalt beam and the rubber foundation [4]. He concluded that the asphalt beam should be glued on the rubber foundation in order to simulate full contact and full friction. When no glue was used, partial slip could occur between the beam and the rubber. Due to the full contact, the crack propagation speed under a symmetric load decreased strongly when the crack length reached about 60% of the height of the beam; at that moment the crack entered the compression zone and no further propagation was observed.

Furthermore, the BOEF setup was also used for reflective cracking analysis. Molenaar investigated the effect of stress absorbing membrane interlayers (SAMI) using the BOEF test setup [9]. During the testing both vertical deflection and horizontal tensile displacements were monitored. A special clamp with a strain gauge was developed to monitor the displacements due to the vertical

crack propagation. It was observed that the crack was retarded by using the SAMI. A similar setup was successfully adopted by Brown [10] and Rowe [5] for the characterisation of reinforcing interlayer materials.

Roesler and Gaedicke applied the BOEF setup for concrete crack investigations [11-13]. A pre-notched concrete beam was placed on a clay subgrade. Post-peak loading-unloading-reloading cycles were used to investigate the failure envelope of concrete materials. In order to do so, they measured load-crack opening displacement (COD) curves. When the results of the BOEF tests were compared with the results obtained on simply supported beams, the maximum load on the BOEF beam was higher than that of the simply supported beam because of the presence of the elastic foundation. Another interesting observation was that after a certain crack opening, the load increased again, which may be due to the load transfer through the elastic foundation.

It can be concluded from the literature that the BOEF setup is useful for cracking and healing investigations because of the following reasons:

- o a well defined crack can be observed and investigated in this test which is very useful for healing investigations.

- o the elastic foundation absorbs most of the vertical deformation, which helps for healing investigations and eliminates the influence of permanent deformation;

- o after a loading-unloading cycle, the elastic foundation will help to close the crack during unloading and will support in this way the healing process of asphalt mixtures.

Hence, the BOEF setup is chosen for self healing investigations of asphalt mixtures in this study.

6.2 Experiments

6.2.1 Materials

6.2.1.1 Asphalt mixtures

A dense asphalt mixture type DAC 0/8 was used in this study. The target air voids content was 4%. Figure 6-1 shows the gradation curve of this asphalt mixture which is in accordance with the Dutch specifications [14]. Information of the materials used is given in Table 6-1.

As shown in Figure 6-2, asphalt mixture blocks were produced using a PresBox shear box compactor with a size of 450mm*175mm*150mm[15]. The BOEF beams with a size of 400mm*70mm*35mm were sawn from the blocks. A small notch was sawn in the middle of the beam with a width of 3.5mm and a depth of 15mm.
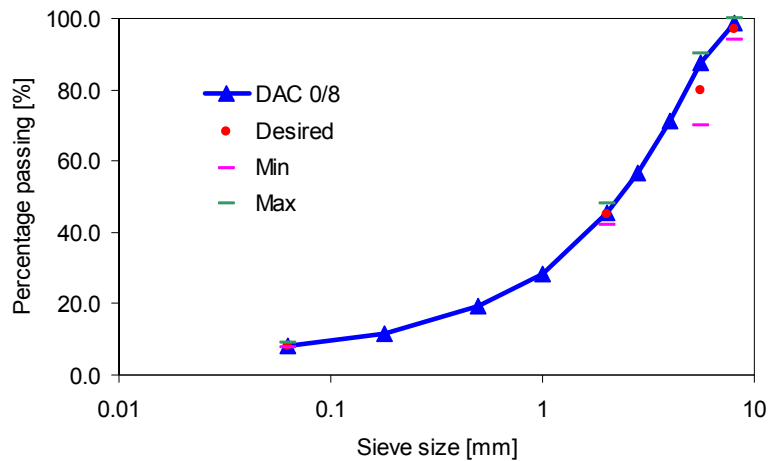
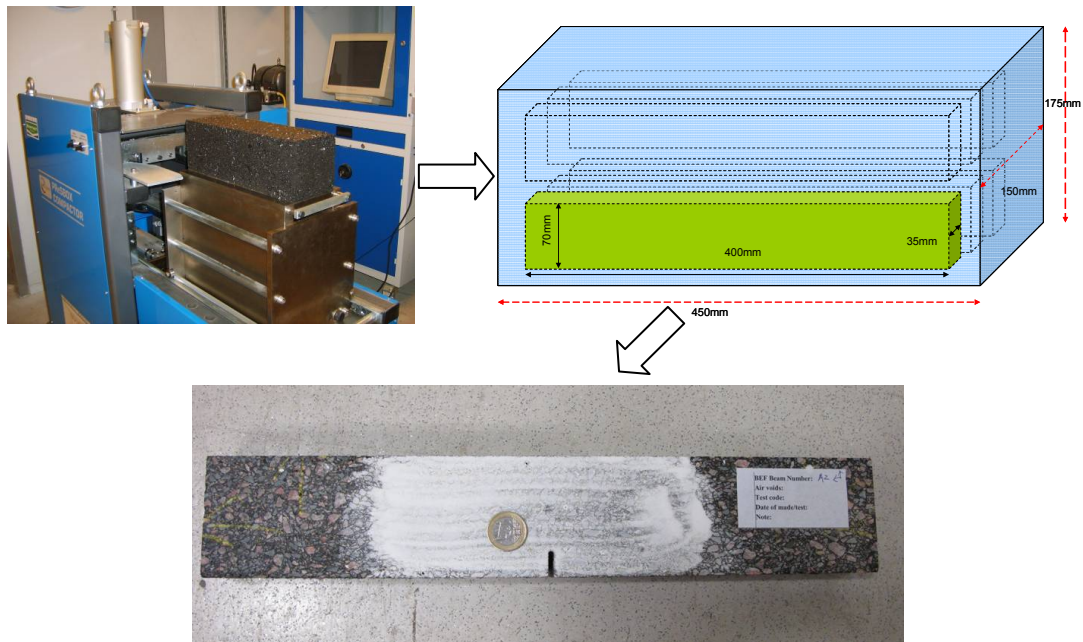Figure 6-1 Gradation curve of DAC 0/8 asphalt mixtures

Figure 6-2 Production of the BOEF asphalt beam

Table 6-1 List of materials used in the DAC 0/8 asphalt mixture

Materials	Scottish Granite 8-5.6mm	Scottish Granite 5.6-4mm	Norwegian Bestone 6-2mm	Crushed Sand 2-1mm	Crushed Sand 1-0mm	Wigro Filler	70/100 penetration bitumen
Proportions by mass [%]	11.2	19.6	21.5	16.8	16.8	7.5	6.5
Density [g/mm³]	2.576	2.576	2.643	2.677	2.677	2.750	1.025

6.2.1.2 Rubber

Neoprene rubber was selected as elastic foundation, with a hardness of 40° shore and a thickness of 20mm. The Young's modulus of the rubber was 6.5MPa. Another type of rubber with a Young's modulus of 15MPa was used as a loading pad. This pad had a size of 20mm*10mm*35mm.

6.2.1.3 Others

A steel plate with a thickness of 10mm was used as foundation. Epoxy glue Rengel SW 404 was used to glue the asphalt beam to the rubber foundation and to glue the rubber foundation to the steel plate. It was selected for its excellent workability and its good adhesion to asphalt-rubber and rubber-steel.

A Canon G11 camera with remote control was used for monitoring the crack propagation in the asphalt beam. White paint was used to make the cracks visible. A ruler marker with 5mm, 10mm and 20mm in length was used to quantify the crack length on the photos.

6.2.2 Test setup

Figure 6-3 shows the BOEF setup developed in this study. In order to ensure full contact between asphalt beam and rubber foundation, the asphalt beam was fully glued on the rubber except 10mm away from each side of the notch. This was to avoid glue under the notch. In addition, the rubber-steel interface was also fully glued. The load was applied in the middle of the beam through a rubber pad. At three places displacements were measured throughout the test (see Figure 6-3): the vertical displacement at the top of the rubber pad, VD; the crack opening displacement, COD, which was located right under the crack tip with a measuring distance of 20mm; and the side displacement, SD, which was located 10mm away from the edge of the beam.

6.2.3 Test procedure

Figure 6-4 illustrates the test procedure. Both monotonic loads and dynamic loads were applied in the test program. The general test procedure for the monotonic load was as follows.

- o The tests were conduced at 5°C. First a load was applied at a constant COD speed of 0.001mm/s until the target COD level was reached. Three target COD levels were selected: 0.2mm, 0.6mm and 0.9mm, respectively.

- o After the target COD level was reached, the specimen was unloaded with a COD closing speed of -0.001mm/s till the load level had returned to 0. At that moment, the external load was removed.

- o A rest period of 1 hour was first applied at 5°C. Then healing periods of 3 hours and 24 hours and healing temperatures of 5°C and 40°C were applied, respectively.

o After the healing period, the specimens were reloaded at a temperature of 5 ºC using a COD speed of 0.001mm/s till a COD level of 1.5mm. For specimens healed at a temperature of 40ºC, a conditioning time of at least 2 hours at 5 ºC was applied.
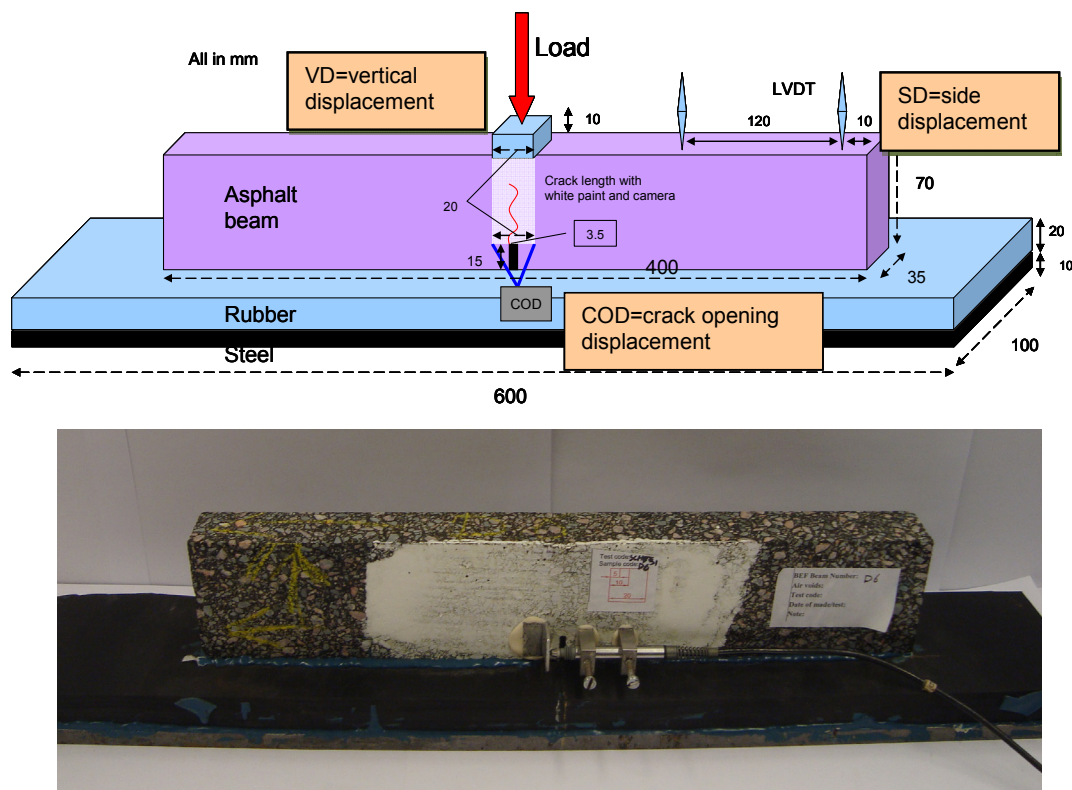

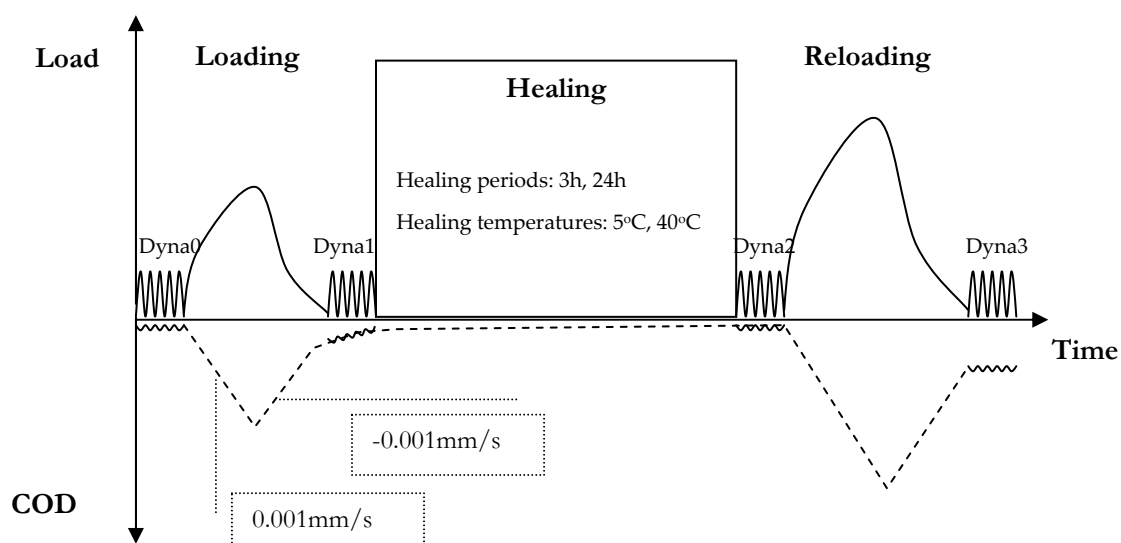Figure 6-3 Schematic of the BOEF setup (upper) and the real TUDelft BOEF setup (lower)

Figure 6-4 Illustration of the BOEF test procedure

Apart from the monotonic loading described above, series of force controlled dynamic loads were also applied between the loading-healing-reloading tests as shown in Figure 6-4. It should be noted that the dynamic loads were just to monitor the change in stiffness. The terms Dyna0, Dyna1, Dyna2 and Dyna3 were used for the dynamic loading before monotonic loading, immediately after loading (before healing), after healing and after reloading, respectively. During the dynamic loading, a small load amplitude of 300N and a frequency of 5Hz for 25 cycles were used at a temperature of 5^oC. The dynamic response of the COD was measured. The applied dynamic load was very small, and no influence on the healing process was expected. For specimens healed at a temperature of 5^oC, the dynamic loads were also applied during the self healing periods. An "apparent modulus" was calculated from the dynamic data as following.

$$M_{COD} = \frac{L_{dyna}}{C_{dyna}}$$
6-1

where,

M_{COD} = apparent modulus of the BOEF beams, N/mm;

L_{dyna} = maximum dynamic load applied, 300 N;

C_{dyna} = measured maximum of the dynamic response of the COD, mm.

It is expected that the M_{COD} will decrease in the case of crack growth during loading. After healing it is expected that the M_{COD} will recover at least partly due to healing. It should be noted that the M_{COD} is an "apparent stiffness" of the notched BOEF beam; it is a system value and not a material modulus.

6.3 Cracking of Asphalt Mixtures

Figure 6-5 shows the load-COD (abbreviation LC) curves obtained from the monotonic BEOF tests (MBT). Because of the influence of the rubber foundation, the LC curve does not show abrupt failure like observed in loading tests on simply supported beams.

- o At a COD level around 0.2mm, the slope of the load-COD curve decreases which may be seen as the start of cracking.

- o When comparing the different COD speeds, a higher COD speed shows a higher load value where the slope of the load-COD curves decrease. However, the differences in different COD speeds are not so evident when the repeatability of the tests is considered.
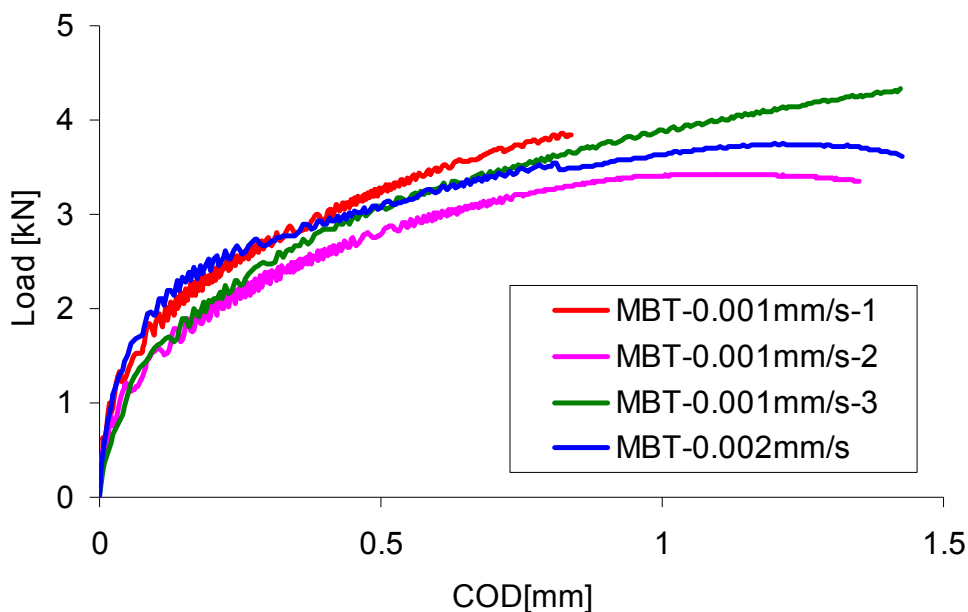

Figure 6-5 Monotonic BOEF test results (Three different tests were carried out at a COD speed of 0.001mm/s to check the variability of the BOEF test)

Figure 6-6 shows an example of the VD and SD as measured during the MBT test. It is recalled that the tests were COD controlled implying a constant increase in COD during time. As one will observe, the development of the VD is nonlinear. The VD-COD curve has a similar trend as the load-COD curve which is shown in Figure 6-5.

In addition, the SD shows different phases. Please note that a negative value of the SD means that the side of the beam is moving downwards, and a positive value means that the side of the beam is moving upwards. The phases for SD are:

- o The SD shows a slight increase at the beginning of the test until a COD level of proximately 0.02mm is reached. This implies that at the beginning the whole beam moves downwards.

- o Then, the SD starts to decrease linearly with increasing COD, which means the beam starts to bend.
- o After a certain moment, the rate of the SD decreases, implying that a non-linear second phase has started. The start of this second phase in the SD curve marks the initiation of cracking. Interestingly, the start of the second phase also correlates with the change of the slope of the load-COD curve and the change of the slope of the VD-COD curve.

In order to determine the crack propagation speed, camera assisted crack length measurements were made. Figure 6-7 shows an example of the development of the crack length at different COD values.
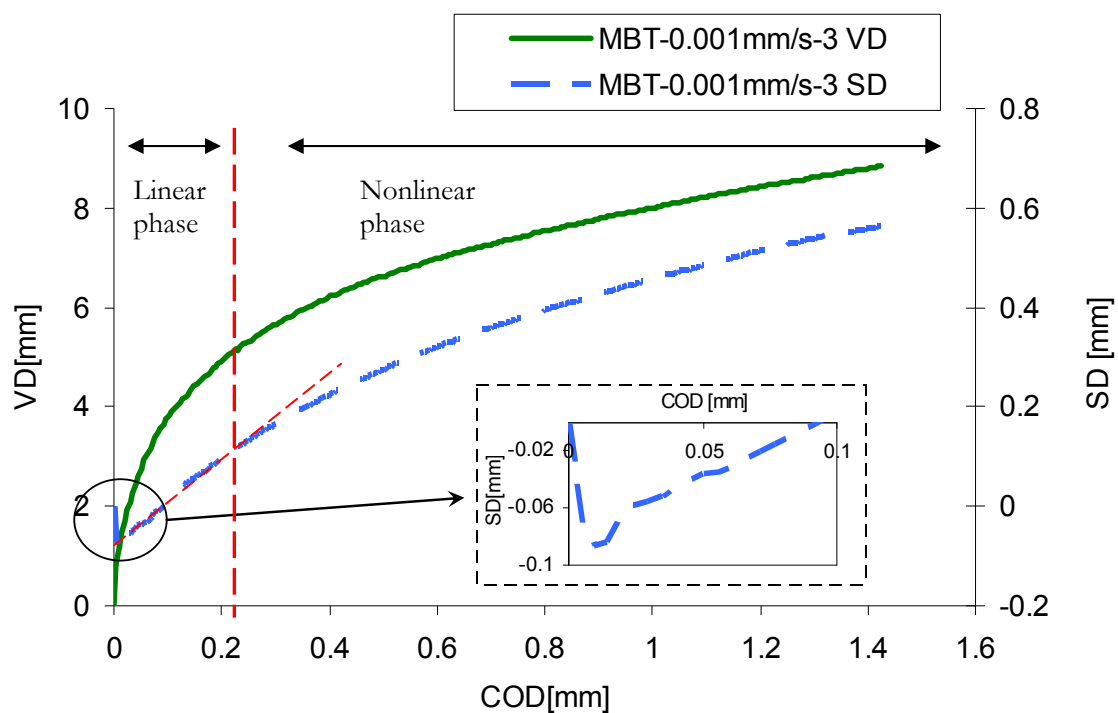

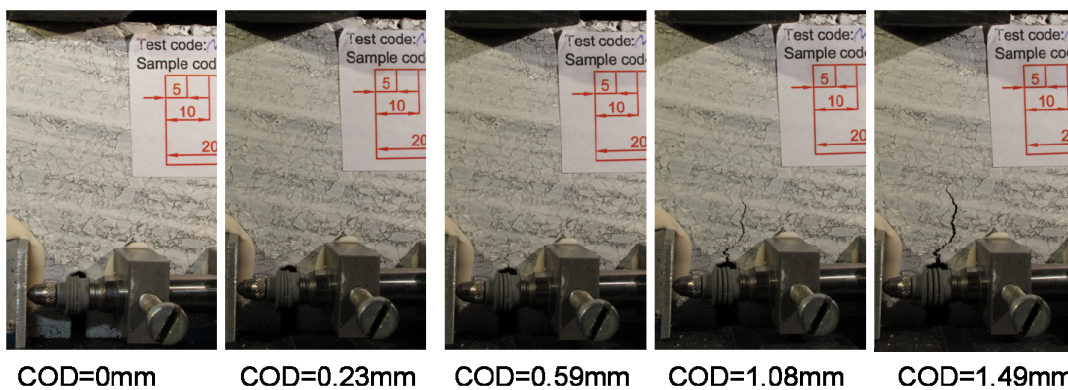Figure 6-6 Development of VD and SD for a COD speed of 0.001mm/s during a MBT test

Figure 6-7 Crack observations for the MBT test at a COD speed of 0.001mm/s

167

Figure 6-8 shows the development of the visible crack length and the visible crack width at the notch. The crack length refers to the visible crack development in the vertical direction and the crack width refers to the visible crack opening in the horizontal direction along the notch. It can be seen that the crack becomes visible after a COD level of 0.2mm and develops further. The development of the crack length tends to slow down after a COD level of 1mm because at that moment the crack is entering the compression zone. In addition, a continuous growing crack width at the notch can also be observed after the crack has become visible.
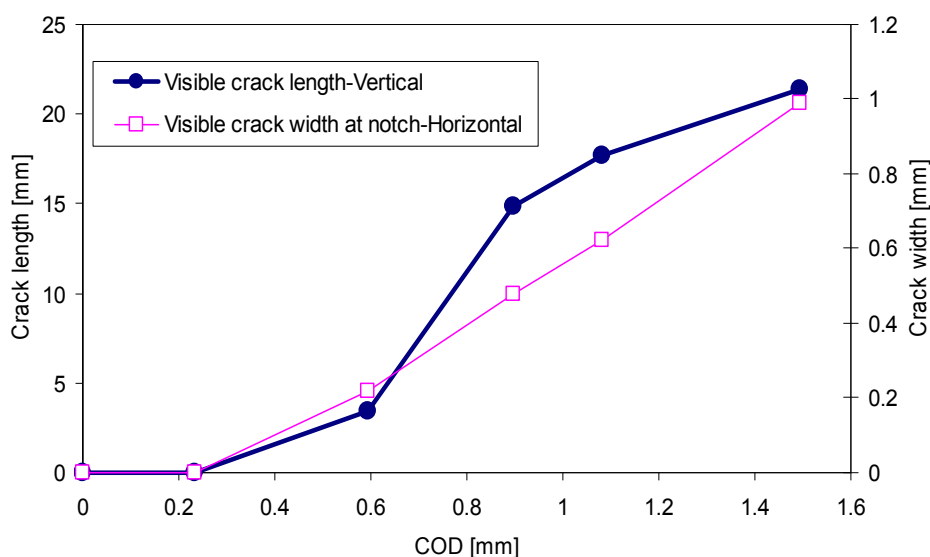

Figure 6-8 Development of the visible crack for a COD controlled MBT test
(speed of 0.001mm/s)

From the results in Figure 6-5 to Figure 6-8, the following crack phases in relation to the increase of the COD can be observed:

o   Preloading phase (about 0 - 0.02mm COD): the BOEF setup is under compression due to the low stiffness of the rubber foundation.

o   No visible crack phase (about 0.02mm - 0.2mm COD): the BOEF beam is bending. However, due to the visco-elastic effect, no visible crack can be observed.

o   Crack propagation phase (about 0.2mm - 1mm COD): the crack develops fast with increasing COD. The side displacement, SD, enters the non-linear second phase.

o   Crack propagation phase in the compression zone of the bending beam (COD ≥ 1mm): the crack propagation speed slows down with increasing COD.

Because the healing behaviour can be dependent on the amount of damage, healing tests were carried out on specimens cracked to different levels. As a result, three COD levels were selected to which specimens were loaded and

subjected to a healing period afterwards. The three selected COD levels are 0.2mm, 0.6mm and 0.9mm. The related crack lengths are no visible crack, 3-5mm and 8-10mm, respectively.

6.4   Unloading

When the target COD level was reached during loading, the unloading was carried out with a COD speed of -0.001mm/s. The external load facility was removed when the load became zero. After that, the setup is subjected to an autonomous process which means that the setup is left alone and that all the recovery which is observed after removal of the load is due to recovery of the BOEF test setup (beam and rubber foundation).

The development of the SD is shown in Figure 6-9. The recovery of the SD indicates the recovery of the curvature of the asphalt beam. This implies the macroscopic structural recovery of the BOEF asphalt beam due to confining effect of the rubber foundation. It can be observed that all the beams were recovering to the initial position shortly after the load was removed.
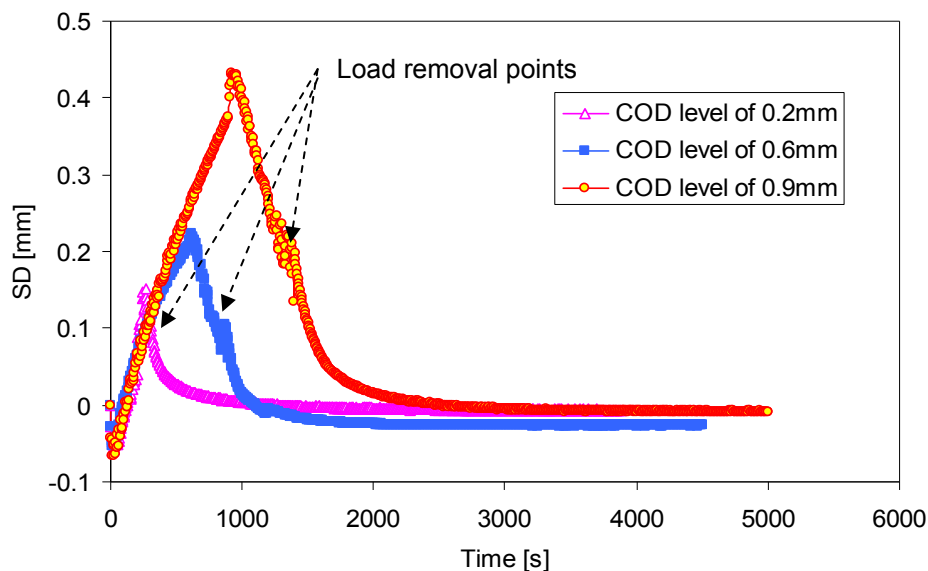

Figure 6-9 Recovery of the SD during unloading

Figure 6-10 shows the COD development curve during the unloading process. A nonlinear recovery of the COD can still be observed after removing the external load; even when the SD is constant. This is probably caused by the visco-elastic relaxation of the internal stress of the asphalt concrete beam and the closing of the crack due to the confinement of the rubber foundation. Most of the recovery occurs at the beginning of the process and is finished approximately one hour after the load was removed. As also shown in Figure 6-10, a residual COD even after the rest period can be observed for different target CODs. The residual COD can be explained by the deformation of the asphalt concrete beam or the mismatch of the crack faces.
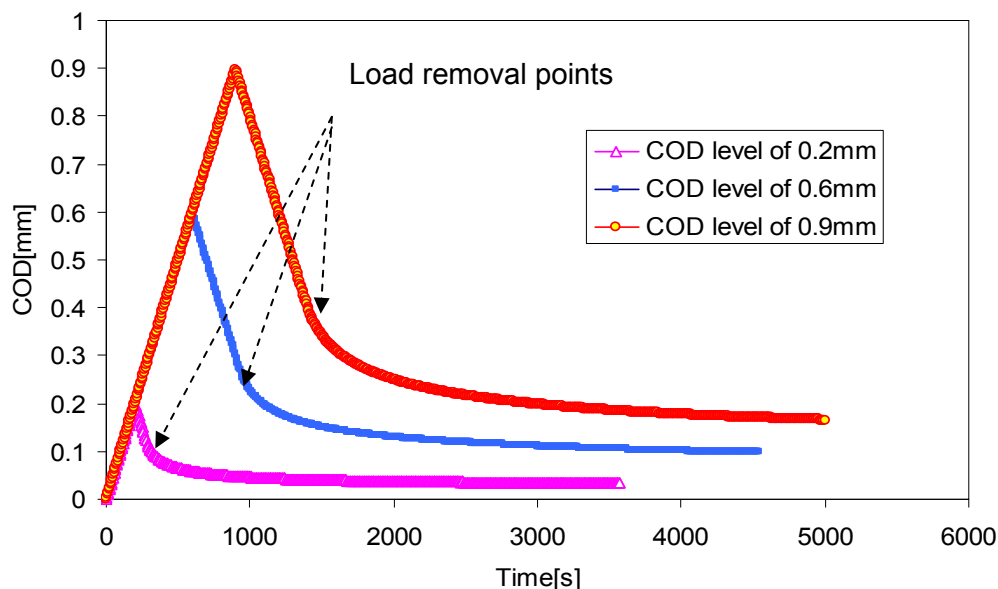
Figure 6-10 Recovery of the COD during unloading

To further clarify the reason of the residual COD during the unloading process, the crack observation photos at different conditions are compared; an example is shown in Figure 6-11. It can be observed that the visible crack which developed during the loading process is fully closed after unloading. This confirms that the residual COD is not because of the mismatch of the crack surfaces but due to the visco-elastic deformation of the asphalt concrete beam. In another word, the BOEF setup allows the autonomous fully closure of the crack surfaces. This offers the great opportunity to investigate the self healing behaviour of the asphalt mixture at any crack status.

(a)   (b)   (c)   (d)
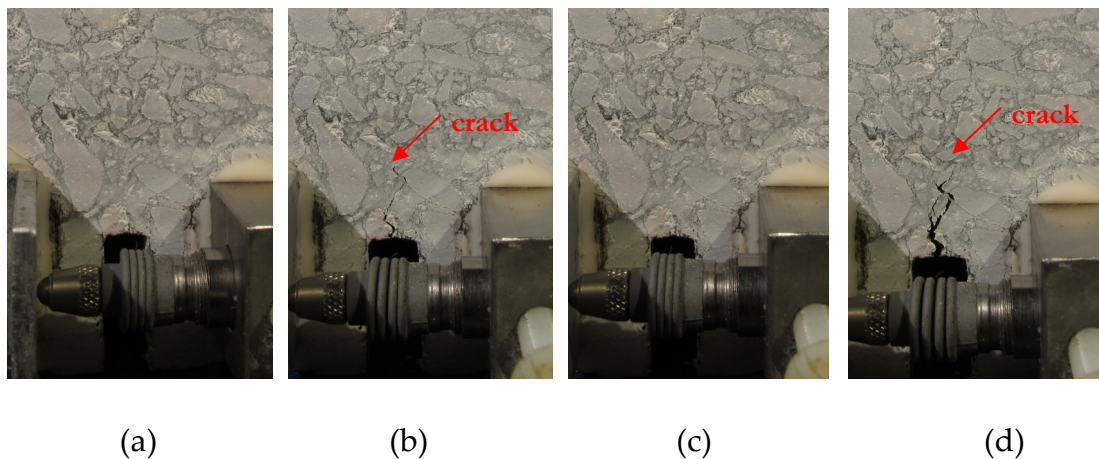
Figure 6-11 Example of crack formation and closure: (a) before loading; (b) loading till COD of 0.9mm; (c) unloading; (d) reloading till COD of 1.5mm

6.5   Healing of Asphalt Mixtures

Figure 6-12 shows the BOEF test results at different target COD levels. The changes in reloading curves which can be observed are due to different healing conditions. The analysis of the test results is given in detail in the following sections.

- o Section 6.5.1 presents the immediate reloading behaviour, which represents the reloading without any healing period.

- o Section 6.5.2 shows the development of the reloading strength of the BOEF asphalt beams under different healing conditions.

- o Section 6.5.3 shows the development of the reloading curves under different healing conditions.

- o Section 6.5.4 discusses the development of the COD during healing periods.

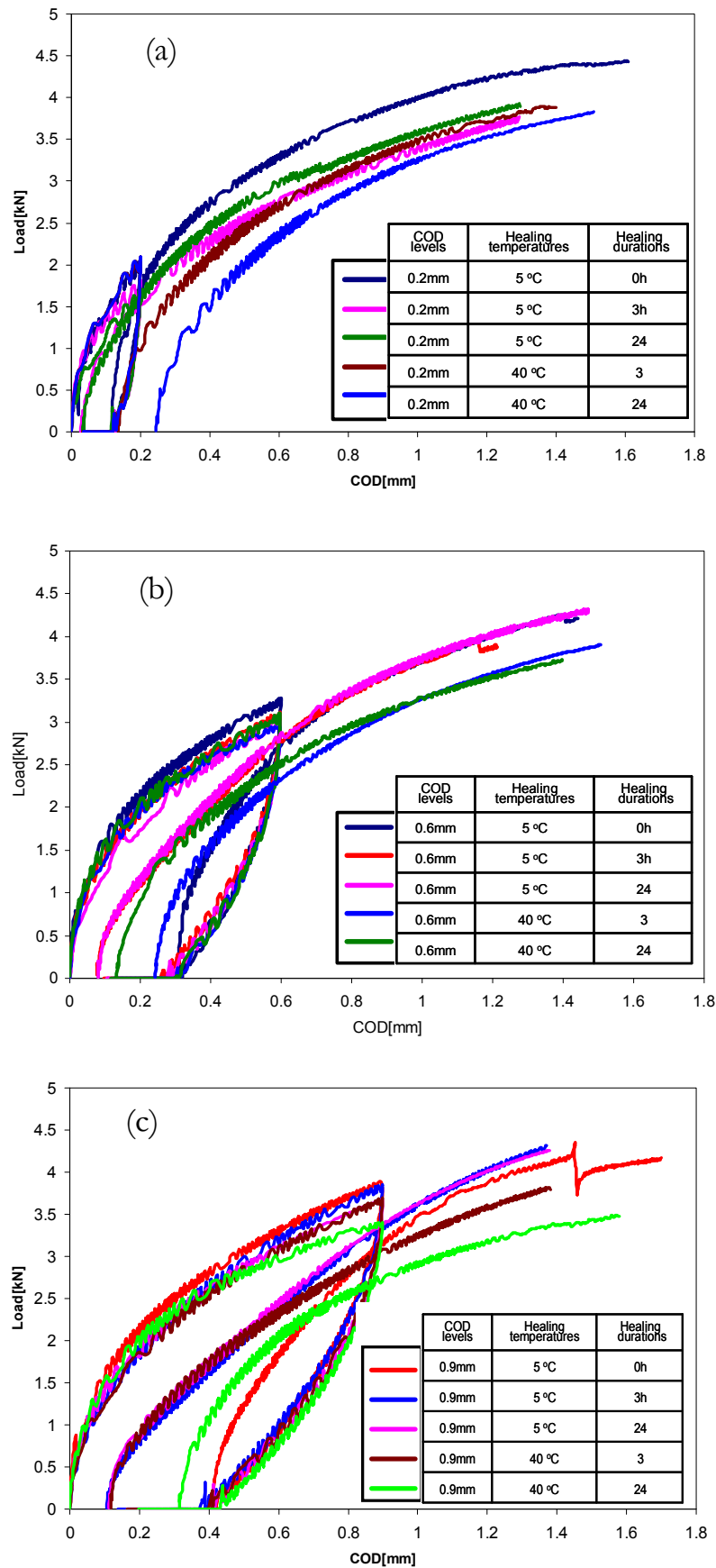- o Section 6.5.5 presents the development of the dynamic response of the BOEF asphalt beams.

Figure 6-12 BOEF test curves at COD levels of (a) 0.2mm, (b) 0.6mm, (c) 0.9mm

6.5.1 Immediate reloading

Figure 6-13 illustrates the results of reloading without application of a rest period for different target CODs. An MBT test to failure result is also presented. It can be seen that all loading-reloading curves are within the MBT curve. The MBT curve can be seen as a failure envelope for the loading-reloading curves. In addition, it appears that after the reloading cycle, the curve will not return to the same point of the loading curve where it unloaded from, but to a point which belongs to a lower load value. This difference increases with the increase of the target COD level applied. This phenomenon is due to the damage which is caused in such an unloading-reloading loop [16].

Figure 6-14 compares the immediate reloading and a reloading after a short healing period of 3 hours at a temperature of 5°C. It can be observed that after a short healing period the reloading load-COD curve shows a less steep slope. This is because of the relaxation of the asphalt beam and the confinement of the rubber foundation. Because of that, a recovery of the COD is observed.
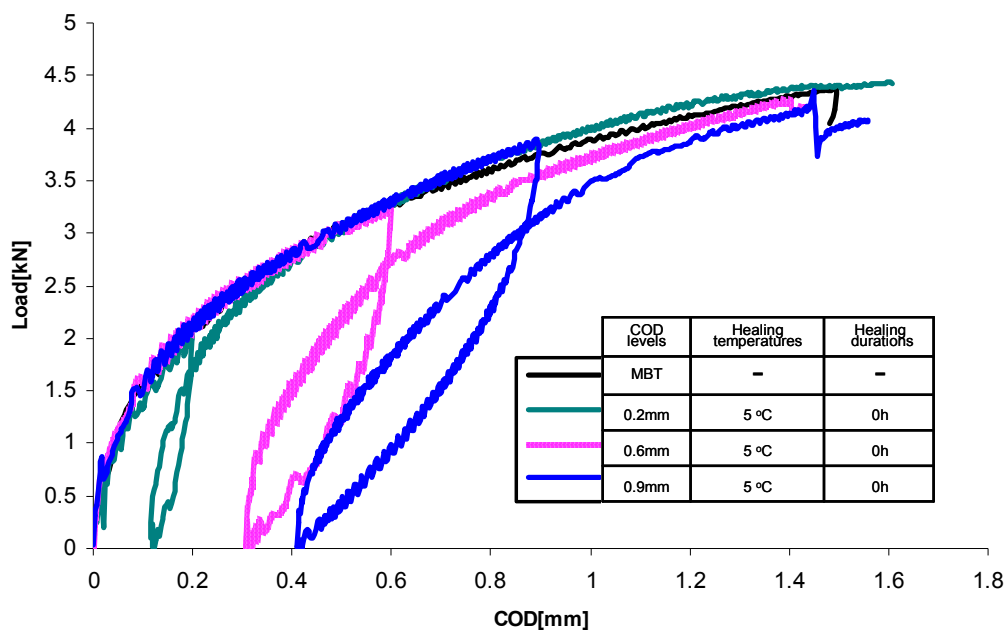

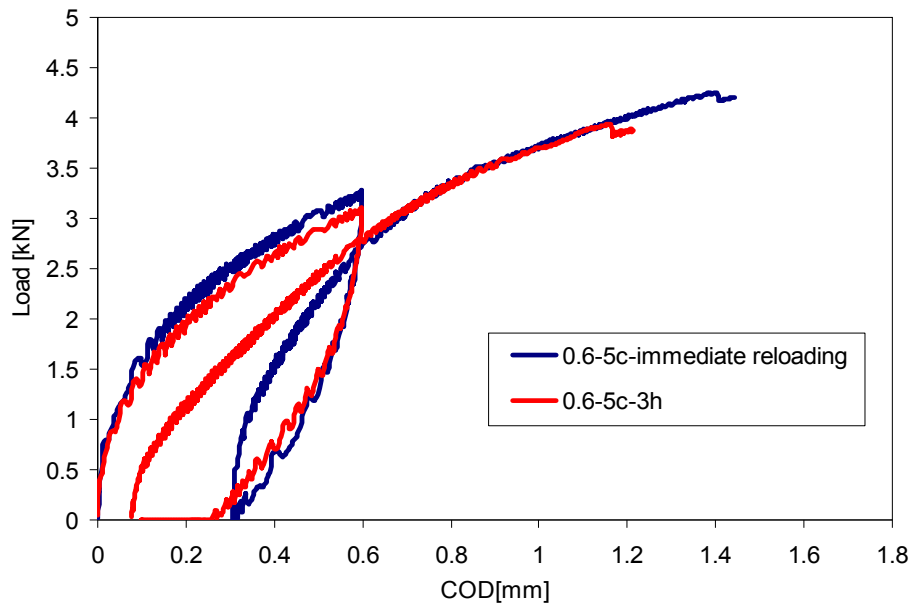Figure 6-13 Illustration of the BOEF envelopes

Figure 6-14 Comparison of immediate reloading and reloading after 3 hours at a healing temperature of 5oC for a target COD level of 0.6mm

6.5.2 BOEF strength

In order to further investigate the healing behaviour of asphalt beams with the BOEF test setup, a parameter called the BOEF strength was introduced. Figure 6-15 shows the determination of the BOEF strength. The BOEF strength was defined as the transition load from the no visible crack phase to the crack propagation phase. The load value corresponding to the linear-nonlinear transition of the SD-COD curve has been used to quantify this transition load. It should be noted that this strength is not exactly the strength of the asphalt beam, which represents the load applied to the whole BOEF system to start a crack. The BOEF strength is a combination of the strength of the beam and the reaction load from the rubber foundation.

Table 6-2 lists all the measured BOEF strength values. It can be observed that the loading strengths of all the beams are almost constant. An average value around 2.1kN was obtained.
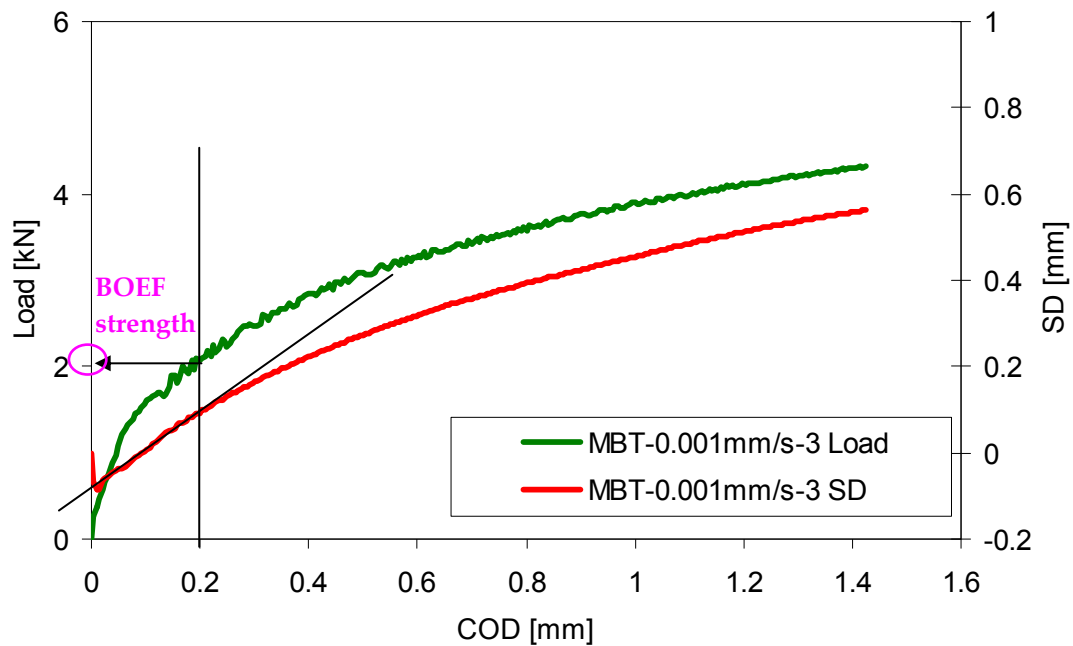
Figure 6-15 Determination of the BOEF strength

Table 6-2 List of the BOEF strength results

(0.2-5C-3h means the BOEF test was carried out with the target COD level of
0.2mm and the healing time was 3 hours at a temperature of 5 ℃)

	BOEF loading strength	BOEF reloading strength	Reloading percentage
	[kN]	[kN]	[%]
0.2-5C-3h	1.7	2.3	134.7
0.2-5C-24h	1.7	2.2	133.3
0.2-40C-3h	2	2.5	125.3
0.2-40C-24h	2	1.7	85.3
0.6-5C-3h	2.2	1.5	68.2
0.6-5C-24h	2.5	2	80
0.6-40C-3h	1.8	1.6	88.9
0.6-40C-24h	2.2	2.1	95.5
0.9-5C-3h	1.7	0.9	52.9
0.9-5C-24h	2.2	1.4	64.8
0.9-40C-3h	2.3	1.7	73.9
0.9-40C-24h	2.2	1.8	80.5

Figure 6-16 shows the BOEF reloading strength percentages for different healing conditions. The BOEF reloading strength percentage is defined by the BOEF reloading strength divided by the BOEF loading strength.

The following can be observed for the results.

- o A clear time and temperature dependency of the development of the reloading strength percentages can be observed. A longer healing time and a higher healing temperature are beneficial.

- o It can be observed that all the reloading strength values at the COD level of 0.2mm above 100%. This is because when determining the BOEF strength from the COD-2mm loading curves, the SD-COD change is still in the linear range. So the maximum load value of the load-COD curve was used as loading strength.

- o It can also be observed at the COD level of 0.2mm that almost no change of the BOEF strength can be observed as a result of healing. It seems that during unloading at this COD level, the not yet visible crack heals immediately. Or the assumption that there was some damage at COD level of 0.2 mm is incorrect; perhaps there was not yet damage.

- o At the COD levels of 0.6mm and 0.9mm, all the reloading strengths are less compared to the loading strength. An increase of the reloading strength percentage due to different healing conditions can also be observed. The reloading strength recovers slightly faster at the COD level of 0.6mm than at the COD level of 0.9mm when the beam is more damaged.
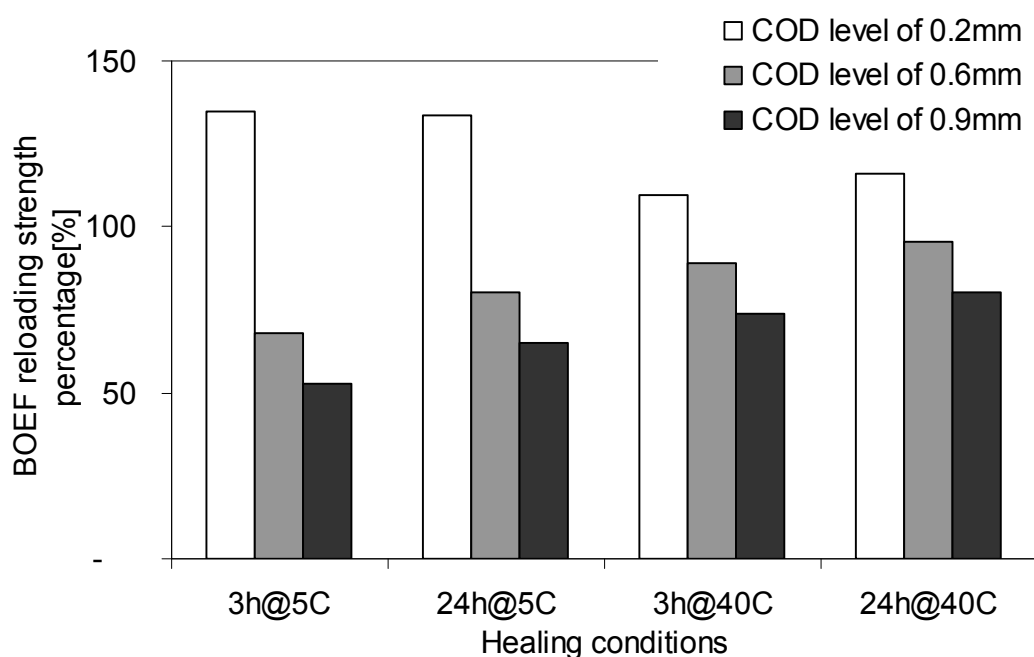

Figure 6-16 Comparison of the BOEF strength percentages under different healing conditions

6.5.3 BOEF curves

Prior to the comparison of the BOEF curves, the loading and reloading LC curves were smoothened by using a power function as shown in Equation 6-2.

$$L = m \cdot C^n$$

6-2

where,

L	= load, N;
C	= value of the COD, mm;
m and n	= regression parameters.

In addition, the reloading curves are normalized using the function given in Equation 6-3. All the normalized reloading curves are compared to avoid sample to sample variation.

$$L_{norm}(C) = \frac{L_{reloading}(C)}{L_{loading}(C)} L_{ref}(C) = \frac{m_2 C^{n_2}}{m_1 C^{n_1}} \cdot m_{ref} C^{n_{ref}}$$

6-3

Table 6-3 shows the regression parameters for different loading and reloading curves.

Figure 6-17 gives and example of simulating the MBT curve with the exponential function, which was used as the reference.

In Figure 6-18, the normalized LC curves for all the healing conditions are compared. An increase of the slope of the LC curve is observed for increasing healing time and increasing healing temperature. It can also be seen that at a longer COD levels of the reloading curve, the reloading after high temperature healing shows a slight tendency to decrease. This can be explained by the following reasons: a. the conditioning time at 5°C before the reloading was not enough; b. some permanent deformation occurred during the high healing temperature.

Table 6-3 Regression results for different LC curves

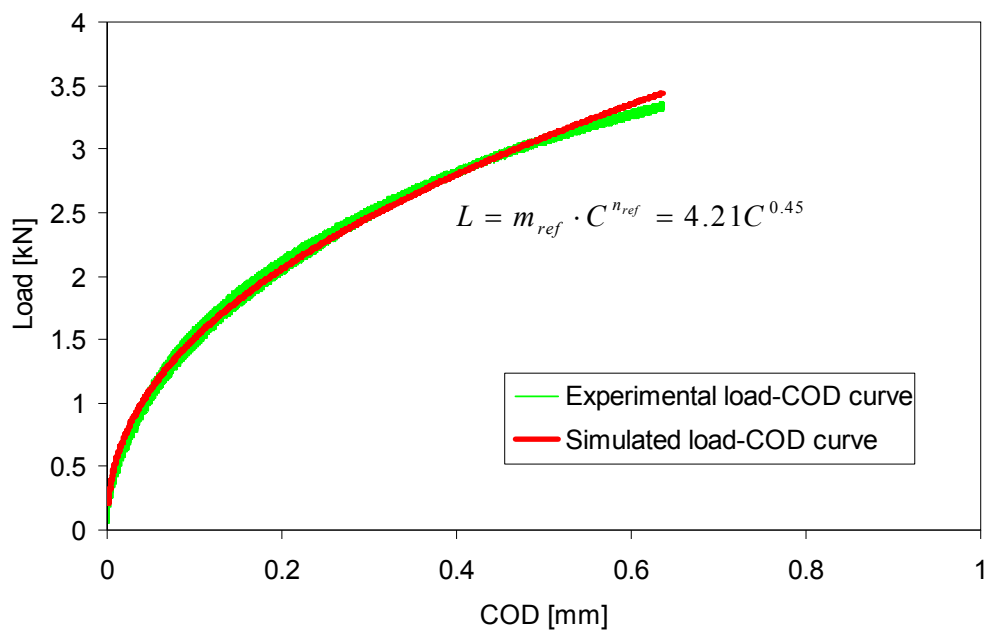| Code	Loading		Reloading	
	m_1	n_1	m_2	n_2
0.2-5C-3h	3.37	0.40	3.64	0.48
0.2-5C-24h	3.72	0.51	4.20	0.55
0.2-40C-3h	3.93	0.44	3.89	0.47
0.2-40C-24h	4.16	0.50	3.88	0.49
0.6-5C-3h	3.91	0.44	4.13	0.62
0.6-5C-24h	3.82	0.48	4.18	0.60
0.6-40C-3h	3.93	0.44	3.82	0.48
0.6-40C-24h	3.87	0.47	3.51	0.48
0.9-5C-3h	3.54	0.50	3.23	0.67
0.9-5C-24h	3.92	0.45	3.73	0.60
0.9-40C-3h	3.95	0.48	3.46	0.55
0.9-40C-24h	3.76	0.41	3.66	0.49
Reference	4.21	0.45		

$$L = m_{ref} \cdot C^{n_{ref}} = 4.21 C^{0.45}$$

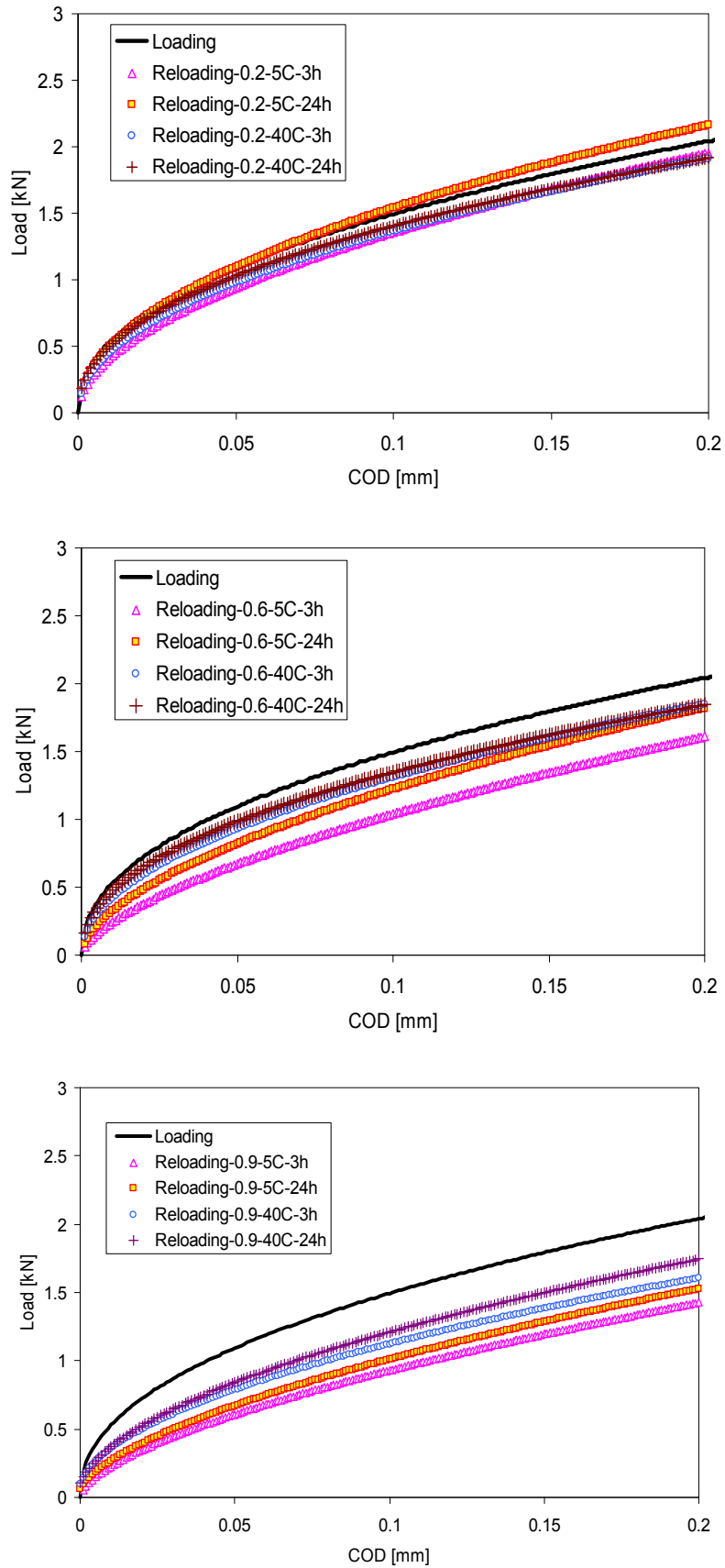Figure 6-17 Simulating the LC curve of the reference MBT curve with a power function

Figure 6-18 Comparison of normalized loading and reloading curves: (a) COD level of 0.2mm; (b) COD level of 0.6mm; (c) COD level of 0.9mm
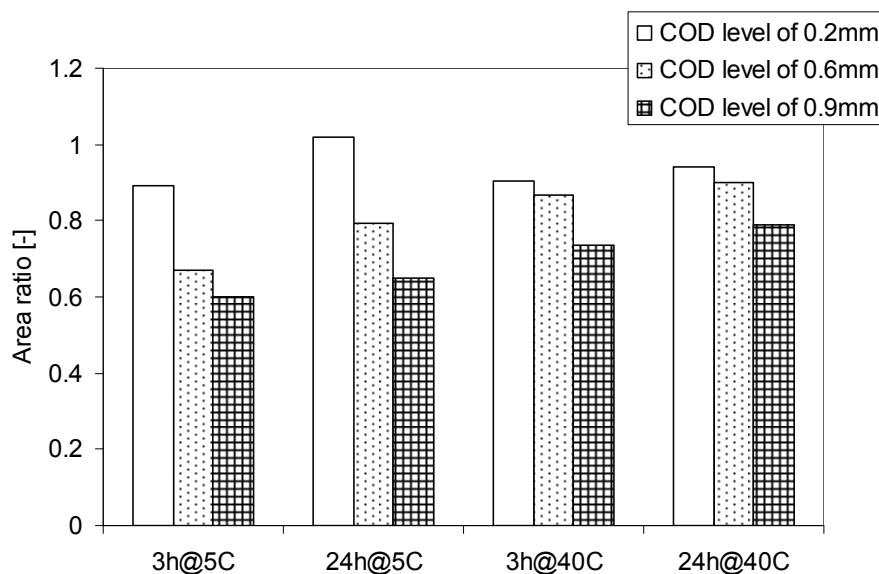
Figure 6-19 Comparison of the area ratio under the reloading LC curve

In Figure 6-19 the area change of the LC curve for each healing condition is given. The area is calculated to a COD level of 0.2 mm. This was done to minimize unexpected tendencies at high temperatures. The following observations can be made.

- o The increase of the area is dependent on healing time and healing temperature.
- o Because of the limited damage, the area change at a target COD level of 0.2mm is limited.
- o The area changes faster at the target COD level of 0.6mm than the COD level of 0.9mm.

6.5.4 COD recovery

Figure 6-20 shows the COD development at different healing conditions. From the figure the following can be observed.

- o The residual COD decreases in all cases during healing. However, an almost constant COD can be seen after 3 hours healing at 5 °C. A residual COD value ranging from 0.03mm to 0.11mm was obtained. This can be caused by a mismatch of the crack faces at either side of the crack and/ or permanent deformation occurring in the asphalt beam because of the visco-elastic behaviour.

- o When comparing the different target COD levels, a higher target COD value shows a higher residual COD. However, a higher target COD level shows a faster recovery of the COD, which may be due to residual compressive stresses and confinement from the rubber foundation.

- o When the beam is subjected to a healing temperature of 40°C, the residual COD increases. It is believed that this increase of the residual COD is caused by an artefact caused by subjecting the BOEF setup to

thermal cycles of 5°C - 40°C - 5°C. Further investigations are needed to clarify this artefact.
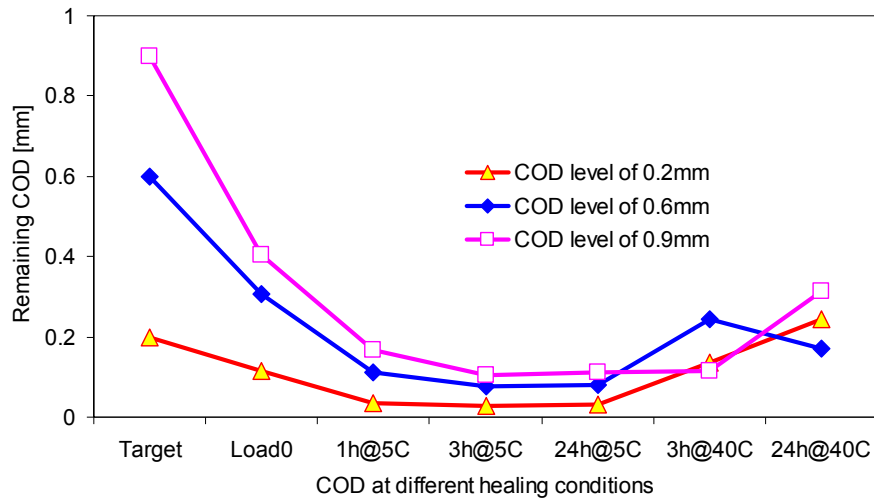

Figure 6-20 COD development at different healing conditions

6.5.5 Dynamic response

Figure 6-21 shows the results of the apparent modulus of the M_{COD} obtained from the dynamic tests at different loading/healing conditions. The M_{COD} of the original beams (Dyna0) was used as a reference and set at 100%. It can be seen that the M_{COD} decreases directly after the loading and reloading process and increases after the healing process. When comparing different COD levels, a higher COD level shows a lower M_{COD} at Dyna1 (M_{COD} after unloading). Since different levels of COD indicate different levels of damage, one can conclude that the M_{COD} can be used to characterize different levels of damage.
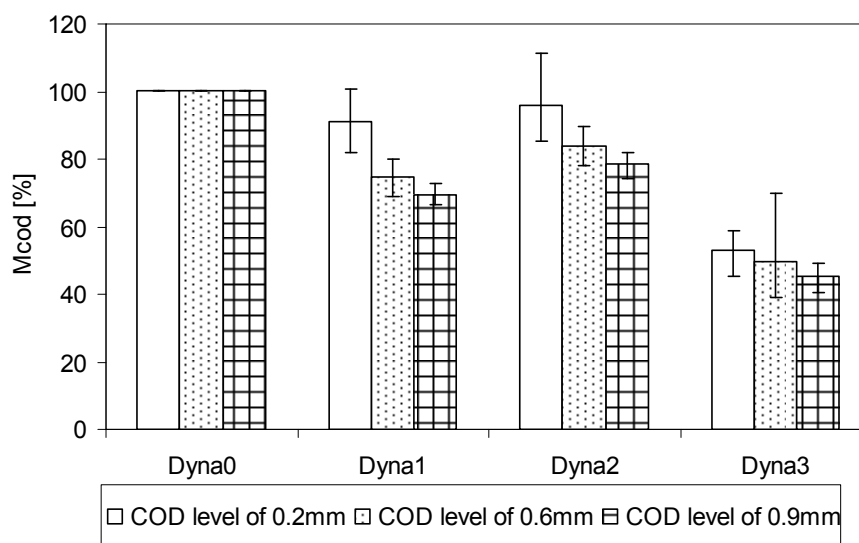
Figure 6-21 Dynamic response of the COD during the BOEF test under dynamic loading of 300N and a frequency of 5Hz

Figure 6-22 illustrates the development of the M_{COD} during the healing process at a healing temperature of 5°C for a rest period of 24 hours. Firstly, all the MCOD developments follow the same trend. A semi-log relationship was used to model this trend. Secondly, for a COD level of 0.2mm, the M_{COD} is approaching 100% due to the fact there is no visible cracking. The M_{COD} recovers slightly faster at a COD level of 0.6mm than at a COD level of 0.9mm with more damage.

Figure 6-22 Development of the M_{COD} at a healing temperature of 5oC for a rest period of 24 hours

Figure 6-23 Healing percentages calculated from the M_{COD} increase for different healing times and temperatures

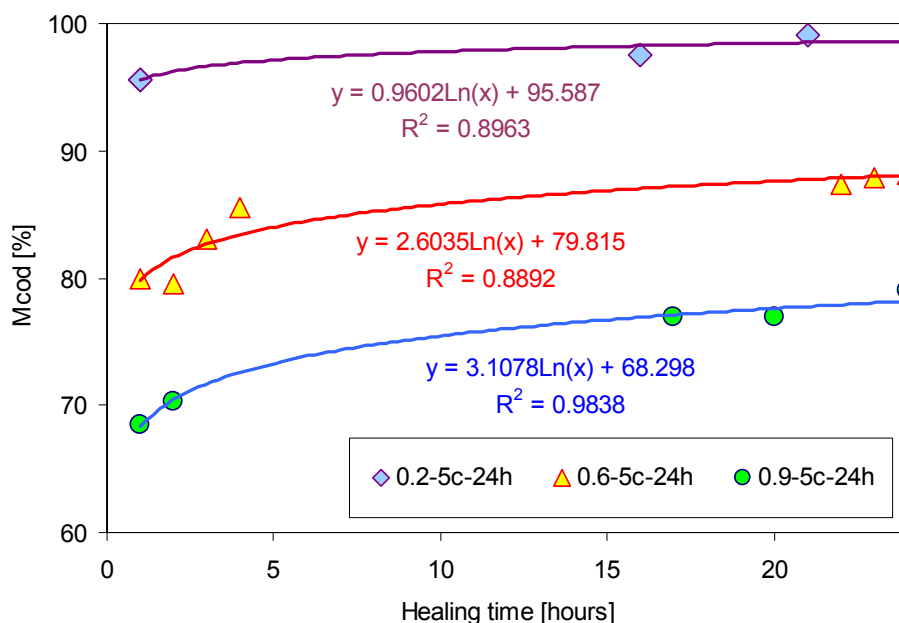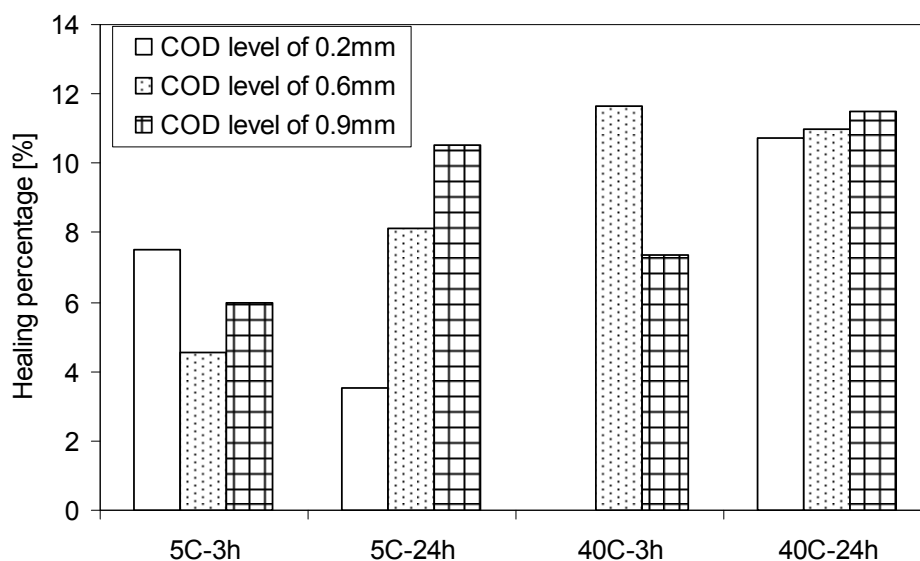Figure 6-23 compares the M$_{COD}$ increase as healing percentage for different conditions. It should be noted that each test condition was carried out on an individual asphalt concrete beam. Because of the uniqueness of the crack distributions in each beam the data were analyzed with care considering the sample-to-sample variation. It can be seen that in general, a longer time and higher temperature results in more M$_{COD}$ improvement. However, the improvement is limited. No clear difference can be observed for different COD levels. For a healing period of 24 hours, an increase in temperature shows limited improvement for the stiffness of the BOEF asphalt concrete beam.

6.5.6 Discussion

When comparing the recovery obtained from the monotonic loading-healing-reloading tests and the recovery from the dynamic response, the recovery from the dynamic response can be related to the crack closure due to the autonomous process. The recovery from the monotonic loading-healing-reloading tests benefits more from healing time and healing temperature, which is believed to be related to the strength regained due to the healing process [6, 17]. However, it should be noted that the above conclusion was made based on the load-COD response of the BOEF setup, which is a system response instead of a material behaviour of an asphalt mixture. This will also has an influence on quantifying the real self healing behaviour. Further research is needed to clarify this influence.

6.6 Summary and Conclusions

The cracking and healing behaviour of an asphalt mixture were investigated with a beam on elastic foundation test setup. Based on the test data and analyses performed, the following can be concluded.

- o The BOEF setup is capable of analyzing the self healing capability of asphalt mixtures under different crack conditions. The following advantages are noted: the setup allows to determine different damage phases by means of a load-COD relationship and the corresponding crack development. The BOEF setup allows fully closure of the crack thanks to the confinement provided by the rubber foundation. Permanent deformation can be neglected. The setup allows easy application and variation of healing time and healing temperature without disturbing the crack situation.

- o The cracking behaviour of an asphalt mix tested by means of the BOEF setup can be investigated with the load-COD curve and camera assisted crack length measurements. At a constant COD development speed, four phases can be observed: preloading phase, no visible crack phase, crack propagation phase and crack propagation phase in compression zone.

- o The healing behaviour of the asphalt mix was investigated at COD levels of 0.2mm, 0.6mm and 0.9mm, corresponding to crack lengths of no visible crack, 3-5mm and 8-10mm, respectively. Certain healing times and temperatures were applied to the test setup. After a healing period, a reloading was applied and the response as a result of this reloading was used as an indicator of healing. The time, temperature and crack size dependency could clearly be observed during the test.

- o The self healing capability observed from the dynamic test results is clearly present at the beginning of the healing process. The self healing capability observed from the monotonic loading-healing-reloading test results is continuously increasing with increasing time and temperature. The healing temperature is more important than the healing time.

- o When comparing the self healing capability observed in the dynamic tests with the healing observed in the monotonic loading-healing-reloading tests, the recovery of the dynamic load response is believed to be related to visco-elasitc recovery and crack closure; the recovery of the monotonic reloading curves is believed to be related to strength gain, which is a flow driven process.

- o The BOEF setup is capable to investigate the self healing capability in a controlled and effective way. This also makes this test useful to clearly differentiate the self healing capability of different types of asphalt mixtures and/or modifications.

References

[1] Soltani A and Anderson DA. New test protocol to measure fatigue damage in asphalt mixtures. Road Materials and Pavement Design 2005;6:485-514.

[2] Di Benedetto H, Quang TN, and Sauzeat C. Nonlinearity, heating, fatigue and thixotropy during cyclic loading of asphalt mixtures. Road Materials and Pavement Design 2011;12:129-58.

[3] Majidzadeh K, Kauffmann EM, and Ramsamooj DV. Application of fracture mechanics in the analysis of pavement fatigue. Journal of Association of Asphalt Paving Technologist 1971;40:227-46.

[4] Molenaar AAA. Structural performance and design of flexible road constructions and asphalt concrete overlays, Delft: Delft University of Technology, PhD thesis, 1983.

[5] Rowe GM, Lewandowski LH, Grzybowski KF, and Rasche J. Development of the beam on elastic foundation for the evaluation of Geo-synthetic materials for reinforcing of asphalt layers. 2009 Annual Meeting of the Transportation Research Board; 2009.

[6] Phillips MC. Multi-step models for fatigue and healing, and binder properties involved in healing. Eurobitume Workshop on Performance Related Properties for Bituminous Binders. Luxembourg; 1998, p. 115.

[7] Bommavaram R, Bhasin A, and Little DN. Determining intrinsic healing properties of asphalt binders: role of dynamic shear rheometer. Transportation Research Record 2009;2126:47-54.

[8] Majidzadeh K, Buranorom C, and Karakouzian M. Application of fracture mechanics for improved design of bituminous concrete. Report FHWA-RD-76-91; 1976.

[9] Molenaar AAA, Heerkens JCP, and Verhoeven JHM. Effects of stress absorbing membrane interlayers. Journal of Association of Asphalt Paving Technologist 1986;55:453-81.

[10] Brown SF, Thom NH, and Sanders PJ. A study of grid reinforced asphalt to combat reflective cracking. Journal of Association of Asphalt Paving Technologist 2001;70:543-70.

[11] Gaedicke C. Fracture-based method to determine the flexural load capacity of concrete slabs, Urbana-Champaign: University of Illinois, PhD thesis, 2009.

[12] Roesler J and Gaedicke C. Fracture-based method to determine the flexural load capacity of concrete slabs. Draft Final Report for Federal Aviation Administration: University of Illinois; 2009.

[13] Roesler J and Gaedicke C. Flexural behavior of boncrete specimens on barious support conditions. 7th International DUT-Workshop on Design and Performance of Sustainable and Durable Concrete Pavements. Seville, Spain; 2010.

[14] CROW. RAW Standard Conditions of Contract for Works of Civil Engineering Construction 2000, Ede, The Netherlands, 2000.

[15] Qiu J, Xuan D, van de Ven MFC, and Molenaar AAA. Evaluation of the shear box compactor as an alternative compactor for asphalt mixture beam specimens. AES - ATEMA'2009, 3rd Int. Conf. on Advances and Trends in Engineering Materials and their Applications. Montreal, Canada; 2009.

[16] Hordijk DA. Local approach to fatigue of concrete, Delft: Delft University of Technology, PhD thesis, 1991.

[17] Qiu J, Van de Ven MFC, Wu SP, Yu JY, and Molenaar AAA. Asphalt pavements are self healing. 1st International Conference on Sustainable Construction Materials: Design, Performance and Application. Wuhan, China; 2010.

7

Modelling Self Healing of Bituminous Materials

Abstract

A s indicated by the experimental results which are presented and discussed in Chapter 4 to Chapter 6, the crack self healing behaviour of bituminous materials is a flow driven process and is dependent on rest periods, temperature and crack phases. In this chapter, the damage and healing behaviour of bituminous materials were investigated through finite element simulations with the finite element code FEMMASSE. By defining both local damage/healing and visco-elastic properties, the self healing phenomenon of bituminous mastics determined using the Direct Tension Test (Chapter 5) and the self healing phenomenon of asphalt mixtures determined using the Beam on Elastic Foundation setup (Chapter 6) were simulated successfully.

S elf healing of bituminous materials has been known for more than fifty years [1-3]. Asphalt pavements are believed to heal under long rest periods and hot summers, hence healing will extend the service life [3, 4]. It has been indicated that the self healing property is complex and very dependent on the duration of rest periods, temperature, crack phases and material properties like viscosity. It is also observed that damage and healing are coupled with the time dependent visco-elasticity [5].

The finite element code FEMMASSE was introduced to model the self healing phenomenon observed from the mechanical testing [6]. This model is capable of linking the physical-chemical (conceptual) based healing model and the mechanical (phenomenological) based healing model. In this chapter, simulations were carried out to model the self healing phenomenon of bituminous mastics (Chapter 5) and asphalt mixtures (Chapter 6) shown in the experimental work. The usefulness of the finite element simulation on further understanding of the self healing phenomenon will be explored.

7.1 Healing Hypothesis

Figure 7-1 hypothesises the crack healing process of bituminous materials. As a cracking process, the crack propagates due to load repetitions and other effects. When the load is removed and a rest period is applied, the crack is subjected to healing. A healing process can be seen as the reverse of the cracking process. Under different healing times and healing temperatures, healing can be seen as a crack repairing process which decreases the crack size by a healing zone.
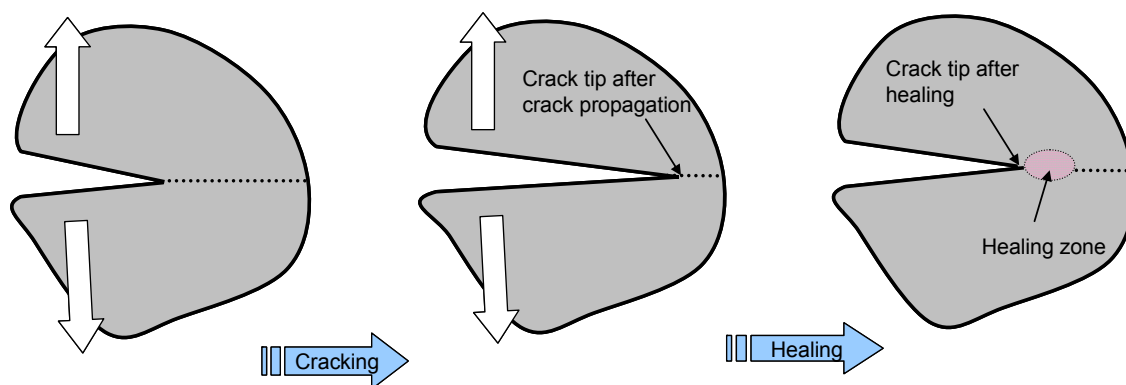

Figure 7-1 Hypothesis of crack healing process

Figure 7-2 shows how the healing zone is developed in bituminous materials. It should be noted that the self healing capability is defined as the recovery of mechanical properties.

In general, the healing process consists two main phases, namely the crack closure and the strength gain. The following explains each process and its

driving force. It should be noted that due to the visco-elastic nature of bituminous materials, the crack closure will not be simply elastic, but is coupled with a visco-elastic feature, such as relaxation.

⇒ **Crack closure (meso crack to micro crack to nano crack)**

    ✓ **Driving force:** thermal induced (flow by temperature) and mechanical induced (by confinement and pressure)

    ✓ **Results:** crack closure and modulus recovery

    ✓ **Others:** visco-elasticity (relaxation)

⇒ **Strength gain (nano crack to full healing)**

    ✓ **Driving force:** thermal induced (wetting and diffusion by temperature) and mechanical accelerated (by confinement and pressure)

    ✓ **Results:** strength gain

As a result, this chapter is aiming to explain the self healing process and to prove the hypothesis using numerical modelling.
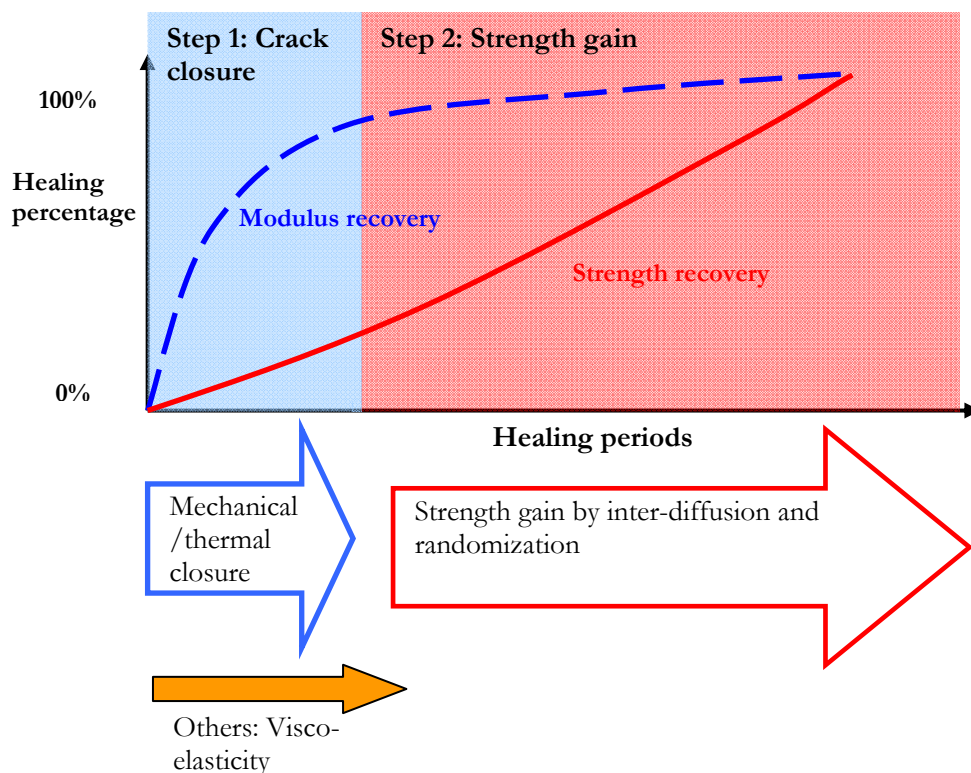

Figure 7-2 Conceptual representation of healing

7.2   Model Implementation

FEMMASSE is a finite element code; its abbreviation stands for Finite Element Modules for MAterials Science and Structural Engineering [6]. It embeds both features of visco-elasticity and smeared crack model. These factors are considered to be the most important factors for modelling the healing process.

7.2.1   Smeared crack model

There are two main categories of models which describe the failure process of bituminous materials: continuum damage mechanics (CDM) and fracture mechanics [7, 8].

The CDM approach treats the evolution of the mechanical properties of a continuum, such as stiffness degradation, as damage evolution. This approach takes into account the bulk rheological material behaviour such as elasticity, visco-elasticity, plasticity and visco-plasticity. The CDM is mostly used to describe the deformation and damage evolution and healing of bituminous materials during load repetitions [9-11]. Because the CDM approach treats heterogeneous asphalt mixtures as macroscopically homogeneous continua, it is easy to be implemented into finite element models. However, the CDM approach is a somewhat phenomenological approach, which can not directly be related to the physical damage phenomena such as the formation and propagation of micro cracks and macro cracks.

Fracture mechanics aims to study the response and failure process as a consequence of crack initiation and propagation. The fracture mechanics approach can account for the initiation of microcracks and the propagation to macrocracks, followed by a complete failure of the structures. In this way, a direct link is formed between the global response (stiffness reduction) and the underlying physics of the damage [8].

A so-called cohesive zone model (CZM), was developed based on non-linear fracture mechanics [12]. As shown in Figure 7-3, a cohesive zone is defined in front of the crack tip with a certain traction-separation behaviour. When the applied local stress is higher than the maximum traction force, the traction-separation behaviour is applied to follow the post-peak softening until the traction diminishes. The cohesive zone model was used successfully to simulate the fracture process of asphalt mixtures at low temperatures [8, 13, 14]. Attempts were also made to simulate the fracture process in a visco-elastic medium with a phenomenological visco-elastic cohesive zone model [15, 16].

The CZM model has two types, a discrete type and a smeared type.

  o In a discrete crack model, all non-linear behaviour is condensed in a stress-crack width relation, while the bulk material behaves linear elastic.

- o In a smeared crack model, the bulk material is assumed to behave non-linear. This is probably more realistic because it does not assume the pre-existence of a crack during the simulation.

It is foreseen that the smeared type cohesive zone model, which is directly related to the cracking process of materials, has a potential to be used for healing simulations and to prove the healing hypothesis as proposed above.
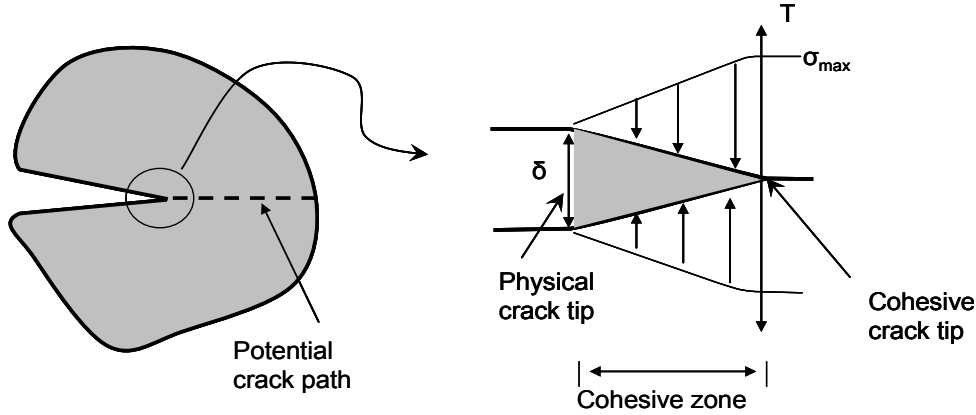
Figure 7-3 Illustration of cohesive zone model

As shown in Figure 7-4, damage is composed of two phases in the FEMMASSE analysis, namely the hardening phase and the softening phase according to references [17, 18].

- o The hardening phase is activated with a corresponding volumetric length (L_{vol}), which is taken as the length of the specimen. By dividing the crack width in the hardening phase by the volumetric length L_{vol}, a normalized strain value for the hardening phase can be obtained.

- o The softening phase is activated as isotropic softening with a characteristic length (L_{ch}). To achieve mesh size independence, the square root of the determinant of the Jacobian matrix (sqrt(D_{Jac})) of the integration points was taken as the characteristic length [18]. By dividing the crack width in the softening phase by this characteristic length L_{ch}, a normalized strain value for the softening phase can be obtained.

Figure 7-4 Illustration of stress-strain relation in FEMMASSE

The following gives the stress-strain relations.

Strain decomposition
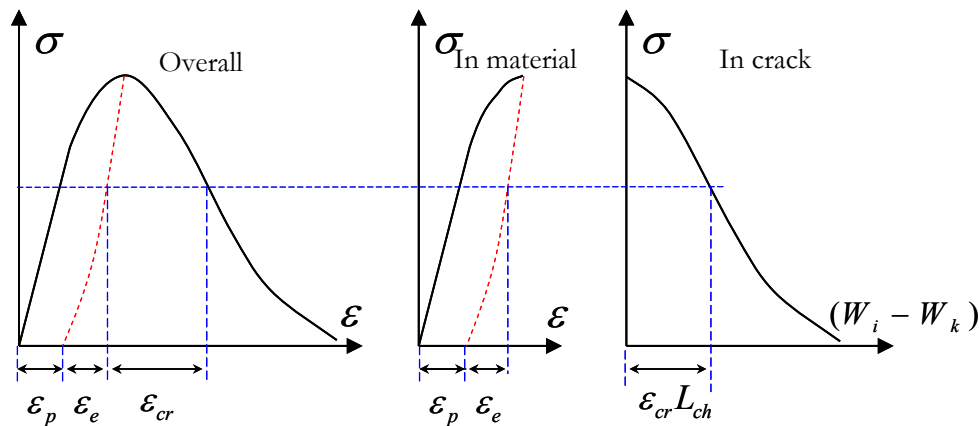
$$\varepsilon_i = \varepsilon_{ei} + \varepsilon_{pi} + \varepsilon_{cri}$$

7-1

In the elastic phase

$$\varepsilon_i = \frac{\sigma_i}{E}$$

7-2

In the hardening phase ($W_i \leq W_k$)

$$\varepsilon_i = \frac{\sigma_i}{E} + \frac{W_i}{L_{vol}}$$

7-3

In the softening phase ($W_i > W_k$)

$$\varepsilon_i = \frac{\sigma_i}{E} + \frac{W_k}{L_{vol}} + \frac{W_i - W_k}{2 \times L_{ch}}$$

7-4

where,

σ_i	= stress in the time interval i;
ε_i	= strain in the time interval i;
ε_{ei}	= elastic strain in the time interval i;
ε_{pi}	= plastic strain (hardening) in the time interval i;
ε_{cri}	= crack strain (softening) in the time interval i;
E	= material modulus;
W_i	= crack width at the time interval i [mm];
W_k	= crack width at which the tensile strength σ_{max} is reached [mm];
L_{vol}	= volumetric length for hardening [mm];
L_{ch}	= characteristic length for softening [mm].

As shown in Figure 7-5, the damage-healing rule is defined in a stress-crack width relation. During the simulation, the stress-crack width relation for the smeared crack model is defined in a multi-linear tubular form. After the analysis, the information of stress, strain and crack width of each individual integration point are available. The stress-strain relationship combines both information of visco-elasticity and cracking. In order to eliminate the effect of visco-elasticity on the healing process, the stress-crack width relationship of a single crack was used hereafter to define the crack healing process.

Assume that the material is loaded such that it reaches state A which implies that the material is loaded until a certain crack size has developed. After reaching A an unloading-reloading loop is applied.

- o A→O: The material is unloaded till point O considering pure elastic crack;

- o O→B: The material is reloaded till point B which has more damage, indicating damage development during reloading;

o O→C: The material is reloaded till point A which has less damage, indicating healing.

In the following sections, the usefulness of this local damage-healing definition will be discussed.
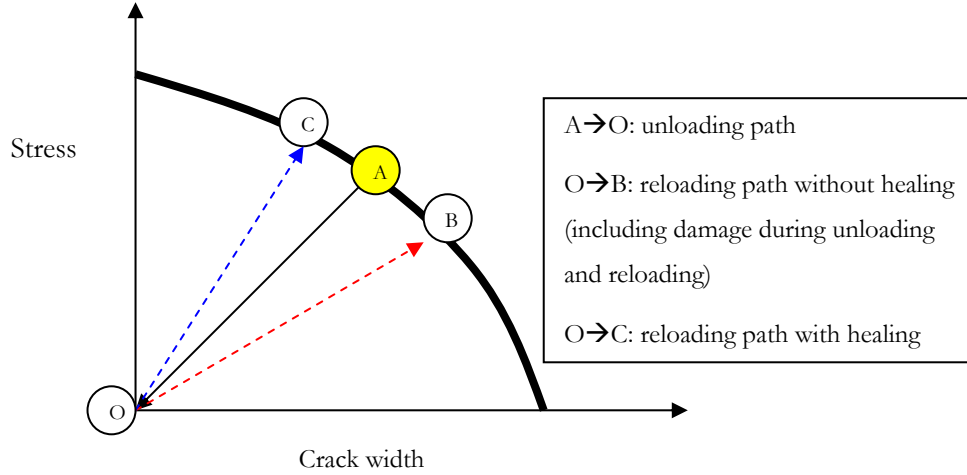
Figure 7-5 Illustration of local damage-healing rule in a stress-crack width curve

7.2.2   Generalized Maxwell model

A generalized Maxwell model is used in FEMMASSE for modelling the time dependent visco-elastic behaviour (Figure 7-6).

Figure 7-6 Generalized Maxwell Model

In the constitutive equation, the incremental strain rate $\Delta \varepsilon^i$ from time t^i until time t^{i+1} is assumed to be constant. The stress at the end of the interval is given as follows:

The total stress follows from the summation of all Maxwell units and reads:

$$\sigma^{i+1} = E_{VE}\Delta \varepsilon^i + \sigma^i \qquad\qquad 7\text{-}5$$

where,

$$E_{VE} = \sum_{k=1}^{m} \frac{\tau_k}{\Delta t} E_k \left(1 - e^{-\frac{\Delta t}{\tau_k}} \right) \qquad \text{7-6}$$

$$\sigma^i = \sum_{k=1}^{m} \sigma_k^i e^{-\frac{\Delta t}{\tau_k}} \qquad \text{7-7}$$

where,

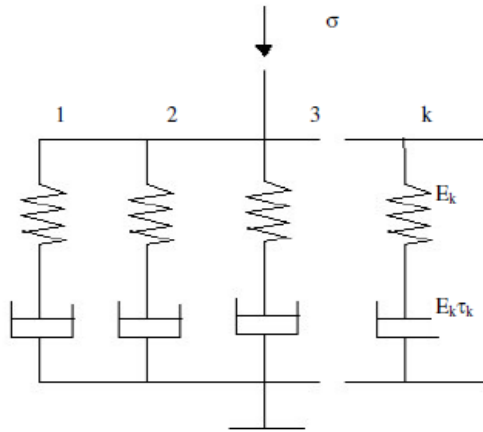|	
σ^{i+1}	= stress at the end of the time interval i;
σ^i	= stress at the beginning of the time interval i;
σ_k^i	= stress in Maxwell unit k at the beginning of the time interval i;
$\Delta \varepsilon^i$	= total strain increment at the time interval i;
τ_k	= model parameter, relaxation speed of the Maxwell unit k;
Δt	= duration of the time interval.

7.2.3 Summary

FEMMASSE is capable to define both visco-elastic and smeared crack behaviour. It has a potential to simulate the cracking and healing process of bituminous materials. In the section 7.3, the FEMMASSE model is used to model the test results of the self healing phenomenon of bituminous mastics which were obtained by the direct tension test. And in section 7.4, it is used to model the test results of the self healing phenomenon of asphalt mixtures by means of the beam on elastic foundation test.

7.3 Modelling of Self Healing of Bituminous Mastics using the DTT

7.3.1 Problem statement

Figure 7-7 shows results of the damage and healing development in the experiments on bituminous mastics reported in Chapter 5. The tests were carried out using the direct tension test with a displacement speed of 10mm/min at 0°C. The DTT machine was programmed to stop at a displacement of 0.15mm, 0.8mm, 1.5mm, 2mm, 3mm and when the specimen was totally broken. After the displacement was reached, some specimens were unloaded and an immediate reloading (rest period of 0 hour) was applied to investigate the damage behaviour. The other specimens were placed back into the silicon rubber mould to heal for 5 minutes, 30 minutes and 3 hours at a temperature of 20°C. After healing, the reloading was applied using the same loading condition till total failure.
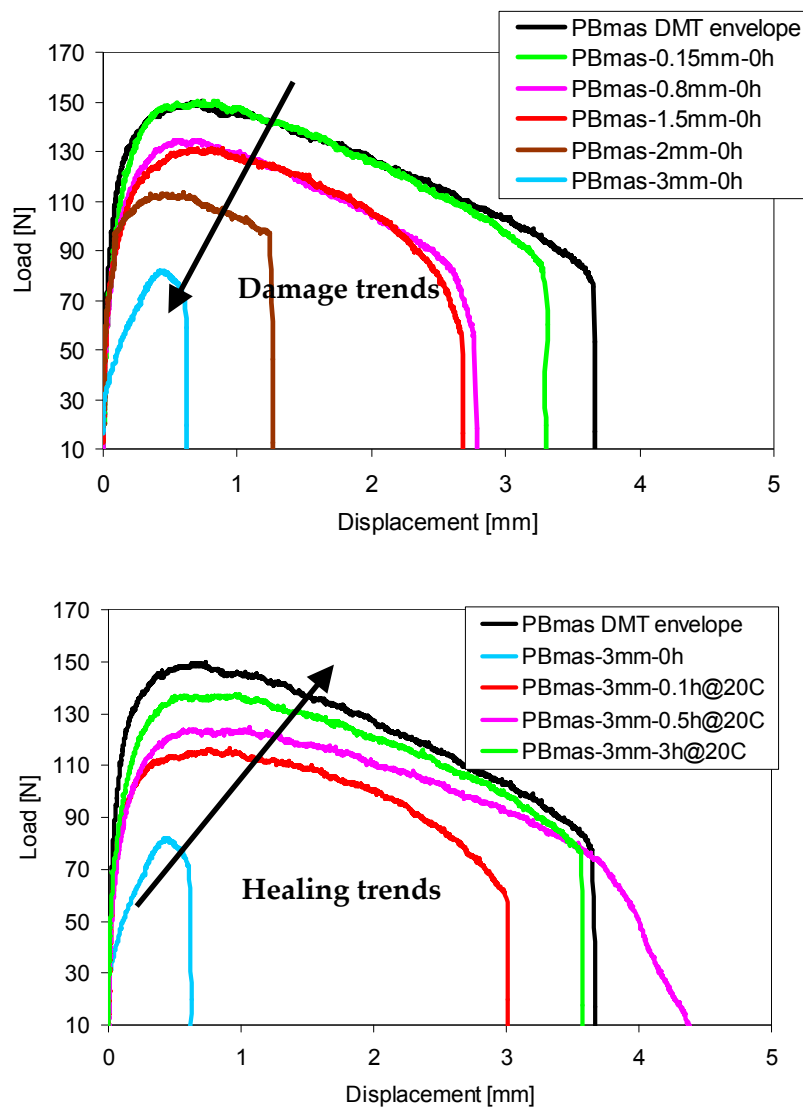
Figure 7-7 Development of damage and healing observed using the DTT

When comparing the damage process of immediate reloading at different displacements with the healing process of specimens which were loaded till 3mm and then were allowed to heal, the damage and healing process are clearly visible. In addition, both the damage and healing processes are coupled with visco-elastic behaviour. In order to further understand the damage and healing process and the effect of visco-elasticity, the DTT test is simulated using the FEMMASSE model.

7.3.2 FEM model for DTT setup

Table 7-1 lists the material properties of the bituminous mastics. A 5-term Maxwell model was used to model the visco-elastic behaviour. The data was back-calculated from the complex modulus master-curve of the sample at a test temperature of $0{}^{o}C$.

Table 7-1 List of material parameters of bituminous mastics

E_0 [MPa]	2306	Poisson's ratio	0.35	Strength [MPa]	5
5-Term Maxwell model					
k	1	2	3	4	5
E_k / E_0 [-]	0.523185976	0.322064934	0.132783536	0.020001	0.001964
τ_k [hours]	5.98454E-07	1.28933E-05	0.000277778	0.005985	0.128933

Figure 7-8 shows the multi-linear smeared crack model used in the FEMMASSE analysis. The parameters were obtained by fitting the global monotonic load-displacement curve, which will be shown in Section 7.3.3.1. In addition, an Alfa factor was also introduced to consider the unloading path after cracking. Alfa factors of 0 and 1 were selected to investigate the influence of the unloading path on the data simulation.

Figure 7-9 shows the bituminous mastic specimen during the DTT test and its modelling. A parabolic shape was used for the specimen with a width of 5mm at the middle part, and 20mm at the end. The total length of the bituminous mastic specimen was 20mm and the sample thickness was 6mm. A displacement speed of 10mm/min was applied at the temperature of $0{}^{o}C$.

The corresponding meshes and the boundary conditions in the FEMMASSE program are also shown in Figure 7-9. The aluminium top and the bottom caps were simulated as well. In addition, a 5 mm high damage-healing zone was defined for further healing investigation; this area is indicated in red. Initially, both parts of the bituminous mastics follow the same damage rule. During the healing process, the material properties within the damage-healing zone can be changed, which will be discussed later.

Figure 7-9c and Figure 7-9d are examples of the simulation results of the tensile stress distribution and the crack propagation, respectively.
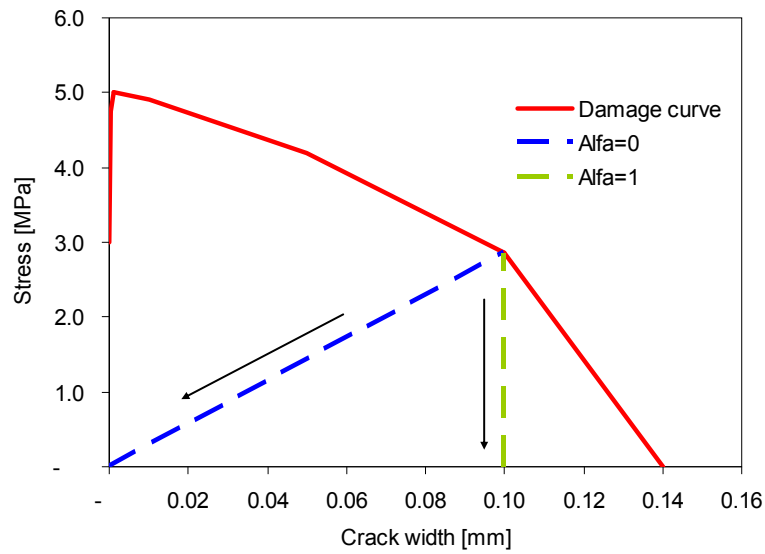

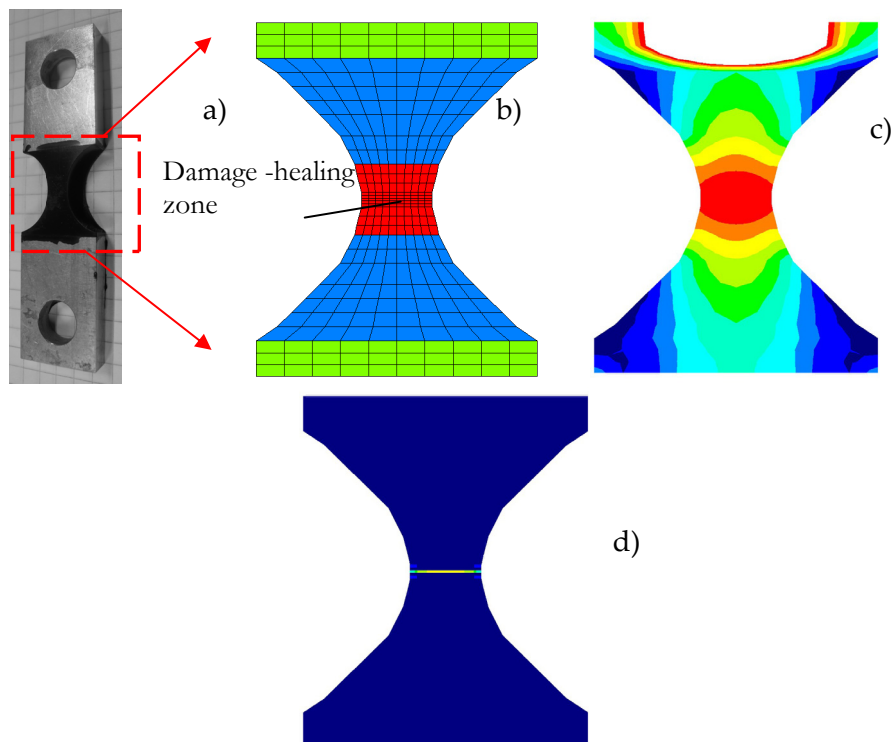Figure 7-8 Illustration of the local damage criteria

Figure 7-9 Illustration of the DTT test sample and its FEM model
a) DTT specimen; b) FEM meshes; c) Tensile stress distribution; d) Crack propagation

7.3.3   Modelling of damage behaviour

7.3.3.1   Monotonic test

Figure 7-10 shows the modelling results of the monotonic DTT test at 0°C with a displacement speed of 10mm/min. One will observe that the measured curve was very well simulated. In addition, the development of the crack width is also similar to the development of the single crack width as reported in Chapter 5 [5]. It should be noted that the experimental curve was shifted a little bit in order to correct for differences between the experimental displacement speed at the very beginning of the test and the constant speed of 10mm/min which was assumed in the simulation. The differences were caused by the fact that in the very beginning of the test the equipment was unable to give a constant displacement speed of 10mm/min.
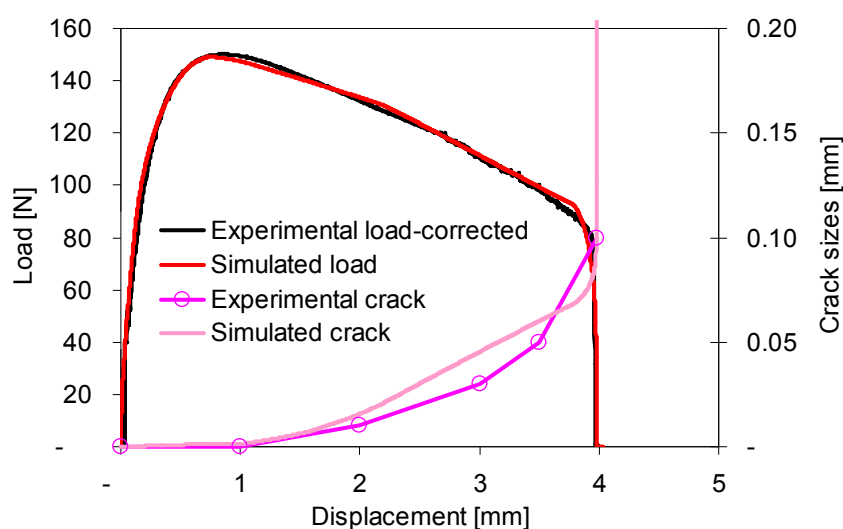
Figure 7-10 Modelling of the VED full curve of bituminous mastic with Alfa=0
(displacement speed of 10mm/min at 0°C)

7.3.3.2   Post-peak relaxation

The relaxation behaviour is very important for characterizing the visco-elasticity of undamaged bituminous materials [19, 20]. It is shown in literature that for concrete materials the post-peak relaxation is also very interesting for investigating the coupled damage - visco-elastic behaviour [21, 22]. However, it should be noted that bituminous materials show quite a large amount of relaxation compared with concrete materials even in the presence of damage.

In order to quantify the effect of damage coupled relaxation, simulations of the relaxation behaviour were made with and without taking into account the damage function. In the following text, VE stands for a linear visco-elastic simulation without the damage function; VED is the VE with the damage function.

Figure 7-11 shows simulation of relaxation at elongation of 1mm. The force needed to get that one mm displacement is just after reaching the peak load implying that the relaxation is measured on a damaged specimen. The figure shows that when comparing the simulated relaxation curves with and without damage feature, the trends are similar. The F_0 and t_0 correspond to the load and time when relaxation starts. The figure shows that both the relaxation of the VE simulation and the VED simulation are the same as the experimentally determined relaxation curve.
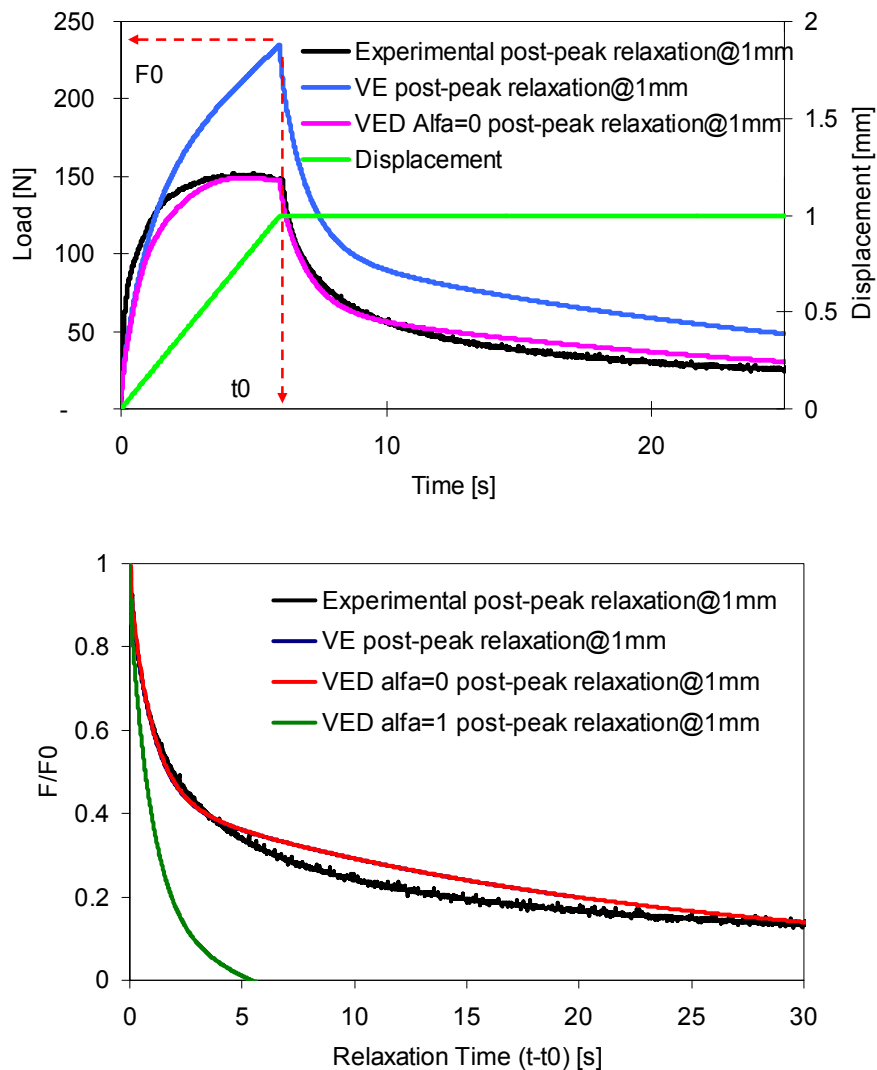
Figure 7-11 Modelling of the damage coupled relaxation:
Simulation of post-peak relaxation test (upper); Comparison of post-peak relaxation curves (lower)

It seems that the damage only decreases the load level to obtain a certain deformation before relaxation starts but the shape of the relaxation curve of the damaged specimen is still the same as the undamaged one. The post-peak relaxation is largely because of the time dependent visco-elastic effect.

The Alfa value also influences the simulated post-peak relaxation behaviour. Considering the damage coupled effect, it seems that the crack closure effect influences the relaxation. To have a good simulation, the Alfa value should be 0. Hence, the combination of visco-elasticity plus local damage (Alfa=0) seems to be capable to give a satisfactory VED simulation.

7.3.3.3 Post-peak unloading

Figure 7-12 shows the simulation of the unloading process after loading till certain target displacement.
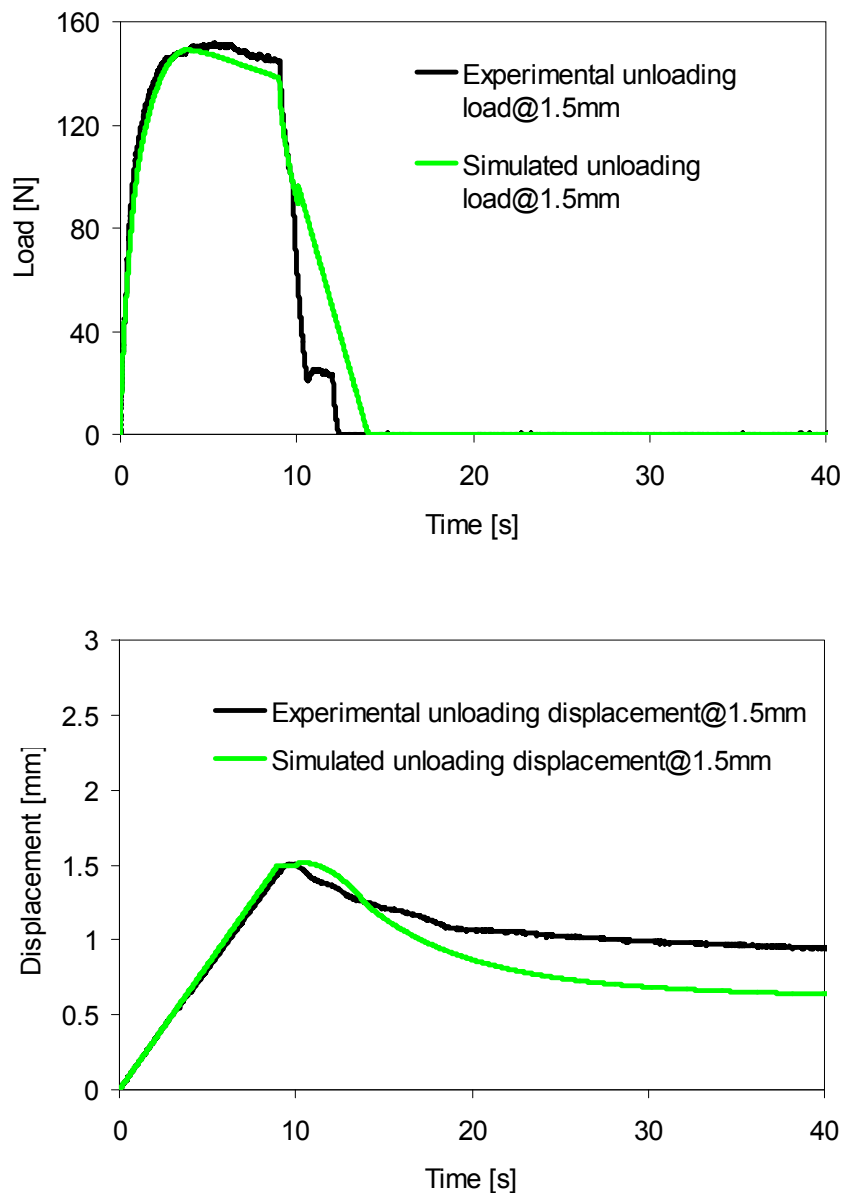

Figure 7-12 Modelling of the VED unloading: Load signal (upper); b) Displacement signal (lower)

The loading experiment was displacement controlled. In the unloading part it was planned to remove the load immediately after it had reached the target

displacement. However, removing the load immediately was not possible in the experiment. There was always some delay. The simulated displacement signal shows good agreement with the experimental data. However, the simulated displacement decreases a bit faster during unloading. This can be related to the intrinsic feature of the smeared crack model. For simplicity, FEMMASSE defines a linear unloading path for the crack closure. And the crack closure is directly related to current stress state in the element. This implies that if there is no external stress present, the crack is assumed to be closed immediately (given the condition that Alfa=0). This simplification can be applied successfully for concrete materials. However, due to the visco-elastic nature, the crack closure process of bituminous materials is nonlinear and closely related to the internal stress which is introduced due to the visco-elastic recovery.

7.3.3.4 Immediate reloading

Figure 7-13 shows the representation of the smeared crack model for immediate reloading. Hordijk showed that when simulating immediate reloading an extra damage term needed to be introduced to the smeared crack model to take into account the fact that the reloading curve not goes to point A but to point B [23] The reloading follows the same route as the unloading curve and then follows the re-damage curve with a lower strength.
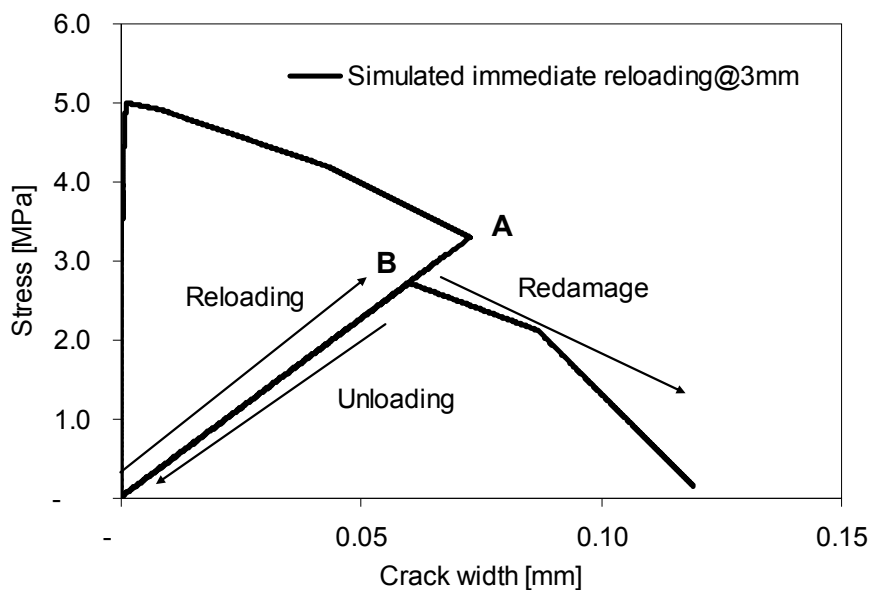
Figure 7-13 Smeared crack model for immediate reloading with a decrease of the reloading strength

Figure 7-14 compares the simulated immediate reloading with the experimental results. It can be seen that the simulations are in line with the experimental results. However, the simulated reloading curve seems to be larger than the experimental curve at a higher reloading displacement level. This may due to

the rapid crack accumulation during the experiment which is not taken care for by the model.
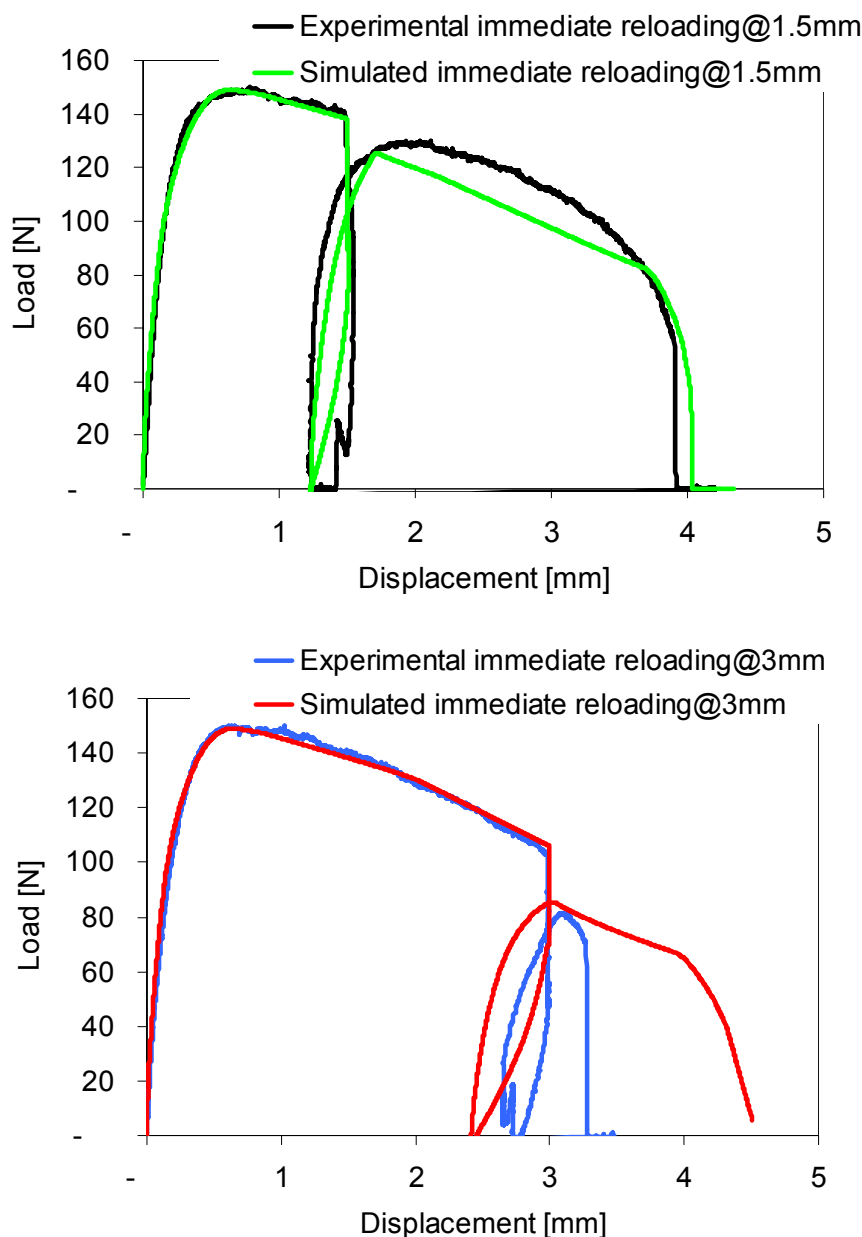
Figure 7-14 Modelling of the VED immediate reloading (Alfa=0)
a) Simulation of immediate unloading at displacement of 1.5mm; b) Simulation of immediate unloading at displacement of 3mm

7.3.4   Modelling of healing behaviour

As indicated above, the time dependent visco-elasticity has a big influence on the post-peak damage and unloading behaviour of bituminous mastics. It is expected that visco-elasticity will also influence the healing process as represented by the reloading curves after a certain healing period has been applied. As a result, the healing which is believed to be visible in the reloading curve is in fact for a part visco-elastic recovery (VER) and for a part real healing

or damage recovery [5]. These two processes are interacting with each other. VER is faster than the damage recovery. From the definition of the model, the VER is defined as the pure visco-elastic recovery without taking into account any damage development. The damage recovery can be divided into the stiffness (crack) recovery (StiffR) and the strength recovery (StrenR).

Figure 7-15 shows how stiffness (crack) recovery can be simulated within a smeared crack model. By increasing the reloading slopes, the stiffness recovery of a crack can be simulated. This also implies a decrease of the crack size in the model. How strength recovery can be simulated is also shown in Figure 7-15; it results in a higher failure envelope. The ratio of the StiffR means the ratio of the slope of the reloading curve over the slope of the unloading slope. The ratio of the StrenR means the ratio of the maximum point of the reloading curve over the original reloading strength.
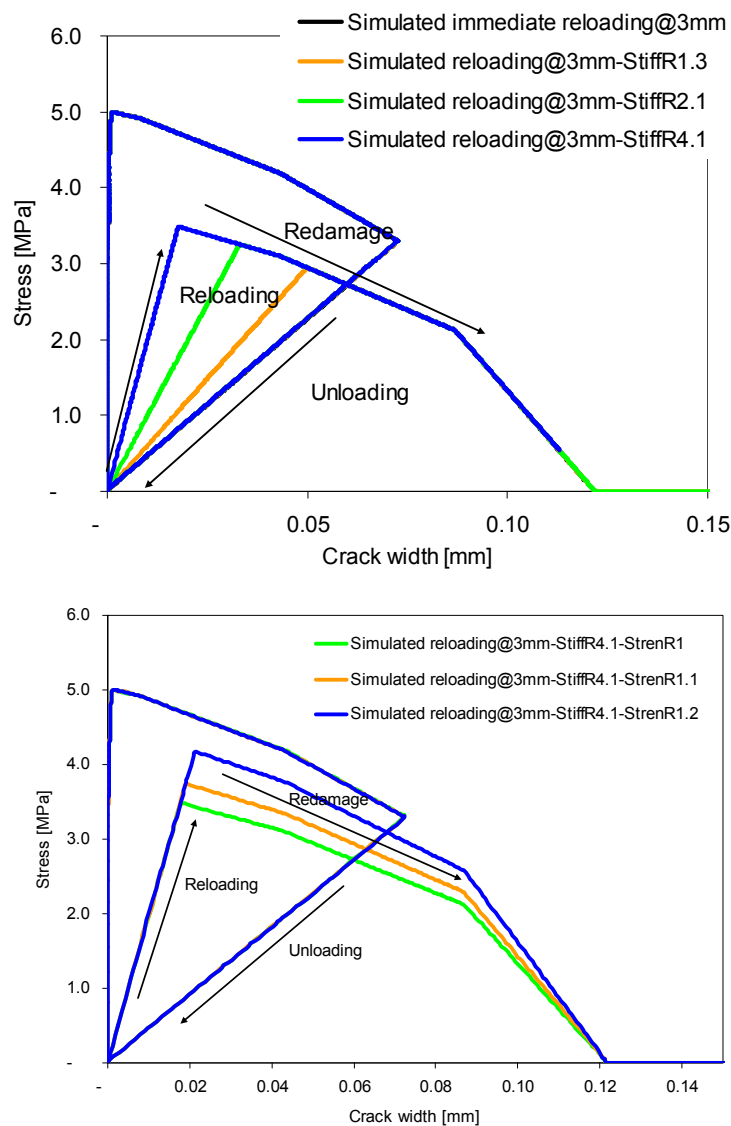
Figure 7-15 Modelling of stiffness recovery and strength recovery on local damage criteria: a) Stiffness recovery; b) Strength recovery

Figure 7-16 shows the simulation results of the global load-displacement curve. The following can be observed:

- o If only visco-elastic behaviour is applied and no change in the smeared crack model, the global curve will result in a decrease of the reloading stiffness. This is because of the relaxation of the bulk material.

- o If a stiffness recovery in the smeared crack model is applied, the improvement of the reloading stiffness and slightly of the reloading strength is observed.

- o The strength recovery shows improvement in the reloading strength. No change is observed in the reloading stiffness.

- o As observed from the experimental results, the reloading stiffness after healing was always higher than the one with immediate reloading [5]. This implies that the visco-elastic recovery and the stiffness recovery process of the crack happen together at the beginning of the healing process, and is then followed by the strength recovery process.
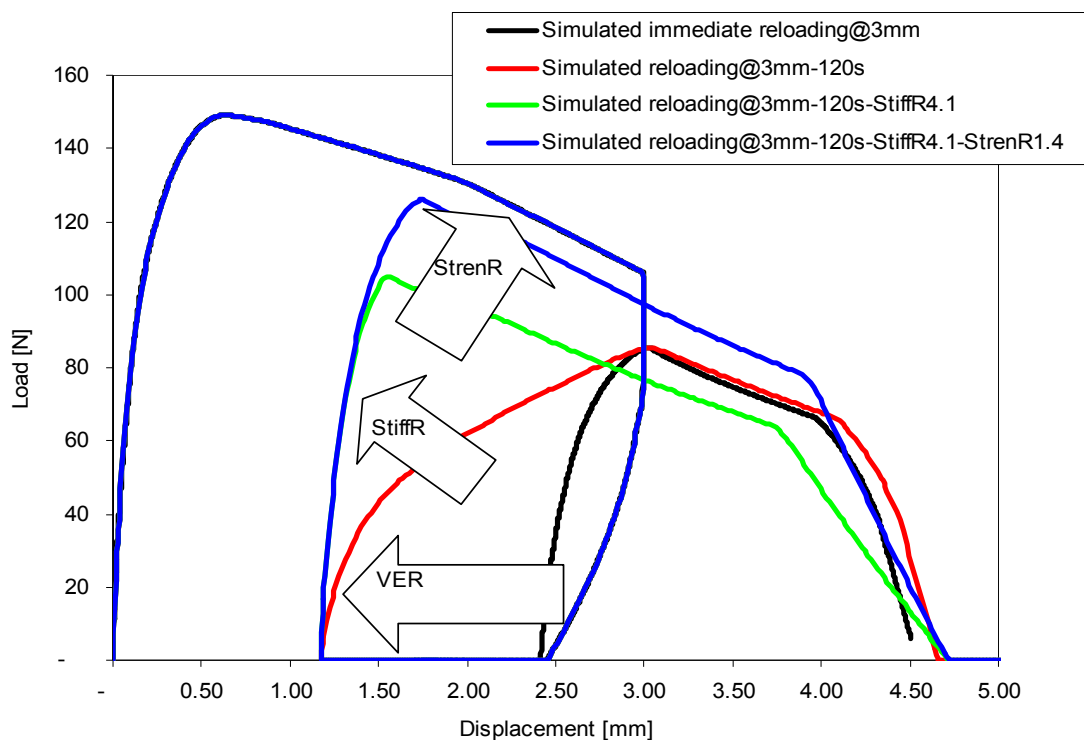
Figure 7-16 Illustration of visco-elastic coupled healing decomposition

Figure 7-17 shows the modelling results of the visco-elastic coupled healing. The results are believed to be in reasonable agreement with the experimental observations. The reason for the not so optimal fit curve is the due to the definition of the smeared crack model as indicated in Equation 7-4. The crack development is independent of the visco-elastic property. The visco-elastic property only controls the elastic part of the model, while the crack development part of the model is still rigid. This would cause the consequences that the time dependency of the reloading curve during simulation, which dominates by the crack closure and development, is lacking. Further research is needed to fully couple the visco-elastic property to the smeared crack model in order to obtain an optimal fit of the test results.

Figure 7-17 Modelling of visco-elastic coupled healing results

(Test was done at 0°C and 10mm/min displacement speed, healing was done at 20°C)

7.4 Modelling Self Healing of Asphalt Mixtures using the BOEF Setup

7.4.1 Problem statement

As shown in Chapter 5, an autonomous self healing setup was developed namely the beam on elastic foundation healing setup. This setup consists of a notched asphalt beam glued on a soft rubber foundation. Under a loading-unloading-healing-reloading procedure, the self healing capability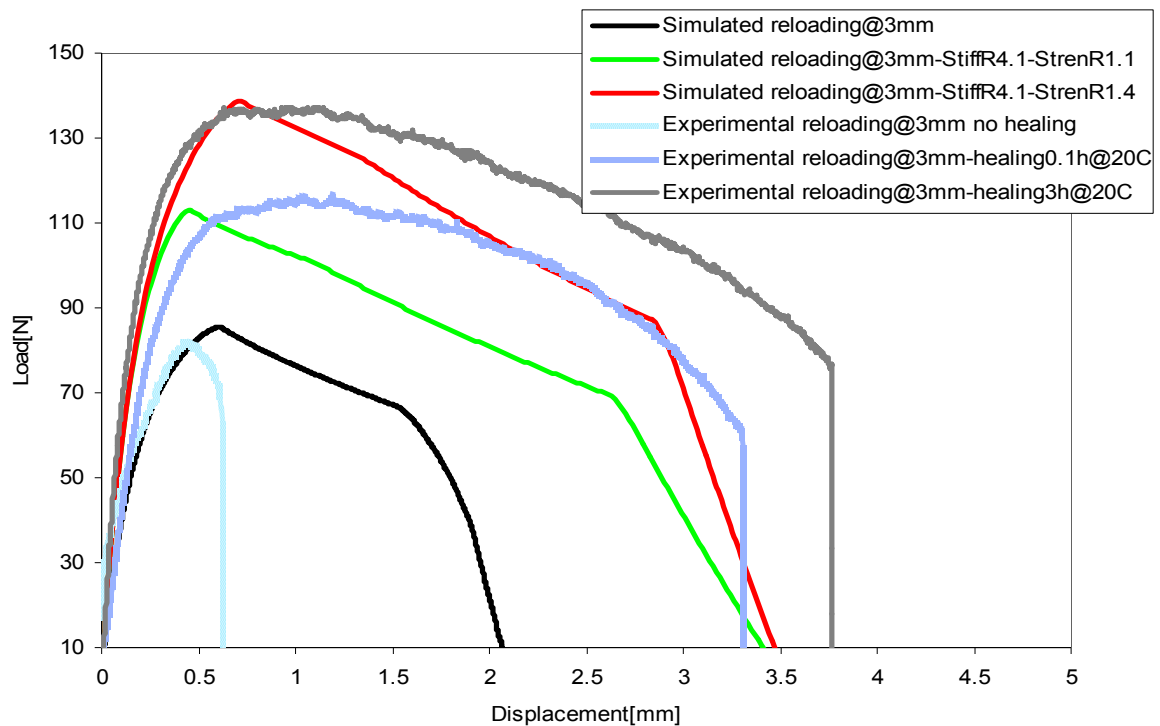 of asphalt mixtures can be characterized at different healing rest period, healing temperature and crack phases. Figure 7-18 shows typical load-crack opening displacement (abbreviation LC) curves from the BOEF setup under different healing conditions. It should be noted that, the reloading curves were shifted such that they can be compared directly with the loading curve. Because of the influence of the rubber foundation, the LC curve does not show the abrupt failure which is observed in tests on simply supported beams. When considering the reloading curve at different healing conditions, if there is no healing, the reloading curves would be independent of the healing conditions. However, the increase of the reloading curves marks the existence of the self healing phenomenon of asphalt mixtures and the self healing capability increases with the increasing healing time and healing temperature. Because of the complexity of the BOEF setup, these experimental results indicate a structural response rather than only the material response. Hence, modelling the self healing occurring in the BOEF test is of importance to further understand the self healing phenomenon at mixture level in a real structure.
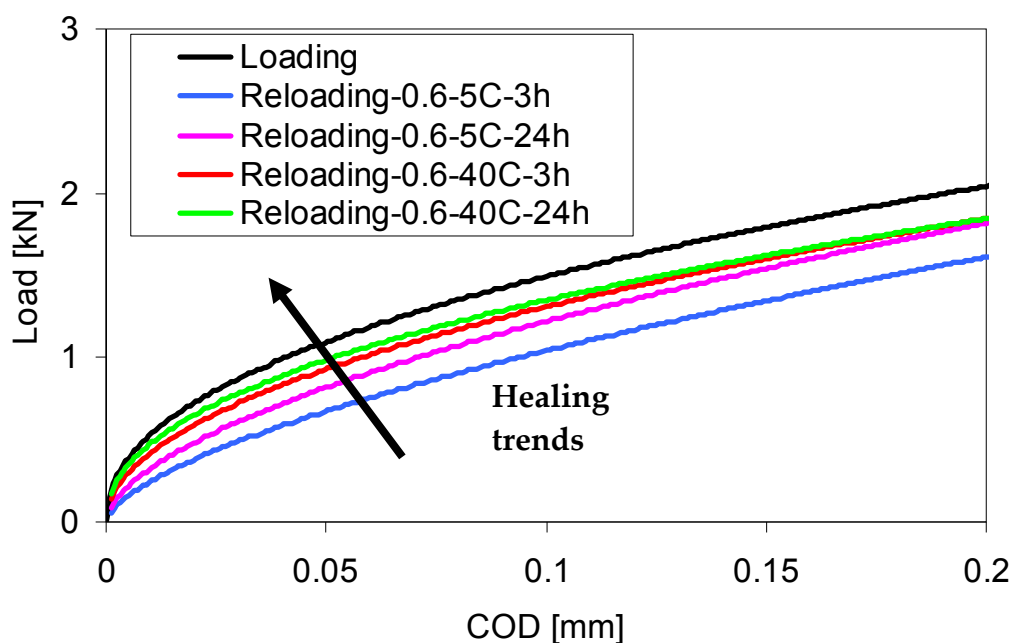

Figure 7-18 Typical BOEF test results under different healing conditions for a target COD level of 0.6mm

7.4.2 FEM model for BOEF setup

Table 7-2 lists the material parameters that were used for the BOEF analysis. Elastic material properties were assigned to all materials, only the asphalt mixture was modelled visco-elastically. The visco-elastic properties of the asphalt mixture were back-calculated from information on the mixture stiffness as a function of loading frequency and temperature which was collected using a dynamic tension-compression test.

Table 7-2 Material parameters for BOEF analysis

Elastic material parameters				
	Rubber pad	Rubber foundation	Glue	Steel
E [MPa]	15	6.5	4000	200000
Poisson's ratio	0.49	0.49	0.15	0.15

Visco-elastic material parameters for asphalt mixes							
E_0 [MPa]	k	1	2	3	4	5	6
19956	E_k / E_0 [-]	4.52E-01	2.85E-01	2.00E-01	5.71E-02	5.09E-03	6.92E-04
	τ_k [s]	8.47E-07	2.19E-05	2.70E-04	3.19E-03	4.72E-02	2.78E-01

Figure 7-19 shows the finite element model developed in FEMMASSE to model the BOEF test. A 2D model was developed and plain stress conditions were assumed to occur. The thickness of the model was 35mm.

Due to the complication of keeping a constant COD by applying a vertical load in the FEM simulation, the simulation was carried out with an experimental load as input, which is shown in Table 7-3.

Table 7-3 Comparison of experiment and FEM simulation on obtaining Load-COD curves for BOEF analysis

	Controlled parameter	Measured parameter
Experiment	COD (0.001mm/s) by LVDT	Vertical load by actuator
FEM simulation	Vertical load using the measured value	COD by two nodes over the notch

Displacements were calculated at three locations, including the crack opening displacement (COD), which is located over the notch with a measuring distance of 20mm; the vertical displacement (VD), which is located over the rubber loading pad on top of the asphalt beam; and the side displacement (SD), which is located 10mm away from the side of the BOEF beam.

A thin layer of elements right above the notch was defined with both visco-elastic and smeared crack properties. For simplicity, a linear smeared crack model was defined to this layer of elements. The strength and the maximum crack width were chosen as 3MPa and 0.001mm, respectively.
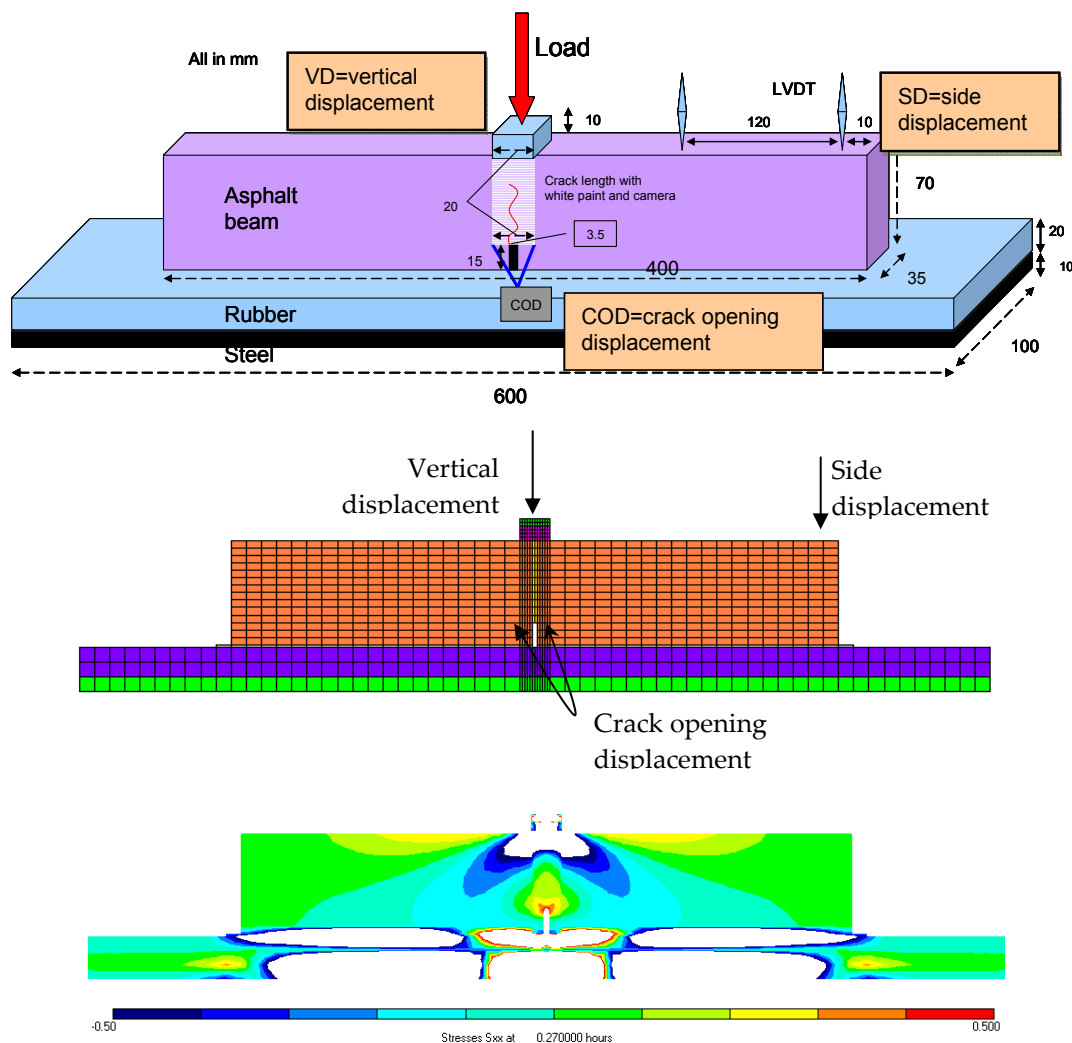

Figure 7-19 FEM model assembly of BOEF setup (a) BOEF-2D FEM modelling using FEMMASSE; (b) Horizontal stress distribution Sxx (the white areas are the areas where the stresses are less than -0.5MPa or higher than 0.5MPa)

7.4.3   Visco-elastic analysis

Figure 7-20 shows the results of the visco-elastic simulation. The following observations can be made:

- o The simulated LC curve shows a similar slope at the beginning but a higher slope after the COD level of 0.2mm when compared to the experimental LC curve. It should be noted that the simulation was carried out assuming no damage is present in the specimen. So the difference in slope can be because of damage, which will be further verified.

- o The SD curve shows the curvature of the BOEF beam during bending. The simulated SD curve shows the similar changes as observed in the Load-COD curve. A small drop is observed at the very beginning for both simulation and experiment, which is due to the preloading of the BOEF set-up. After that, the BOEF beam starts to bend. After 200s, the simulation curve tends to have a nonlinear decreasing slope, while the experimental curve is still increasing. This can also be seen as an indication of damage.

- o The VD curve measures the overall displacement of the BOEF set-up. No clear differences can be observed. This might be because the rubber pad is contributing most to the vertical displacement.

- o As a result, the LC curve is more appropriate for measuring and evaluating local cracking and healing behaviour. This is also proved experimentally in the literature [24].
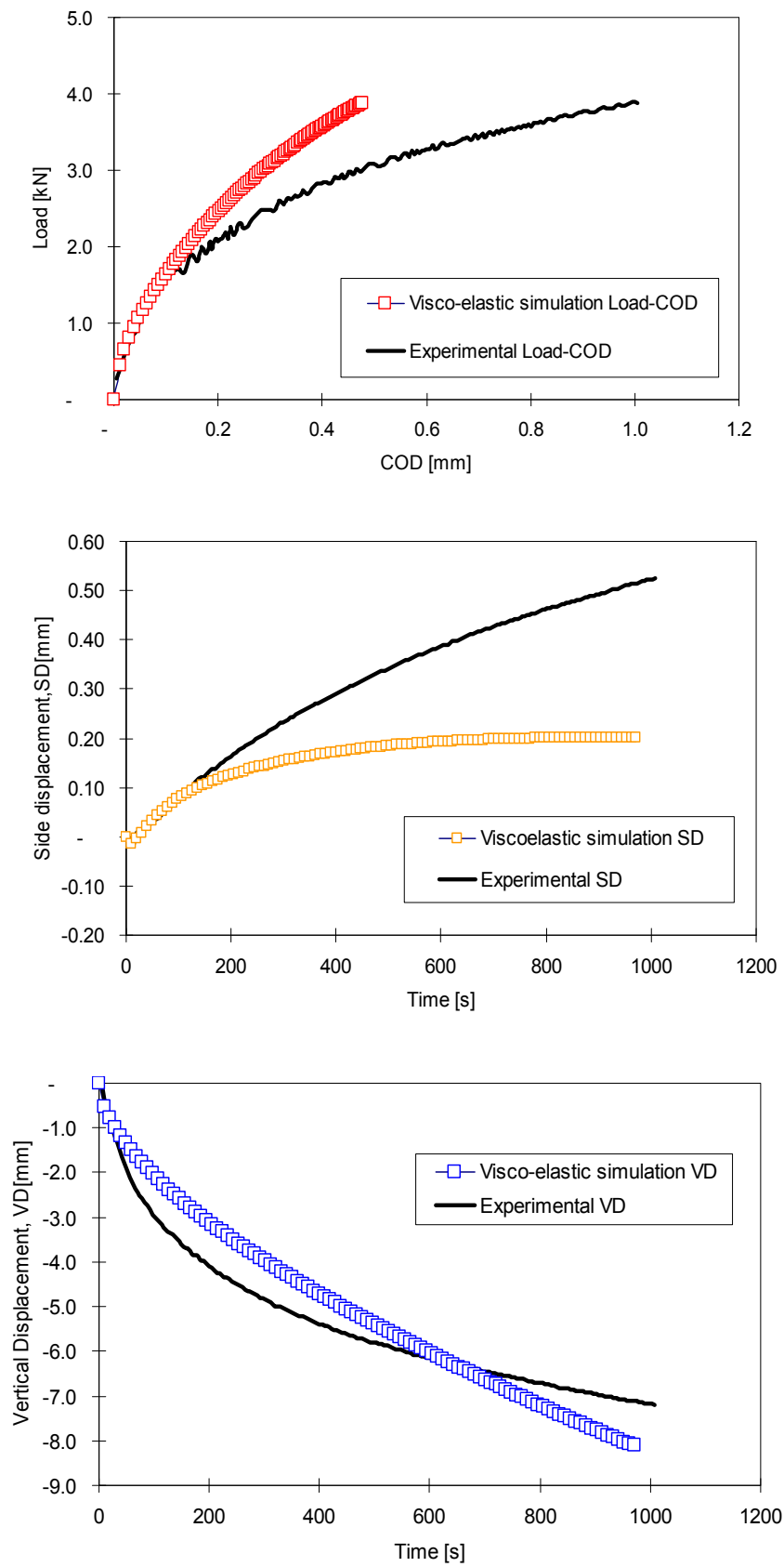
Figure 7-20 Simulation of monotonic BOEF test at 5°C: (a) Load-COD curve; (b) SD-time curve; (c) VD-time curve

7.4.4 Modelling of cracking behaviour

7.4.4.1 Load-COD curve

Figure 7-21a compares the simulated COD development with and without damage. The modelling with damage indicates that at a certain displacement, a crack has initiated, and the displacement increases because of crack propagation. Figure 7-21b compares the simulated and experimental LC curves. It can be seen that the LC relationship can be simulated successfully if the damage is modelled appropriately.

Figure 7-21 Modelling of cracking behaviour: (a) comparison of crack opening displacement with and without damage; (b) simulation of Load-COD curve with CZM

7.4.4.2   Unloading

Figure 7-22 shows the simulation results of the unloading curves. It can be seen that the model cannot fully simulate the unloading behaviour. The simulated COD recovers immediately to zero after unloading, which overestimates the experimental COD recovery speed. This is because the experimental crack closure process is a nonlinear process, which is related to the internal compressive stress state due to confining effect of the rubber foundation and relaxation of the asphalt beam.
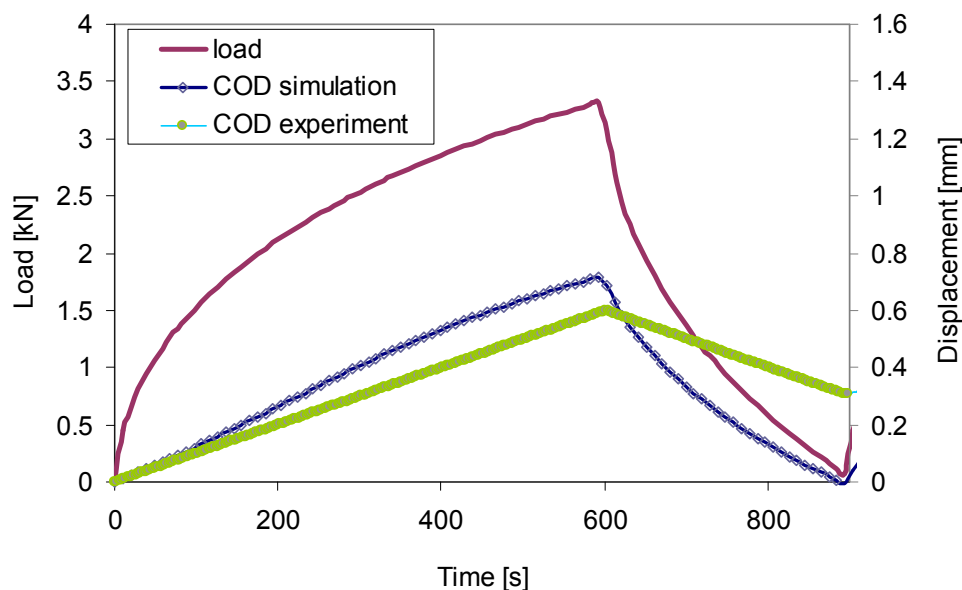
Figure 7-22 Simulation of unloading behaviour

7.4.5   Modelling of healing behaviour
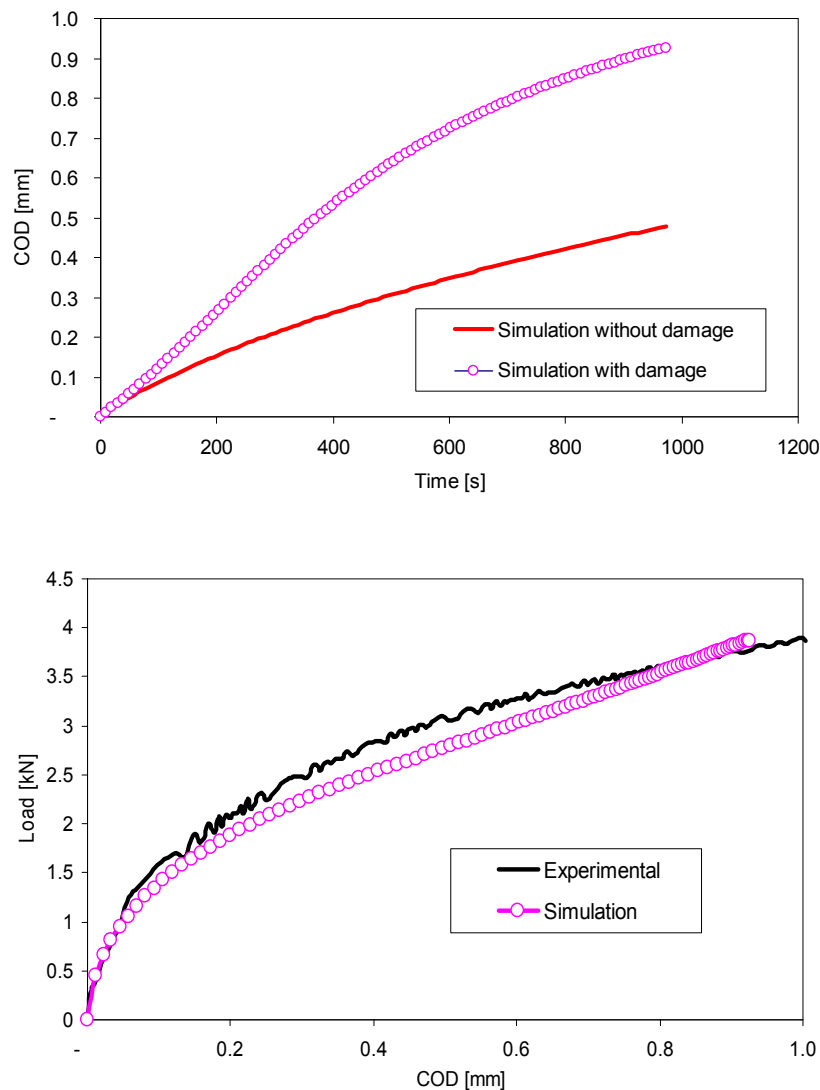
Figure 7-23 shows the simulation results of the reloading behaviour. It is shown earlier that unloading and a short term healing results in closure of the crack. So the reloading includes two possible processes, the crack reopens and further crack propagation. It is hypothesised that the crack reopening process is more sensitive to healing. Due to healing, the crack tip regained its stiffness and strength. A healing approach adopted from the DTT simulation was used to simulate the stiffness and strength recovery of the crack. However, limited difference can be noticed in a macroscopic load-COD curve.

It was then hypothesised further that the crack tip is not only healed totally but also reduces in length due to healing. During the simulation, a deduction of the crack length after healing was included manually. The same load was applied in all cases in order to see the difference. As shown from Figure 7-23b, the simulation shows agreement with the experimental results, which proves the hypothesis. The pre-defined crack length of 10mm is similar with the experimental result from short period healing (3 hours at 5°C). When increasing healing times and healing temperatures, the reloading curve after healing is

similar to a crack length of 5mm or even lower. It implies that healing behaviour can be seen as a crack repairing process with increasing healing times and healing temperatures. However, the pre-defined crack length of 10mm is not exactly the same as the experiment result of 5mm at a COD level of 0.6mm, more research needs to be carried out to minimize this difference.
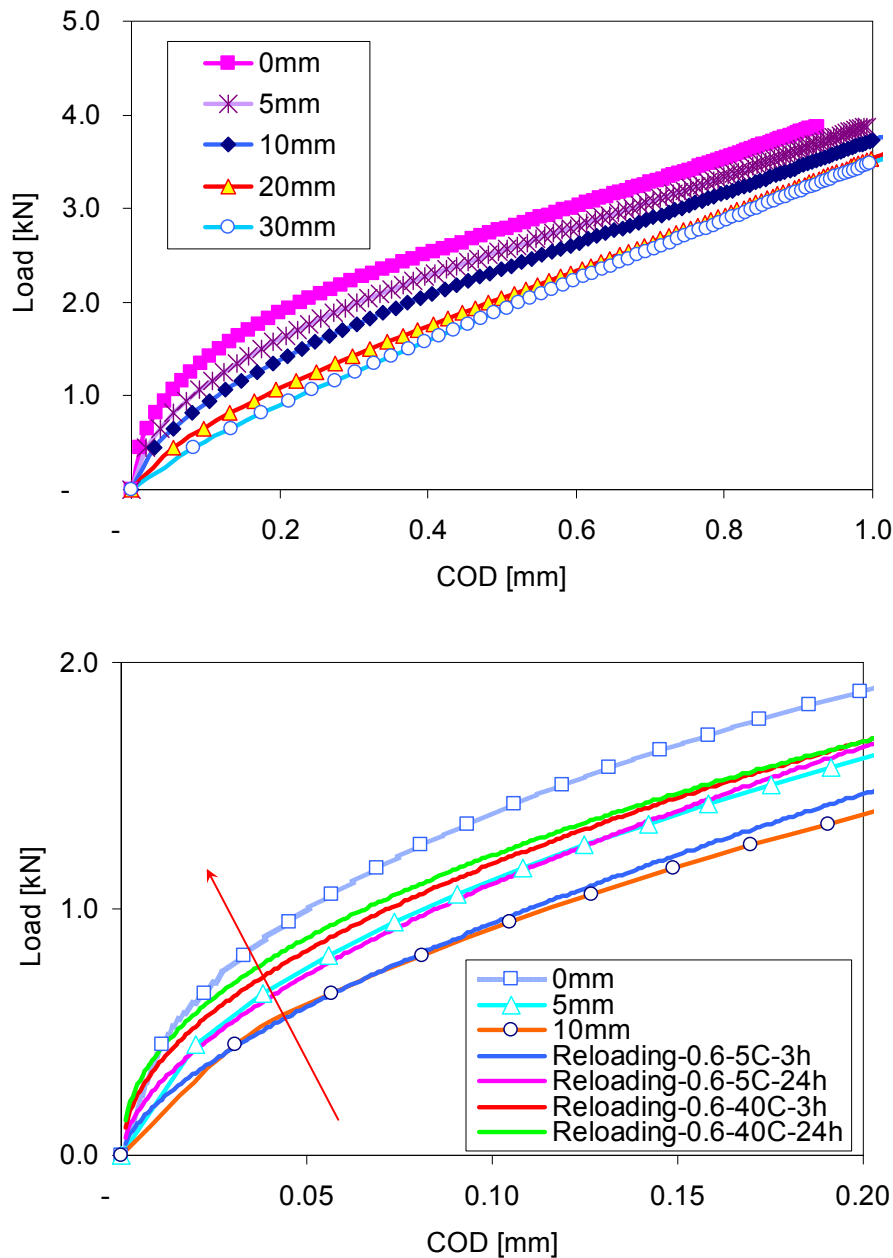

Figure 7-23 Simulation of reloading behaviour with different pre-defined crack lengths (e.g. 5mm means that the length of the pre-defined crack length above notch is 5mm) (a) full reloading LC curves; (b) comparison of simulation with experiment results

7.5 Conclusions

A healing model was developed by using the finite element program named FEMMASSE. The model combines a smeared type cohesive zone model and visco-elastic behaviour. Based on the observations and the simulation results, the following can be concluded:

- o With regard to modelling self healing of bituminous mastics using the DTT:

  - ➢ The viscoelastic coupled damage and healing behaviour of bituminous mastics can be simulated by defining both local damage-healing and visco-elastic properties.

  - ➢ The visco-elastic-damage interactions were observed to be important for damage simulation of bituminous mastics such as post-peak relaxation, unloading and reloading.

  - ➢ The visco-elastic coupled healing process can be de-composed into visco-elastic recovery and damage recovery including stiffness recovery and strength recovery. The visco-elastic recovery and the stiffness recovery developed after a short healing time and the strength recovery after a long healing time.

- o With regard to modelling self healing of asphalt mixtures using the BOEF setup:

  - ➢ The load-COD curve is shown to be the most appropriate relationship for experimentally indentifying the cracking and healing behaviour. Upon defining the local cohesive zone parameters, the global load-COD curve can be simulated successfully.

  - ➢ During the unloading process, the experimental crack closes slowly when the COD is decreasing. Due to the simplicity of the unloading nature of the smeared crack model, the crack surface closes totally after the load was removed. This overestimates the crack closure speed in reality.

  - ➢ The reloading behaviour after different healing conditions can be simulated by decreasing the crack lengths. The healing behaviour is then directly related to a decreasing crack length as a crack repairing process.

References

[1] Bazin P and Saunier JB. Deformability, fatigue and healing properties of asphalt mixes. Proceedings of the Second International Conference on the Structural Design of Asphalt Pavements. Ann Arbor, Michigan, USA; 1967, p. 553-69.

[2] Francken L. Fatigue performance of a bituminous road mix under realistic best conditions. Transportation Research Record 1979;712:30-4.

[3] Lytton RL, Chen CW, and Little DN. Fundamental properties of asphalts and modified asphalts - task K: microdamage healing in asphalt and asphalt concrete. FHWA Final Report DTFH61-92-C-00170; 1998.

[4] Phillips MC. Multi-step models for fatigue and healing, and binder properties involved in healing. Eurobitume Workshop on Performance Related Properties for Bituminous Binders. Luxembourg; 1998, p. 115.

[5] Qiu J, Van de Ven MFC, Wu SP, Yu JY, and Molenaar AAA. Asphalt pavements are self healing. 1st International Conference on Sustainable Construction Materials: Design, Performance and Application. Wuhan, China; 2010.

[6] FEMMASSE. *User manual MLS version 8.5*. 2006.

[7] Mazars J and Pijaudier-Cabot G. From damage to fracture mechanics and conversely: A combined approach. International Journal of Solids and Structures 1996;33:3327-42.

[8] Kim YR. Cohesive zone model to predict fracture in bituminous materials and asphaltic pavements: state-of-the-art review. International Journal of Pavement Engineering 2011;12:343-56.

[9] Abu Al-Rub RK, Darabi MK, Little DN, and Masad EA. A micro-damage healing model that improves prediction of fatigue life in asphalt mixes. International Journal of Engineering Science 2010;48:966-90.

[10] Lee H and Kim Y. Viscoelastic continuum damage model of asphalt concrete with healing. J. Eng. Mech. 1998;124:1224.

[11] Pronk A. PH model in 4PB test with rest periods. Road Materials and Pavement Design 2009;10:417-26.

[12] Hillerborg A, Modeer M, and Petersson PE. Analysis of crack formation and crack growth in concrete by means of fracture mechanics and finite elements. Cement and Concrete Research 1976;6:773-81.

[13] Song SH, Paulino GH, and Buttlar WG. Simulation of crack propagation in asphalt concrete using an intrinsic cohesive zone model. Journal of Engineering Mechanics 2006;132:1215-23.

[14] Li X and Marasteanu M. Cohesive modeling of fracture in asphalt mixtures at low temperatures. International Journal of Fracture 2005;136:285-308.

[15] Kim YR, Allen DH, and Little DN. Damage-induced modeling of asphalt mixtures through computational micromechanics and cohesive zone fracture. Journal of Materials in Civil Engineering 2005;17:477-84.

[16] Allen DH and Searcy CR. A micromechanical model for a viscoelastic cohesive zone. International Journal of Fracture 2001;107:159-76.

[17] Sadouki H and Denarié E. Modelling of UHPFRC in composite structures. Sustainable and Advanced MAterials for Road InfraStructure WP 14: High Performance Fibre Reinforced Cementitious Composites for rehabilitation D26; 2006.

[18] Denarié E, Habel K, and Brühwiler B. Structural behavior of hybrid elements with Advanced Cementitious Materials (HPFRCC) 4th International Workshop on High Performance Fiber Reinforced Cement Composites Ann Arbor, Michigan, USA; 2003.

[19] Lundstrom R. On rheological testing and modelling of asphalt mixtures with emphasis on fatigue characterization: KTH Royal Institute of Technology, 2004.

[20] Woldekidan M, Huurman M, and Mo L. Testing and modeling of bituminous mortar response. Journal of Wuhan University of Technology--Materials Science Edition 2010;25:637-40.

[21] Bazant ZP and Gettu R. Rate effects and load relaxation in static fracture of concrete. ACI Materials Journal 1992;89:456-68.

[22] Denarié E, Cécot C, and Huet C. Characterization of creep and crack growth interactions in the fracture behaviour of concrete. Cement and Concrete Research 2006;36:571-5.

[23] Hordijk DA. Local approach to fatigue of concrete, Delft: Delft University of Technology, PhD thesis, 1991.

[24] Wagoner M, Buttlar W, and Paulino G. Disk-shaped compact tension test for asphalt concrete fracture. Experimental Mechanics 2005;45:270-7.

8

Conclusions and Recommendations

Abstract

In this chapter, the conclusions and recommendations of this thesis are presented. The conclusions in this chapter are rather general in comparison with the detailed conclusions discussed in individual chapters. The recommendations outline the possibilities for future research.

T he main goal of this research was to understand the self healing mechanism of bituminous materials. The three objectives of this research were "what is healing", "how to measure healing effectively" and "how to modify it if possible". Three areas of the self healing phenomenon were explored including mechanical assessment, material modifications and modelling simulations. In Chapter 3 to Chapter 7, the details of the work conducted in this research were discussed. In each of the chapters the important findings were reported at the end of the chapter.

In this final chapter, the generalized conclusions and recommendations are presented. Section 8.1 gives the conclusions and Section 8.2 addresses recommendations for future work.

8.1 Conclusions

In order to achieve the three objectives of this thesis (what is healing, how to measure healing effectively and how to modify it if possible) attention was paid to test methods which can be used, material aspects and how healing can be modelled. The following conclusions have been drawn.

8.1.1   With regard to testing

o Three test methods are developed to indentify the self healing phenomenon with regard to crack healing of bituminous materials. In each of these test methods, cracks were produced first in a controlled way, and the healing process of these cracks was investigated by means of these tests. The tests involved self healing tests on bituminous binders using the DSR, self healing tests on bituminous mastics using the DTT and self healing tests on asphalt mixtures using the BOEF test. The first two tests were developed from material point of view, and the last test was developed from structural point of view.

o The DSR can be used to investigate the self healing capability of bitumen using the two-piece healing set-up. The development of the complex shear modulus can be used as an indicator for the healing capability. Healing can be divided into two phases namely the initial healing phase and the time dependent healing phase. The initial healing phase mimics the crack closure process of the healing process, and the time dependent healing phase mimics the healing in time. It was demonstrated that many factors influence the complex shear modulus measurement results obtained by using the DSR parallel-plate geometry; especially the compressive force applied perpendicular to the crack phases plays an important role. Special attention must be paid to distinguish the real healing effect from those factors that may not really contribute to the healing of bitumen.

o The DTT test with a fracture-healing-refracture (FHR) procedure was successfully applied to investigate the self healing capability of an open crack. A strength recovery master curve can be obtained using the time-temperature superposition principle. The strength increases with increasing healing time and increasing healing temperature. When comparing the crack closure process observed by using fluorescence microscopy and the strength recovery master curve, the completion of the crack closure process does not mark a full recovery of the strength. The DTT test with a loading-healing-reloading (LHR) procedure can be applied to investigate the self healing capability of meso cracks in a specimen. The healing observed in this test is dependent on healing time, damage levels and material type. A higher self healing capability can be obtained when the healing time is longer and/or crack phase is smaller.

o The asphalt beam glued on a rubber foundation test, the BOEF test, is capable of analyzing the self healing capability of asphalt mixtures under different conditions (crack phases, time, and temperature). The BOEF setup allows fully closure of the crack due to the confinement of the rubber foundation. After a healing period, the beams were reloaded and the response was used as an indicator of healing. The self healing capability increases with increasing healing time, temperature and when the crack size is small.

o These three test methods are capable of ranking the self healing capability of bitumen, bituminous mastics and asphalt mixtures at different healing times, temperatures and damage levels.

8.1.2 With regard to materials

o The self healing process of damage in bituminous materials consists of two main phases, namely the crack closure and the strength gain phase. The driving force for the crack closure phase can be either thermal (flow by temperature) or mechanically (by confinement, pressure). This is also coupled with the visco-elastic behaviour of bituminous materials. The crack closure phase results in closing of the crack and recovering of the material stiffness. The driving force for the strength gain phase is thermally (by wetting and diffusion by temperature), where mechanical pressure perpendicular to the crack phases is also necessary to ensure the occurrence of the wetting and diffusion process. The strength gain phase results in recovering of material strength.

o In the exploration phase of this research, many different types of self healing material systems were studied as potential modifiers to improve the self healing capability of bituminous materials. These included inonomers, supramolecular rubbers and nanoparticles. The experimental results showed that a pure soft bitumen is an excellent healer compared

to all the self healing material systems introduced. All the novel self healing modifiers that were tested are not very beneficial. The addition of the novel modifiers either increases the stiffness of the material like ultrafine fillers or can not work effectively due to segregation.

o A clear influence of an SBS polymer modification on the self healing capability was observed. A negative effect is observed when considering healing of an open crack. A positive effect can be observed at a lower damage level where micro cracks develop. This positive effect can be explained by the confinement effect from the undamaged SBS polymer network.

8.1.3 With regard to modelling

o The viscoelastic coupled damage and healing behaviour of bituminous mastics and asphalt mixtures can be simulated by defining both visco-elastic and cohesive zone properties in a finite element program. The visco-elastic coupled healing process of bituminous mastics using the DTT can be de-composed into visco-elastic recovery and damage recovery including stiffness recovery and strength recovery. For the healing simulation of the BOEF test, the healing phenomenon can be simulated by a reduced crack length, which can be directly linked to a crack repairing process.

8.2 Recommendations

From the experience obtained from this study, the following aspects are important for further research:

8.2.1 With regard to testing

o For the self healing test methods developed in this thesis, further research is needed to validate and implement these methods into practice. The test methods can be used for ranking the self healing capabilities of different types of materials and modifications in relation to the physical-chemical, rheological and micro-structural properties. More variables should also be considered including aging, moisture and so on. In addition, it is also recommended to apply these developed methods to evaluate the crack-sealing capability of sealants and joint materials.

o When considering the difference between modulus recovery and strength recovery, hardly any research is available on the strength recovery aspect. Due to the importance of the strength recovery in healing characterization shown in this thesis, assessment of the self healing capability should be investigated on that aspect.

o The complexity and artefacts during self healing assessments should be taken good care of. Especially, the visco-elastic behaviour, the geometry effect and the plastic behaviour, which might occur during the measurements should be recognized and taken into account.

8.2.2   With regard to materials

o Because of its low viscosity, pure soft bitumen exhibits an excellent self healing capability of itself when compared to polymer modified bitumen. However, to improve the self healing capability of bituminous materials in time, an ageing inhibitor or anti-ageing product is needed to lower the viscosity of aged bitumen. A rejuvenation technology can also be considered as an effective method to upgrade the self healing capability during the service life

o In order to ensure the healing capability of bituminous materials during their service life, an effective material modification is recommended. Polymer modified bitumen is capable of improving the high and low temperature performance. However, the application of the polymer modified bitumen for improving the self healing capability should be undertaken with care. It limits the self healing capability when the polymer network is broken. When the polymer network is not broken, the elastic recovery of the network can act as confinement to accelerate the self healing process.

o It is also suggested to build a self healing material system (encapsulation system, micro-vascular system for example) to improve the self healing capability of bituminous materials instead of modifying a material itself. However, this research should also be preceded by research into the feasibility of such systems. Questions like will they survive e.g. the harsh conditions occurring during mixing, laying and compaction should be answered.

o The mixing methods strongly influence the performance of the modified bitumen. Further research on the effect of the mixing methods is necessary.

8.2.3   With regard to modelling

o Fracture mechanics based modelling should be improved to incorporate time, temperature and loading rate dependent behaviour. Due to the elastic nature of the smeared crack model, it overestimates the crack development and crack closure speed of bituminous materials in reality.

o Bituminous materials are very complex. When subjected to mechanical loading, different types of behaviour and processes occur at the same time including visco-elastic, visco-plastic behaviour, cracking, etc. A numerical model combining continuum damage mechanics and fracture

mechanics is thus needed to fully simulate the performance of bituminous materials.

8.2.4 With regard to durable asphalt pavements

Healing can be very important in a durable asphalt pavement. Through healing, cracks can repair themselves. This process is very sensitive to environmental conditions such as temperature, confining compressive stresses etc. This means that the healing behaviour of an asphalt mixture in a pavement structure can be optimized. This will result in pavements with an enhanced durability. However, the optimization of the self healing capability should be undertaken under the condition that all the other structural and functional performances are fulfilled.

o When considering self healing as it can occur in different types of asphalt layers in a pavement structure, dense asphalt concrete will show a much better healing potential than porous asphalt concrete. The reason is that the dense asphalt concrete has a bitumen rich system and a cohesive type crack is likely to occur and to be healed. Furthermore the bituminous binder in porous asphalt concrete will age much more rapidly than dense asphalt concrete because of its much higher void content. Ageing will reduce the self healing capability.

o When considering the possibility of self healing occurring in different positions of the pavement, bottom-up cracks are expected to heal faster than top-down cracks. This is because ageing and ingress of water, which occur at the pavement surface, will have a negative influence on the self healing process.

o When considering the influence of the crack size on healing one can state that a narrow crack size is favourable for a fast healing. To this end, healing can be used to balance the damage process. Or, in other words, a long service life can be obtained when the healing process is balancing the damage development. In this way, a long life asphalt pavement can be constructed.

o The healing factors applied in current pavement design methods are too simple and empirical. They should be improved in order to be able to take into account time/temperature/crack size dependency of the self healing behaviour.

Curriculum Vitae

Name	Jian Qiu
Date and Place of Birth	16 September, 1982, Liaozhong, China
E-mail:	j.qiu@tudelft.nl, pidqiu@hotmail.com

Experience

2007- 2012	PhD Researcher at Road and Railway Engineering Delft University of Technology, The Netherlands
	Title of PhD thesis: Self Healing of Asphalt Mixtures
2005- 2007	Master of Science in Material Science
	Wuhan University of Technology, P. R. China
	Title of Master thesis: Design and Application of Recycled Asphalt Mixture
2001- 2005	Bachelor of Science in Material Science and Engineering
	Wuhan University of Technology, P. R. China

Publications

1. **Qiu J**, Molenaar AAA, van de Ven MFC, Wu S, Yu J. Investigation of self healing behaviour of asphalt mixes using beam on elastic foundation setup. Materials and Structures, 2012, 45(5): 777-791.

2. **Qiu J**, van de Ven MFC, Wu S, Yu J, Molenaar AAA. Evaluating self healing capability of bituminous mastics. Experimental Mechanics, DOI: 10.1007/s11340-011-9573-1, 2012.

3. **Qiu J**, van de Ven MFC, Wu S, Molenaar AAA, Yu J. Self healing characteristics of bituminous mastics using a modified direct tension test. Submitted to Journal of Intelligent Material Systems and Structures, JIM-11-200, 2012.

4. **Qiu J**, van de Ven MFC, Wu S, Yu J, Molenaar AAA. Crack healing mechanisms in bituminous materials, Submitted to Journal of Materials in Civil Engineering, ASCE, 2012.

5. **Qiu J**, Molenaar AAA, van de Ven MFC, Wu S. Development of an autonomous setup for evaluating self healing capability of asphalt mixes. Transportation Research Board 91st Annual Meeting, Washington DC, USA, January 22-26, 2012.

6. **Qiu J**, van de Ven MFC, Schlangen E, Wu SP, and Molenaar AAA. Characterization and modelling of self healing behaviour of bituminous materials towards durable asphalt pavement design. ISAP 2012 International Symposium on Heavy Duty Asphalt Pavements and Bridge Deck Pavements. Nanjing, China, May 23-25, 2012.

7. **Qiu J**, van de Ven MFC, Schlangen E, Wu SP and Molenaar AAA. Cracking and healing modelling of asphalt mixes. 7th RILEM International Conference on Cracking in Pavements, Delft, the Netherlands, June 20-22, 2012.

8. **Qiu J**, van de Ven MFC, Wu S, Yu J, Molenaar AAA. Investigating self healing behaviour of pure bitumen using dynamic shear rheometer. Fuel, 2011, 90(8): 2710-2720.

9. **Qiu J**, van de Ven MFC, Wu S, Yu J, Molenaar AAA. Self healing of road-use bituminous materials: mechanical characterization and its modelling, Third International Conference on Self-Healing Materials 2011, Bath, UK. June 27-29, 2011.

10. **Qiu J**, van de Ven MFC, Wu S, Yu J, Molenaar AAA. Asphalt pavements are self healing, 1st International Conference on Sustainable Construction Materials: Design, Performance and Application, Wuhan, China, August 10-12, 2010.

11. **Qiu J**, van de Ven MFC, Wu S, Yu J, Molenaar AAA. Investigating the self healing capability of bituminous binders. Road Material and Pavement Design, 2009,10(SI) p.81-94.